Generation of 2-D Digital Filters with Variable Magnitude Characteristics starting from a Particular Type of 2-Variable Continued Fraction Expansion

SHIVANI HARIDAS

A Thesis

in

The Department

of

Electrical and Computer Engineering

Presented in Partial Fulfillment of the Requirements for the
Degree of Master of Applied Science at
Concordia University
Montreal, Quebec, Canada, H3G 1M8

July 2006

Your file Votre référence
ISBN: 978-0-494-20748-2
Our file Notre référence
ISBN: 978-0-494-20748-2

ABSTRACT

Generation of 2-D Digital Filters with Variable Magnitude Characteristics starting from a Particular Type of 2-Variable Continued Fraction Expansion

Shivani Haridas

A new approach to generate 2-D filters having variable magnitude characteristics has been proposed. In this work, 2-D digital filters starting from a singly terminated network is generated. A new type of Continued Fraction Expansion obtained from a singly terminated network is considered, its stability defined and stable 2-D analog lowpass filters have been generated. The 2-D analog lowpass filters have been transformed to digital domain by applying generalized bilinear transformation. The 2-D digital lowpass filters give rise to 2-D digital highpass, bandpass and bandstop filters. The 2-D highpass and bandstop filters have been generated from 2-D lowpass filters using appropriate transformations. The 2-D bandpass filter has been obtained by a combination of lowpass and highpass filters.

The 2-D digital filters are classified into four sets. The classification of four sets is based on the coefficients of the Continued Fraction Expansion. Each set is further classified into four cases. The classification of four cases in each set is based on the coefficients of the generalized bilinear transformation.

The effects of the coefficients of the generalized bilinear transformation in each case and the effects of the coefficients of the Continued Fraction Expansion (CFE) in each set are studied.

In the end, some basic examples of implementation of 2-D digital lowpass filters in image processing are illustrated. The examples include reducing added Gaussian noise from images by using 2-D lowpass filtering.

ACKNOWLEDGEMENTS

I am deeply privileged to work under the thesis supervision of Dr. Venkat Ramachandran. It was Dr. Ramachandran's invaluable thoughts at the macro level which helped me to mould me on a technical plane. I am deeply indebted to him for providing me an opportunity to work with him. It was Dr. Ramachandran's vision and ideas that provided the foundation for this thesis. He has been extremely helpful, understanding and extra-ordinarily patient in the critical review of my thesis. It has been a great privilege to work with him which will result in the writing of a few invaluable research papers which we will submit in future. I also sincerely thank Dr. Anjali Agarwal and Dr. Wenfang Xie for their suggestions during the final submission of the thesis.

I am heartily grateful to my mother, Ms. Padmini G. Rao and grand father, Mr. P.K.G. Rao, for their encouragement and support which have always been the key factor behind my every success in life. I would like to thank them for their love and sacrifices. I would also like to express my gratitude to my aunts, uncles and cousins, whose help made this dream come true. It was a pleasure to work with my colleagues and friends Karthikeyan Sundaram, Ajit Singh Sandhu and Serguei Mokhov who provided valuable help during the various stages of this work.

Shivani Haridas, July 2006

Dedicated to my Grand Mother,

Late Mrs. Sharada G. Rao

Contents

List of Figures

List of Symbols and Abbreviations

s_1, s_2	: Laplace domain parameter in two dimensions
z_1, z_2	: Z-domain parameter in two dimensions
H	: Transfer function of a filter in analog domain
H_d	: Transfer function of a filter in digital domain
Σ	: Summation
$\in$	: Belongs to
M	: Order of filter
B_k	: Coefficients required for the filtering function
$a_{00}, a_{01}, a_{10}, a_{11}$	: Coefficients of the generalized doubly terminated network
$b_{00}, b_{01}, b_{10}, b_{11}$	considered by using the CFE
k_1, k_2	: Bandwidth affecting coefficients of generalized bilinear transformation
a_1, a_2	: Gain affecting coefficients of generalized bilinear transformation
b_1, b_2	: Polarity affecting coefficients of generalized bilinear transformation
μ	: Mean of average value of the noise function
σ	: Standard deviation of the noise function
M, N	: Number of columns and rows of a digital image
*	: Convolution
N-D	: N-Dimensional, where N is positive integer, e.g., 2-D for Two-Dimensional

D_a	: Denominator of a transfer function
N_a	: Numerator of a transfer function
SHP	: Strictly Hurwitz Polynomial
VSHP	: Very Strict Hurwitz Polynomial
CFE	: Continued Fraction Expansion
BIBO	: Bounded Input Bounded Output
FIR	: Finite Impulse Response
IIR	: Infinite Impulse Response
DFT	: Discrete Fourier Transform
IDFT	: Inverse Discrete Fourier Transform
MSE	: Mean Square Error
PSNR	: Peak Signal-to-Noise Ratio
PDF	: Power Density Function

Chapter 1

Introduction

The topic of Multi-dimensional system (MDS) analysis and design of multi-dimensional filters has increasingly attracted considerable attention during the recent years and is still receiving significant interest by both theorists and practitioners. Multi-dimensional signal processing has many applications in modern day devices and many practical systems, because of which, this subject is still being investigated in such important areas as facsimile, television, sonar, bio-medicine, remote sensing, underwater acoustics, moving-objects recognition, robotics and so on [1].

Specifically, researchers have been drawn into the area of two-dimensional (2-D) digital systems due to several reasons: high efficiency, high speed computations, permitting high quality image processing and analysis, great application flexibility and adaptability, decreasing cost of software and hardware implementations due to large expansion and evolution of microcomputers, microprocessors and high-integration digital circuits [1].

The two-dimensional digital systems perform important operations which include: 2-D digital filtering, 2-D digital transformations, local space processing, data compression and pattern recognition. Digital filtering, digital transformations and local space operators play important roles in preprocessing of images, performing smoothing, enhancement, noise reduction, extracting boundaries and edges before pattern recognition, data compres-

sion operations permitting the reduction of large number of data representing the images in digital form and minimizing transmission and storage problems. Pattern recognition operations permit the extraction of significant information and configures from the images for final interpretation and utilization [1][2][3].

The 2-D digital filters have numerous applications in various fields such as image processing and seismic signal processing. In many of these applications, the signal does not have any preferred spatial direction and so the required filter functions possessing circular, elliptical and other symmetric frequency response characteristics are finding great importance. Also 2-D filters find increasing applications in image restoration and enhancement [1]. As an example, two dimensional high pass filtering removes the unwanted background noise from an image so that the details contained in the higher spatial frequencies are easier to perceive.

1.1 Two-Dimensional Digital Filters

The 2-D filters can be classified into two main groups. The first group comprises a finite sequence transfer function and so the filters in this group are called Finite Impulse Response (FIR) filters. The second group comprises an infinite sequence transfer function and so the filters in this group are called Infinite Impulse Response (IIR) filters.

1.1.1 Finite Impulse Response Filters (FIR Filters)

The transfer function of 2-D FIR filters can be described by using 2-D z-transform as follows [1]:

$$H(z_1,z_2) = \sum_{n1=0}^{M} \sum_{n2=0}^{N} A_{n_1 n_2} z_1^{-n_1} z_2^{-n_2} \tag{1.1}$$

Eqn.(1.1) implies that some of the 1-D design methods can be directly extended to two (2-D) or more dimensions (M-D) by appropriate modifications in the design procedures. It should also be noted that a straight extension of 1-D technique to 2-D design may not

always be possible. In the 2-D FIR filters, problems of stability do not occur since the impulse response is bounded and exists only for finite time duration and the stability of H(z_1, z_2) is guaranteed. Therefore,

$$\sum_{n_1=0}^{M} \sum_{n_2=0}^{N} |H(z_1, z_2)| < \infty \tag{1.2}$$

for all finite values of M and N.

1.1.2 Infinite Impulse Response Filters (IIR Filters)

The transfer function of 2-D IIR filters can be described by using 2-D z-transform [1] and can be expressed as a ratio of two variable polynomials as follows:

$$H(z_1, z_2) = \frac{N(z_1, z_2)}{D(z_1, z_2)} = \frac{\sum_{i=0}^{I} \sum_{j=0}^{J} a_{ij} z_1^{-i} z_2^{-j}}{\sum_{k=0}^{K} \sum_{l=0}^{L} b_{kl} z_1^{-k} z_2^{-l}} \tag{1.3}$$

where b_{00}=1, a_{ij} and b_{kl} are real coefficients.

For any input signal $X(z_1, z_2)$, the output $Y(z_1, z_2)$ of the filter is given by,

$$Y(z_1, z_2) = H(z_1, z_2) \cdot X(z_1, z_2) \tag{1.4}$$

In the 2-D IIR filters, one important problem to be dealt with is stability. According to the stability theorem [4][5], the 2-D IIR filter is guaranteed to be stable in the bounded-input bounded-output (BIBO) sense, if there exists no value of z_1 and z_2 for which $D(z_1, z_2) = 0$ for both $|z_1| \geq 1$ and $|z_2| \geq 1$ [1]. This means it is highly preferable that the given analog transfer function must have a Very Strict Hurwitz Polynomial (VSHP) denominator [5]. Therefore, the design of a 2-D IIR filter requires obtaining the coefficients a_{ij} and b_{kl} in eqn.(1.3) so that $H(e^{j\omega_1 t_1}, e^{j\omega_2 t_2})$ approximates a given response G(jω_1, jω_2) where ω_1 and ω_2 are horizontal and vertical spatial frequencies respectively, which also ensures the

stability of the filter.

1.2 Stability of 2-D filters

In one-dimensional (1-D) systems (both analog and discrete), one can use suitably chosen transfer functions having no common factors between the numerator and the denominator in order to design a filter having required specifications. Let $H_a(s) = \frac{N_a(s)}{D_a(s)}$ be a transfer function in the analog domain with $N_a(s)$ and $D_a(s)$ being relatively prime. For the transfer function $H_a(s)$ to be stable, $D_a(s)$ should be a strictly Hurwitz polynomial (SHP). A SHP contains its zeros strictly in the left-half of the s-plane. Similarly, if $H_d(z) = \frac{N_d(z)}{D_d(z)}$ be a transfer function in the discrete domain with $N_d(z)$ and $D_d(z)$ being relatively prime, then $D_d(z)$ should be a Schur polynomial in order that the function $H_d(z)$ shall be stable. A Schur polynomial contains its zeros strictly within the unit circle [5].

In the case of 2-D analog systems, it is possible that both the even and the odd parts of a polynomial may become simultaneously zero at specified sets of points, but not in their neighbourhood. If this occurs in the denominator of the transfer function, it is called a non-essential singularity of the first kind. In addition, in 2-D transfer functions, both the numerator and the denominator polynomials can become zero simultaneously at a given set of points. When this happens, it is known as non-essential singularity of the second kind. Mathematically, for a 2- D analog transfer function $H_a(s_1, s_2) = \frac{N_a(s_1,s_2)}{D_a(s_1,s_2)}$, the above two cases may be expressed as [5]

(a) $D_a(s_1, s_2) = 0$ and $N_a(s_1, s_2) \neq 0$ constitute non-essential singularity of the first kind at (s_1, s_2).

(b) $D_a(s_1, s_2) = 0$ and $N_a(s_1, s_2) = 0$ constitute non-essential singularity of the second kind at (s_1, s_2).

A similar situation exists in the case of 2-D discrete systems also. One of the well-known methods of designing digital filters is to start from a given analog filter transfer

function and then apply the generalized bilinear transformation $s_i \rightarrow k_i \frac{z_i+a_i}{z_i+b_i}$, $i = 1, 2$, in order to obtain the corresponding digital transfer function [6].

The occurence of the non-essential singularity of the first kind always results in an unstable filter and hence cannot be used in the design of stable filters. The occurence of the non-essential singularity of the second kind in a transfer function may or may not cause instability. It is not possible to determine the stability by inspection [7][8].

As mentioned in Sec 1.1, one important issue concerning the above types of filters is the stability of the filter. It is known that FIR filters are inherently stable. IIR filters may or may not be stable depending upon the transfer function.

The most commonly used stability criterion is based on the bounded-input bounded-output (BIBO) criterion [9]. This criterion states that a filter is stable if its response to a bounded input is also bounded. Mathematically, for causal linear shift-invariant systems, this corresponds to the condition that

$$\sum_{n_1=0}^{\infty} \sum_{n_2=0}^{\infty} |h(n_1, n_2)| < \infty \tag{1.5}$$

where $h(n_1, n_2)$ is the impulse response of the filter.

Eqn.(1.5) points out an important observation that the stability criterion is always verified, if the number of terms of the impulse response is finite, which is the case with FIR filters. However, the above condition does not prove feasible to the test of stability for IIR filters. In the 1-D filters, it is possible to relate the BIBO stability condition to the positions of the z-domain transfer function poles which have to be within the unit circle and it is possible to test the stability by determining the zeros of the denominator polynomial. Similarly, in the 2-D case, a theorem establishing the relationship between the stability of the filter and the zeros of the denominator polynomial can be formulated. This theorem states that [10], for 2-D IIR causal quater-plane filters, if $B(z_1, z_2)$ is a polynomial in z_1 and z_2, the real transfer function of the form $\frac{1}{B(z_1,z_2)}$ is stable if and only if,

$$B(z_1, z_2) \neq 0 \, for \, |z_1| \geq 1, |z_2| \geq 1 \tag{1.6}$$

The above theorem has the same form as in the 1-D case, i.e., it relates the stability of the filter to the singularities of the z-transform. However, in the 2-D case such a formulation for stability condition does not produce an efficient method for stability test, as in 1-D, due to the lack of appropriate factorization theorem of algebra. Therefore, it is necessary in principle, to use an infinite number of steps to test the stability. Also, even if it is possible to find methods to test conditions equivalent to eqn.(1.6) in a finite number of steps [11], computationally it is not easy to incorporate them in a design method and there is a problem of stabilizing the filters which may become unstable.

A widely used approach involves the design of two-variable stable analog transfer function and use bilinear transformations to obtain digital transfer function. For example, first design a two-variable passive (hence guaranteed stable) analog filter via a computer-aided optimization technique and then obtained a 2-D IIR transfer function by applying a double bilinear transformation on the transfer function of the analog filter [12,13].

The 2-D filter stability testing problem can also be avoided by designing a separable 2-D IIR filter approximating the frequency response characteristic. For separable filter, the 2-D transfer function $H(z_1, z_2)$ can be expressed as a product of two 1-D transfer functions, i.e., $H(z_1, z_2) = H(z_1).H(z_2)$. In this case, the testing of stability reduces to that of checking the stability of the 1-D filters, which is considerably simpler. Moreover, a separable filter is also more economical to implement. For example, [14] describes a computer-aided method of designing separable filters.

Therefore, from the point of view of stability tests, there can be two different approaches that can be considered, in designing an IIR filter. One method is to carry out the stability test in every stage of the filter design so that the eventual filter is stable. In the second method, stability is not considered as a part of the design and a magnitude-squared transfer function is first designed. Then a stable filter is obtained, by choosing the poles in

the stability region. Such an approach is convenient, because squared magnitude functions can be in a simple form and it is easy to find the poles of the filter.

In view of all the above difficulties in 2-D design, it will be highly convenient, if we start with Very Strict Hurwitz Polynomials (VSHP) in the denominator of a 2-D transfer function, because such polynomials do not contain non-essential singularities of the second kind. This ensures stability of the designed filter. We will briefly review some of its properties in the next section.

1.3 Review of VSHP and its properties

A class of polynomials which do not contain singularities (discussed in Sec. 1.2) is called Very Strict Hurwitz Polynomials (VSHP) [5]. A VSHP is defined as follows:

"$D_a(s_1, s_2)$ is a VSHP, if $\frac{1}{D_a(s_1,s_2)}$ does not possess any singularities in the region $\{(s_1, s_2) \mid Re\, s_1 \geq 0,\ Re\, s_2 \geq 0,\ |s_1| \leq \infty\ and\ |s_2| \leq \infty\}$".

As per this definition, a VSHP has to be necessarily a Strictly Hurwitz Polynomial (SHP) [5]. After ensuring that a given two-variable polynomial is a SHP, then one can proceed further to ascertain the absence of singularities at points of infinity. The points of infinity are studied by considering the reciprocal of the variable. In view of the two variables considered, the following possibilities exist:

(a) $s_1 \rightarrow \infty$, s_2= finite,

(b) s_1= finite, $s_2 \rightarrow \infty$,

(c) $s_1 \rightarrow \infty$ and $s_2 \rightarrow \infty$.

That is, in (a) and (b), only one of the variables goes to infinity, while the other remains finite, whereas in (c), both the variables go to infinity simultaneously. Another alternate definition for a VSHP is proposed in [15].

A relatively prime two-variable function, $H(s_1, s_2) = \frac{A(s_1,s_2)}{B(s_1,s_2)}$, having no second kind singularities is a reactance function if and only if $A(s_1, s_2) + B(s_1, s_2)$ is a VSHP. Such

functions are called proper reactance functions [16] and are useful as transformation functions to generate a (structurally stable) 2-D network from a stable 1-D network. This is one of the main applications of VSHPs and is utilized in the design of 2-D stable digital filters.

Now, we shall discuss some of the properties of VSHP. The proofs of the properties and a comprehensive study of two variable Hurwitz polynomials are contained in [5][17].

Property 1

The transfer function $H_a(s_1, s_2)$ (defined in [18]) does not possess any singularity in the closed right-half of the (s_1, s_2) biplane, if and only if $D_a(s_1, s_2)$ is a VSHP.

In the above, the closed right-half biplane is

$$\{(s_1, s_2) \mid Re\, s_1 \geq 0,\ Re\, s_2 \geq 0,\ |s_1| \leq \infty\ and\ |s_2| \leq \infty\}$$

Property 2

$D(s_1, s_2) = [D_1(s_1, s_2)].[D_2(s_1, s_2)]$ shall be a VSHP, if and only if $[D_1(s_1, s_2)]$ and $[D_2(s_1, s_2)]$ are individually VSHPs.

This property demonstrates clearly that a product of two VSHPs results in a VSHP. Also, if a VSHP is product-separable, the individual factors shall be VSHPs.

Property 3

If $D_a(s_1, s_2)$ is a VSHP, $\frac{\partial D_a(s_1,s_2)}{\partial s_1}$ and $\frac{\partial D_a(s_1,s_2)}{\partial s_2}$ are also VSHPs.

Property 4

The polynomials $E_i(s_2)$, i=0, 1, 2, ..., p and $F_j(s_1)$, j=0,1,2,...,q defined in [19] are SHPs (Strictly Hurwitz Polynomials) in s_1 and s_2, respectively.

Property 5

Each of the functions $\frac{E_i(s_2)}{E_{i-1}(s_2)}$, i=1, 2, ..., p is a minimum reactive positive real function in s_2 (where a positive real function E(s) is called minimum reactive (susceptive), if it has no poles or zeros on the imaginary axis of s). Similarly, each of the functions $\frac{F_j(s_1)}{F_{j-1}(s_1)}$, j=1, 2, ..., q is a minimum reactive positive real function in s_1.

1.4 Generation of VSHP

When VSHP is used in the denominator of a 2-D analog transfer function, it is guaranteed that the resulting 2-D digital bilinear transfer function obtained through the application of the well-known bilinear transformation is stable [8],[20]. Therefore, VSHP is highly useful in the 2-D digital filter design. We can first generate a two-variable Very Strictly Hurwitz Polynomial (VSHP) using its various properties and assign the generated VSHP to the denominator of the 2-D analog transfer function, then obtain the digital transfer function through double bilinear transformations. Here, we review some methods, which are used to generate VSHP.

1.4.1 Using Terminated n-port Gyrator Networks[21]

For a n-port gyrator network, its ports are terminated by capacitances. In such a case, the overall admittance matrix will be

$$A = \begin{bmatrix} \mu & g_{12} & g_{13} & \cdots & g_{1n} \\ -g_{12} & \mu & g_{23} & \cdots & g_{2n} \\ -g_{13} & -g_{23} & \mu & \cdots & g_{3n} \\ \vdots & \vdots & \vdots & \ddots & \vdots \\ -g_{1n} & -g_{2n} & -g_{3n} & \cdots & \mu \end{bmatrix} \tag{1.7}$$

The determinant of the matrix A can be expressed as

$$\begin{aligned} D_n = \sum_{1 \le i \le n} \mu_i \left|A_i\right| + \sum_{1 \le i_1 < i_2 < i_3 < n} \mu_{i_1}\mu_{i_2}\mu_{i_3} \left|A_{i_1 i_2 i_3}\right| \\ + \ldots + \mu_1\mu_2\mu_3 \ldots \mu_n (n \; is \; odd) \end{aligned} \tag{1.8}$$

or

$$D_n = |A_n| + \sum_{1\le i_1<i_2<n} \mu_{i_1}\mu_{i_2}\,|A_{i_1 i_2}| + \sum_{1\le i_1<i_2<i_3<i_4<n} \mu_{i_1}\mu_{i_2}\mu_{i_3}\mu_{i_4}\,|A_{i_1 i_2 i_3 i_4}| \\ +\ldots + \mu_1\mu_2\mu_3\ldots\mu_n (n\,is\,even) \tag{1.9}$$

where $|A_{i_1 i_2}|$is the determinant of the sub-matrix of A obtained by deleting both i_1^{th} and i_2^{th} rows and columns, the same holds for $|A_{i_1 i_2 i_3}|$, $|A_{i_2 i_3 i_4}|$, etc.,

By making some of the μ_i's equal to s_1 and some of μ_i's equal to s_2, under certain \ noindentconditions, eqn.(1.8) and eqn.(1.9) will yield two-variable VSHPs.

1.4.2 Using the properties of positive semi-definite matrices[22]

In this case, we first define three $n\times n$ square matrices A, μ and G as

$$A = \begin{bmatrix} a_{11} & a_{12} & \cdots & a_{1n} \\ a_{21} & a_{22} & \cdots & a_{2n} \\ \vdots & \vdots & \ddots & \vdots \\ a_{1n} & a_{2n} & \cdots & a_{nn} \end{bmatrix} \tag{1.10}$$

$$\mu = \begin{bmatrix} \mu_1 & \cdots & \cdots & \cdots & 0 \\ \vdots & \mu_2 & & & \vdots \\ \vdots & & \mu_3 & & \vdots \\ \vdots & & & \ddots & \vdots \\ 0 & \cdots & \cdots & \cdots & \mu_n \end{bmatrix} \tag{1.11}$$

$$G = \begin{bmatrix} 0 & g_{12} & g_{13} & \cdots & g_{1n} \\ -g_{12} & 0 & g_{23} & \cdots & g_{2n} \\ -g_{13} & -g_{23} & 0 & \cdots & g_{3n} \\ \vdots & \vdots & \vdots & \ddots & \vdots \\ -g_{1n} & -g_{2n} & -g_{3n} & \cdots & 0 \end{bmatrix} \tag{1.12}$$

where A is a general symmetrical $n \times n$ square matrix, μ is an $n \times n$ diagonal matrix and G is an $n \times n$ skew-symmetric matrix. These matrices A, μ and G are physically realizable.

Now, we define a matrix C as:

$$C = A\mu A^T + G \tag{1.13}$$

The determinant of matrix C is given by

$$M = det(C) \tag{1.14}$$

The polynomial M_n

$$M_n = M + \sum_{j=1}^{n} k_j \frac{\partial M}{\partial \mu_i} \tag{1.15}$$

is a two-variable VSHP when some of the μ_i's are properly made equal to s_1 and some of the μ_i's equal to s_2 and it is made sure the requirements of VSHP are met.

1.4.3 Using the properties of the derivative of even or odd parts of Hurwitz polynomial'[23, 24]

From eqn.(1.10) and eqn.(1.11), one can obtain an n^{th} order polynomial M_n as

$$M_n = det[\mu I + A] \tag{1.16}$$

From, the diagonal expansion of the determinant of matrix, M_n can be written as eqn.(1.8) and eqn.(1.9). We can observe that M_n is the odd (even) part of a n- variable Hurwitz polynomial when n is odd (even), so $\frac{\frac{\partial M_n}{\partial \mu_i}}{M_n}$ is a reactance function. Therefore,

$$M_n = M + \sum_{j=1}^{n} k_j \frac{\partial M}{\partial \mu_i} \tag{1.17}$$

is a n- variable Hurwitz polynomial.

Assigning some of μ_i' s to s_1 and some to s_2 and ensuring the conditions of two-variable VSHP, a two-variable VSHP could be generated from eqn.(1.17)

1.5 Symmetry types associated with 2-D transfer functions

Two and higher dimensional systems may possess different types of symmetries. It is observed (for example in [25],[26]) that by taking into account the symmetry constaints, considerable reduction in multiplications can be achieved in the implementation of 2-D filters. Symmetries can also be used to reduce the number of variables in optimization procedure [26].

To understand how symmetry concept is extended to mathematical functions, consider a real function $f(x_1,x_2)$ with $x_1$and x_2 as two independent variables. The function f(x_1, x_2) assigns a unique value to each pair of values of x_1 and x_2 and so, it may be represented by a three dimensional object having (x_1, x_2) plane as the base and the value of the function at each point in the plane as the height. We may say that a function possesses a symmetry, if a pair of operations, performed simultaneously, one on the base of the function object (i.e.,(x_1, x_2)plane), and the other on the height of the object (function value) leaves the function undisturbed.

In other words, existence of symmetry in a function implies that the value of the function at (x_{1T}, x_{2T}) meets a certain requirement, where (x_{1T}, x_{2T}) is obtained by some operation on (x_1, x_2) and this condition being satisfied for all points in the region. The following gives a brief review of the different symmetry constraints.

1.5.1 Displacement (Identity) Symmetry

If a function possesses displacement identity symmetry with a displacement of d, the symmetry conditions on the function can be expressed as

$$f(x+d) = f(x)\, for\, all\, x \in X \tag{1.18}$$

1.5.2 Rotational Symmetry

Choosing the rotational center as the origin and the rotation angle as $\pi/2$ radians, we get the four-fold rotational symmetry condition as

$$f(x_1, x_2) = f(-x_2, x_1)\, for\, all\, x \in X \tag{1.19}$$

following which we have,

$$f(x_1, x_2) = f(-x_2, x_1) = f(-x_1, -x_2) = f(x_2, -x_1) \tag{1.20}$$

1.5.3 Centro-Symmetry

In the two-variable case, twofold rotational symmetry (rotation by π radians) is called centro-symmetry. The required condition for centro-symmetry is

$$f(-x_1, -x_2) = f(x_1, x_2)\, for\, all\, x \in X \tag{1.21}$$

1.5.4 Centro-Anti Symmetry

In the two-variable case, the required condition for centro-anti symmetry is

$$f(-x_1, -x_2) = -f(x_1, x_2)\, for\, all\, x \in X \tag{1.22}$$

1.5.5 Centro-Conjugate Symmetry

In the two variable case, the required condition for centro-conjugate symmetry is

$$f(-x_1, -x_2) = [-f(x_1, x_2)]^* \, for \, all \, x \in X \tag{1.23}$$

1.5.6 Centro-Conjugate Anti-Symmetry

In the two-variable case, the required condition for centro-conjugate anti symmetry is

$$f(-x_1, -x_2) = [-f(x_1, x_2)]^* \, for \, all \, x \in X \tag{1.24}$$

1.5.7 Reflection Symmetry

Reflection about the x_1 axis, the x_2 axis and the diagonals $x_1 = x_2$ and $x_1 = -x_2$ line, respectively, result in reflection symmetries which could be anyone of the following:

$$x_1 \, axis \, reflection \rightarrow f(x_1, -x_2) = f(x_1, x_2) \tag{1.25}$$

$$x_2 \, axis \, reflection \rightarrow f(-x_1, x_2) = f(x_1, x_2) \tag{1.26}$$

$$x_1 = x_2 \, line \, reflection \rightarrow f(x_2, x_1) = f(x_1, x_2) \tag{1.27}$$

$$x_1 = -x_2 \, line \, reflection \rightarrow f(-x_2, -x_1) = f(x_1, x_2) \tag{1.28}$$

$$180 \text{ deg} \, rotation \, about \, the \, origin \rightarrow f(-x_1, -x_2) = f(x_1, x_2) \tag{1.29}$$

$$90 \text{ deg} \, rotation \, about \, the \, origin \rightarrow f(x_2, -x_1) = f(x_1, x_2) \tag{1.30}$$

1.5.8 Quadrantal Symmetry

The condition on the function to possess quadrantal identity symmetry is

$$f(x_1, x_2) = f(x_2, x_1) = f(-x_1, -x_2) = f(x_1, -x_2) \tag{1.31}$$

It is easy to verify that the four quadrants of the X-plane correspond to the four symmetry regions. Hence this symmetry is called quadrantal symmetry.

1.5.9 Diagonal Fourfold Reflection Symmetry

Similar to the quadrantal case, if the function possesses reflection symmetry with respect to $x_1 = x_2$ line and $x_1 = -x_2$ line simultaneously, it is supposed to possess diagonal fourfold reflection symmetry

$$f(x_1, x_2) = f(x_2, x_1) = f(-x_2, -x_1) = f(-x_1, -x_2) \tag{1.32}$$

As in quadrantal symmetry, the function possesses two-fold rotational symmetry when it possesses diagonal four-fold reflection symmetry.

1.5.10 Octagonal Symmetry

In this case, the function possesses quadrantal symmetry and diagonal symmetry simultaneously. The conditions for a function to possess octagonal symmetry are given by

$$\begin{aligned} &f(x_1, x_2) = f(x_1, -x_2) = f(-x_1, x_2) = f(x_2, x_1) \\ &= f(-x_2, -x_1) = f(-x_1, -x_2) = f(x_2, -x_1) = f(-x_2, x_1) \end{aligned} \tag{1.33}$$

1.5.11 Circular Symmetry

Mathematically, circular symmetry in 2-D filter responses can be defined as the filter response being able to satisfy the general equation of a circle, according to which,

$$\omega_1^2 + \omega_2^2 = M \tag{1.34}$$

where ω_1 and ω_2 are the frequencies in the two dimensions, and M is the magnitude response which needs to be a constant in order to satisfy the circular symmetry property.

The function relation for circular symmetric response in ω plane is given by [27]

$$\hat{H}_1(\omega_1^2)\hat{H}_2(\omega_2^2) = H_s(\omega_1^2 + \omega_2^2) \tag{1.35}$$

where $\hat{H}(\omega_1^2)$ and $\hat{H}(\omega_2^2)$ are the transfer functions of both the dimensions.

It has been clearly proved in [27][28] that, it is not possible to obtain exact circular symmetric stable rational transfer function with denominator other than unity in the analog domain. In order to approximate circular symmetry, a product separable function given by, $H(s_1, s_2) = h_1(s_1)h_2(s_2)$ is considered. Therefore, the following can be deduced:

1. Any separable function, $H(s_1, s_2) = h_1(s_1)h_2(s_2)$ is quadrantally symmetric.

2. When $h_1(.) = h_2(.)$, $H(s_1, s_2)$ is also octagonally symmetric, where $h_1(.)$ is a single variable function.

3. For the magnitude of circular symmetry being the main criterion, $|h_1(j\omega_1)|^2$ should approximate $\lambda e^{\alpha\omega_1^2}$ for suitable values of λ and α.

4. When stable, all-pole 2-D transfer functions are considered to possess quadrantal symmetry, they turn out to be separable.

5. $H(s_1, s_2)$ is said to possess circular symmetry if its magnitude is invariant on a set of specified circular paths around the origin in the ω plane.

1.5.12 Elliptical Symmetry

Similar to the circular case, elliptical symmetry in 2-D filter responses can be defined as the filter response being able to satisfy the general equation of an ellipse, according to which,

$$\frac{\omega_1^2}{a_1^2} + \frac{\omega_2^2}{a_2^2} = 1 \tag{1.36}$$

where ω_1 and ω_2 are the frequencies in the two dimensions, and M is the magnitude response which needs to be a constant in order to satisfy the elliptical symmetry property. The Magnitude 'M' takes both the axes (major and minor) into account when a constant value for it is chosen and a_1 & a_2 corresponding to a magnitude M.

By replacing ω_1 by $\alpha\omega_1$ and ω_2 by $\beta\omega_2$ in eqn.(1.23), we obtain the function relation for elliptic symmetric functions. Thus an ideal elliptical symmetric 2-D magnitude squared function is given by [25]

$$H(\omega_1^2, \omega_2^2) = \lambda e^{(\alpha\omega_1^2 + \beta\omega_2^2)} \tag{1.37}$$

1.6 Scope of the thesis

In this thesis, we will propose a new technique for generating 2-D digital filters having variable magnitude characteristics. Different types of CFE's have been considered [29, 30]. These CFE's are in 1-D discrete domain. The 2-D and multidimensional CFEs were introduced in [31], which were realized as multi-variable ladder networks. The approach used in this thesis is to generate 2-D digital filters starting with a singly terminated network. Here, we will consider a new type of CFE obtained from the singly terminated network, define its stability and design it as a stable 2-D digital lowpass filter. The design of 2-D lowpass filters will be further extended to 2-D digital highpass, bandpass and bandstop filters. In addition, we will also show some basic examples of 2-D filter application in image processing.

In Chapter 2, we will generate 2-D digital lowpass filters from a new type of Continued Fraction Expansion (CFE) obtained from singly terminated network and study their characteristics. The stability of the 2-D analog lowpass filters will be defined and proved by verifying the denominator of the transfer function polynomial to be a Very Strict Hurwitz Polynomial (VSHP). The 2-D analog lowpass filters will be transformed to digital domain by applying generalized lowpass bilinear transformation. The 2-D digital lowpass filters are classified into four sets. Each set is further classified into four cases. The classification of four sets is based on the coefficients of the CFE; and the classification of four cases in each set is based on the coefficients of the generalized bilinear transformation. The effect of the coefficients of the generalized bilinear transformation in each case and the effect of the coefficients of the CFE in each set on the amplitude frequency response will be studied.

In Chapters 3 and 4, we will generate 2-D digital highpass filters and 2-D digital bandpass filters respectively by using the 2-D digital lowpass filters proposed in Chapter 2. Similar to 2-D digital lowpass filters, the four different sets and four cases involved in each set proposed earlier in Chapter 2 will be classified and the effect of the coefficients on the amplitude frequency response will be studied.

In Chapter 5, we will generate 2-D digital bandstop filters from 2-D analog lowpass filter used in Chapter 2. The 2-D analog lowpass filter is transformed to 2-D analog bandstop filter using lowpass to bandstop transformation. The 2-D digital bandstop filter will then be generated by applying the generalized bilinear transformation to the 2-D analog bandstop filter. Similar to Chapters 2, 3 and 4, the 2-D digital bandstop filters will be classified into four sets and four cases and the effect of the coefficients on the amplitude frequency response will be studied.

In Chapter 6, we will show some basic examples of the application of 2-D digital lowpass filters in image processing. The examples will include recovering standard images corrupted by the added Gaussian noise using 2-D digital lowpass filtering.

In Chapter 7, we will discuss the conclusions and some directions for future work.

Chapter 2

Two Dimenional Low Pass Filters from CFE

2.1 Introduction

In various applications, we already have an existing network or we have to implement a multidimensional stable filter that does not have its 1-D equivalents. In multidimensional domain, filter design and analysis becomes a tedious process. Often, design of such filters are based on various conditions and assumptions, which will still make the solutions practically feasible. Hence, if we consider a transfer function obtained from a Continued Fraction Expansion (CFE), its generation as a stable 2-D filter requires certain conditions to be satisfied. But in a 2-D network, specifying necessary and sufficient conditions for the coefficients of the filter is often a tedious task. Our emphasis on this chapter will be to find simple possible ways to specify the conditions to achieve the desired response in 2-D digital filters.

In this chapter, we will design 2-D low-pass filters in digital domain by considering the transfer function obtained from a new type of Continued Fraction Expansion (CFE). The different types of CFEs are discussed in Sec. 2.2. In Sec. 2.3, we will obtain 2-D analog

lowpass filters from the inversion of analog CFE and ensure its stability by verifying it to be a VSHP. By applying the generalized bilinear transformation, the analog LPF can be transformed to its digital domain. In Section 2.4, we will discuss the four sets that were formed based on the values of the coefficients of the CFE and four different cases involved in each set based on the coefficients of the generalized bilinear transformation. In Sec. 2.5, we will discuss each set in particular and study the effect of the coefficients of the filter on the amplitude-frequency response. Sec. 2.6 gives the summary and discussions of the results contained in this chapter.

2.2 Different types of CFEs

A Digital Reactance Function (DRF) is the ratio of a mirror-image polynomial (MIP) and an anti-mirror-image polynomial (AMIP) or from the inverse of that ratio. The two polynomials are obtained from $D(z)$ (whose order is n), the denominator of a stable digital transfer function as

$$MIP : F_1(z) = \frac{1}{2}[D(z) + z^n D(z^{-1})] \tag{2.1}$$

$$AMIP : F_2(z) = \frac{1}{2}[D(z) - z^n D(z^{-1})] \tag{2.2}$$

It has been shown that the DRF given by $[F_1(z)/F_2(z)]$ or $[F_2(z)/F_1(z)]$ can always be expanded into different Continued Fraction Expansions (CFEs)

CFE1:

$$A_1 + \cfrac{1}{A_2 + \cfrac{1}{A_3 + \ldots}} \tag{2.3}$$

where $A_i = a_i \frac{z-1}{z+1}$.

CFE2:

$$B_1 + \cfrac{1}{B_2 + \cfrac{1}{B_3 + \ldots}} \tag{2.4}$$

where $B_i = b_i \frac{z+1}{z-1}$.

CFE3:

$$C_1 + \cfrac{1}{C_2 + \cfrac{1}{C_3 + \ldots}} \tag{2.5}$$

where $C_i = c_i \frac{z-1}{z+1} + d_i \frac{z+1}{z-1}$.

CFE4:

$$D_1 + \cfrac{1}{D_2 + \cfrac{1}{D_3 + \ldots}} \tag{2.6}$$

where $D_i = \frac{k_i(z^2-1)}{z^2+\gamma_i z+1}$ and $k_i > 0$, $|\gamma_i| < 2$ [29, 30].

The above CFEs are in 1-D discrete domain. The 2-D and multidimensional CFEs were introduced in [31] which were realized as multivariable ladder networks. In what follows, we consider another type of CFE in order to obtain the required VSHP.

2.3 Transfer Function of 2-D lowpass filter obtained from the inversion of analog CFE

CFE can be obtained either in the analog domain or in the digital domain. One can start from the analog CFE and then apply the required generalized bilinear transformation [6]

$$s_i \rightarrow k_i \frac{z_i - a_i}{z_i + b_i} \tag{2.7}$$

where i=1, 2 for 2-D filters, to obtain the required digital filter transfer function. For the resulting 2-D filter to be stable, it is required that $k_i > 0$, $0 \leq a_i \leq 1$ and in particular $b_i = 1$ for a lowpass filter. If the filter in the analog domain is stable, then by applying the generalized bilinear transformations, and satisfying the stability criteria, the digital filter

will also be stable. Alternatively, one can start with the CFE in the digital domain and invert it to obtain the discrete filter transfer function.

Consider the polynomial

$$D_a(s_1, s_2) = a_{00} + a_{10}s_1 + a_{01}s_2 + a_{11}s_1s_2 \tag{2.8}$$

which is a VSHP [5].

The corresponding reactance function is

$$G_a(s_1, s_2) = \frac{a_{11}s_1s_2 + a_{00}}{a_{10}s_1 + a_{01}s_2} \tag{2.9}$$

Using eqn.(2.9), the generalized expression of the Continued Fraction Expansion (CFE) can be written as

$$F(s_1, s_2) = \frac{a_{11}s_1s_2 + a_{00}}{a_{10}s_1 + a_{01}s_2} + \frac{1}{\frac{b_{11}s_1s_2+b_{00}}{b_{10}s_1+b_{01}s_2} + \frac{1}{\ldots}} \tag{2.10}$$

Inverting the above equation and restricting ourselves to the coefficients of a 's and b 's only, we get

$$F(s_1, s_2) = \frac{\left(\frac{a_{11}s_1s_2+a_{00}}{a_{10}s_1+a_{01}s_2}\right)\left(\frac{b_{11}s_1s_2+b_{00}}{b_{10}s_1+b_{01}s_2}\right) + 1}{\left(\frac{b_{11}s_1s_2+b_{00}}{b_{10}s_1+b_{01}s_2}\right)} \tag{2.11}$$

The resulting two-variable reactance function is given by

$$F(s_1, s_2) = \frac{P(s_1, s_2)}{Q(s_1, s_2)} \tag{2.12}$$

$$F(s_1, s_2) = \frac{\begin{array}{c} a_{11}b_{11}s_1^2s_2^2 + (a_{11}b_{00} + a_{00}b_{11} + a_{10}b_{01} + a_{01}b_{10})s_1s_2 \\ +a_{10}b_{10}s_1^2 + a_{01}b_{01}s_2^2 + a_{00}b_{00} \end{array}}{a_{10}b_{11}s_1^2s_2 + a_{01}b_{11}s_1s_2^2 + a_{10}b_{00}s_1 + a_{01}b_{00}s_2} \tag{2.13}$$

The analog filter transfer function is given by

$$H(s_1, s_2) = \frac{N(s_1, s_2)}{D(s_1, s_2)} \tag{2.14}$$

$$D(s_1, s_2) = P(s_1, s_2) + Q(s_1, s_2) \tag{2.15}$$

$$D(s_1, s_2) = s_1^2 \begin{bmatrix} a_{11}b_{11}s_2^2 \\ +a_{10}b_{11}s_2 \\ +a_{10}b_{10} \end{bmatrix} + s_1 \begin{bmatrix} a_{01}b_{11}s_2^2 + \\ \begin{pmatrix} a_{11}b_{00} + a_{00}b_{11} \\ +a_{10}b_{01} + a_{01}b_{10} \end{pmatrix} s_2 \\ +a_{10}b_{00} \end{bmatrix} + \begin{bmatrix} a_{01}b_{01}s_2^2 \\ +a_{01}b_{00}s_2 \\ +a_{00}b_{00} \end{bmatrix} \tag{2.16}$$

$$H(s_1, s_2) = \frac{A_0}{s_1^2 \begin{bmatrix} a_{11}b_{11}s_2^2 \\ +a_{10}b_{11}s_2 \\ +a_{10}b_{10} \end{bmatrix} + s_1 \begin{bmatrix} a_{01}b_{11}s_2^2 + \\ \begin{pmatrix} a_{11}b_{00} + a_{00}b_{11} \\ +a_{10}b_{01} + a_{01}b_{10} \end{pmatrix} s_2 \\ +a_{10}b_{00} \end{bmatrix} + \begin{bmatrix} a_{01}b_{01}s_2^2 \\ +a_{01}b_{00}s_2 \\ +a_{00}b_{00} \end{bmatrix}} \tag{2.17}$$

Since the stability of the filter is defined by the denominator of the transfer function, we have taken the numerator of the transfer function in eqn.(2.14) as a constant A_0. To define the stability of the filter, we have to make the filter's transfer function free from singularities of the first and the second kind (Sec.1.2). Therefore, we should prove the denominator polynomial to be a VSHP [5]. If we simplify the denominator polynomial i.e., eqn.(2.16), it can be readily verified that the denominator polynomial is a Strictly Hurwitz Polynomial

(SHP) [5]. Further, based on the test methodology to check for VSHP [5], we get,

$$D(s_1, s_2) = D\left(\tfrac{1}{s_1}, s_2\right) = D\left(s_1, \tfrac{1}{s_2}\right) = D\left(\tfrac{1}{s_1}, \tfrac{1}{s_2}\right) \neq \tfrac{0}{0} \tag{2.18}$$

where $s_1 = 0$ and $s_2 = 0$.

Since the non-essential singularities of the first and the second kind are ruled out, we can conclude that the denominator polynomial, $D(s_1, s_2)$ is a VSHP. If we go into the discrete (z) domain (by applying analog to digital transformation, the generalized bilinear transformation), the transfer function so obtained will be stable.

The constant A_0 in the numerator of eqn.(2.17) is adjusted such that the amplitude at $\omega_1 = 0$ and $\omega_2 = 0$ shall be unity, i.e.,

$$|H_a(0,0)| = \left|\frac{A_0}{D_a(0,0)}\right| = 1 \tag{2.19}$$

Therefore, the value of the numerator constant, A_0 after simplifying eqn.(2.19) is $a_{00}b_{00}$.

The 2-D filter transfer function in the analog domain is

$$H(s_1, s_2) = \frac{a_{00}b_{00}}{s_1^2\begin{bmatrix} a_{11}b_{11}s_2^2 \\ +a_{10}b_{11}s_2 \\ +a_{10}b_{10} \end{bmatrix} + s_1\begin{bmatrix} a_{01}b_{11}s_2^2+ \\ \left(\begin{array}{c} a_{11}b_{00}+a_{00}b_{11} \\ +a_{10}b_{01}+a_{01}b_{10} \end{array}\right) \\ +a_{10}b_{00} \end{bmatrix} s_2 + \begin{bmatrix} a_{01}b_{01}s_2^2 \\ +a_{01}b_{00}s_2 \\ +a_{00}b_{00} \end{bmatrix}} \tag{2.20}$$

Applying the generalized bilinear transformation [6],

$$s_1 \rightarrow k_1\frac{z_1 - a_1}{z_1 + b1} \tag{2.21}$$

$$s_2 \rightarrow k_2 \frac{z_2 - a_2}{z_2 + b_2} \tag{2.22}$$

where $k_1 > 0, k_2 > 0$, $0 \leq a_1 \leq 1$, $0 \leq a_2 \leq 1$ and $b_1 = b_2 = 1$ in particular to obtain a lowpass filter transfer function, to eqn.(2.20),

$$H(z_1, z_2) = \frac{a_{00}b_{00}(z_1 + b_1)^2(z_2 + b_2)^2}{\begin{array}{l} k_1^2(z_1 - a_1)^2 \left[\begin{array}{l} a_{11}b_{11}k_2^2(z_2 - a_2)^2 \\ +a_{10}b_{11}k_2(z_2 - a_2)(z_2 + b_2) \\ +a_{10}b_{10}(z_2 + b_2)^2 \end{array}\right] + \\ k_1(z_1 - a_1) \left[\begin{array}{l} a_{01}b_{11}k_2^2(z_2 - a_2)^2(z_1 + b_1) \\ +\left(\begin{array}{l} (a_{11}b_{00} + a_{00}b_{11} + a_{10}b_{01} + a_{01}b_{10})k_2 \\ (z_2 - a_2)(z_2 + b_2)(z_1 + b_1) \end{array}\right) \\ +a_{10}b_{00}(z_2 + b_2)^2(z_1 + b_1) \end{array}\right] + \\ \left[\begin{array}{l} a_{01}b_{01}k_2^2(z_2 - a_2)^2(z_1 + b_1)^2 \\ + a_{01}b_{00}k_2(z_2 - a_2)(z_2 + b_2)(z_1 + b_1)^2 + \\ a_{00}b_{00}(z_1 + b_1)^2(z_2 + b_2)^2 \end{array}\right] \end{array} \tag{2.23}$$

2.4 Classification of 2-D Low Pass Filters

The 2-D lowpass filters are classified into four sets and each set is further classified into four cases. The classification of the four sets is formed based on the coefficients of the CFE and the classification of the four cases involved in each set is based on the coefficients of the generalized bilinear transformation.

2.4.1 The four types of sets

The different sets are formed based on the coefficients of the transfer function, i.e., eqn.(2.20). In all the four sets, the values of b_1 and b_2 are set to 1 for a lowpass filter. The values of

a_1 and a_2 vary between 0 and 1 and the values of k_1 and k_2 are greater than 0 to obtain a stable filter.

In **set 1**, the values of all the coefficients of the CFE, i.e., eqn.(2.20) are the same, i.e

$$a_{00} = a_{01} = a_{10} = a_{11} = b_{00} = b_{01} = b_{10} = b_{11} \tag{2.24}$$

Different magnitude and contour plots are obtained by varying the values of a_1, a_2, k_1 and k_2.

In **set 2**, we have

$$\begin{aligned} a_{00} = a_{01} = a_{10} = a_{11} \\ b_{00} = b_{01} = b_{10} = b_{11} \end{aligned} \tag{2.25}$$

Different magnitude and contour plots are obtained by varying the values of a_1, a_2, k_1 and k_2.

In **set 3**, we have

$$\begin{aligned} a_{00} &= a_{11} \\ a_{01} &= a_{10} \\ b_{00} &= b_{11} \\ b_{01} &= b_{10} \end{aligned} \tag{2.26}$$

Different magnitude and contour plots are obtained by varying the values of a_1, a_2, k_1 and k_2 .

In **set 4**, we have

$$a_{00} \neq a_{01} \neq a_{10} \neq a_{11} \neq b_{00} \neq b_{01} \neq b_{10} \neq b_{11} \tag{2.27}$$

Different magnitude and contour plots are obtained by varying the values of a_1, a_2, k_1 and k_2.

2.4.2 The different cases involved in the 4 sets

There are four different cases involved in each set. The four cases are formed based on the coefficients of the generalized bilinear transformation, i.e., a_1, a_2, k_1 and k_2. In all the four cases the values of b_1 and b_2 are set to 1 in order that we design low pass filters. The contour responses of the low pass filter exhibit elliptical to circular nature based on the values of a_1, a_2, k_1 and k_2.

Case 1:

$a_1 = a_2 \quad , \quad k_1 \neq k_2 \quad , \quad b_1 = b_2 = 1$

Case 2:

$a_1 \neq a_2 \quad , \quad k_1 = k_2 \quad , \quad b_1 = b_2 = 1$

Case 3:

$a_1 \neq a_2 \quad , \quad k_1 \neq k_2 \quad , \quad b_1 = b_2 = 1$

Case 4:

$a_1 = a_2 \quad , \quad k_1 = k_2 \quad , \quad b_1 = b_2 = 1$

2.5 Frequency Responses of 2-D digital lowpass filter

The reactance function eqn.(2.9) obtained from the chosen VSHP polynomial eqn.(2.8) is applied to the generalized expression of CFE. The resultant transfer function eqn.(2.20) obtained from the inversion of CFE is digitized by applying the generalized bilinear transformation, ie., eqn.(2.7). The eqn.(2.23) gives the transfer function of the 2-D digital low pass filter. To investigate the manner in which each coefficient of the generalized bilinear transformation affects the frequency response of the resulting 2-D low pass filter, we apply the four cases to each set of 2-D lowpass filter transfer function.

Let us consider the 2-D lowpass filter coefficients and the generalized bilinear transformation coefficients to be unity i.e., $a_1 = 1$, $a_2 = 1$, $b_1 = 1$, $b_2 = 1$, $k_1 = 1$, $k_2 = 1 \, and \, a_{00} = 1$, $a_{10} = 1$, $a_{01} = 1$, $a_{11} = 1$, $b_{00} = 1$, $b_{10} = 1$, $b_{01} = 1$, $b_{11} = 1$. Under

this condition, the 3-D amplitude-frequency response and contour plots of the 2-D digital lowpass filter are shown in Fig. 2.1.

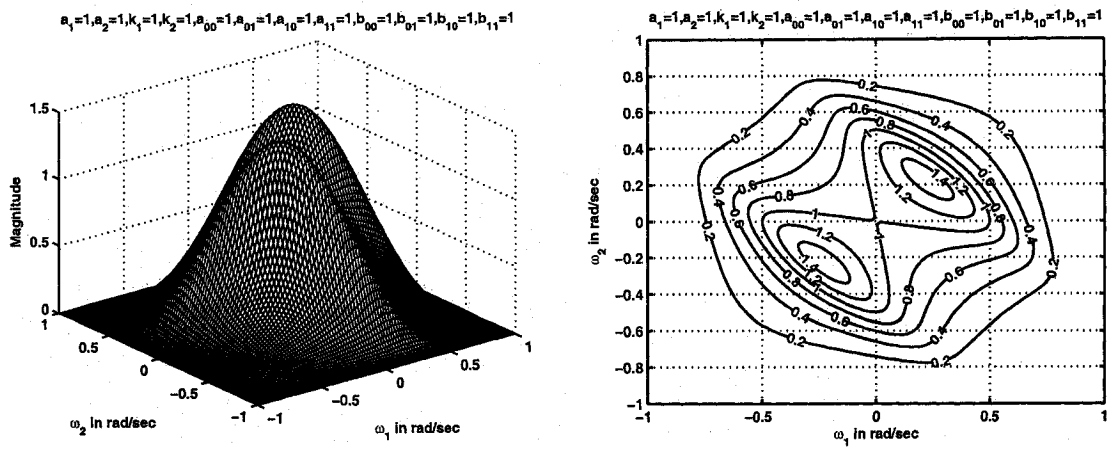

Figure 2.1: 3-D amplitude-frequency response and contour response of the 2-D digital lowpass filter when all the coefficients are unity

It is observed that there is a ripple in the passband at a lower frequency range. The ripple can be removed by reducing the values of a_1 and a_2 by a small fraction as will be later seen in Fig. 2.16 (a). It is important to note that a normalizing constant has to be added to normalize the frequency response. This has been adopted throughout the thesis.

2.5.1 Frequency responses of 2-D discrete lowpass filters in set 1

In this section, we study the manner in which all the four cases in set 1 affect the frequency response behavior of the resulting 2-D discrete low pass filter. In this set, the values of all the coefficients of the transfer function are considered to be the same i.e.,

$$a_{00} = a_{01} = a_{10} = a_{11} = b_{00} = b_{01} = b_{10} = b_{11}$$

Different contour plots are obtained by varying the values of a_1, a_2, k_1 and k_2.

In this set, it is observed in all the four cases that the coefficients k_1, k_2 affect the passband width and the coefficients a_1, a_2 affect the gain of the amplitude-frequency re-

sponse. As k_1 and k_2 values are increased, the passband width of the 2-D lowpass filter decreases and the amplitude of the contour response also decreases. As a_1 and a_2 values are increased, the magnitude of the amplitude-frequency response of the 2-D lowpass filter increases and the passband width decreases. Overall, the passband width decreases when k_1, k_2, a_1 and a_2 values are increased.

Also, when the values of k_1, $k_2 \geq 1$, it can be observed in all the four cases that the contour responses are more elliptical in nature and they are close to circular in nature for further greater values of k_1 and k_2. In this set, there are ripples in the contour response for smaller values of k_1 and k_2 and for larger values of a_1 and a_2.

2.5.1.1 Case 1:

In this case,

$$a_1 = a_2 \quad , \quad k_1 \neq k_2 \quad , \quad b_1 = b_2 = 1$$

As discussed above, the coefficients k_1, k_2 affect the passband width of the frequency response. In Fig. 2.2 (a), (b), (c) and Fig.2.3 (a), (b), there is a gradual decrease in the passband width as the values of k_1, k_2 are increased from 0.25, 0.5 to 8, 10 respectively for the same value of $a_1 = a_2 = 0.25$. At the same time, there is also a decrease in the amplitude from 0.7 to 0.0035 for the same. When the values of k_1 and k_2 are 2 and 10 respectively, the contour response is elliptical in nature which becomes close to circular symmetry when the values of k_1 and k_2 are increased to 8 and 10 respectively as seen in Fig. 2.3 (a), (b).

The coefficients a_1, a_2 affect the amplitude of the frequency response. In Fig. 2.2 (a), Fig. 2.3 (c) and Fig. 2.5 (a), it can be clearly noticed that the amplitude of the contour response increases from 0.7 to 1.1 when the values of a_1, a_2 are increased from 0.25 to 0.75 for the same values of k_1 = 0.25, k_2 = 0.5. Also, it can be seen that there are ripples in

the passband when $a_1 = a_2 \geq 0.5$ and when one of k_1, k_2 values is less than 0.5.

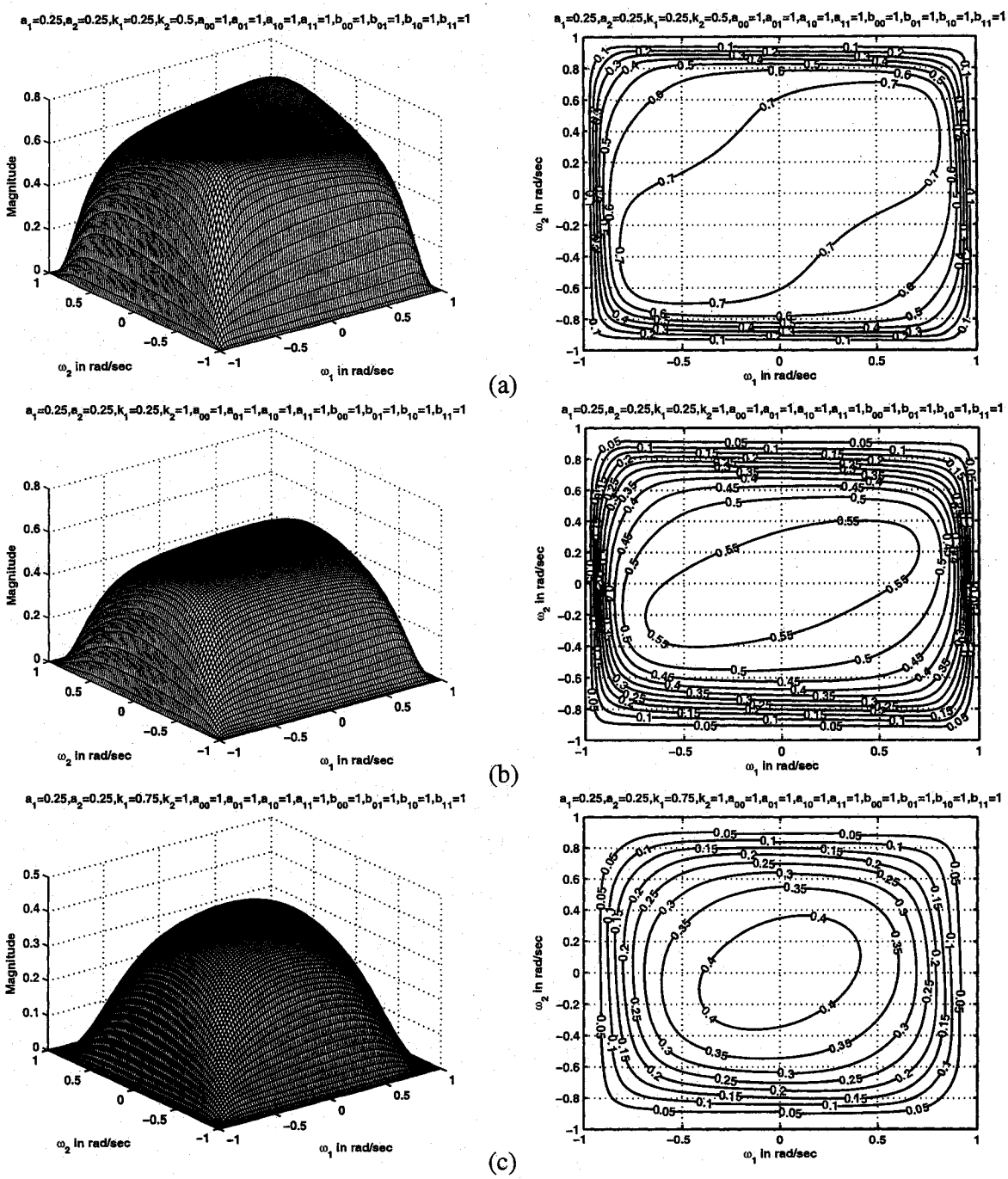

Figure 2.2: 3-D amplitude-frequency response and contour response of the 2-D digital lowpass filter in case 1 of set 1 (when $a_1 = a_2 = 0.25$)

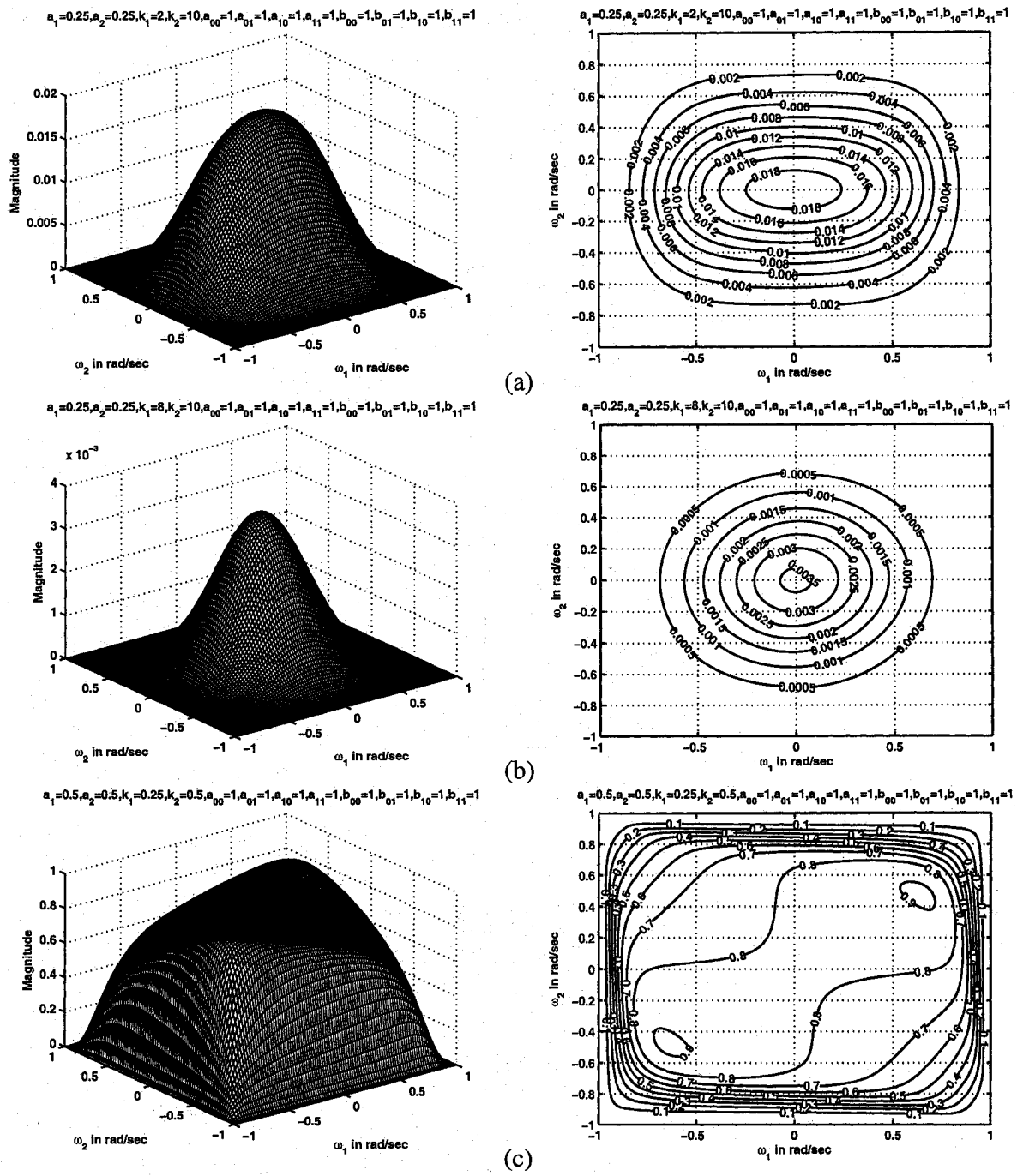

Figure 2.3: 3-D amplitude-frequency response and contour response of the 2-D digital lowpass filter in case 1 of set 1 (when $a_1 = a_2 = 0.25,\ 0.5$)

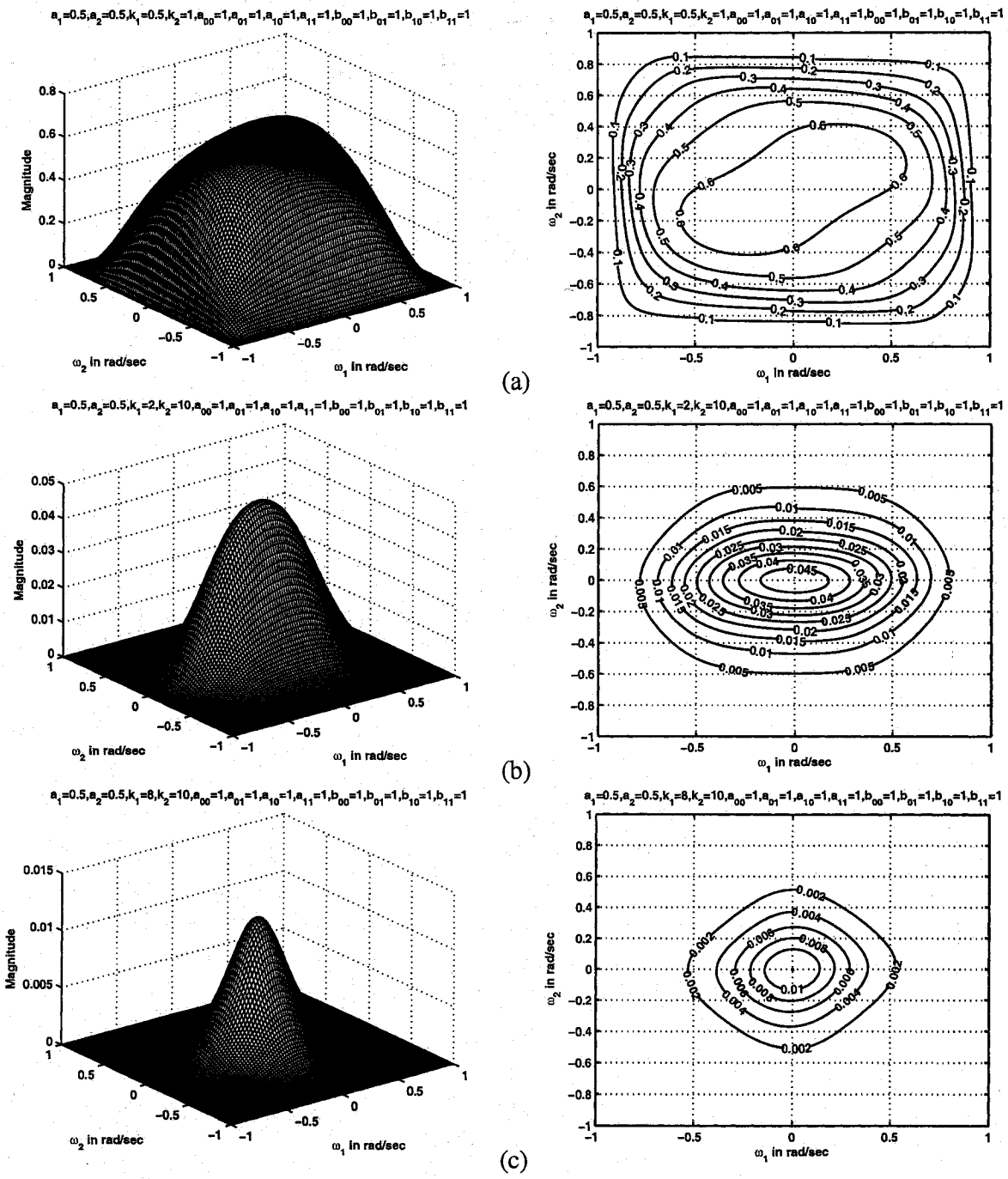

Figure 2.4: 3-D amplitude-frequency response and contour response of the 2-D digital lowpass filter in case 1 of set 1 (when $a_1 = a_2 = 0.5$)

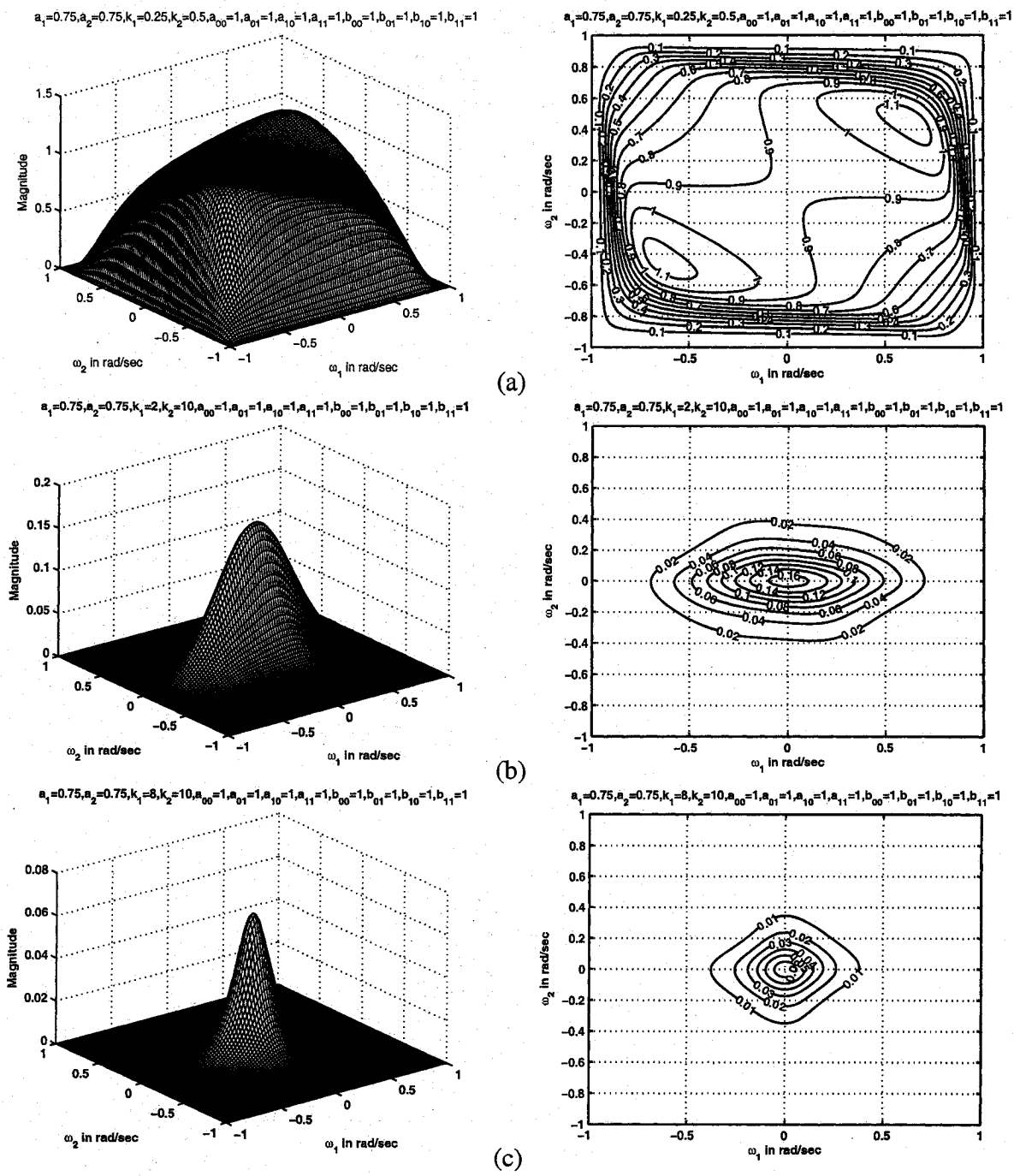

Figure 2.5: 3-D amplitude-frequency response and contour response of the 2-D digital lowpass filter in case 1 of set 1 (when $a_1 = a_2 = 0.75$)

2.5.1.2 Case 2:

In this case,

$$a_1 \neq a_2 \quad , \quad k_1 = k_2 \quad , \quad b_1 = b_2 = 1$$

The coefficients k_1, k_2 affect the passband width of the frequency response. In Fig. 2.6 (c), Fig. 2.7 (c), Fig. 2.8 (c) and Fig. 2.9 (c), there is a decrease in the passband width as the values of k_1, k_2 are increased from 0.5 to 5 for different values of a_1 and a_2. At the same time, there is also a gradual decrease in the amplitude of the frequency response from 1 to 0.25 for the same.

The coefficients a_1 and a_2 affect the amplitude of the frequency response. In Fig. 2.8 (a), (b) and (c), it can be clearly noticed that the amplitude of the contour response increases from 0.4 to 0.8 when the values of a_1, a_2 are increased from 0.25, 0.5 to 0.5, 1 respectively. There are ripples in the contour response for all values of a_1 and a_2 till $k_1 = k_2 \leq 0.75$. When $k_1 = k_2 > 0.75$, ripples in the contour response occur only when both the values of a_1 and a_2 are greater than 0.5. Though there are no ripples in the contour response when the values of $k_1 = k_2 \gg 1$, the contour responses start to lose their elliptical nature for values of a_1 and a_2 greater than 0.5. In Fig. 2.9 (c), when $k_1 = k_2 = 5$, there are no ripples in the contour response when $a_1 = 0.5$ and $a_2 = 1$, but the contour response slightly loses its elliptical nature.

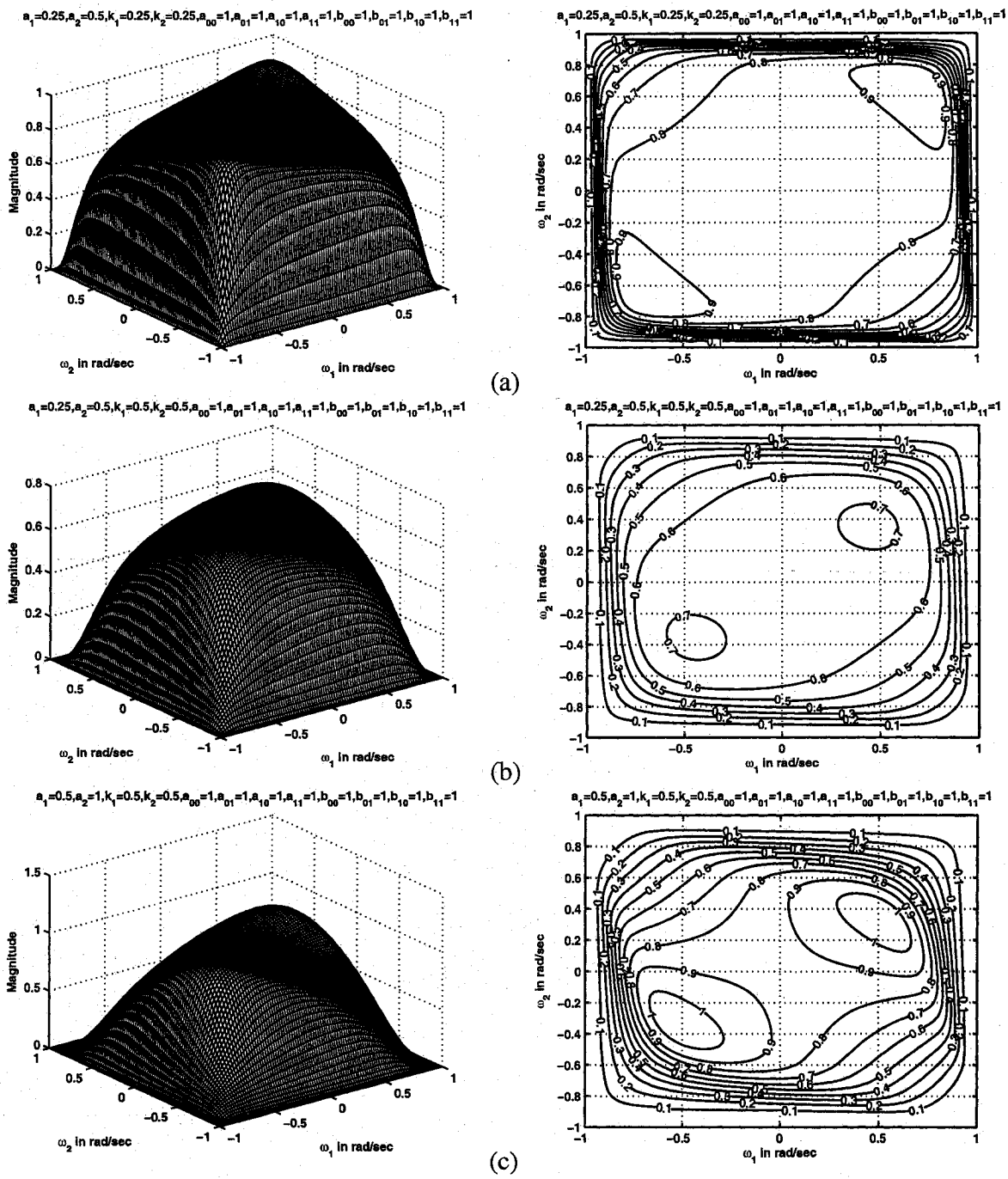

Figure 2.6: 3-D amplitude-frequency response and contour response of the 2-D digital lowpass filter in case 2 of set 1 (when $k_1 = k_2 = 0.25,\ 0.5$)

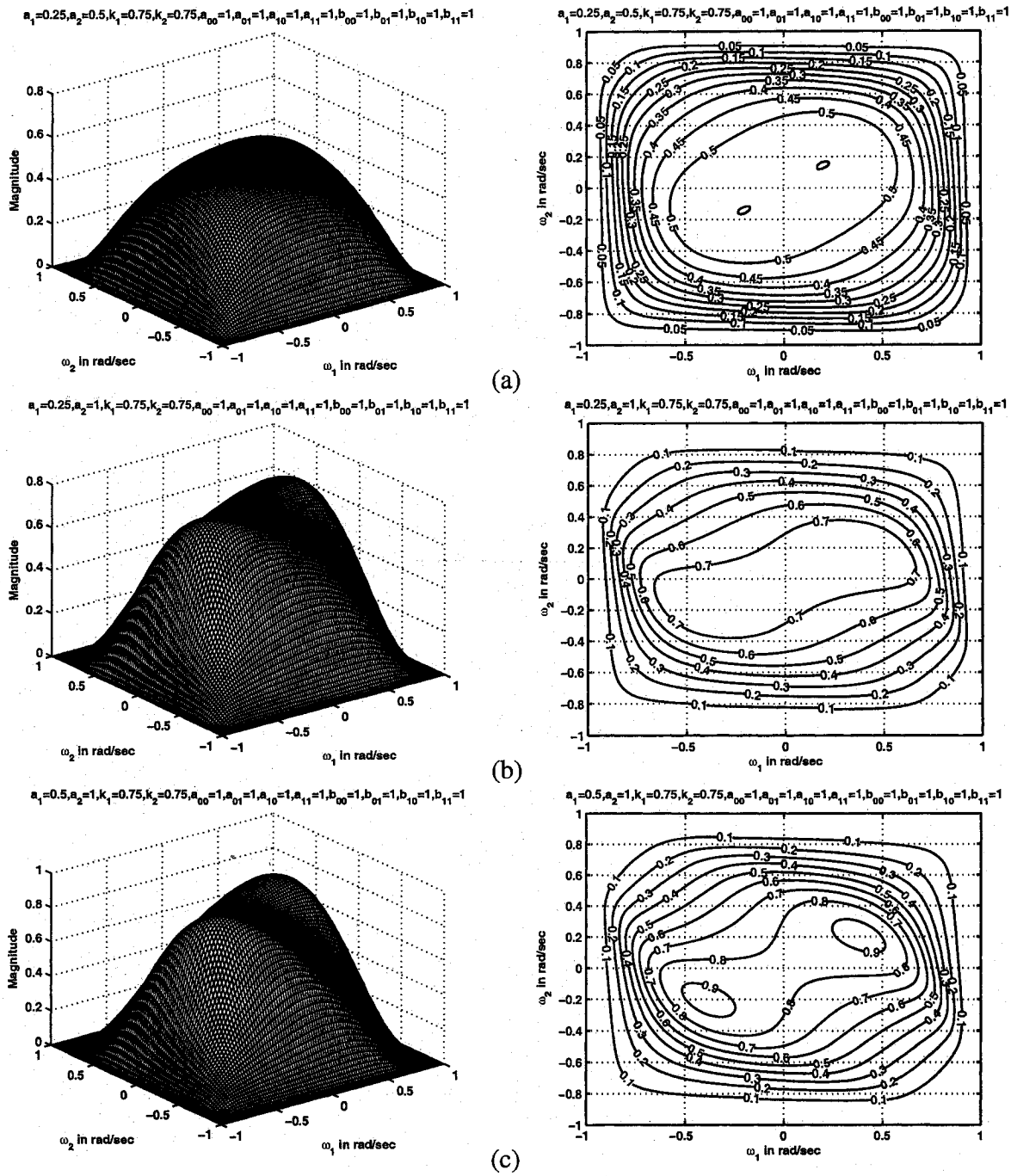

Figure 2.7: 3-D amplitude-frequency response and contour response of the 2-D digital lowpass filter in case 2 of set 1 (when $k_1 = k_2 = 0.75$)

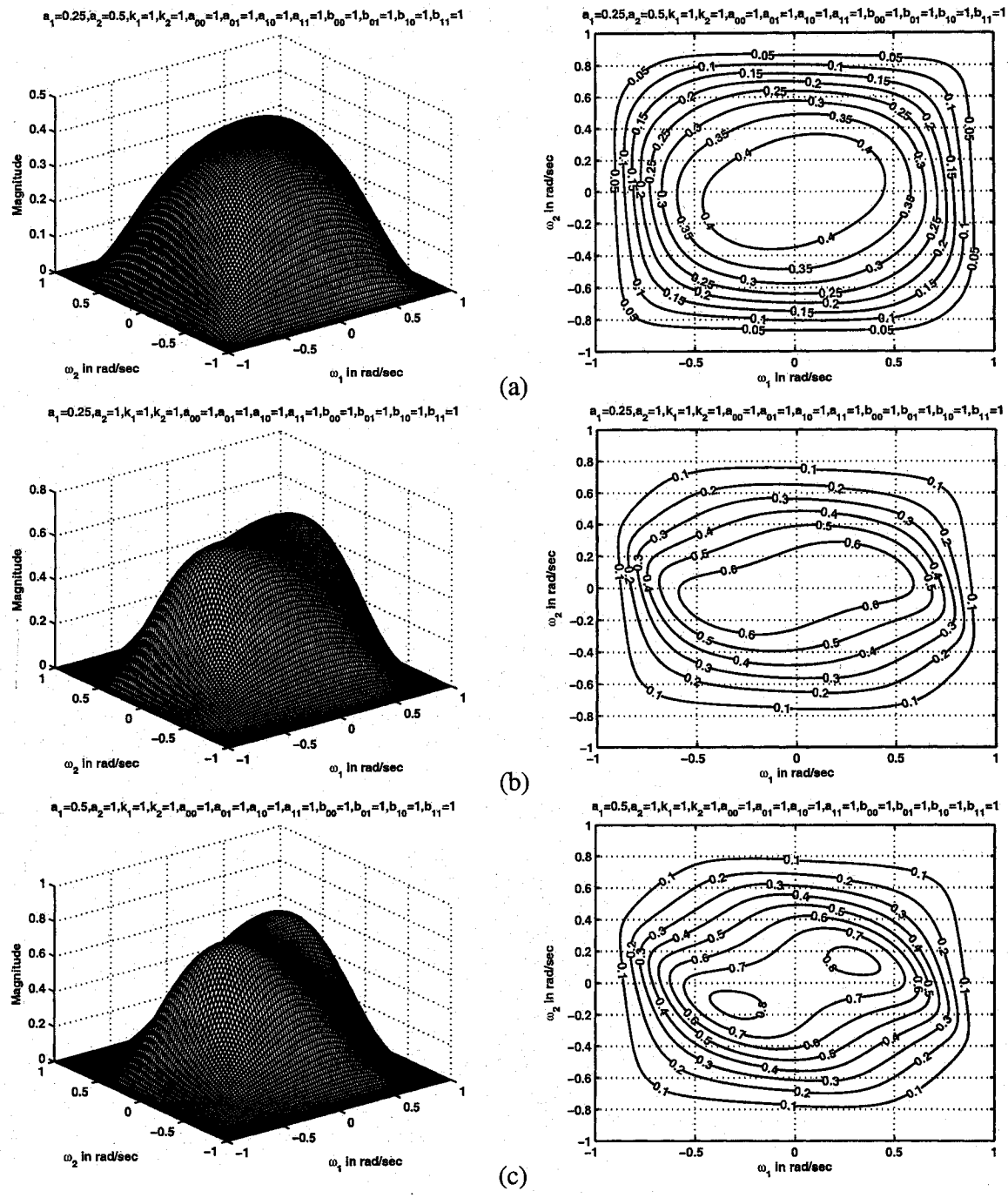

Figure 2.8: 3-D amplitude-frequency response and contour response of the 2-D digital lowpass filter in case 2 of set 1 (when $k_1 = k_2 = 1$)

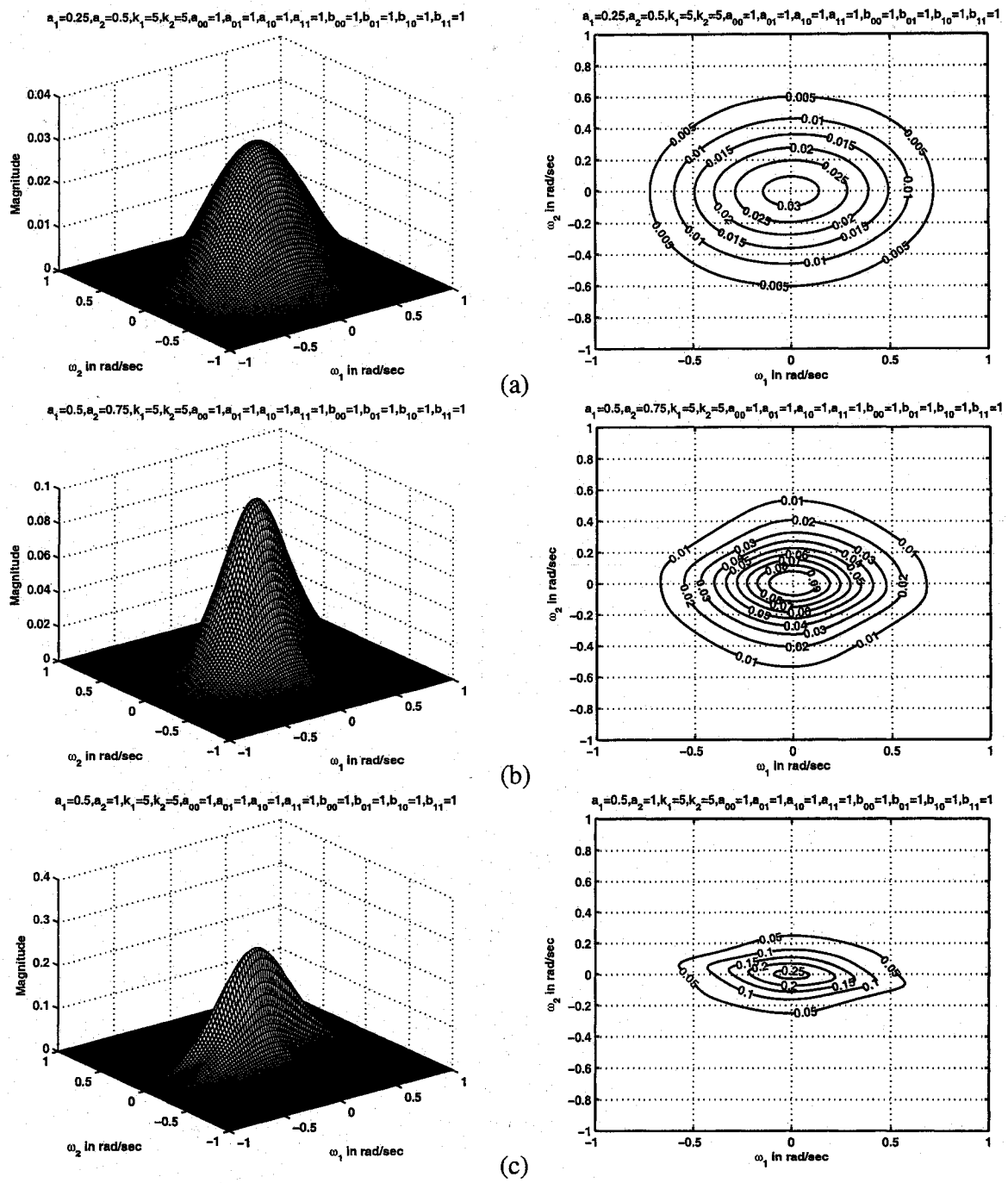

Figure 2.9: 3-D amplitude-frequency response and contour response of the 2-D digital lowpass filter in case 2 of set 1 (when $k_1 = k_2 = 5$)

2.5.1.3 Case 3:

In this case,

$$a_1 \neq a_2 \quad , \quad k_1 \neq k_2 \quad , \quad b_1 = b_2 = 1$$

The coefficients k_1 and k_2 affect the passband width of the frequency response. For example, in Fig. 2.10 (a), (b), (c) and Fig. 2.11 (a), there is a gradual decrease in the passband width as the values of k_1 and k_2 are increased from 0.25, 0.5 to 8, 10 respectively for values of a_1 and a_2 to be 0.25 and 0.5 respectively. At the same time, there is also a gradual decrease in the amplitude from 0.8 to 0.006 for the same.

The coefficients a_1 and a_2 affect the amplitude of the frequency response. In Fig. 2.10 (a), Fig. 2.11 (b) and Fig. 2.12 (c), it can be clearly noticed that the amplitude of the contour response increases from 0.8 to 1.2 when the values of a_1, a_2 are increased from 0.25, 0.5 to 0.75, 0.9 respectively for the same values of $k_1 = 0.25$ and $k_2 = 0.5$. In this case, as $a_1 \neq a_2$ and $k_1 \neq k_2$, ripples in the contour response occur when one of the a_1, a_2 is greater than 0.5 or when one of the k_1, k_2 values is ≤ 0.5. The ripples in the contour response increases as the values of a_1 and a_2 increases as seen in Fig. 2.10 (a), Fig. 2.11 (b) and Fig. 2.12 (c). Though there are no ripples in the contour response when the values of $k_1 = k_2 \gg 1$, the contour responses start to lose their elliptical nature for values of a_1 and a_2 greater than 0.5 as shown in Fig. 2.13 (b), (c).

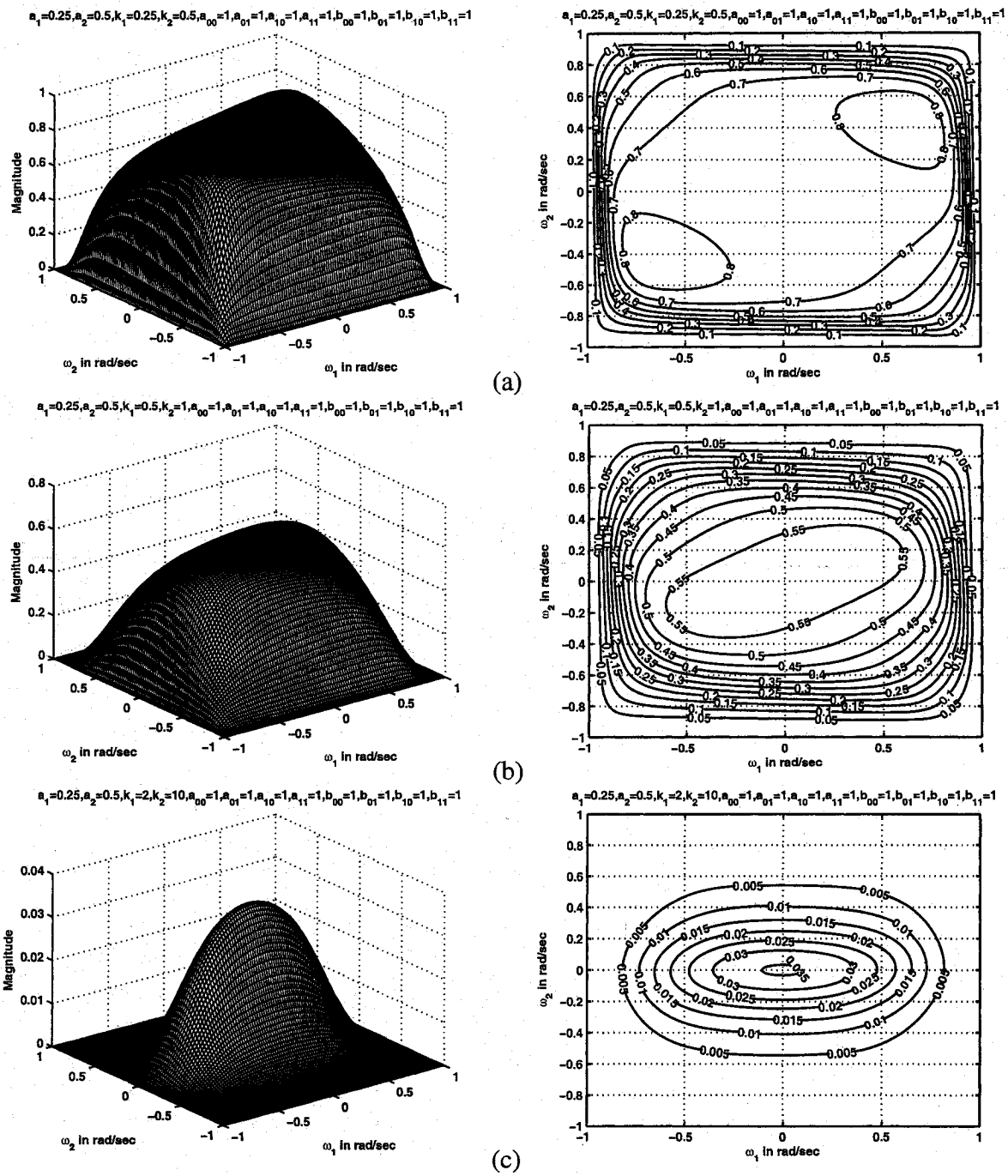

Figure 2.10: 3-D amplitude-frequency response and contour response of the 2-D digital lowpass filter in case 3 of set 1 (when $a_1 = 0.25$, $a_2 = 0.5$)

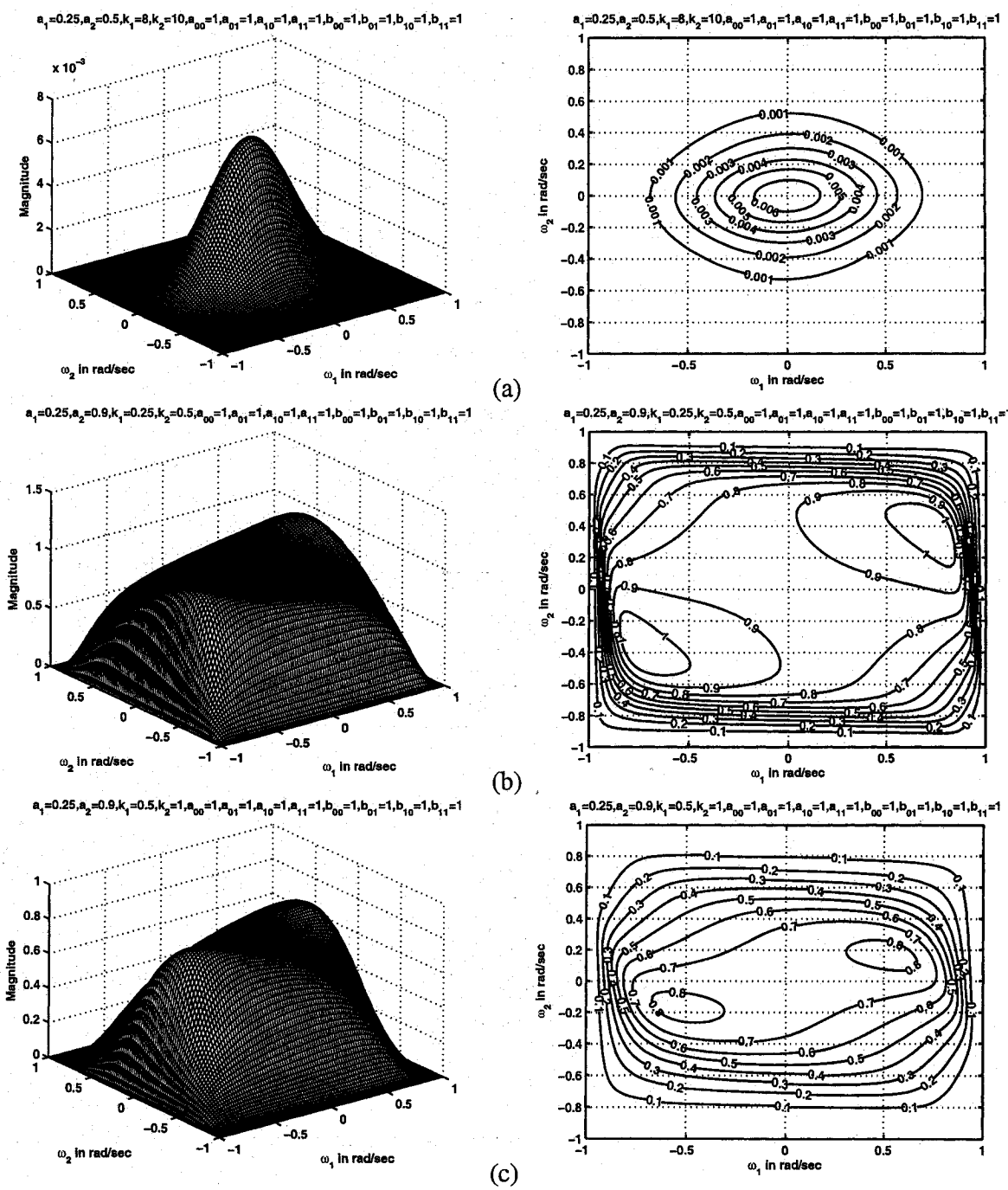

Figure 2.11: 3-D amplitude-frequency response and contour response of the 2-D digital lowpass filter in case 3 of set 1 (when $a_1 = 0.25$, $a_2 = 0.5$, 0.9)

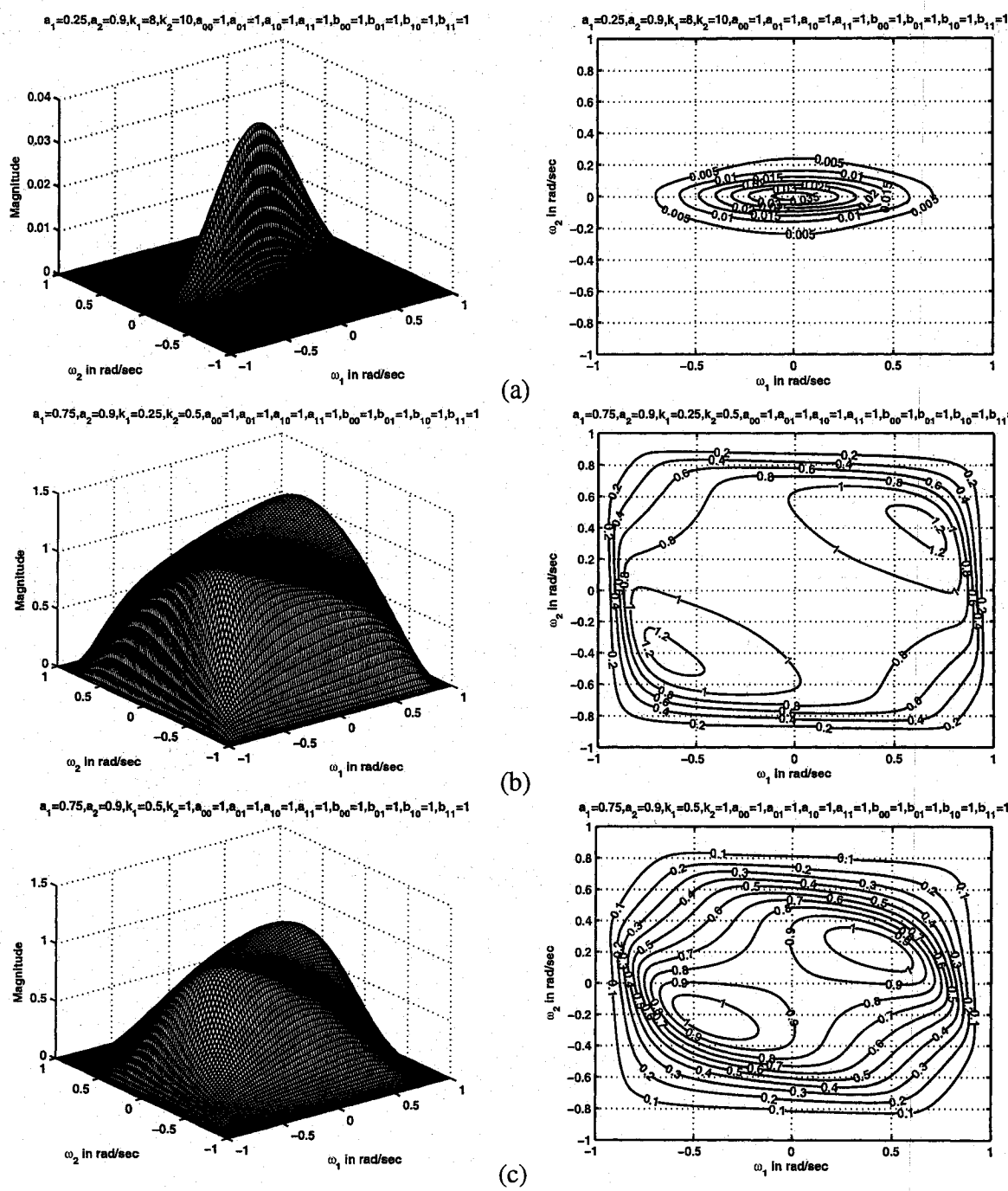

Figure 2.12: 3-D amplitude-frequency response and contour response of the 2-D digital lowpass filter in case 3 of set 1 (when $a_1 = 0.25,\ 0.75,\ a_2 = 0.9$)

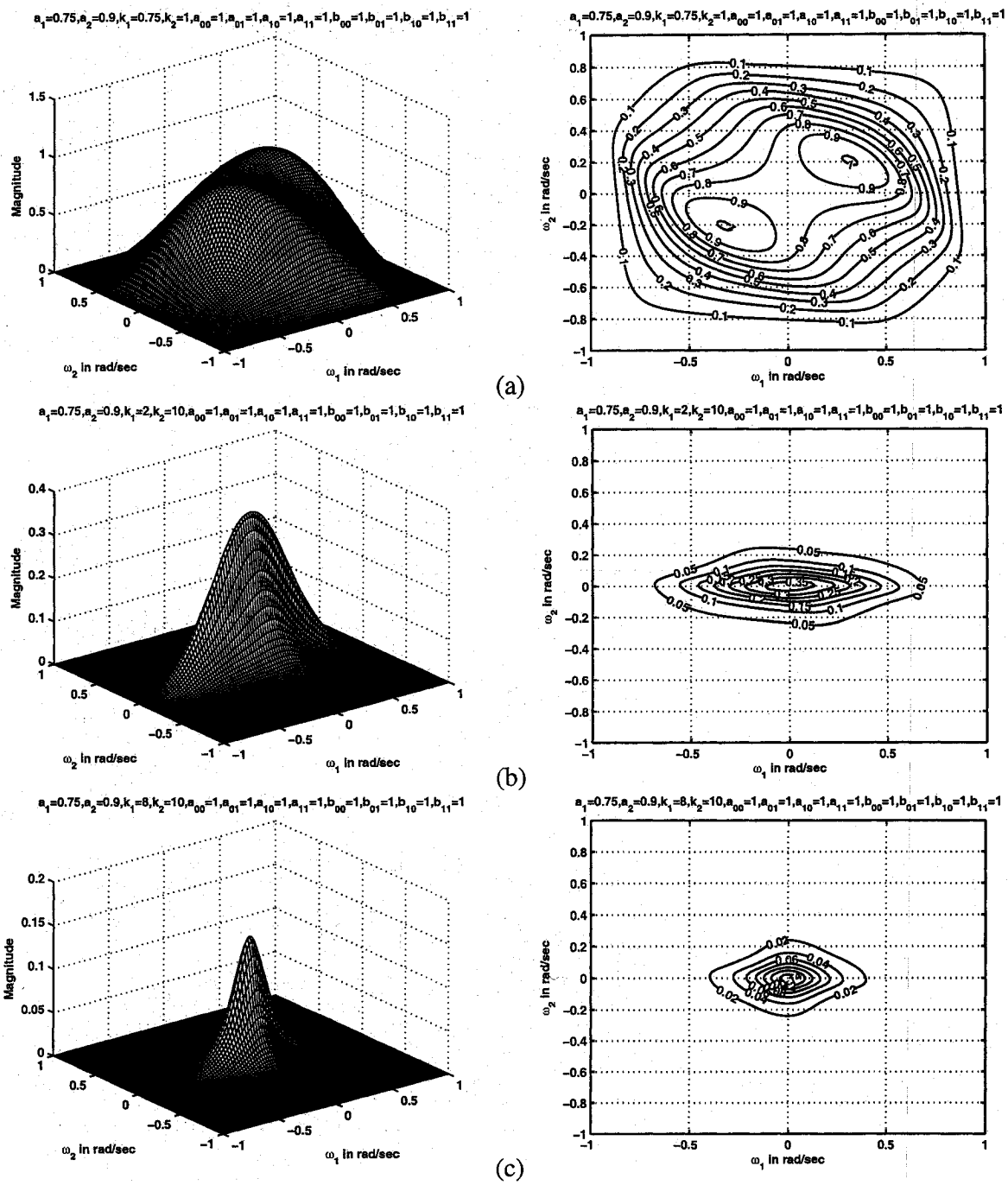

Figure 2.13: 3-D amplitude-frequency response and contour response of the 2-D digital lowpass filter in case 3 of set 1 (when $a_1 = 0.75$, $a_2 = 0.9$)

2.5.1.4 Case 4:

In this case,

$$a_1 = a_2 \quad , \quad k_1 = k_2 \quad , \quad b_1 = b_2 = 1$$

The coefficients k_1 and k_2 affect the passband width of the frequency response. In Fig. 2.14 (a), (c) and Fig. 2.15 (b), Fig. 2.16 (b), there is a decrease in the passband width of the contour response as the values of k_1 and k_2 are increased from 0.25 to 5 for the same values of $a_1 = a_2 = 0.25$. In addition, there is also a gradual decrease in the amplitude from 0.9 to 0.018 for the same.

The coefficients a_1 and a_2 affect the amplitude of the frequency response as seen in Fig. 2.15 (b), (c) and Fig. 2.16 (a) and it can be clearly noticed that the amplitude of the contour response increases from 0.35 to 0.7 when the values of a_1, a_2 are increased from 0.25 to 0.75. There is also a decrease in the passband width of the contour response for the same.

When the values of k_1, $k_2 > 1$, the contour responses are nearly circular in nature as seen in Fig. 2.16 (b). There are ripples in the contour response for values of a_1 and a_2 greater than 0.5 and for values k_1 and k_2 less than 0.5 as shown in Fig. 2.14 (a), (b) and Fig. 2.15 (a). For very high values of k_1 and k_2, the passband width of the frequency response becomes very narrow as shown in Fig. 2.16 (c).

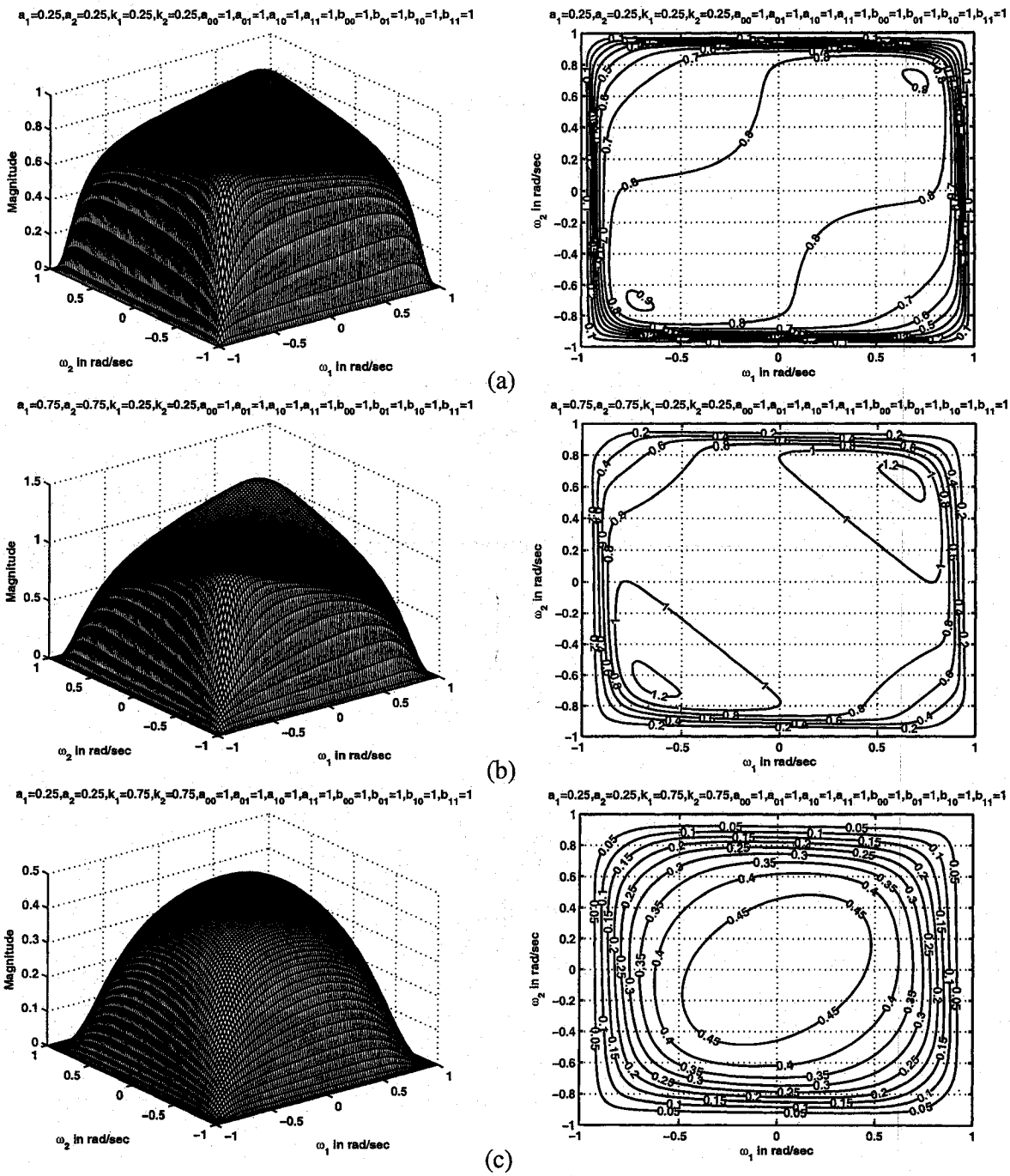

Figure 2.14: 3-D amplitude-frequency response and contour response of the 2-D digital lowpass filter in case 4 of set 1 (when $k_1 = k_2 = 0.25,\ 0.75$)

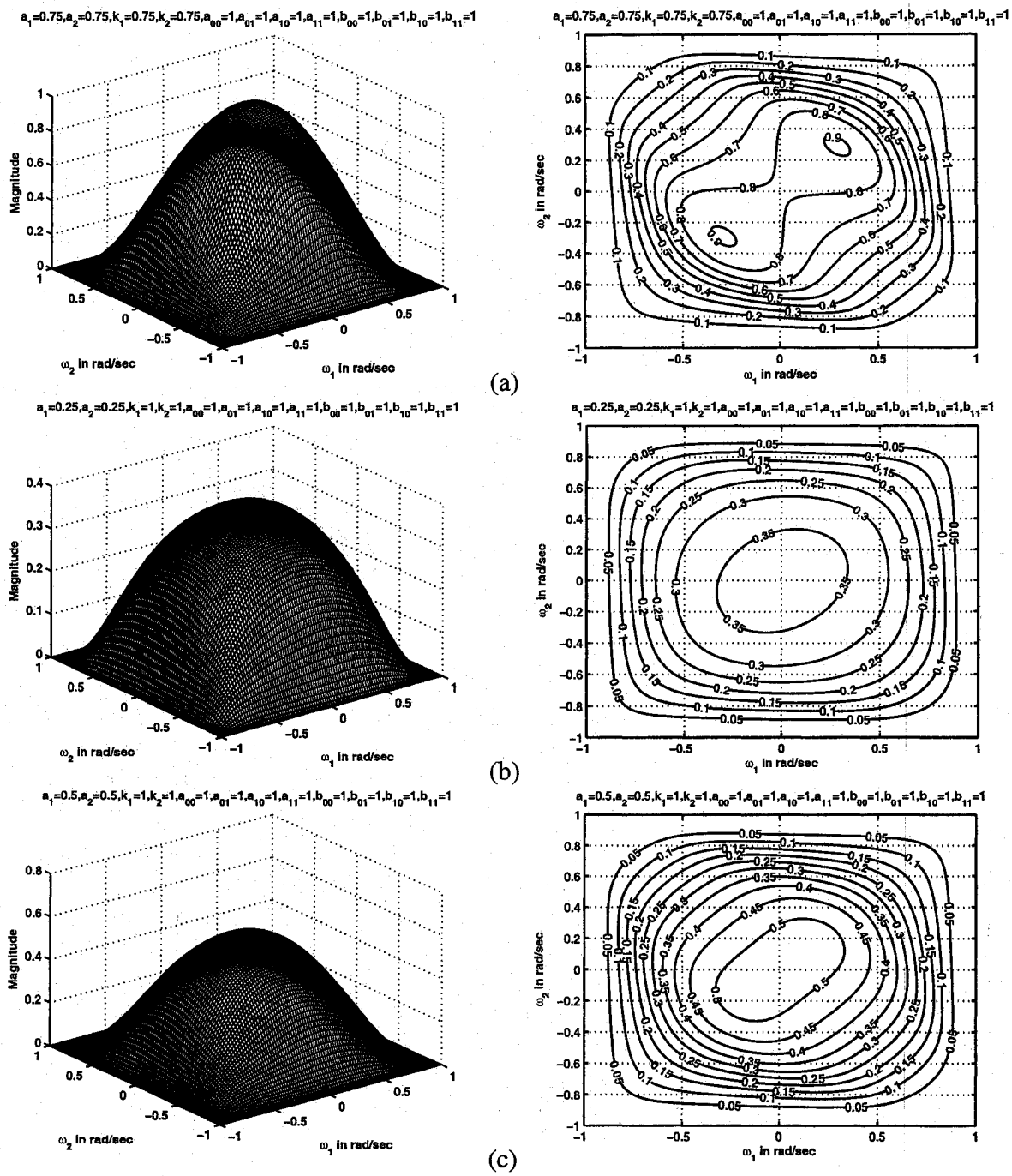

Figure 2.15: 3-D amplitude-frequency response and contour response of the 2-D digital lowpass filter in case 4 of set 1 (when $k_1 = k_2 = 0.75,\ 1$)

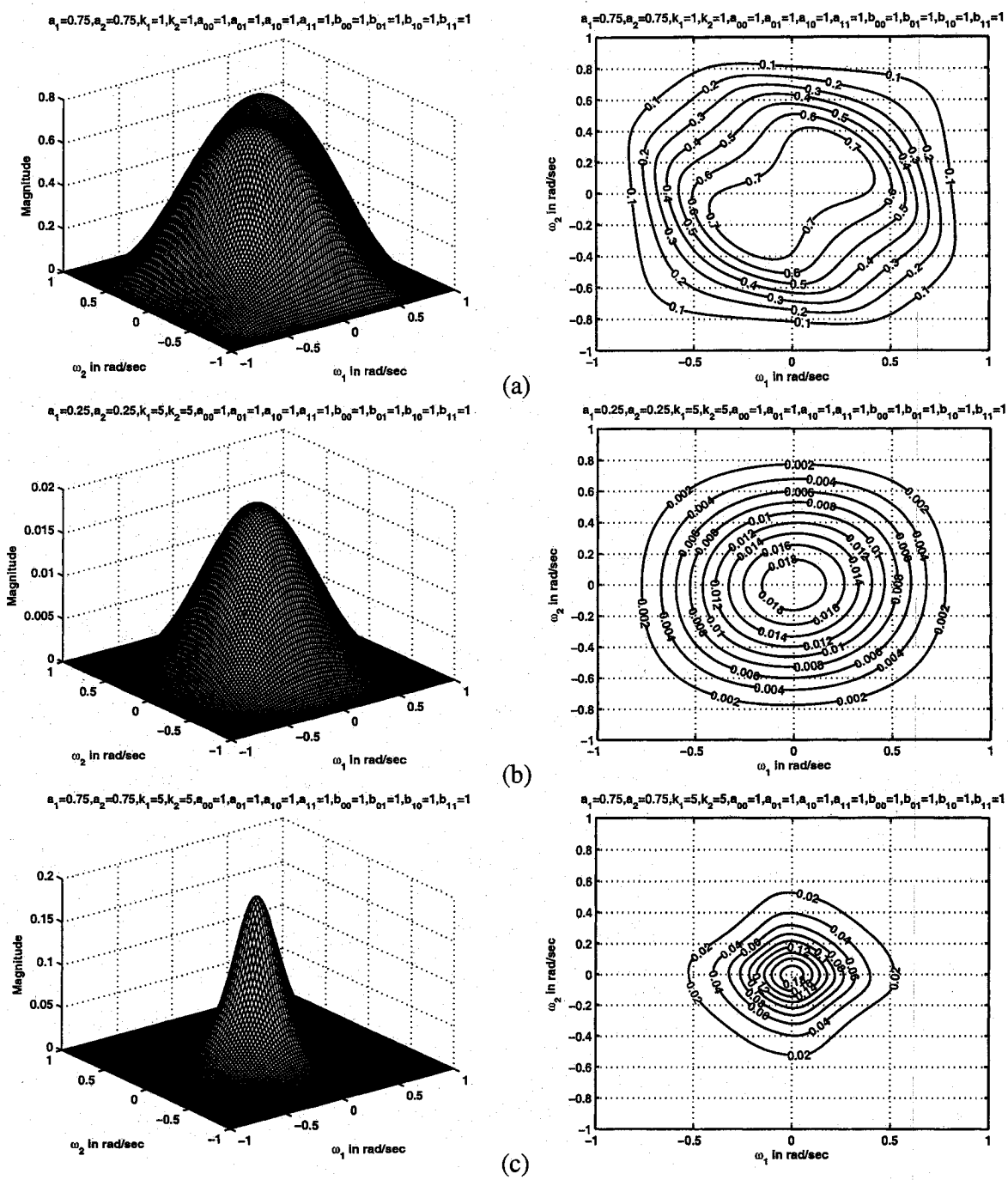

Figure 2.16: 3-D amplitude-frequency response and contour response of the 2-D digital lowpass filter in case 4 of set 1 (when $k_1 = k_2 = 1, 5$)

2.5.2 Frequency responses of 2-D discrete lowpass filters in set 2

In this set,

$$a_{00} = a_{01} = a_{10} = a_{11}$$
$$b_{00} = b_{01} = b_{10} = b_{11}$$

When the above combination of coefficients are substituted in eqn.(2.23), the resulting transfer function is the same as the one used in set 1, as the transfer function does not depend on the coefficients of the CFE. It only depends on the coefficients of the generalized bilinear transformation. Hence the 3-D amplitude and contour responses for set 2 is the same as that of set 1.

2.5.3 Frequency responses of 2-D discrete lowpass filters in set 3

In this section, we study the manner in which all the four cases in set 3 affect the frequency response behavior of the resulting 2-D discrete low pass filter. In this set,

$$a_{00} = a_{11}$$
$$a_{01} = a_{10}$$
$$b_{00} = b_{11}$$
$$b_{01} = b_{10}$$

Different contour plots are obtained by varying the values of a_1, a_2, k_1 *and* k_2.

Similar to set 1, in set 3, it is observed in all the four cases, the coefficients k_1 and k_2 affect the passband width. As k_1 and k_2 values are increased, the passband width decreases and the amplitude of the contour response also decreases. As a_1 and a_2 values are increased, the amplitude of the contour response increases and the passband width decreases. Overall, the passband width decreases when k_1, k_2, a_1 and a_2 values are increased.

It can be observed that there are not many contour responses with ripples in set 3 when

compared to set 1 except under few circumstances which shall be dealt later in this section. Also the amplitude of the contour response is low when compared to set 1 for the same values of k_1, k_2, a_1 and a_2. The frequency responses are more or less similar to set 1 for all values of a_1 and a_2 when k_1, $k_2 > 1$.

2.5.3.1 Case 1:

In this case,

$$a_1 = a_2 \ , \quad k_1 \neq k_2 \ , \quad b_1 = b_2 = 1$$

The coefficients k_1 and k_2 affect the passband width. As k_1 and k_2 values are increased, the passband width decreases and the amplitude of the contour response also decreases. As a_1 and a_2 values are increased, the amplitude of the contour response increases and also, the passband width decreases.

There are no ripples in the contour response for all values of k_1, k_2, a_1 and a_2. The amplitude of the contour response is lower than that of the contour response in case 1 of set 1 for the same values of k_1, k_2, a_1 and a_2. The amplitude of the contour response in Fig. 2.2 (a) of case 1 in set 1 is 0.7 whereas the amplitude for the same values in Fig. 2.17 (a) of set 3 is 0.5 for the same values of $a_1 = a_2 = 0.25$, $k_1 = 0.25$, $k_2 = 0.5$. The contour responses display a square nature for values of k_1, $k_2 < 0.5$. As the values of k_1, k_2 are increased, the contour response display an elliptical nature which gradually changes to nearly circular nature for further increase in the values of k_1, k_2. In Fig. 2.17 (a), (b) and (c) and Fig. 2.18 (a) and (b), the contour response changes from square to nearly circular when the the values of k_1, k_2 are increased from 0.25, 0.5 to 8, 10 respectively.

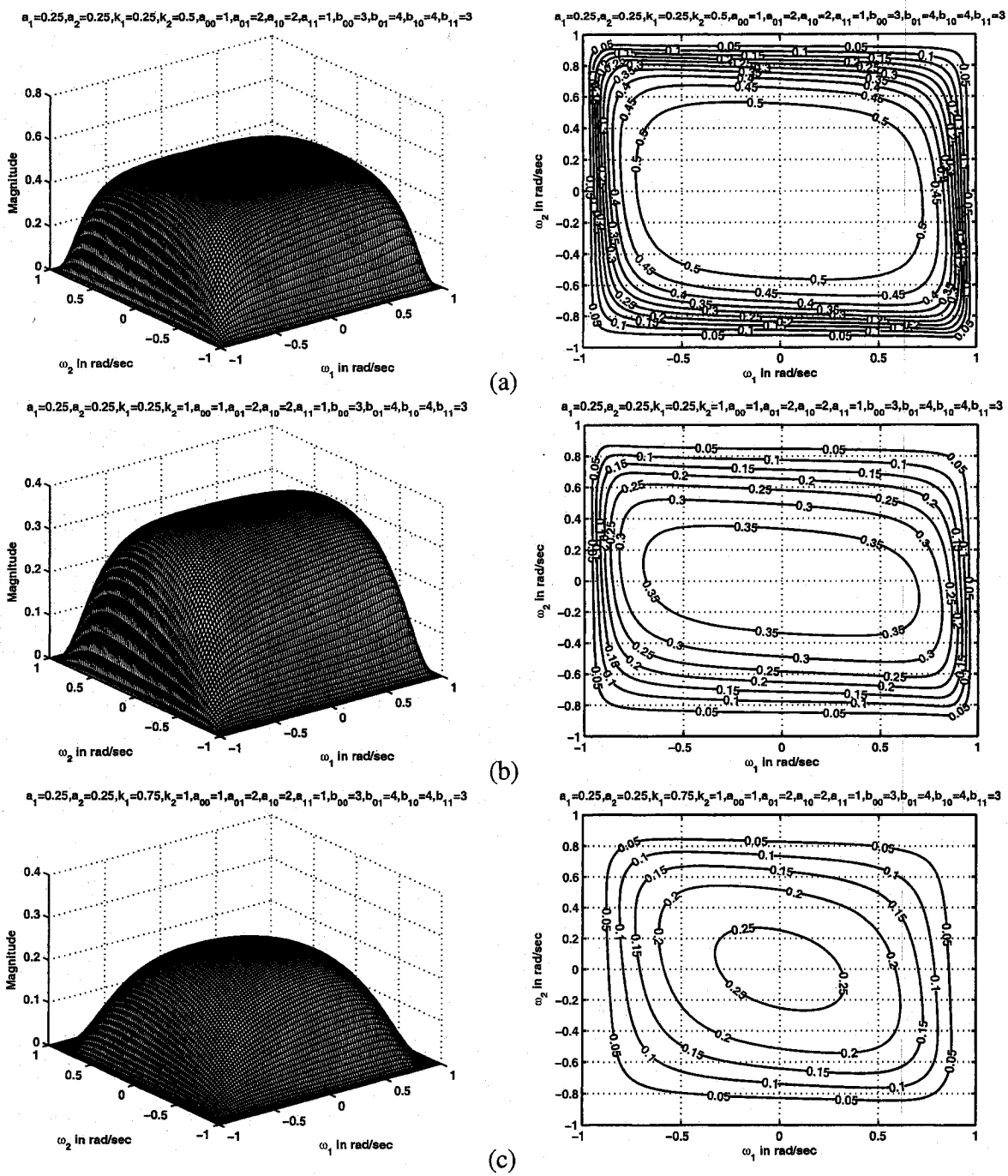

Figure 2.17: 3-D amplitude-frequency response and contour response of the 2-D digital lowpass filter in case 1 of set 3 (when $a_1 = a_2 = 0.25$)

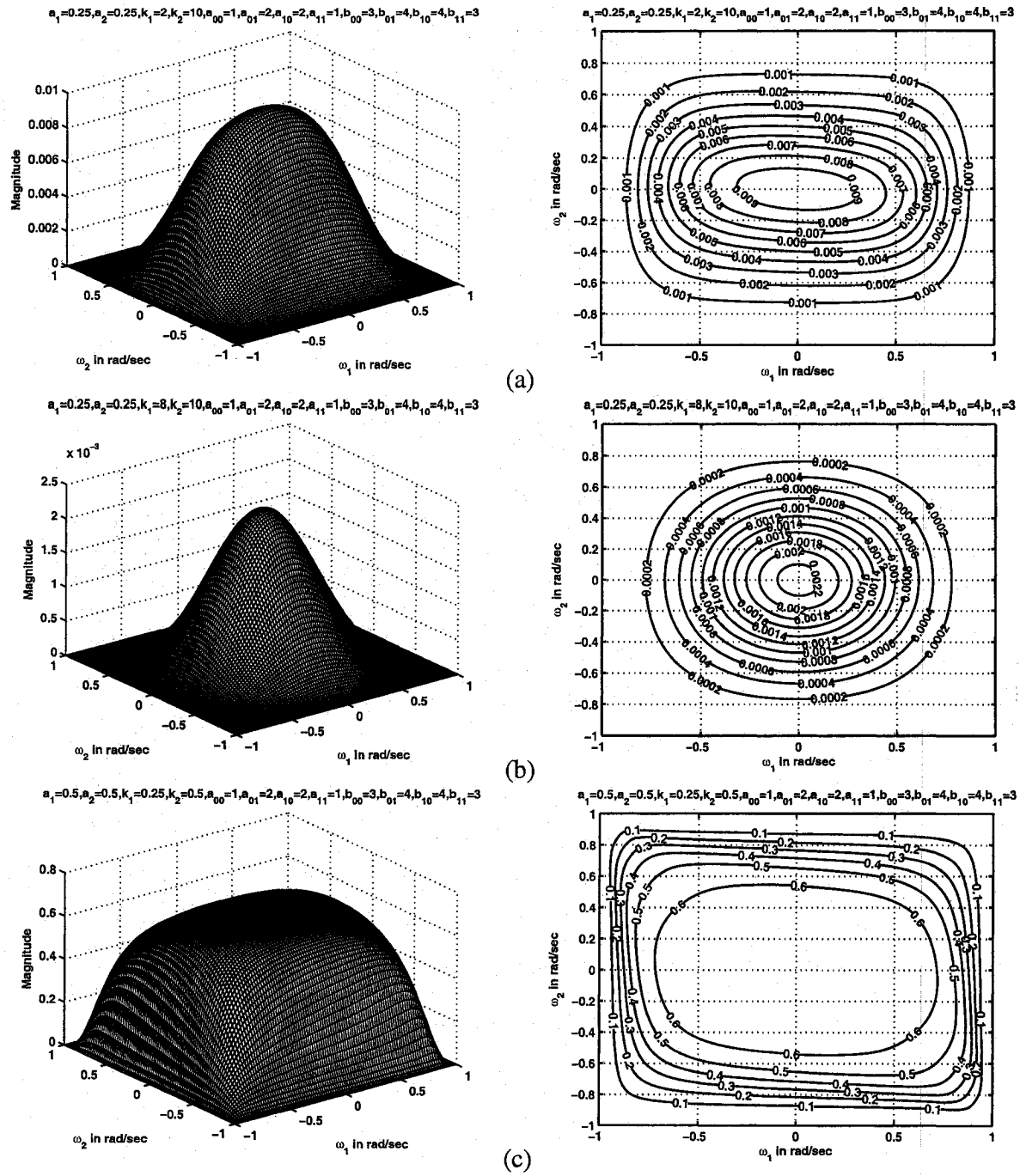

Figure 2.18: 3-D amplitude-frequency response and contour response of the 2-D digital lowpass filter in case 1 of set 3 (when $a_1 = a_2 = 0.25,\ 0.5$)

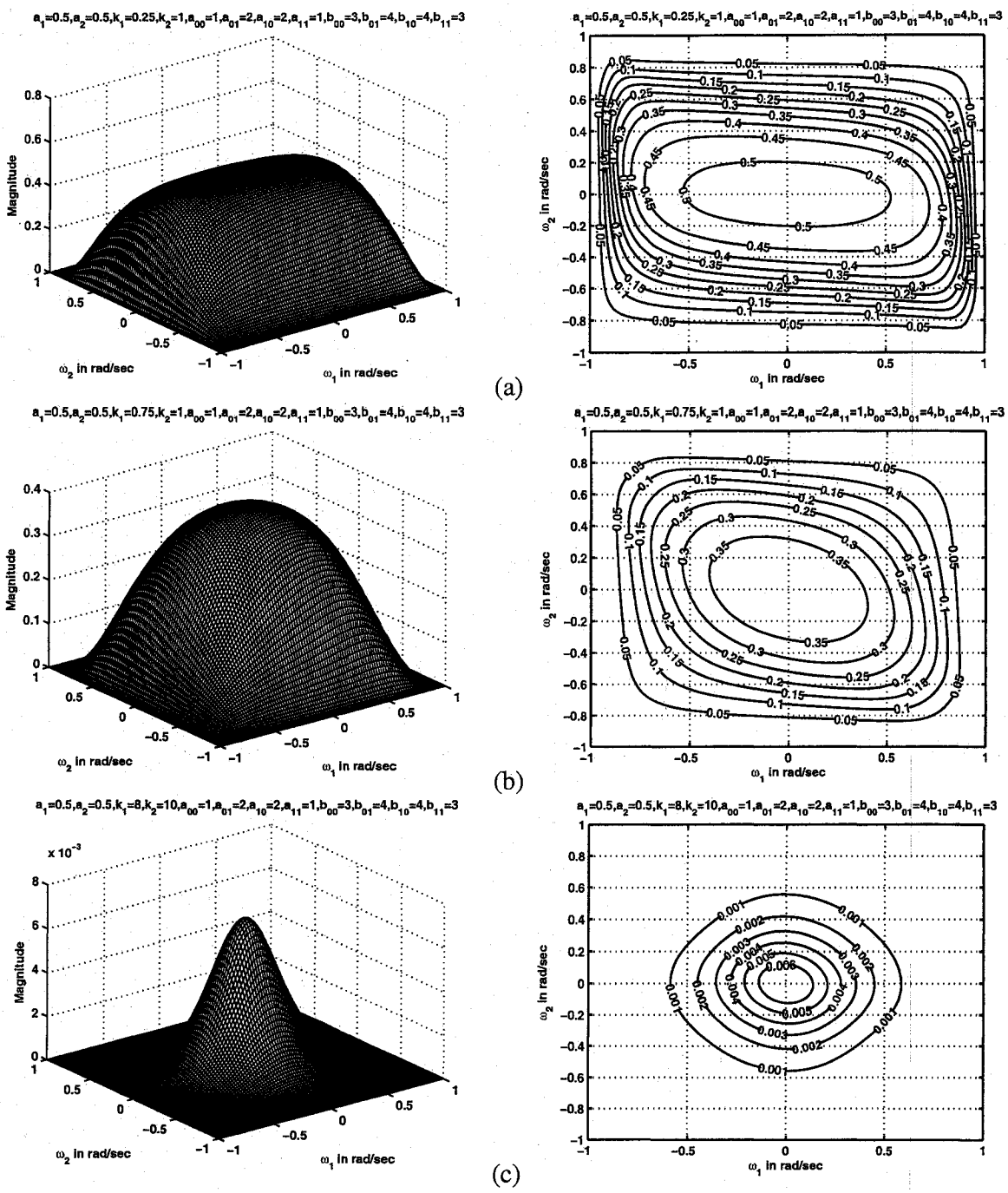

Figure 2.19: 3-D amplitude-frequency response and contour response of the 2-D digital lowpass filter in case 1 of set 3 (when $a_1 = a_2 = 0.5$)

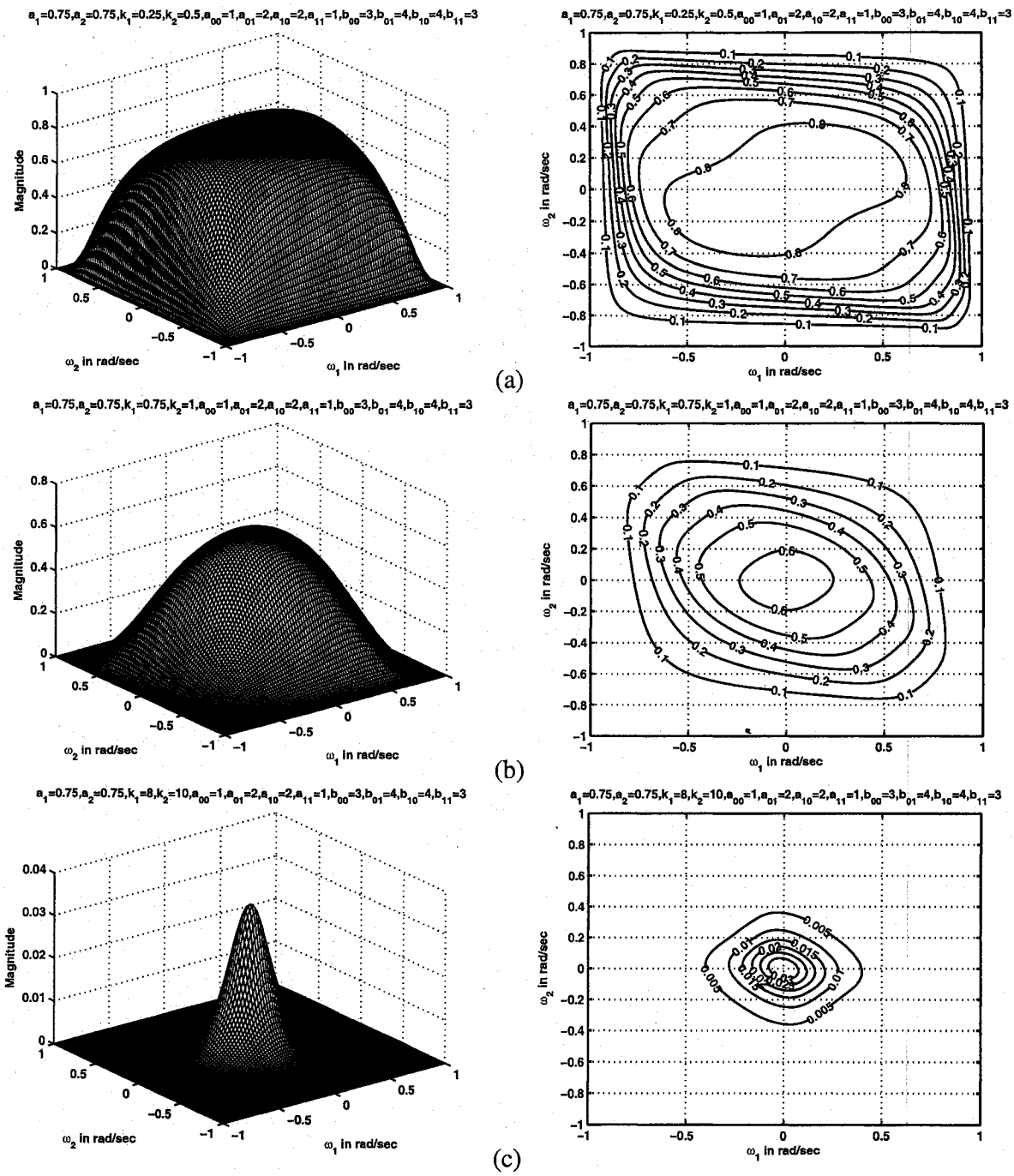

Figure 2.20: 3-D amplitude-frequency response and contour response of the 2-D digital lowpass filter in case 1 of set 3 (when $a_1 = a_2 = 0.75$)

2.5.3.2 Case 2:

In this case,

$$a_1 \neq a_2 \quad , \quad k_1 = k_2 \quad , \quad b_1 = b_2 = 1$$

As mentioned above, it is observed that the coefficients k_1 and k_2 affect the passband width. As k_1 and k_2 values are increased, the passband width decreases and the amplitude of the contour response also decreases. As a_1 and a_2 values are increased, the amplitude of the contour response increases and the passband width decreases. Overall, the passband width decreases when k_1, k_2, a_1 and a_2 values are increased.

There are ripples in the passband of the contour response when the values of k_1, k_2 are as low as 0.25 and for values of a_1, $a_2 \geq 0.5$ as seen in Fig. 2.21 (c). Also, it can be observed that the ripples in the passband occur when the values of $k_1 = k_2 = 0.5$ and for values of a_1, $a_2 \geq 0.75$ as seen in Fig. 2.22 (c). The amplitude of the contour response is lower than that of the contour response in case 2 of set 1 for the same values of k_1, k_2, a_1 and a_2. For example, the amplitude of the contour response in Fig. 2.6 (a) of case 2 in set 1 is 0.9 whereas the amplitude for the same values of $k_1 = k_2 = 0.25$ and $a_1 = 0.25$, $a_2 = 0.5$ in Fig. 2.21 (a) of set 3 is 0.7. The passband becomes very narrow for higher values of k_1 and k_2. As can be shown in Fig. 2.24 (b), when the values of $k_1 = k_2 = 10$, the frequency response has a very narrow passband.

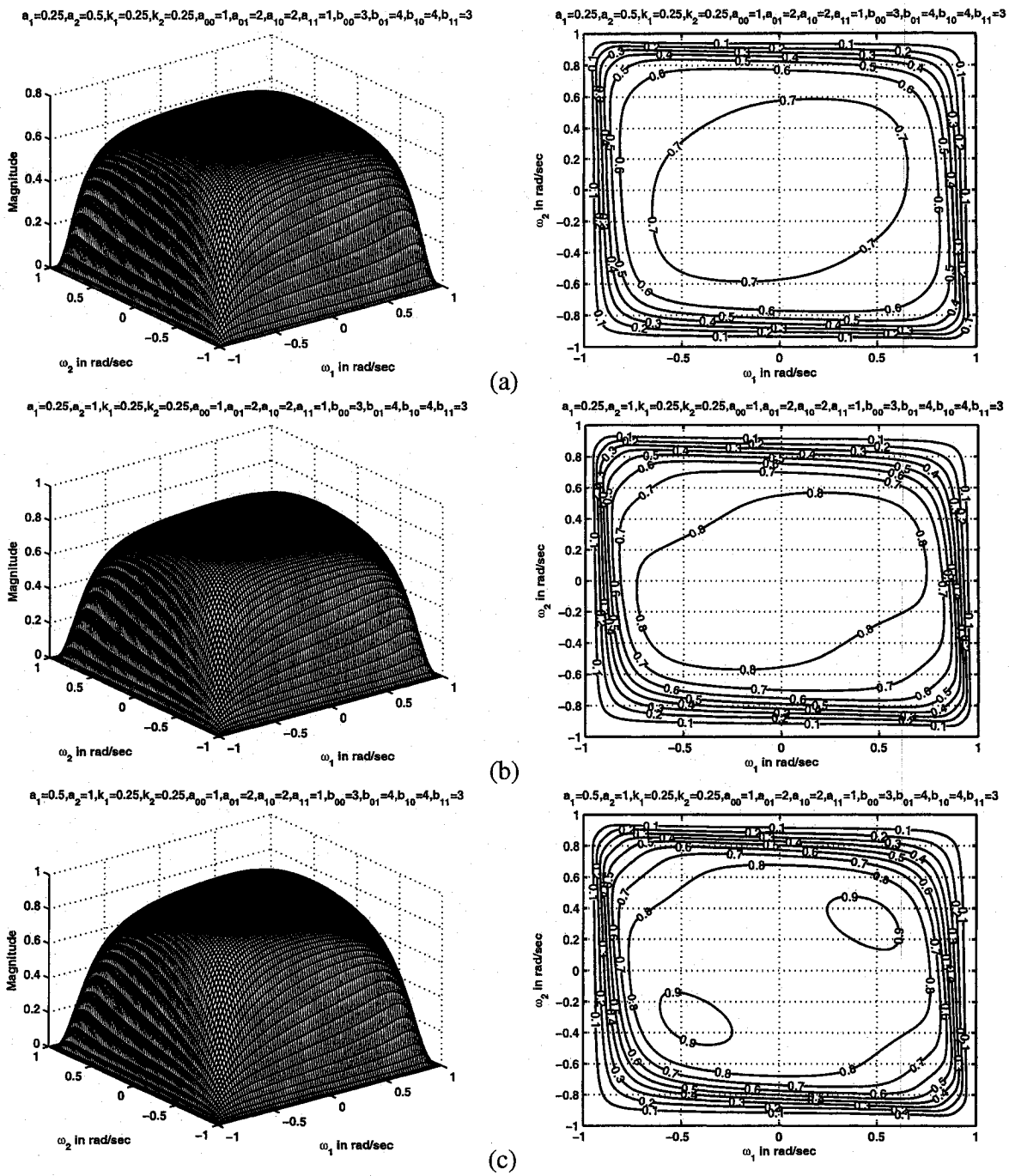

Figure 2.21: 3-D amplitude-frequency response and contour response of the 2-D digital lowpass filter in case 2 of set 3 (when $k_1 = k_2 = 0.25$)

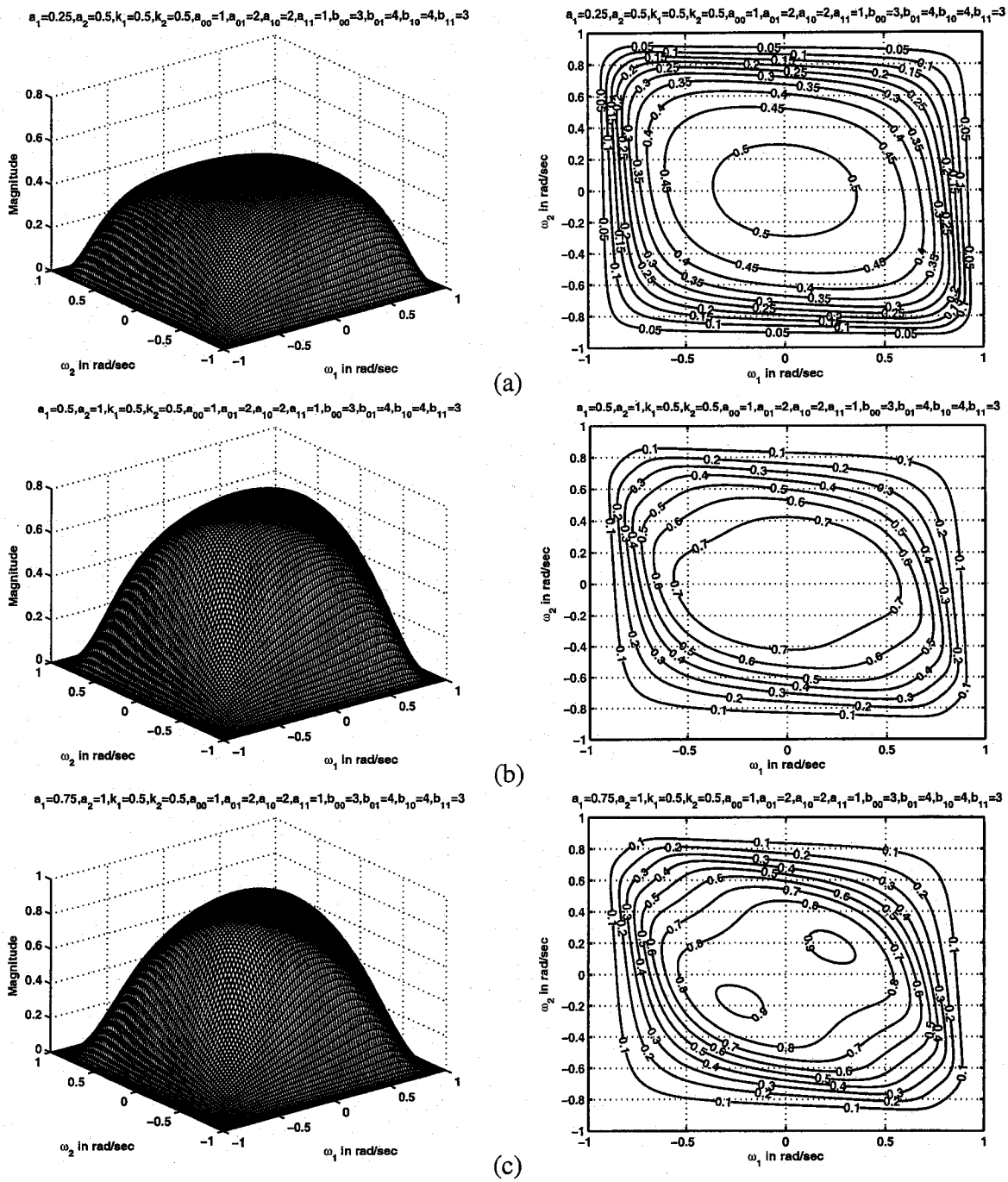

Figure 2.22: 3-D amplitude-frequency response and contour response of the 2-D digital lowpass filter in case 2 of set 3 (when $k_1 = k_2 = 0.5$)

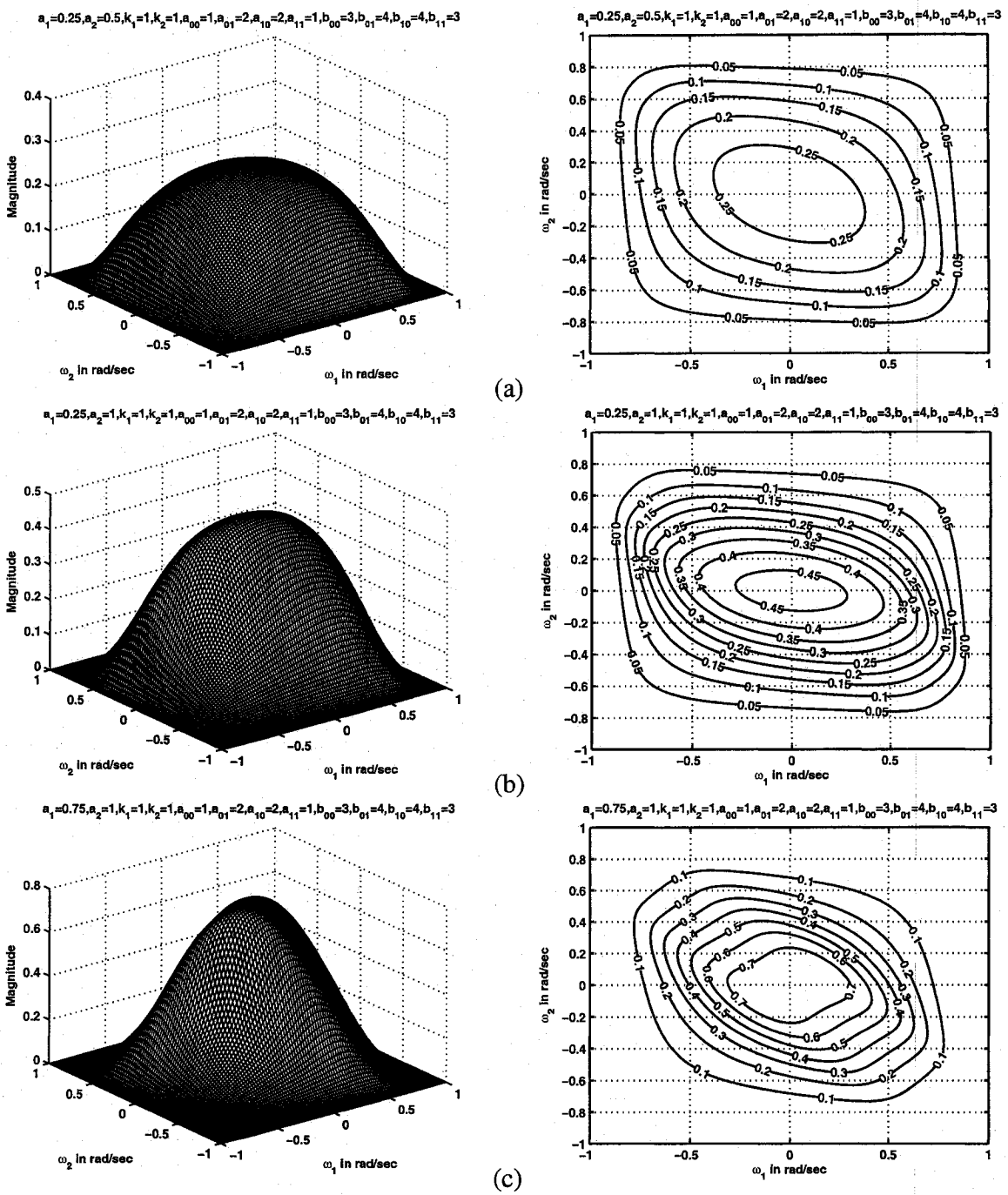

Figure 2.23: 3-D amplitude-frequency response and contour response of the 2-D digital lowpass filter in case 2 of set 3 (when $k_1 = k_2 = 1$)

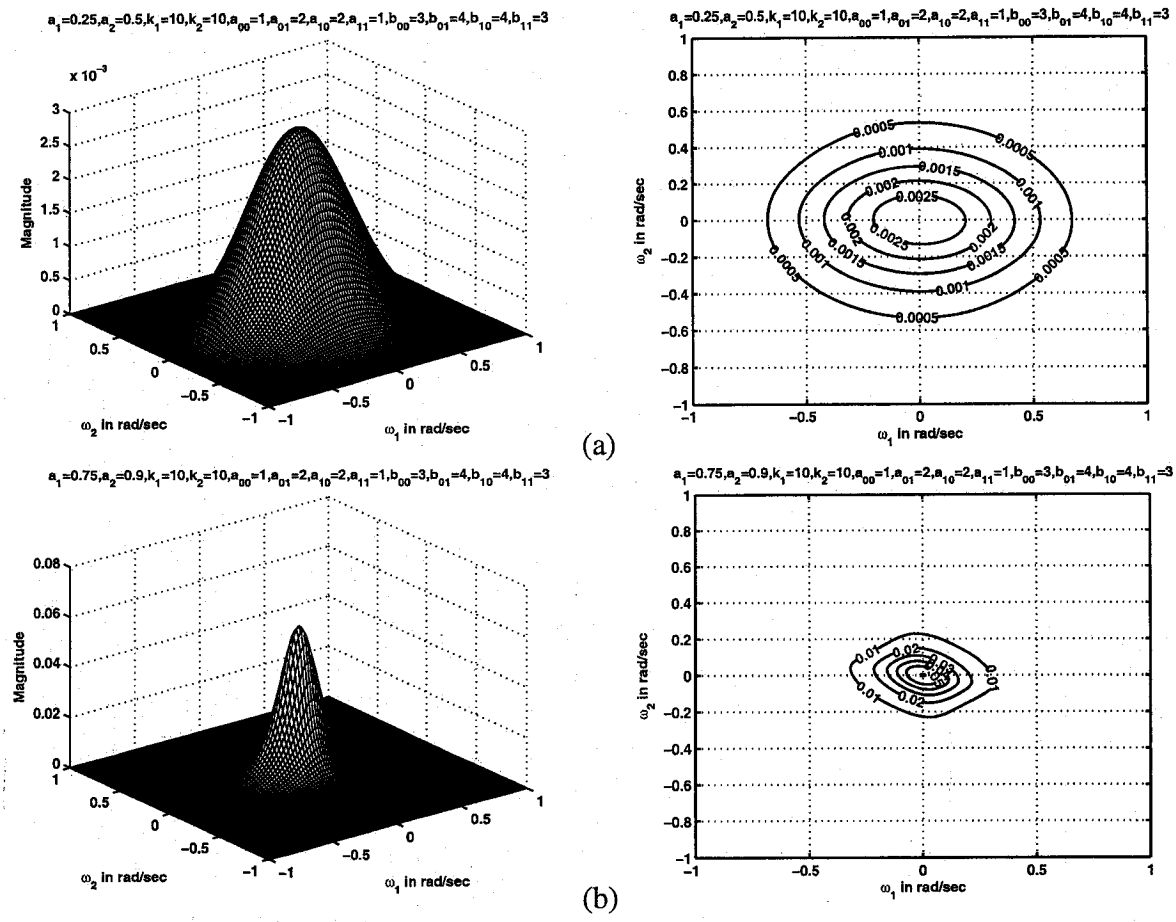

Figure 2.24: 3-D amplitude-frequency response and contour response of the 2-D digital lowpass filter in case 2 of set 3 (when $k_1 = k_2 = 10$)

2.5.3.3 Case 3:

In this case,

$$a_1 \neq a_2 \quad , \quad k_1 \neq k_2 \quad , \quad b_1 = b_2 = 1$$

There are ripples in the passband of the contour response when the values of k_1, k_2 are as low as 0.25 and 0.5 respectively and the values of a_1, a_2 are 0.5 and 1 respectively as shown in Fig. 2.25 (c). Also, it can be observed that the ripples in the passband occur when the values of k_1, k_2 are 0.5 and 1 respectively and the values of a_1, a_2 are 0.75 and 1 respectively as shown in Fig. 2.27 (a). The amplitude of the contour response is lower than that of the contour response in case 3 of set 1 for the same values of k_1, k_2, a_1 and

a_2. For example, the amplitude of the contour response in Fig. 2.10 (b) is 0.55 whereas the amplitude for the same values in Fig. 2.26 (b) is 0.35.

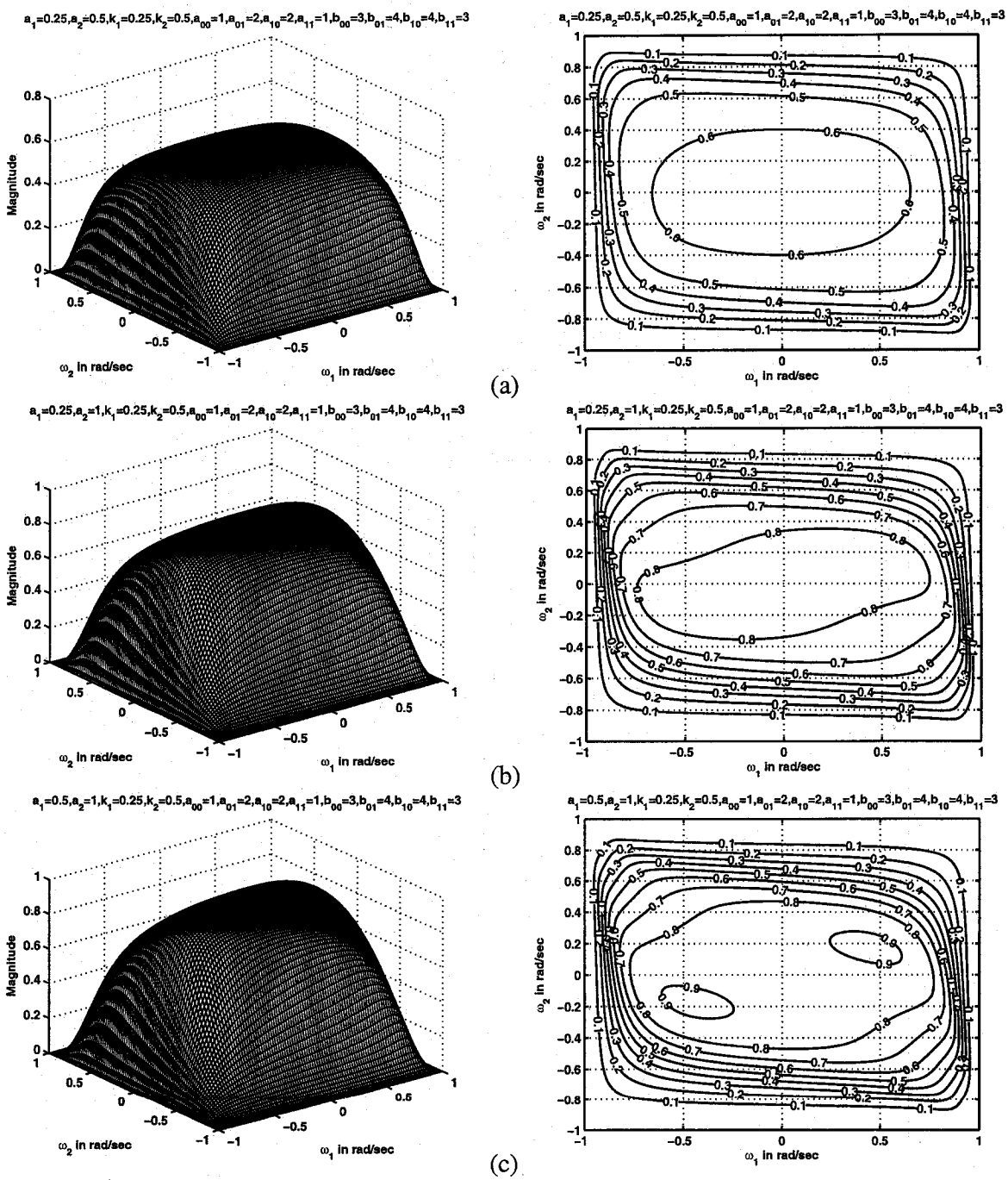

Figure 2.25: 3-D amplitude-frequency response and contour response of the 2-D digital lowpass filter in case 3 of set 3 (when $k_1 = 0.25$, $k_2 = 0.5$)

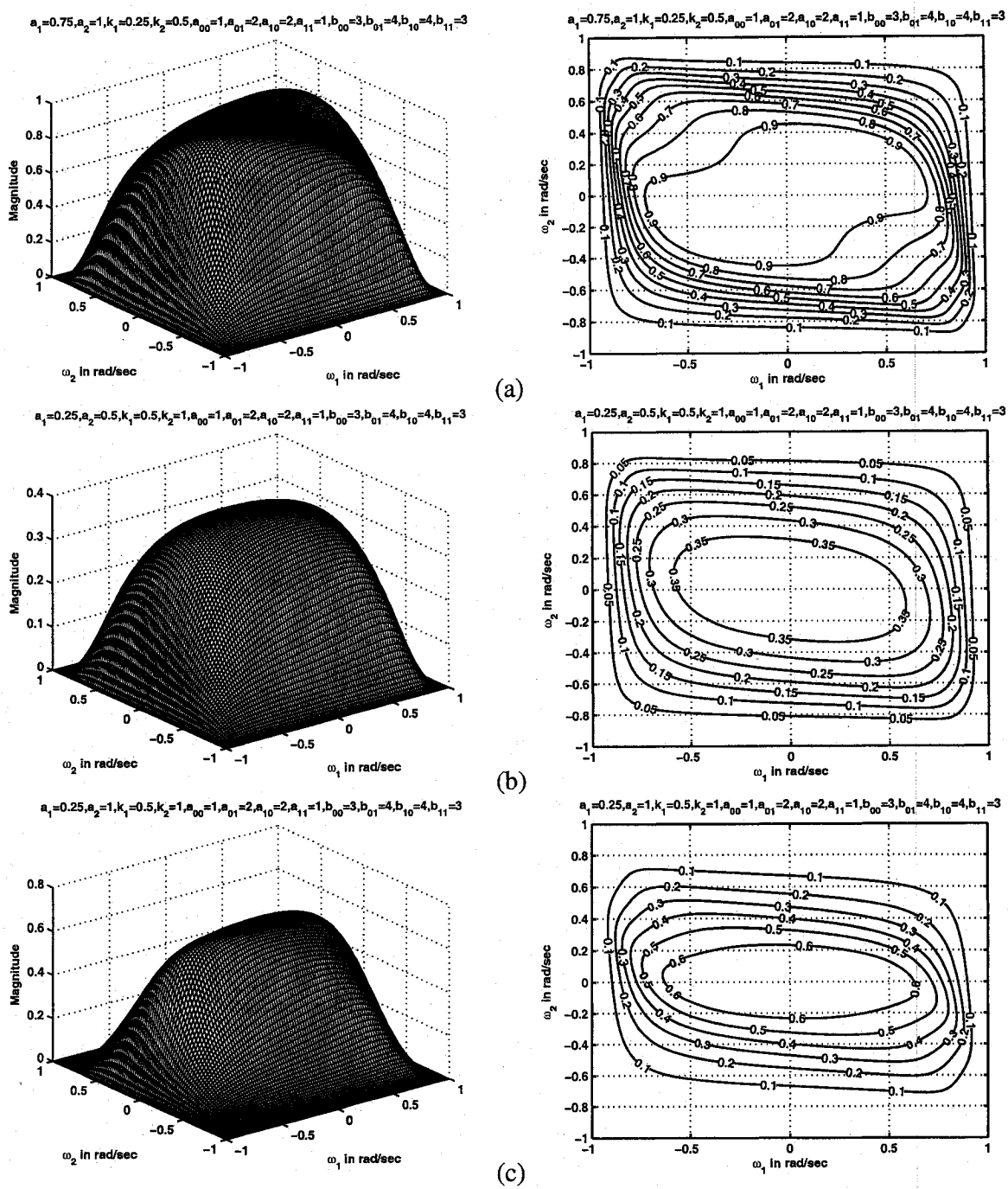

Figure 2.26: 3-D amplitude-frequency response and contour response of the 2-D digital lowpass filter in case 3 of set 3 (when $k_1 = 0.25,\ 0.5,\ k_2 = 0.5,\ 1$)

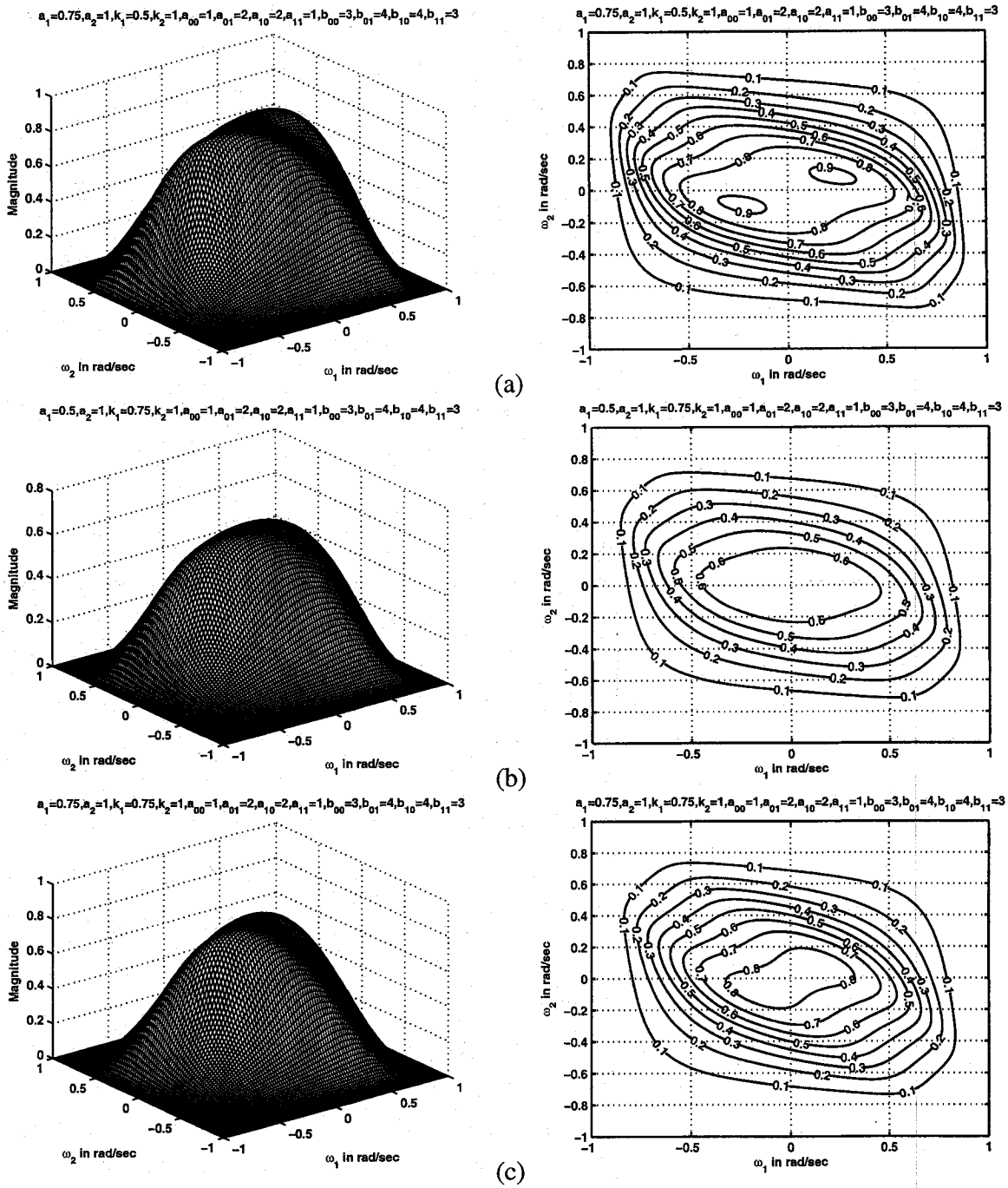

Figure 2.27: 3-D amplitude-frequency response and contour response of the 2-D digital lowpass filter in case 3 of set 3 (when $k_1 = 0.5,\ 0.75,\ k_2 = 1$)

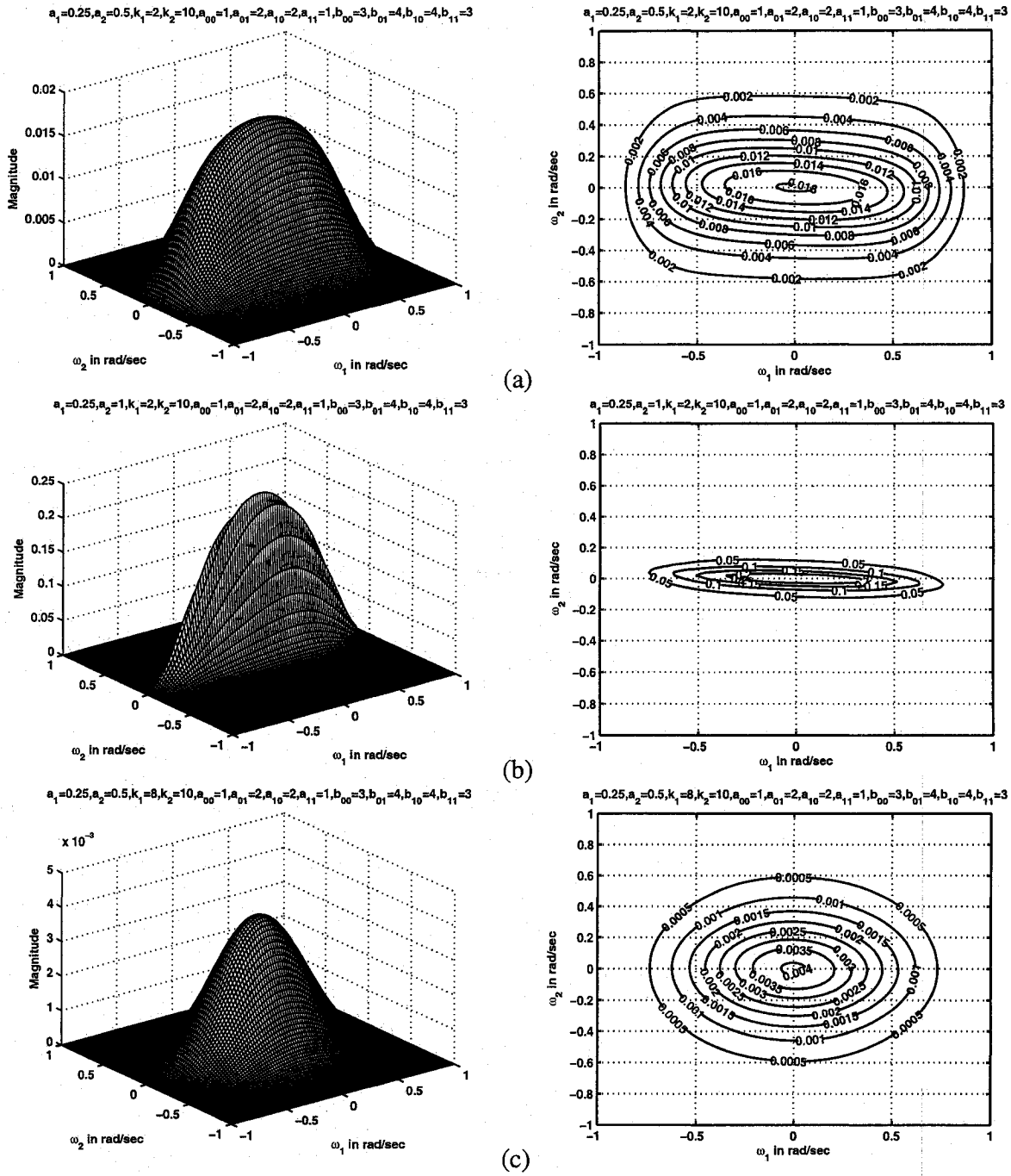

Figure 2.28: 3-D amplitude-frequency response and contour response of the 2-D digital lowpass filter in case 3 of set 3 (when $k_1 = 2,\ 8,\ k_2 = 10$)

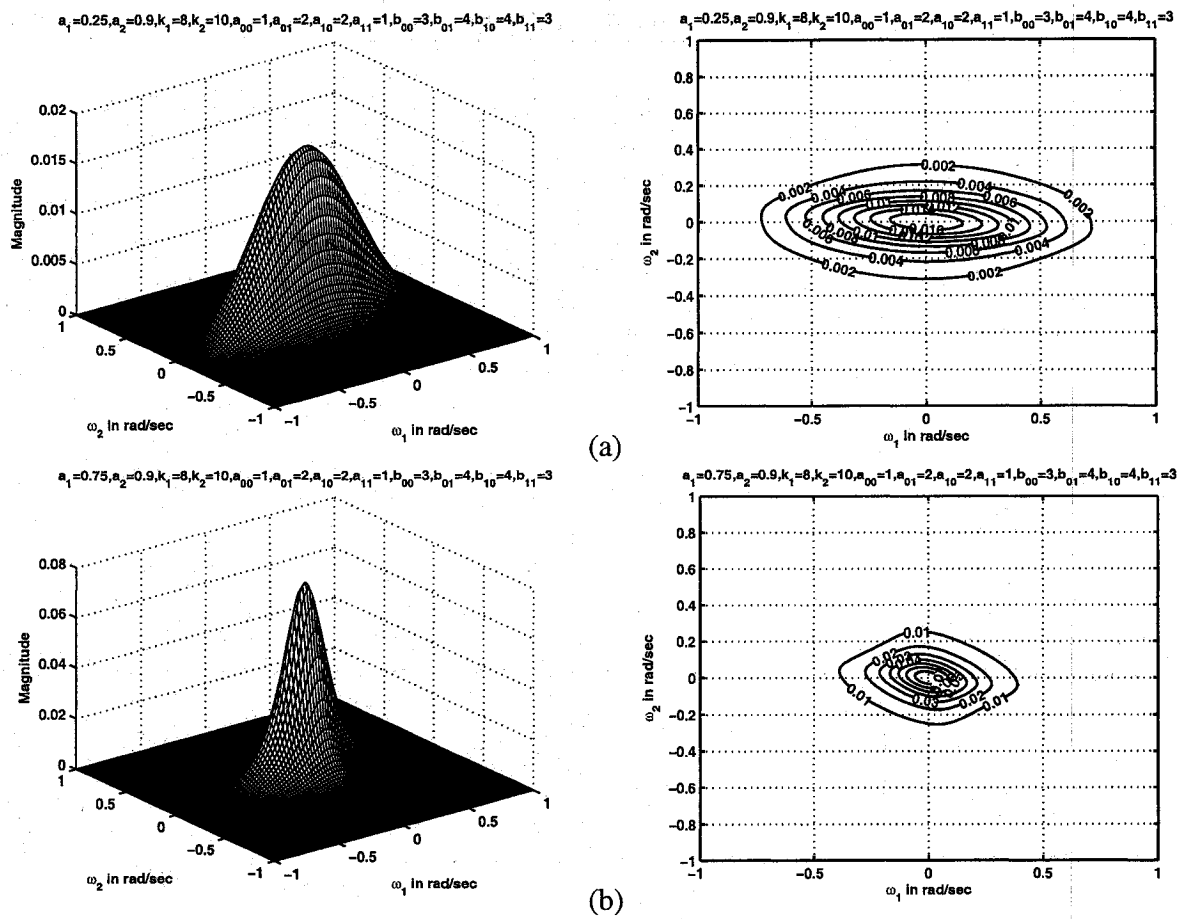

Figure 2.29: 3-D amplitude-frequency response and contour response of the 2-D digital lowpass filter in case 3 of set 3 (when $k_1 = 8$, $k_2 = 10$)

2.5.3.4 Case 4:

In this case,

$$a_1 = a_2 \quad , \quad k_1 = k_2 \quad , \quad b_1 = b_2 = 1$$

There are ripples in the passband of the contour response for the values of $k_1 = k_2 = 0.25$ and for values of $a_1 = a_2 \geq 0.75$ as shown in Fig. 2.30 (b) and (c). When the values of $k_1 = k_2 \gg 1$, the contour responses are more circular in nature. For example, in Fig. 2.33 (a), (b) and (c), the contour responses are nearly circular in nature for all values of a_1

and a_2. The contour responses change from a square nature to a nearly circular nature as the values of k_1 and k_2 increases from 0.25 to 10 as observed in Fig. 2.30 (a), Fig. 2.31 (a), Fig. 2.32 (a) and Fig. 2.33 (a).

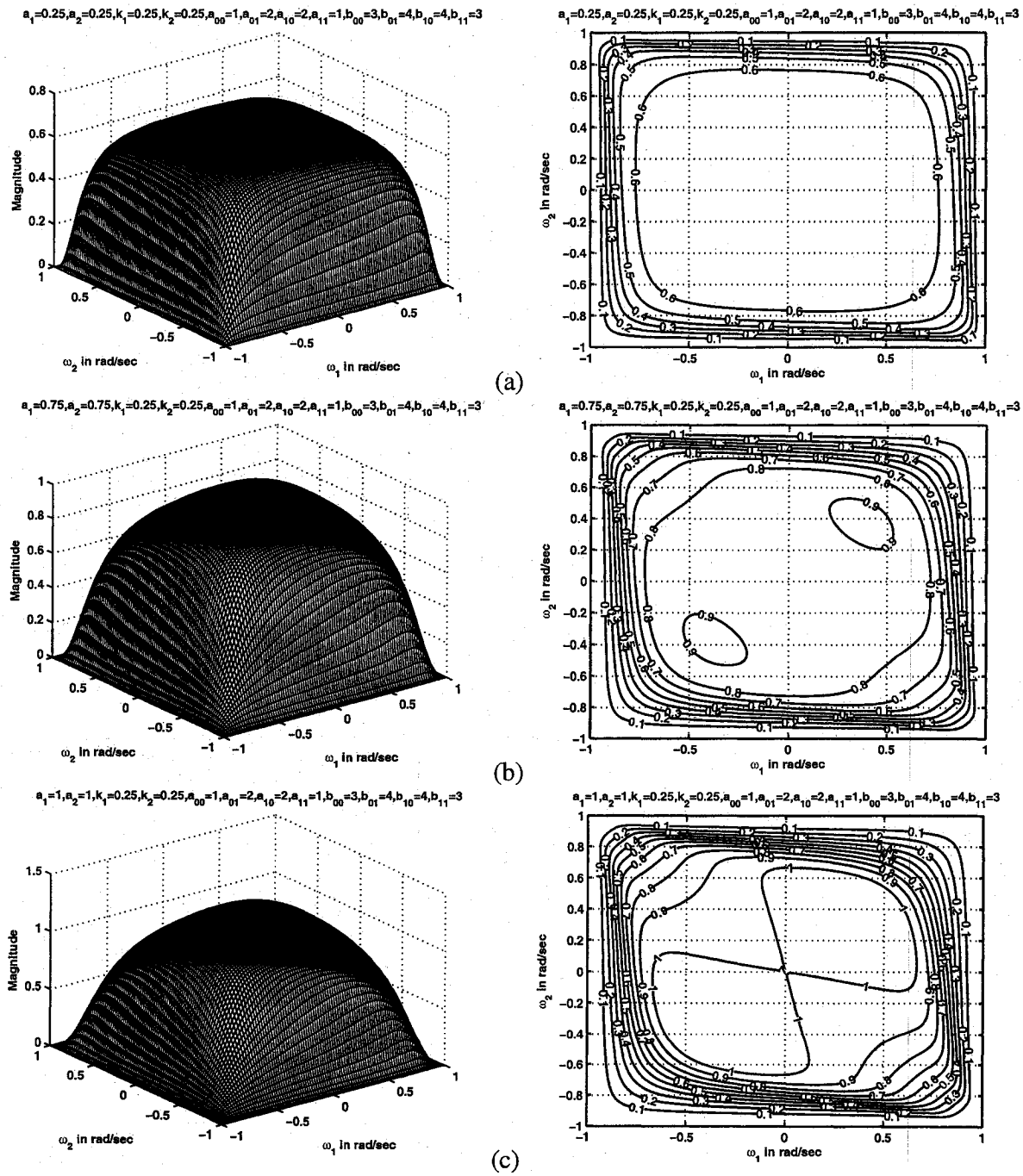

Figure 2.30: 3-D amplitude-frequency response and contour response of the 2-D digital lowpass filter in case 4 of set 3 (when $k_1 = k_2 = 0.25$)

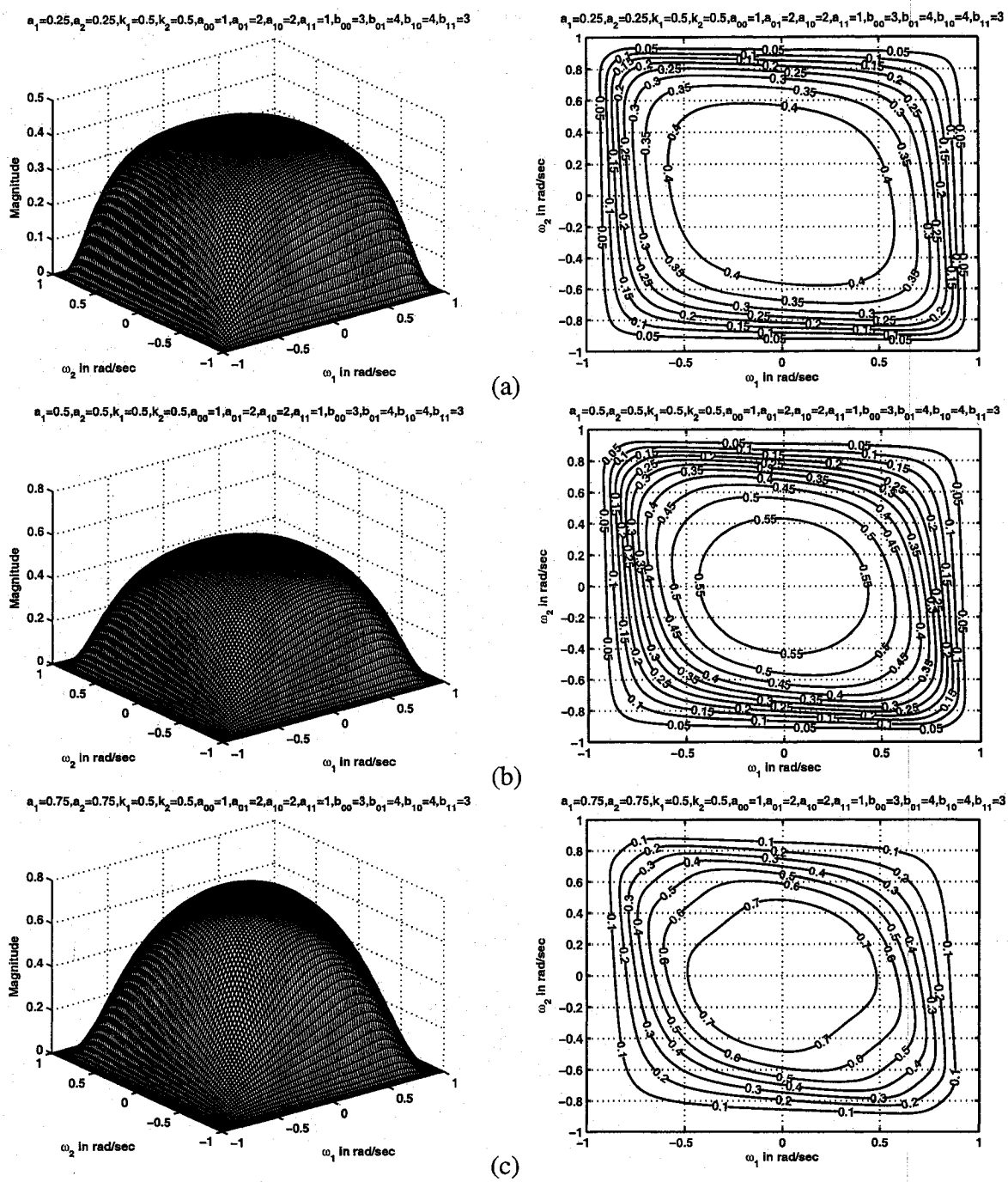

Figure 2.31: 3-D amplitude-frequency response and contour response of the 2-D digital lowpass filter in case 4 of set 3 (when $k_1 = k_2 = 0.5$)

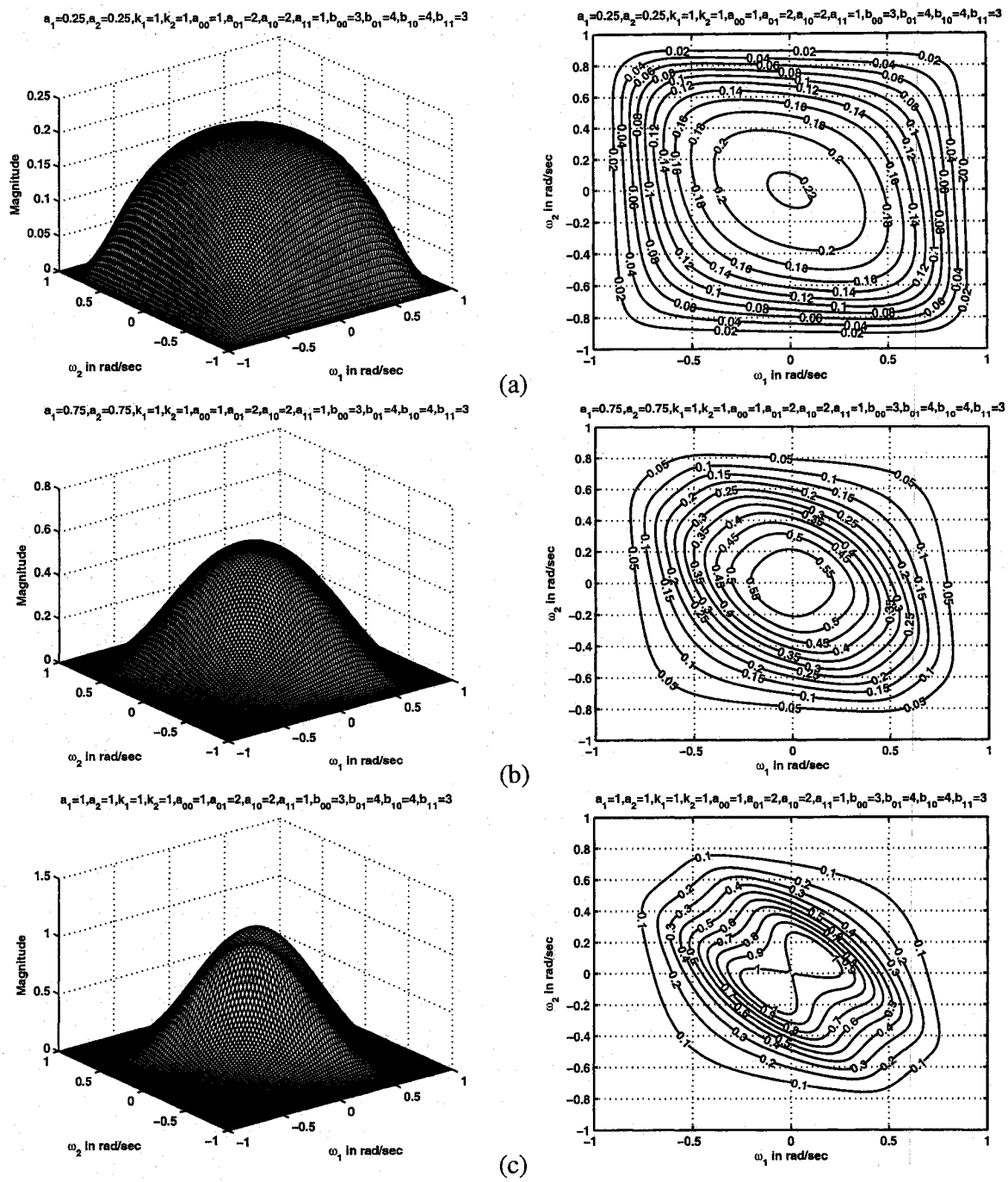

Figure 2.32: 3-D amplitude-frequency response and contour response of the 2-D digital lowpass filter in case 4 of set 3 (when $k_1 = k_2 = 1$)

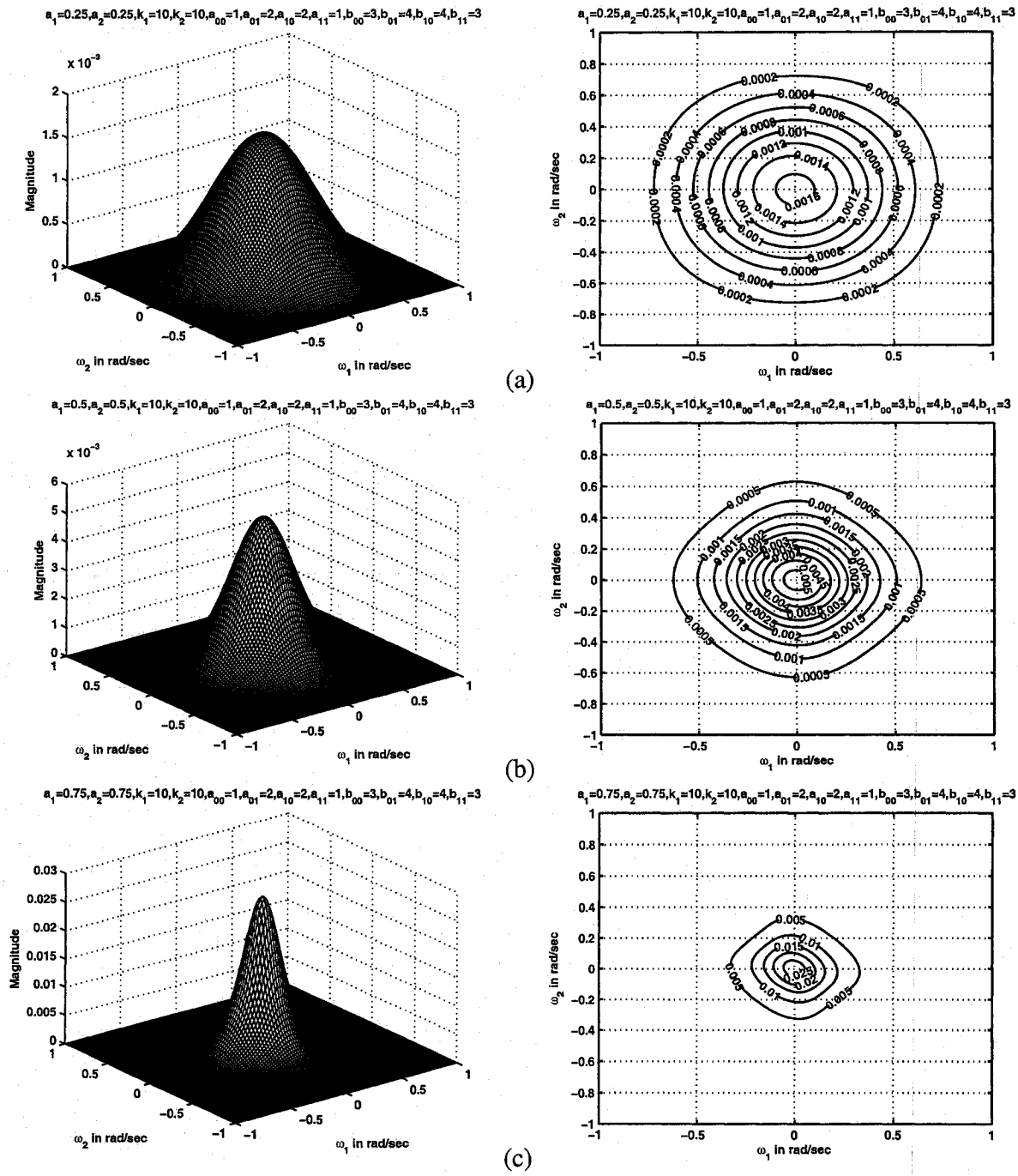

Figure 2.33: 3-D amplitude-frequency response and contour response of the 2-D digital lowpass filter in case 4 of set 3 (when $k_1 = k_2 = 10$)

2.5.4 Frequency responses of 2-D discrete lowpass filters in set 4

In this section, we study the manner in which all the four cases in set 4 affect the frequency response behavior of the resulting 2-D lowpass filter. In this set,

$$a_{00} \neq a_{01} \neq a_{10} \neq a_{11} \neq b_{00} \neq b_{01} \neq b_{10} \neq b_{11}$$

Different contour plots are obtained by varying the values of a_1, a_2, k_1 *and* k_2.

Similar to set 1and set 3, in set 4, it is observed in all the four cases that the coefficients k_1 and k_2 affect the passband width. As k_1 and k_2 values are increased, the passband width decreases and the amplitude of the contour response also decreases. As a_1 and a_2 values are increased, the amplitude of the contour response increases and in addition, the passband width decreases. Overall, the passband width decreases when k_1, k_2, a_1 and a_2 values are increased. For higher values of k_1 and k_2, the contour responses lose their elliptical nature and the passband becomes very narrow.

In set 4, the amplitude frequency responses are similar to that of set 3. But the magnitude of the contour responses is small when compared to that of set 3. Also, the passband width of the contour responses is less when compared to that of set 3. There are not many ripples in the passband of the contour responses except under a few circumstances which will be dealt later in this section.

2.5.4.1 Case 1:

In this case,

$$a_1 = a_2 \quad , \quad k_1 \neq k_2 \quad , \quad b_1 = b_2 = 1$$

The coefficients k_1 and k_2 affect the passband width. As k_1 and k_2 values are increased, the passband width decreases and the amplitude of the contour response also decreases.

As a_1 and a_2 values are increased, the amplitude of the contour response increases and in addition, the passband width decreases.

The contour responses are similar to that of the responses in case 1 of set 3, except that there are ripples in the contour response when $a_1 = a_2 = .75$ and k_1, $k_2 = 0.25, 0.5$ respectively as shown in Fig. 2.37 (b) which were absent in case 1 of set 3 for the same values of a_1, a_2, k_1 and k_2 as observed in Fig. 2.20 (a). The passband of the contour response is smaller than the passband in case 1 of set 3. As an illustration, the passband in Fig. 2.37 (a) of set 4 is smaller than the passband in Fig. 2.4 (c) in case 1 of set 3. Also the magnitude of the contour response is smaller than the magnitude in case 1 of set 3. In Fig. 2.34 (a), (b) and (c), the magnitude of the contour response is slightly smaller when compared to Fig. 2.17 (a), (b) and (c) of case 1 in set 3 for the same values of a_1, a_2, k_1 and k_2.

For higher values of k_1 and k_2, (i.e., when k_1, $k_2 > 1$), the passband of the contour responses decrease gradually as shown in Fig. 2.35 (a), (b) and Fig. 2.36 (c) and Fig. 2.37 (a).

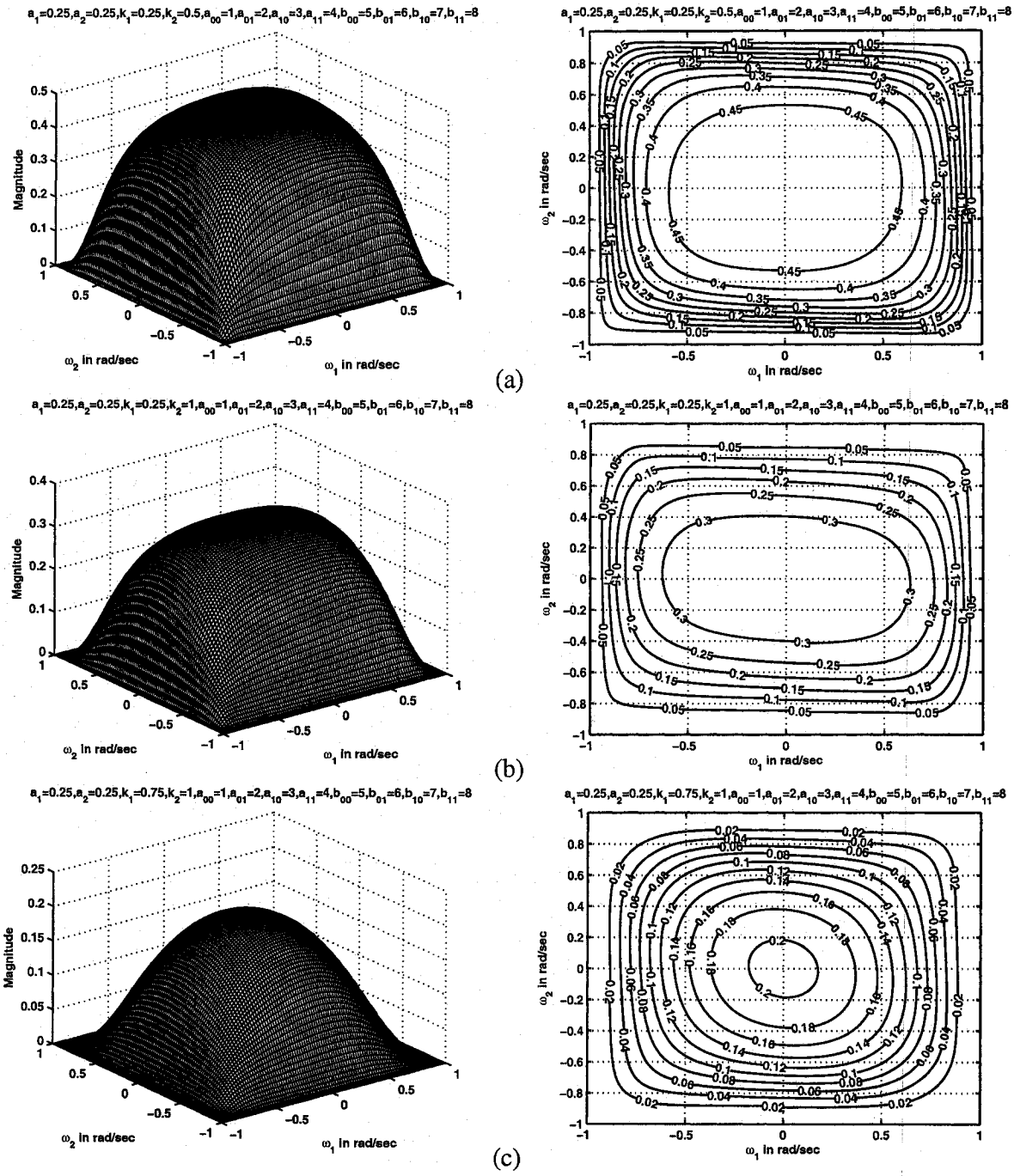

Figure 2.34: 3-D amplitude-frequency response and contour response of the 2-D digital lowpass filter in case 1 of set 4 (when $a_1 = a_2 = 0.25$)

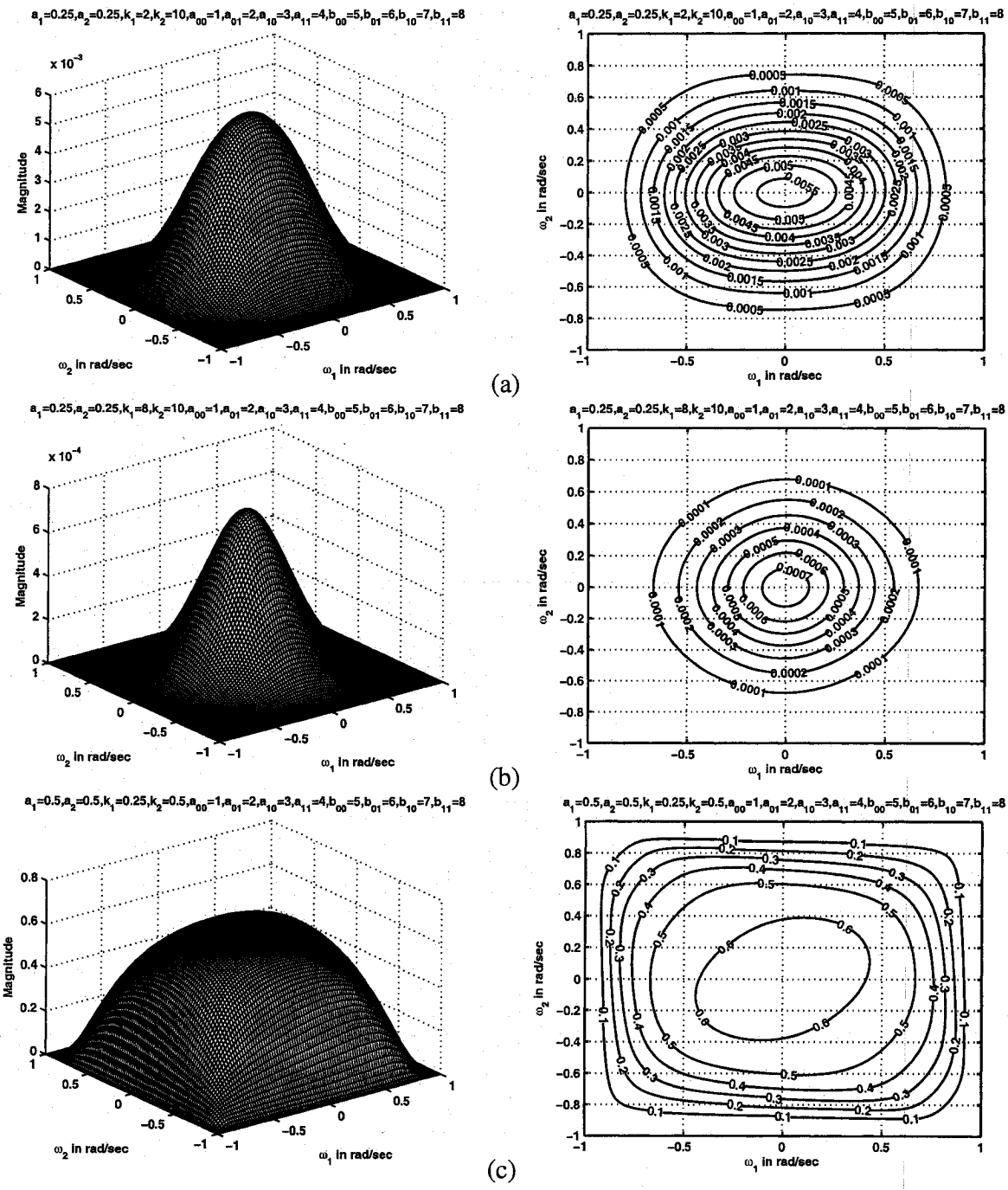

Figure 2.35: 3-D amplitude-frequency response and contour response of the 2-D digital lowpass filter in case 1 of set 4 (when $a_1 = a_2 = 0.25,\ 0.5$)

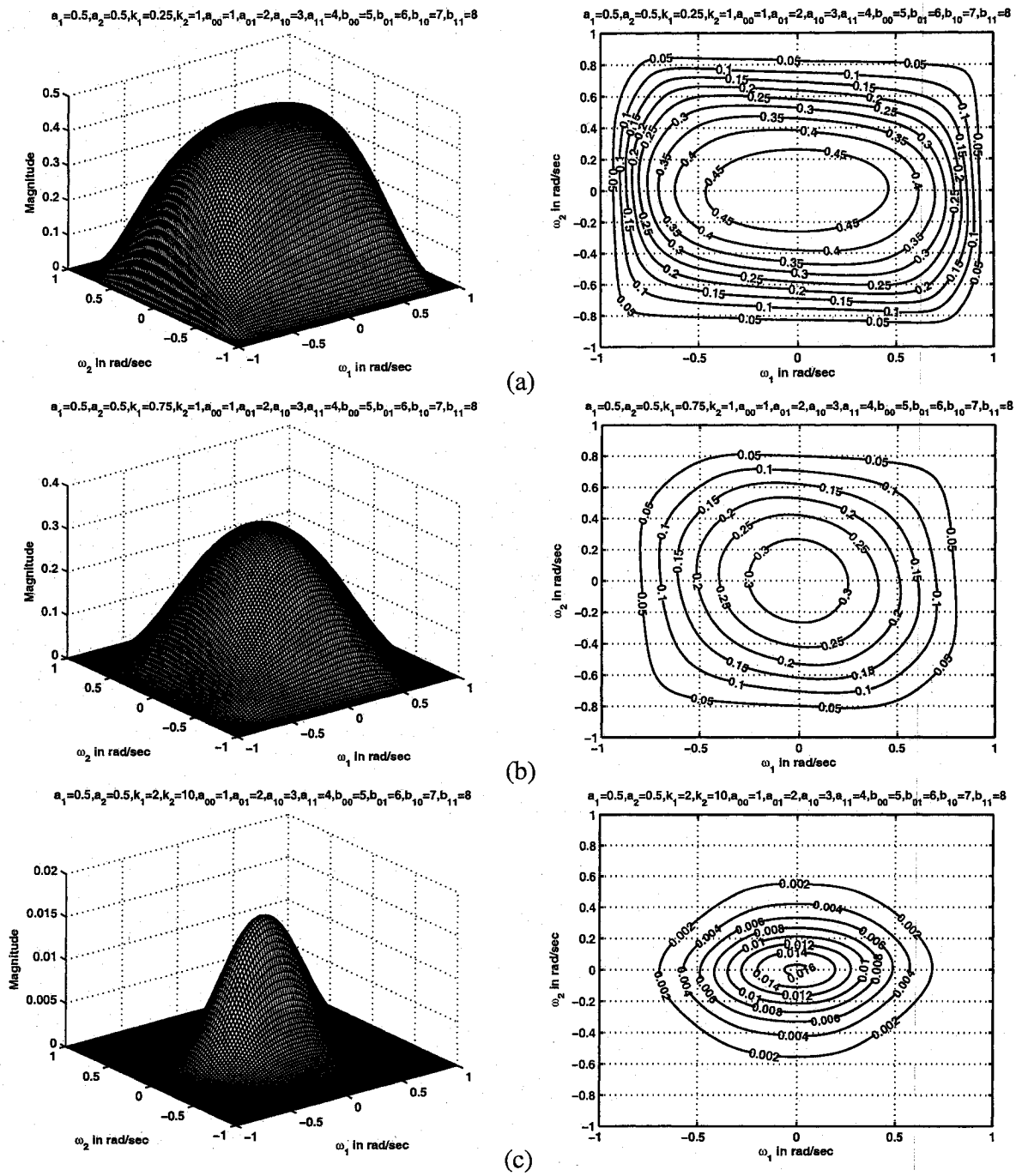

Figure 2.36: 3-D amplitude-frequency response and contour response of the 2-D digital lowpass filter in case 1 of set 4 (when $a_1 = a_2 = 0.5$)

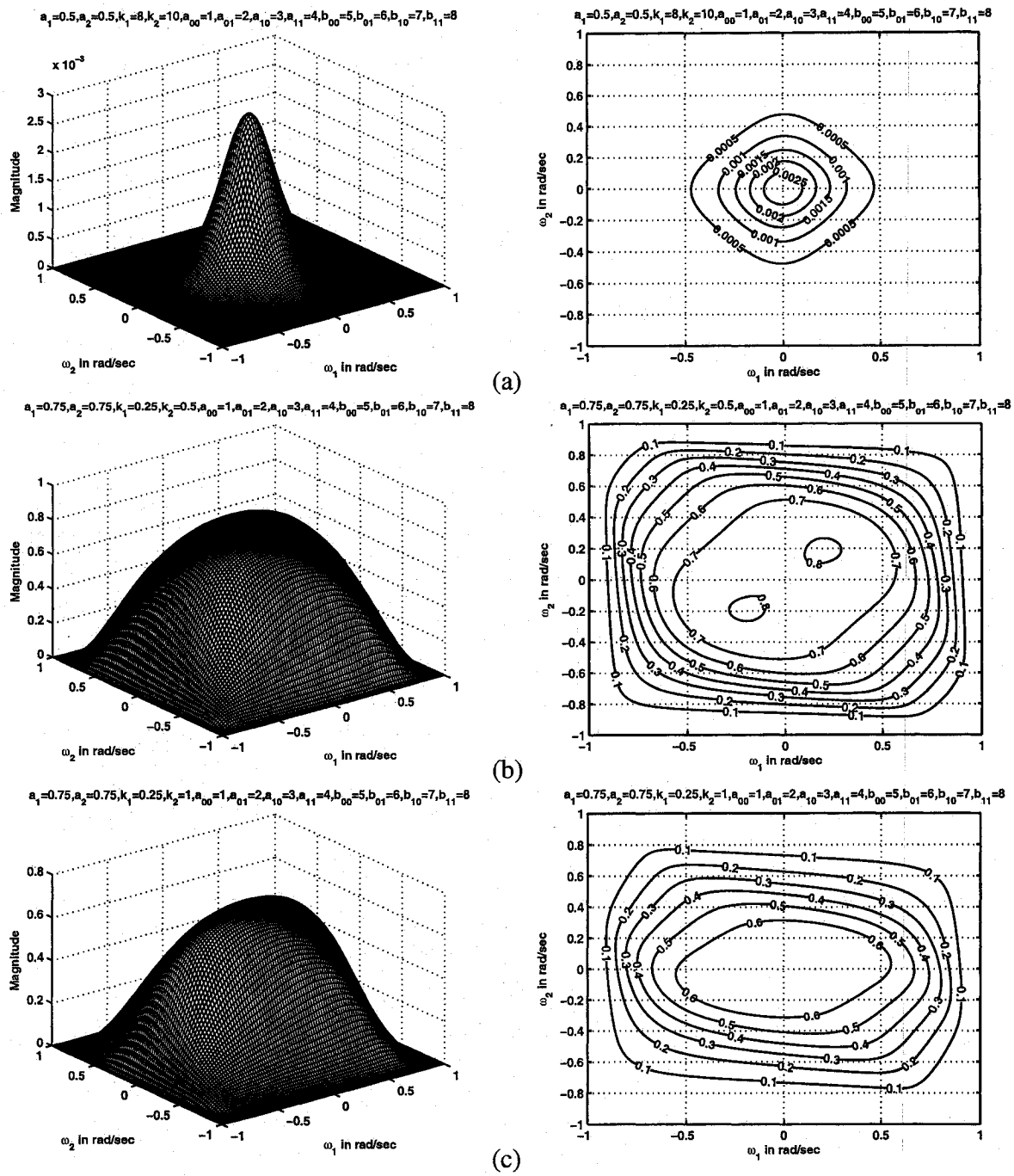

Figure 2.37: 3-D amplitude-frequency response and contour response of the 2-D digital lowpass filter in case 1 of set 4 (when $a_1 = a_2 = 0.5,\ 0.75$)

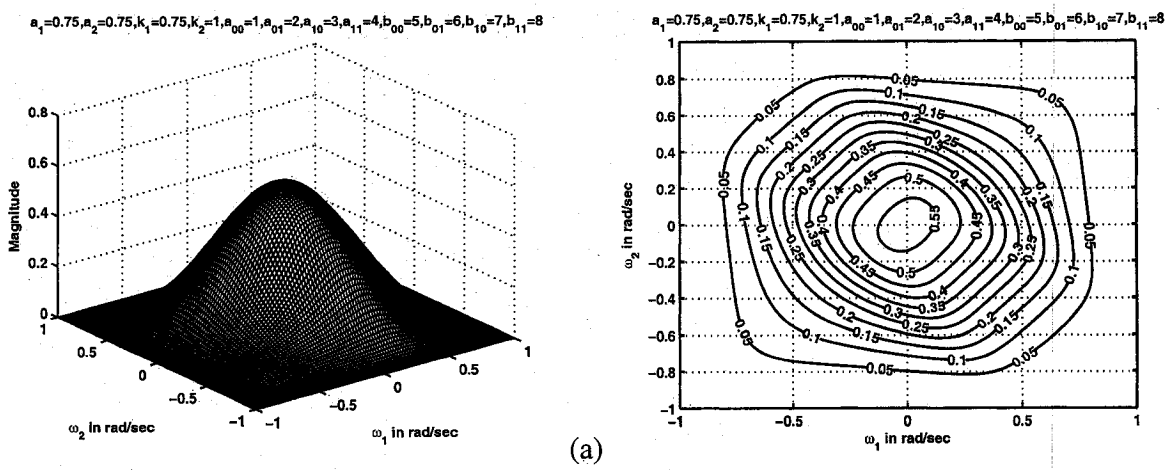

Figure 2.38: 3-D amplitude-frequency response and contour response of the 2-D digital lowpass filter in case 1 of set 4 (when $a_1 = a_2 = 0.75$)

2.5.4.2 Case 2:

In this case,

$$a_1 \neq a_2 \quad , \quad k_1 = k_2 \quad , \quad b_1 = b_2 = 1$$

There are no ripples in the passband of the contour response for all values k_1, k_2, a_1 and a_2. The amplitude of the contour response in this case of set 4 is slightly smaller than that of the contour response in case 2 of set 3 for the same values of k_1, k_2, a_1 and a_2. As can be seen, the amplitude of the contour response in Fig. 2.21 (a) in case 2 of set 3 is 0.7 whereas the amplitude for the same values in Fig. 2.39 (a) of set 4 is 0.6. The passband of the contour response in this case of set 4 is smaller than the passband in case 2 of set 3. As an example, the passband in Fig. 2.41 (c) of set 4 is smaller than the passband in Fig. 2.23 (b) of set 3. The ripples that appear in the passband of the contour responses of case 2 in set 3, when the values of k_1 and k_2 are as low as 0.25 and the values of a_1 and a_2 are ≥ 0.5 as shown in Fig. 2.21 (c) and when the values of $k_1 = k_2 = 0.5$ and the values of a_1 and a_2 are ≥ 0.75 as shown in Fig. 2.22 (c) disappears in this case of set 4. It is shown in Fig. 2.39 (c) and Fig. 2.41 (a).

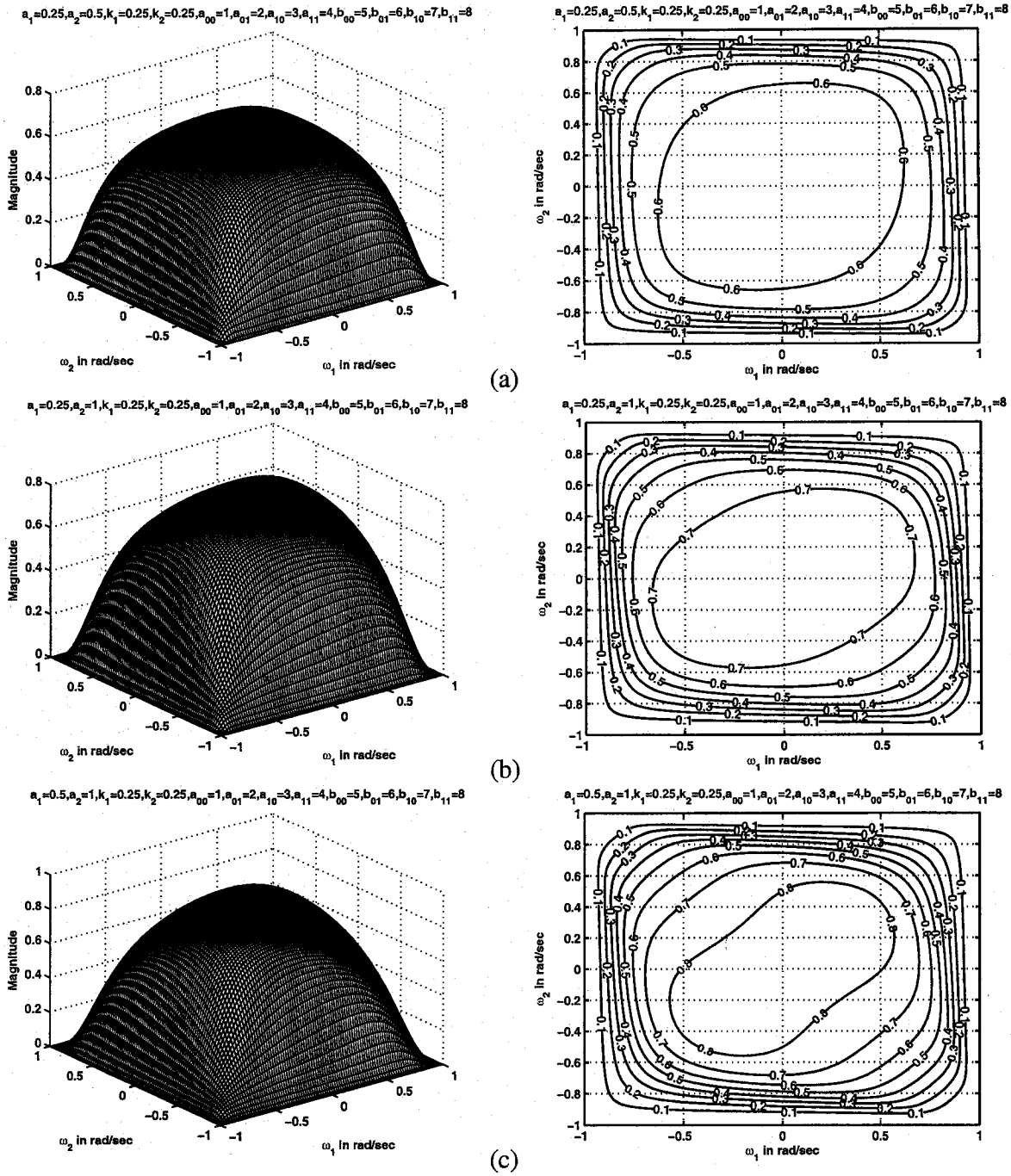

Figure 2.39: 3-D amplitude-frequency response and contour response of the 2-D digital lowpass filter in case 2 of set 4 (when $k_1 = k_2 = 0.25$)

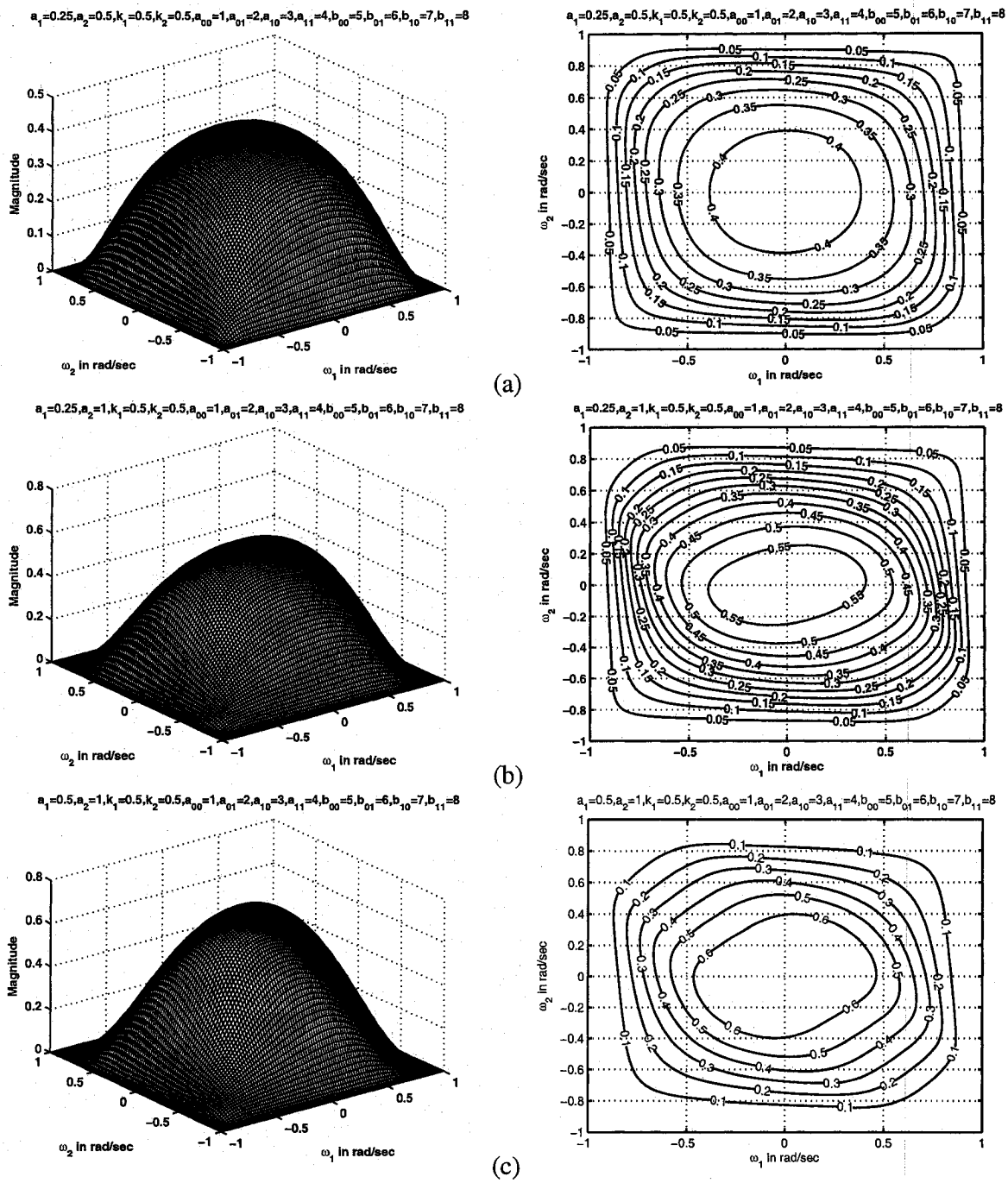

Figure 2.40: 3-D amplitude-frequency response and contour response of the 2-D digital lowpass filter in case 2 of set 4 (when $k_1 = k_2 = 0.5$)

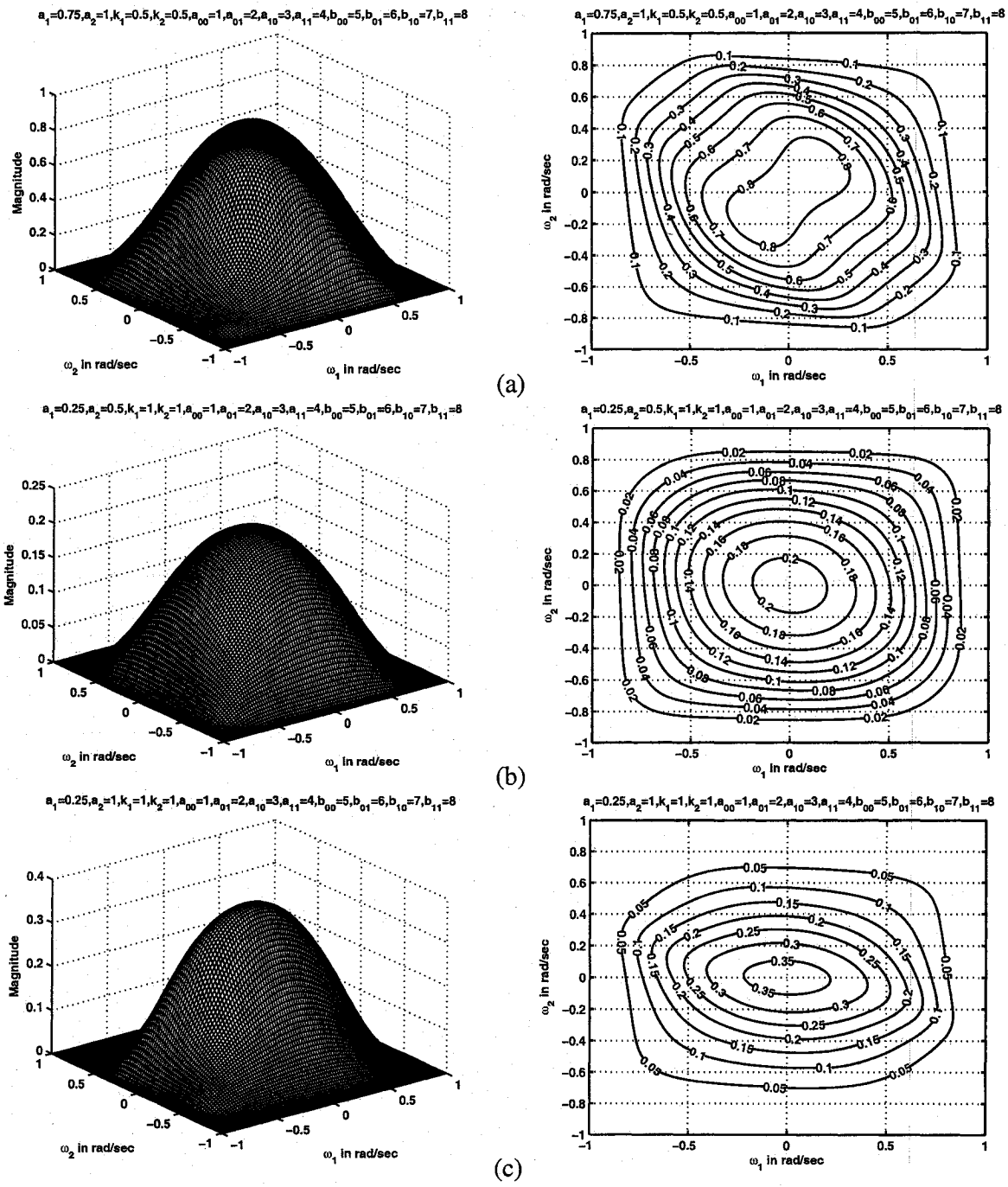

Figure 2.41: 3-D amplitude-frequency response and contour response of the 2-D digital lowpass filter in case 2 of set 4 (when $k_1 = k_2 = 0.5,\ 1$)

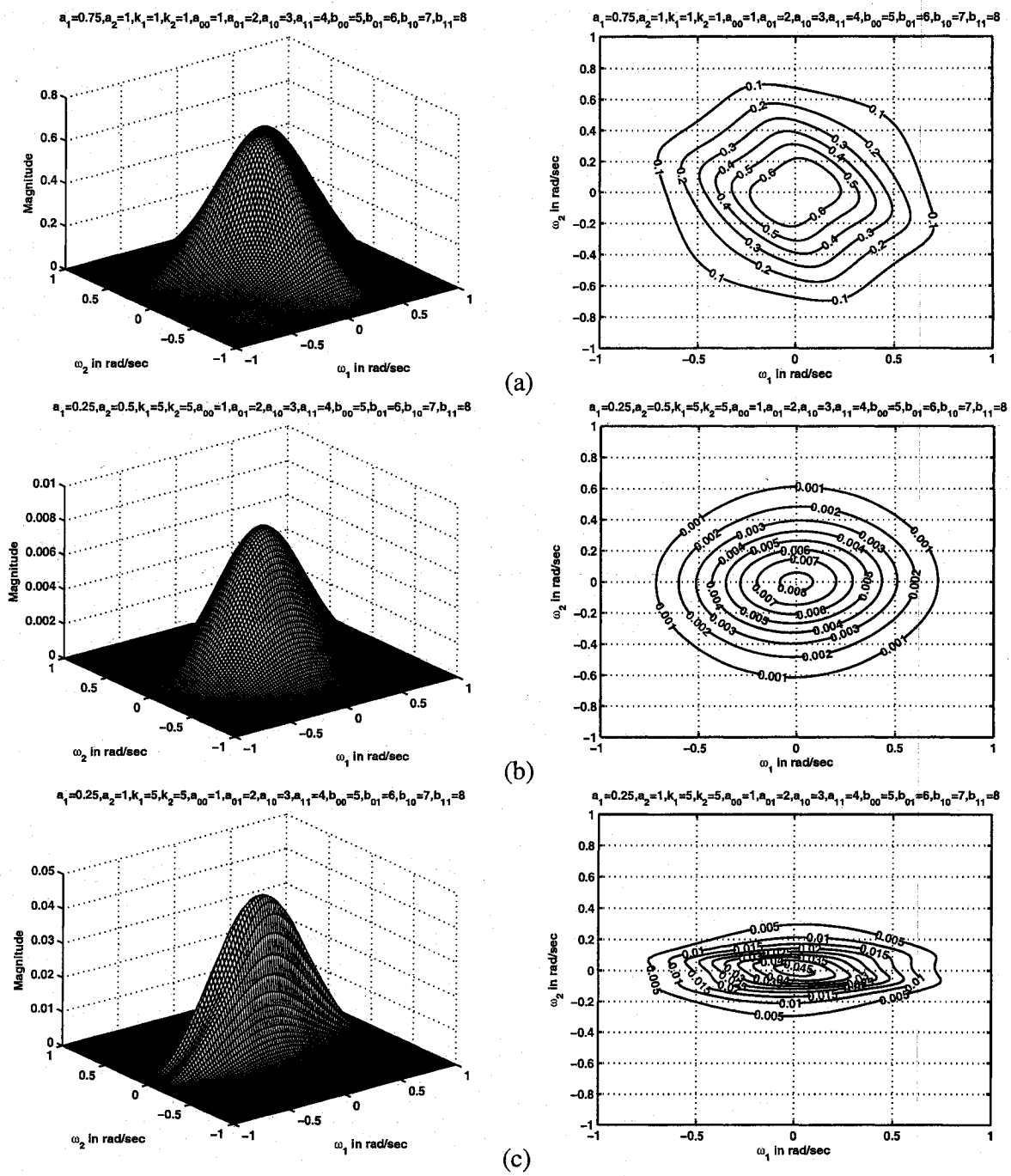

Figure 2.42: 3-D amplitude-frequency response and contour response of the 2-D digital lowpass filter in case 2 of set 4 (when $k_1 = k_2 = 1,\ 5$)

2.5.4.3 Case 3:

In this case,

$$a_1 \neq a_2 \quad , \quad k_1 \neq k_2 \quad , \quad b_1 = b_2 = 1$$

There are no ripples in the passband of the contour response for all values k_1, k_2, a_1 and a_2. The ripples in the passband of the contour responses of case 3 in set 3, when the values of k_1, k_2 are as low as 0.25 and 0.5 respectively and the values of $a_1$and a_2 are 0.5 and 1 respectively, as shown in Fig. 2.25 (c) and when the values of k_1, k_2 are 0.5 and 1 respectively and the values of a_1 and a_2 are 0.75 and 1 respectively, as shown in Fig. 2.27 (a), disappears in this case of set 4 as shown in Fig. 2.43 (c) and Fig. 2.44 (c). The amplitude of the contour response is slightly smaller than that of the contour response in case 3 of set 3 for the same values of k_1, k_2, a_1 and a_2. It is seen that, the amplitude of the contour response in Fig. 2.43 (a) in case 3 of set 4 is 0.55 whereas the amplitude for the same values in Fig. 2.25 (a) in case 3 of set 3 is 0.6. The passband of the contour response is smaller than the passband in case 3 of set 3. The passband in Fig. 2.44 (c) of set 4 is smaller than the passband in Fig. 2.27 (c) of set 3. It can be observed that the contour responses are more elliptical in nature when the values of k_1, $k_2 > 1$ as shown in Fig. 2.46 (a) and (b). Also it begins to lose its elliptical nature for higher values of $a_1$and a_2 as shown in Fig. 2.46 (c) and Fig. 2.47 (a).

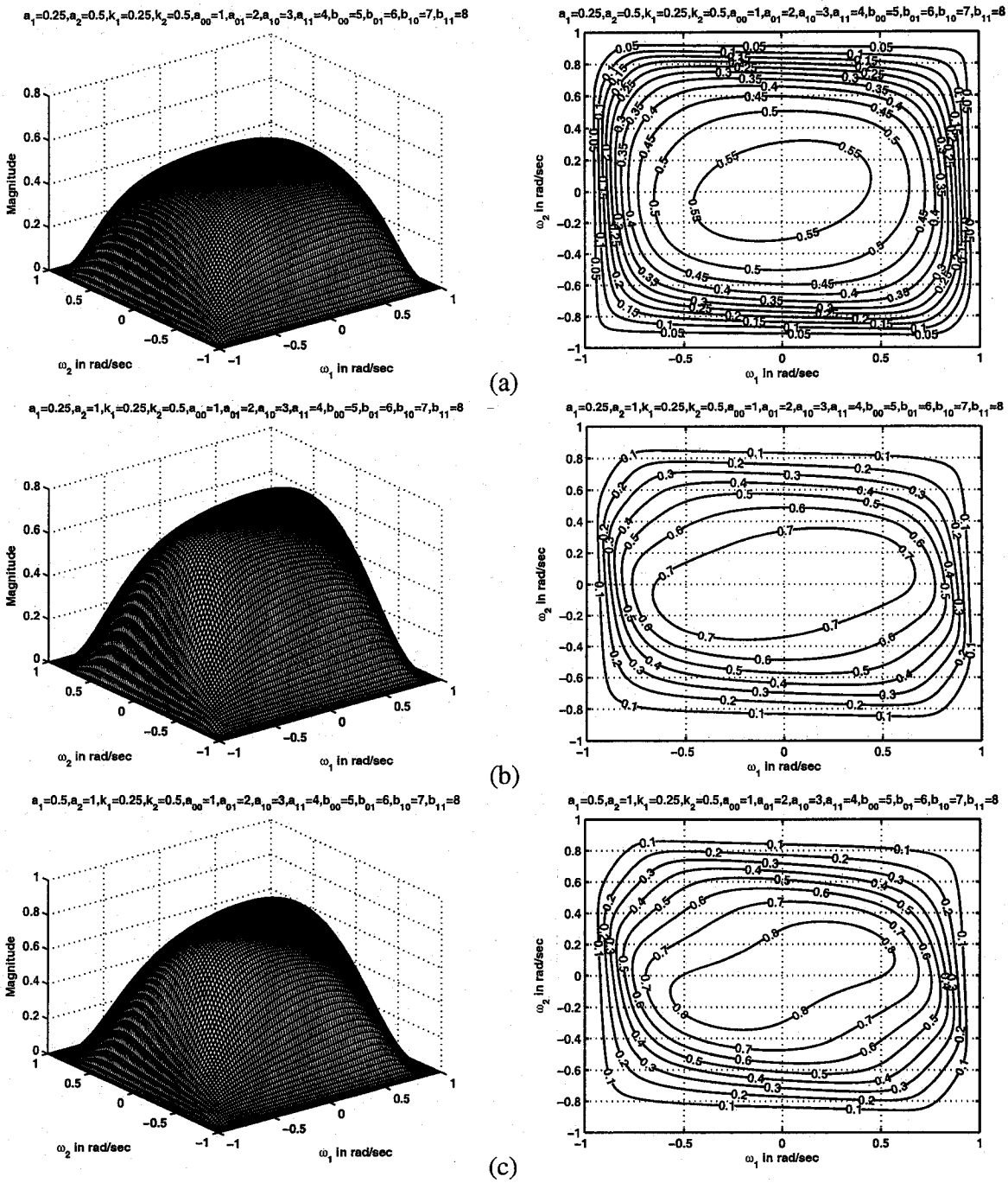

Figure 2.43: 3-D amplitude-frequency response and contour response of the 2-D digital lowpass filter in case 3 of set 4 (when $k_1 = 0.25$, $k_2 = 0.5$)

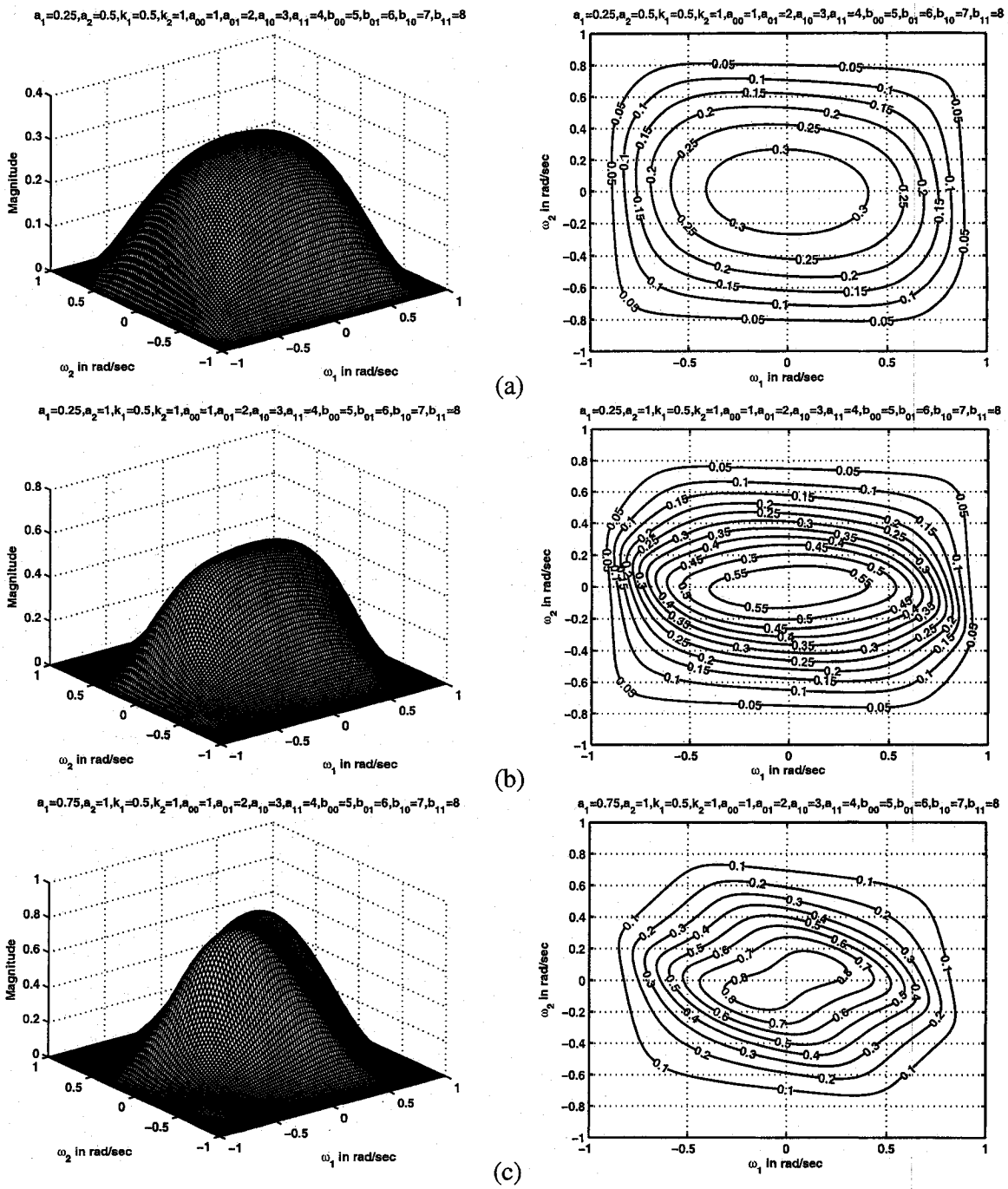

Figure 2.44: 3-D amplitude-frequency response and contour response of the 2-D digital lowpass filter in case 3 of set 4 (when $k_1 = 0.5$, $k_2 = 1$)

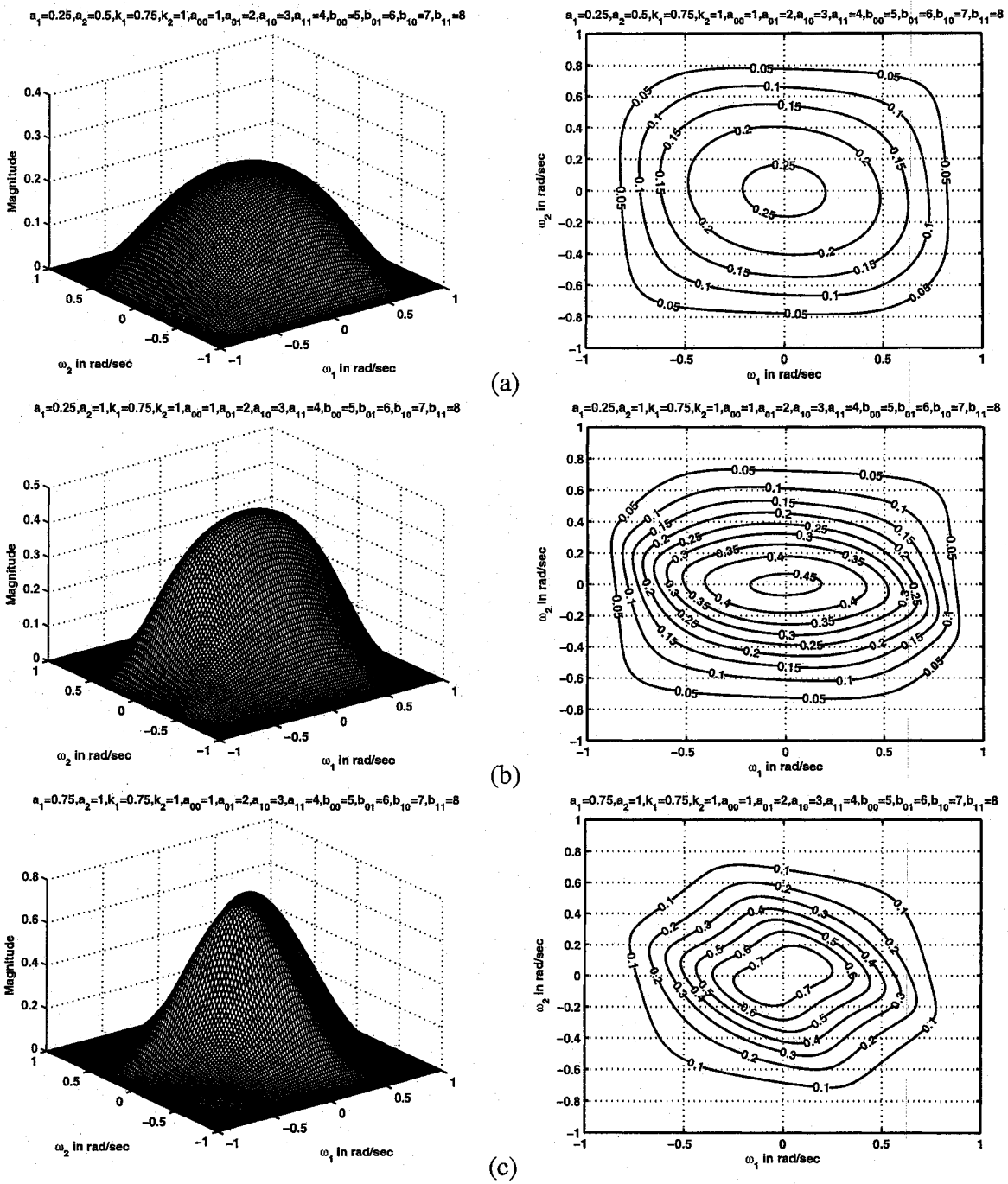

Figure 2.45: 3-D amplitude-frequency response and contour response of the 2-D digital lowpass filter in case 3 of set 4 (when $k_1 = 0.75$, $k_2 = 1$)

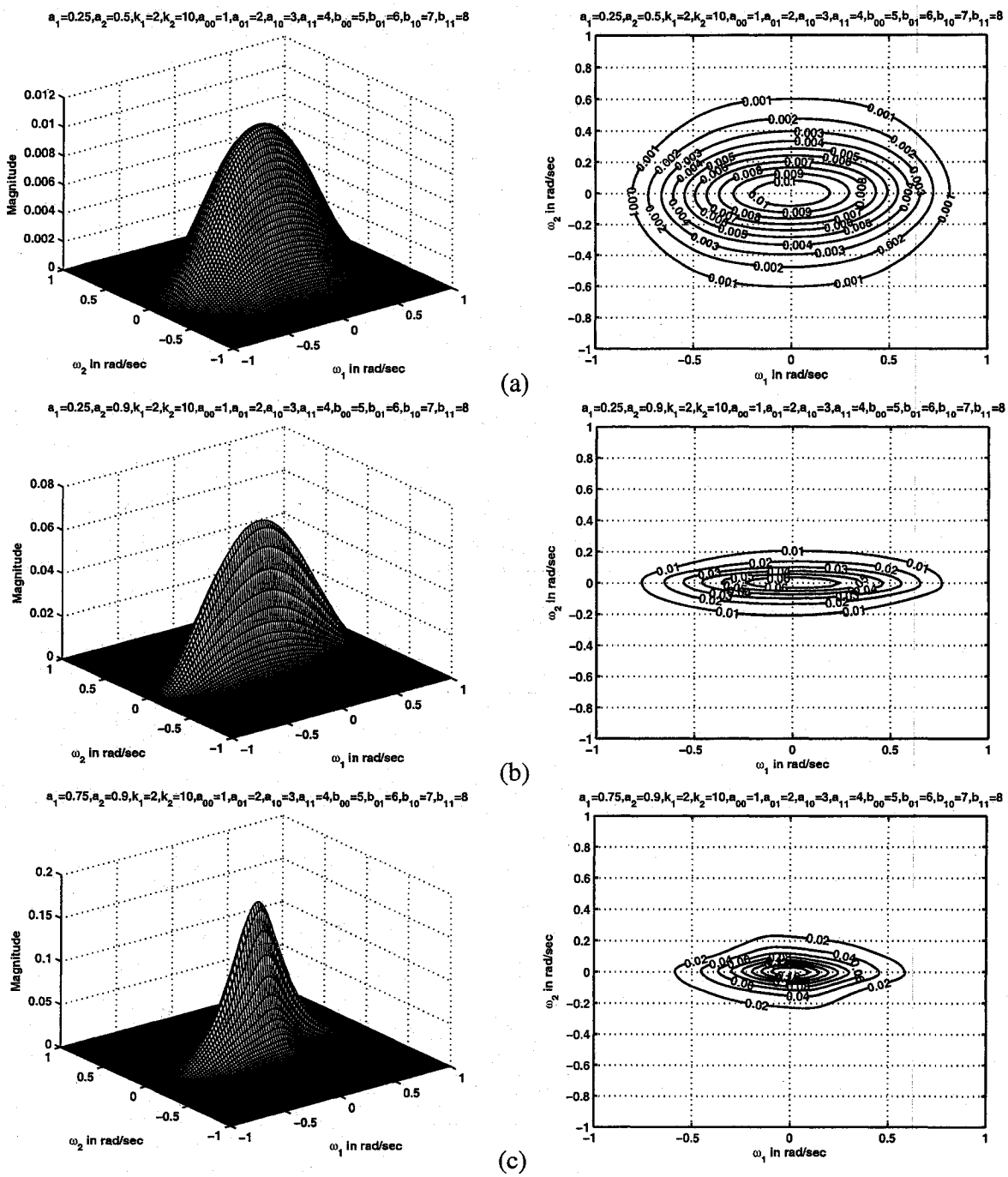

Figure 2.46: 3-D amplitude-frequency response and contour response of the 2-D digital lowpass filter in case 3 of set 4 (when $k_1 = 2,\ k_2 = 10$)

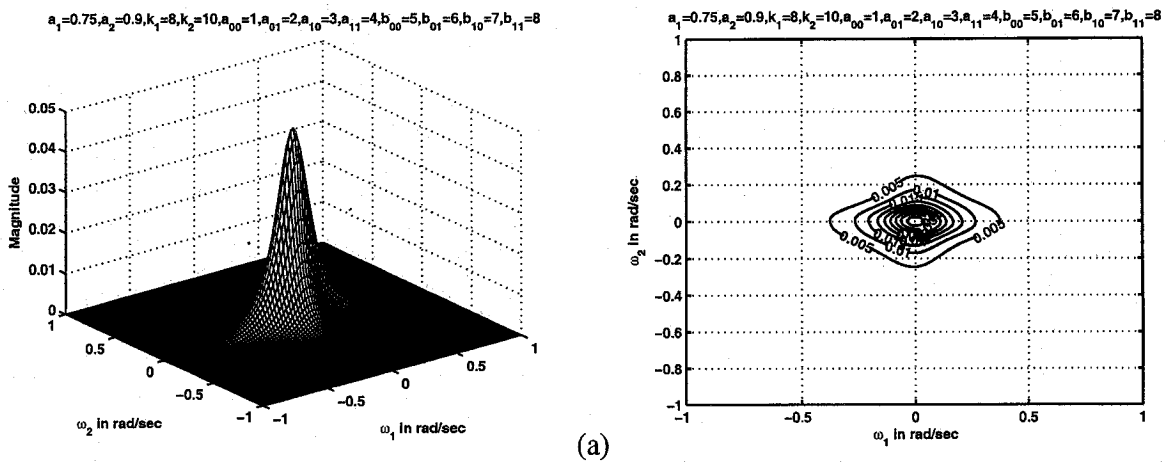

(a)

Figure 2.47: 3-D amplitude-frequency response and contour response of the 2-D digital lowpass filter in case 3 of set 4 (when $k_1 = 8$, $k_2 = 10$)

2.5.4.4 Case 4:

In this case,

$$a_1 = a_2 \quad , \quad k_1 = k_2 \quad , \quad b_1 = b_2 = 1$$

The ripples in the passband of the contour response in case 4 of set 3 for the values of $k_1 = k_2 = 0.25$ and for values of $a_1 = a_2 \geq 0.75$ as shown in Fig. 2.30 (b) disappears in this case of set 4 as shown in Fig. 2.48 (b). Also, in this case, there are ripples in the passband of the contour response for the values of $k_1 = k_2 = 0.5$ and for values of $a_1 = a_2 = 0.9$ as shown in Fig. 2.49 (c). The amplitude of the contour response in this case is slightly lower than that of the contour responses in case 4 of set 3 for the same values of k_1, k_2, a_1 and a_2. This can seen in Fig. 2.48 (b) of set 4 and in Fig. 2.30 (b) of case 4 in set 3. The passband of the contour response in this case of set 4 is smaller than the passband in case 4 of set 3 as shown in Fig. 2.49 (b) of set 4 and in Fig. 2.31 (c) of case 4 in set 3. Also the passband of the frequency response becomes very narrow for greater values of k_1 and k_2 (i.e., $k_1 = k_2 > 1$) as shown in Fig. 2.51 (c).

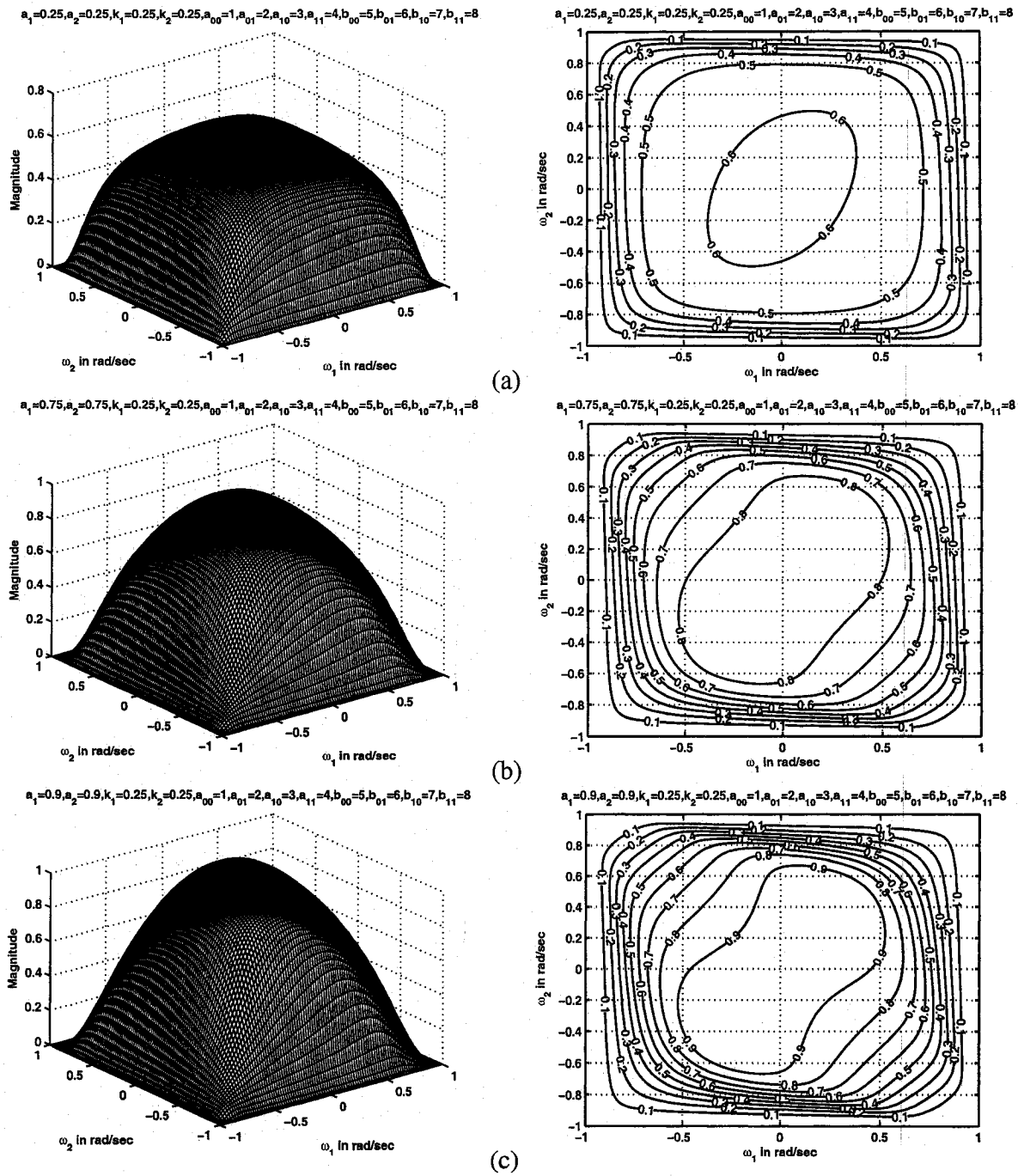

Figure 2.48: 3-D amplitude-frequency response and contour response of the 2-D digital lowpass filter in case 4 of set 4 (when $k_1 = k_2 = 0.25$)

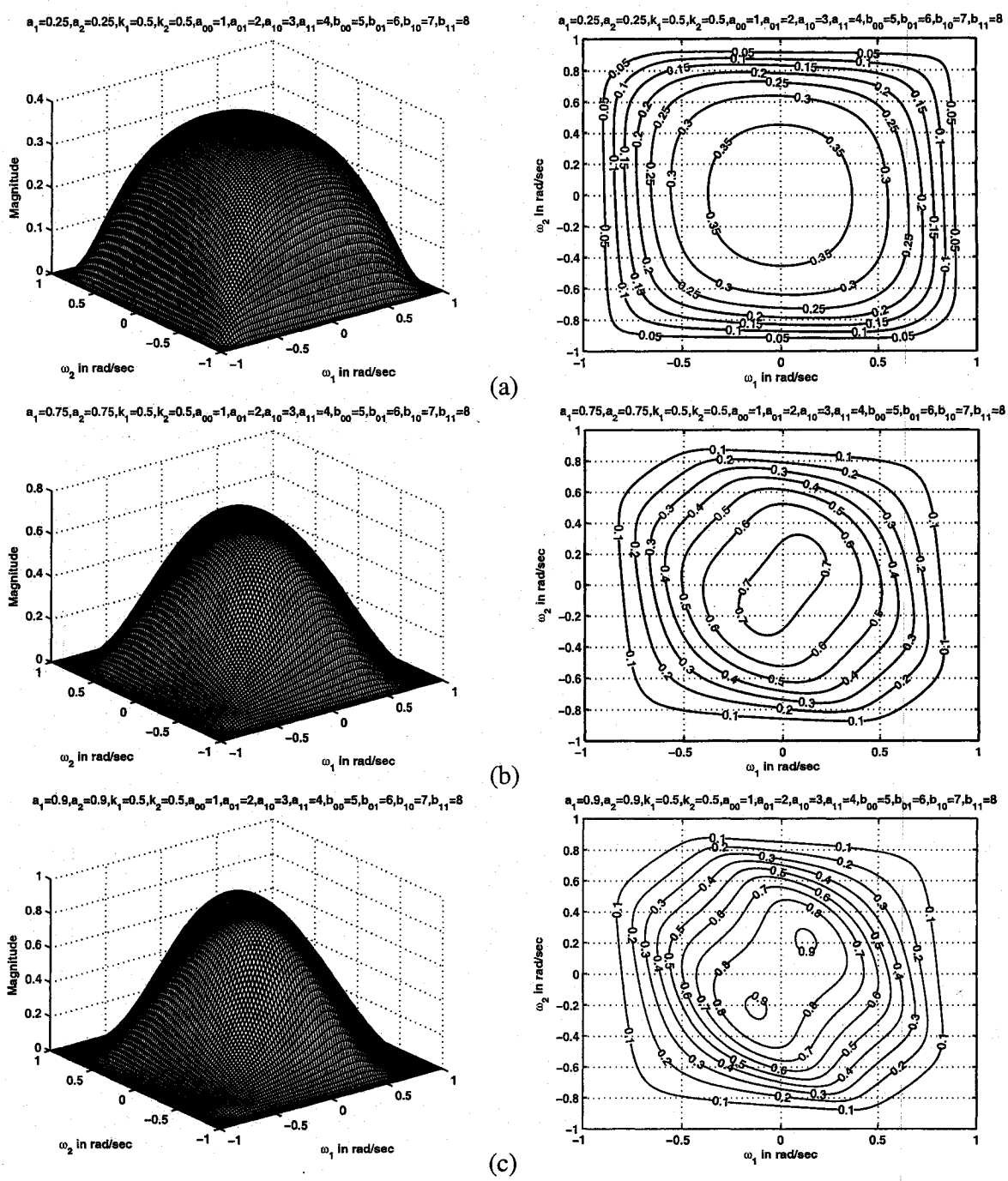

Figure 2.49: 3-D amplitude-frequency response and contour response of the 2-D digital lowpass filter in case 4 of set 4 (when $k_1 = k_2 = 0.5$)

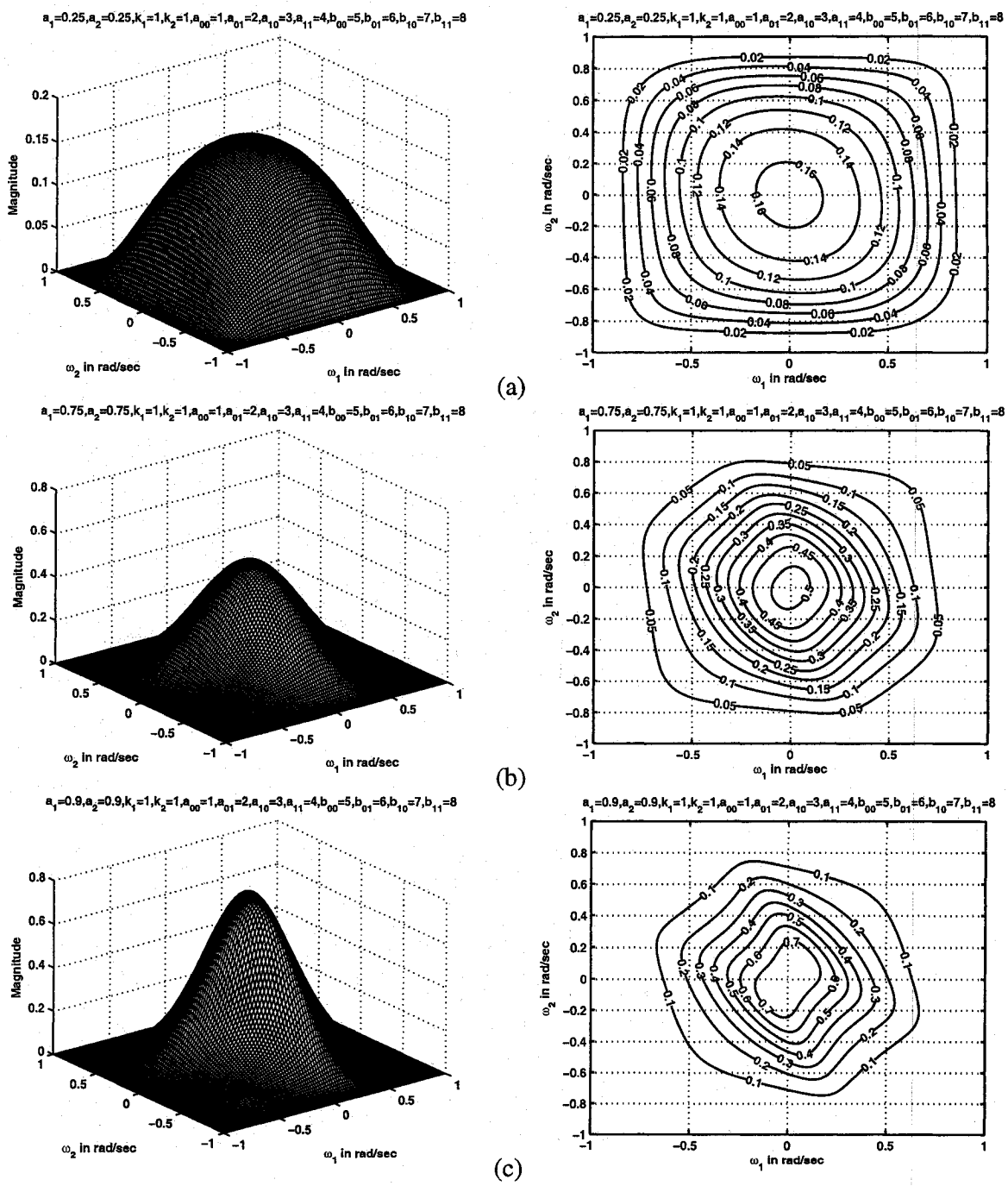

Figure 2.50: 3-D amplitude-frequency response and contour response of the 2-D digital lowpass filter in case 4 of set 4 (when $k_1 = k_2 = 1$)

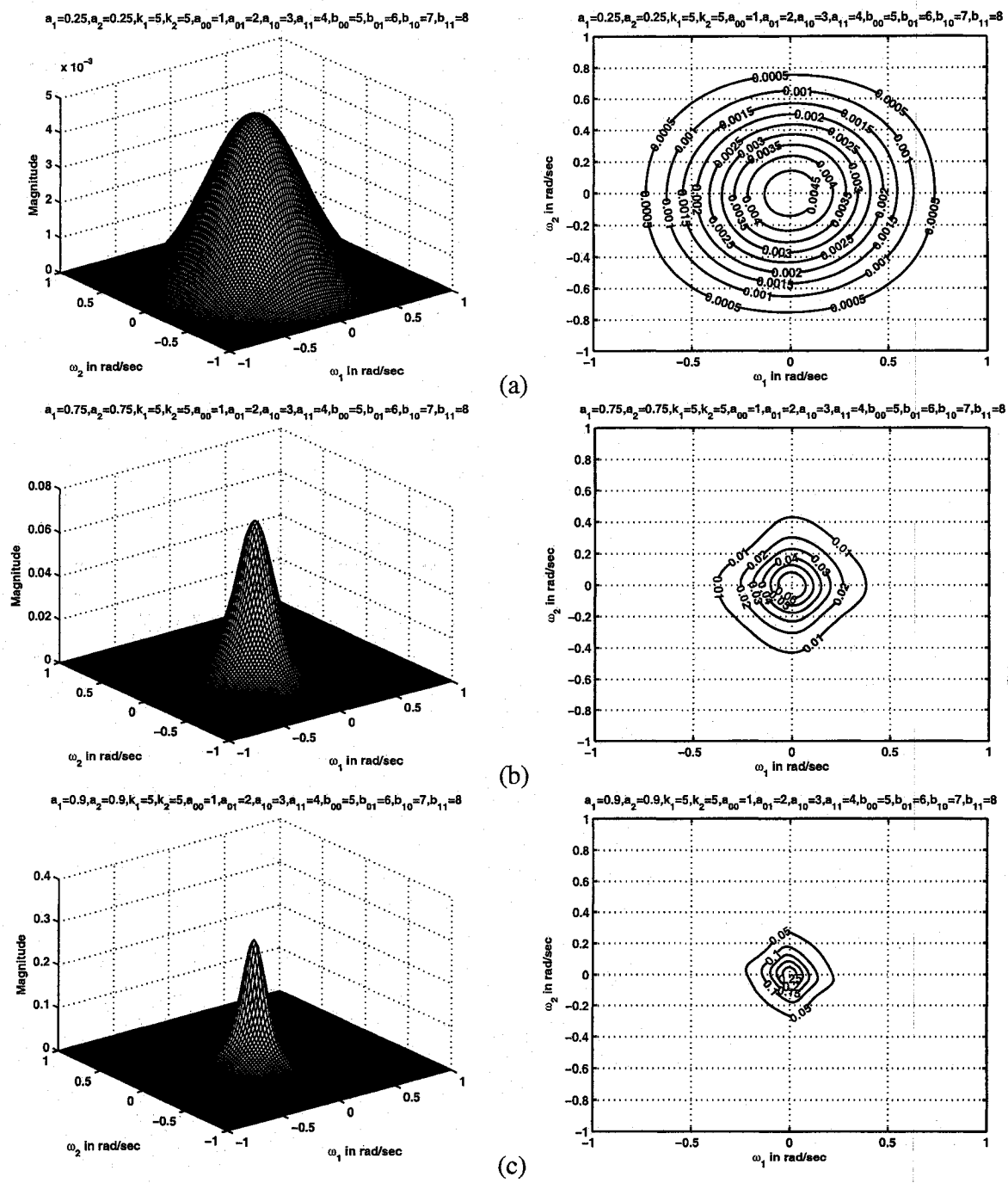

Figure 2.51: 3-D amplitude-frequency response and contour response of the 2-D digital lowpass filter in case 4 of set 4 (when $k_1 = k_2 = 5$)

2.6 Summary

It is observed in all the four cases that the coefficients k_1, k_2 affect the passband width and a_1, a_2 affect the gain of the amplitude-frequency response. As k_1 and k_2 values are increased, the passband width of the 2-D lowpass filter decreases and the amplitude of the contour response also decreases. As a_1 and a_2 values are increased, the magnitude of the amplitude-frequency response of the 2-D lowpass filter increases and the passband width decreases. Overall, the passband width decreases when k_1, k_2, a_1 and a_2 values are increased. Also, when the values of k_1, $k_2 \geq 1$, it can be observed in all the four cases that the contour responses are more elliptical in nature and they are close to circular in nature for further greater values of k_1 and k_2. In all the cases, values of k_1 and k_2 upto 10 have been studied. Higher values are not reported because the responses exhibit a tendency to repeat themselves.

In case 1 of set 1, there are ripples in the contour response for smaller values of k_1 and k_2 (i.e., when k_1, $k_2 \leq 0.5$) and for greater values of a_1 and a_2 (i.e., when a_1, $a_2 \geq 0.5$). In case 2 of set 1, there are ripples in the contour response for all values of a_1 and a_2 till $k_1 = k_2 \leq 0.75$. When $k_1 = k_2 > 0.75$, ripples in the contour response occurs only when both the values of a_1 and a_2 are greater than 0.5. Though there are no ripples in the contour response when the values of $k_1 = k_2 \gg 1$, the contour responses start to lose their elliptical nature for values of a_1 and a_2 greater than 0.5. Similar to case1, in cases 3 and 4, ripples in the contour response occur when one of the a_1, a_2 values is greater than 0.5 or when one of the k_1, k_2 values is ≤ 0.5.

An important obervation to be noted is that the responses for set 2 is the same as that of set 1. This is because of the resulting transfer function for set 2 is the same as the one used in set 1 as the transfer function does not depend on the coefficients of the VSHP polynomial. It only depends on the coefficients of the bilinear transformation.

In set 3, it can be observed that there are not many contour responses with ripples in set 3 when compared to set 1 except under a few circumstances. In case 1, there are no ripples

in the contour response for all values of k_1, k_2, a_1 and a_2. In case 2, there are ripples in the passband of the contour response when the values of k_1, k_2 are as low as 0.25 and for values of a_1, $a_2 \geq 0.5$ and also, the ripples in the passband occurs when the values of $k_1 = k_2 = 0.5$ and for values of a_1, $a_2 \geq 0.75$. In case 3, there are ripples in the passband of the contour response when the values of k_1, k_2 are as low as 0.25 and 0.5 respectively and the values of a_1, a_2 are 0.5 and 1 respectively and also it can be observed that the ripples in the passband occurs when the values of k_1, k_2 are 0.5 and 1 respectively and the values of a_1, a_2 are 0.75 and 1 respectively. In case 4, there are ripples in the passband of the contour response for the values of $k_1 = k_2 = 0.25$ and for values of $a_1 = a_2 \geq 0.75$. Also the amplitude of the contour response is low when compared to set 1 for the same values of k_1, k_2, a_1 and a_2. The frequency responses are more or less similar to set 1 for all values of a_1 and a_2 when k_1, $k_2 > 1$.

In set 4, the responses are similar to that of set 3. But the passband width is smaller in the contour responses of set 4 when compared to that of set 3. Also the magnitude of the contour response is smaller when compared to that of set 3. In case 1, there are ripples in the contour response when $a_1 = a_2$ = .75 and k_1, k_2=0.25, 0.5 respectively. In cases 2 and 3, there are no ripples in the passband of the contour response for all values k_1, k_2, a_1 and a_2. In case 4, there are ripples in the passband of the contour response for the values of $k_1 = k_2 = 0.5$ and for values of $a_1 = a_2 = 0.9$.

Chapter 3

Two Dimensional Highpass Filters from CFE

3.1 Introduction

In Chapter 2, we have discussed the study of lowpass filters. We know that the other types of filters like highpass and bandpass filters can be obtained from the equivalent lowpass filters, or the combinations of the same. Therefore, in this chapter, we will study 2-D digital highpass filters from their equivalent 2-D lowpass filters proposed in Chapter 2.

In Sec. 3.2, we generate 2-D digital highpass filter from its equivalent 2-D analog lowpass filter discussed in Chapter 2. In Sec. 3.3, we shall discuss about the classification of 2-D digital highpass filters. In Sec. 3.4, the different sets and cases in each set, proposed earlier will be discussed and the effect of the coefficients of the 2-D digital highpass filter on the amplitude-frequency response will be studied. Sec. 3.5 gives the summary and discussions of the results contained in this chapter.

3.2 Transfer function of 2-D Highpass Filter

A method of designing 2-D digital highpass filters is to start from the analog lowpass filter transfer function and then apply generalized bilinear transformation, [6], i.e., which is given by $s_i = k_i \frac{z_i + a_i}{z_i + b_i}$ where i=1, 2 for a 2-D filter, to obtain the digital filter transfer function. For the resulting 2-D filter to be stable, it is required that $k_i > 0$ and $0 \leq a_i \leq 1$ and for the filter to be a highpass filter, it is required that $-1 \leq b_i \leq 0$. Here we have assumed $b_i = -1$.

By applying the generalized bilinear transformation, i.e., eqn.(2.7) to the analog transfer function obtained by the inversion of CFE i.e., eqn.(2.20), we get

$$
\begin{aligned}
H(z_1, z_2) = \frac{a_{00}b_{00}(z_1+b_1)^2(z_2+b_2)^2}{} \qquad (3.1)\\
k_1^2(z_1+a_1)^2 \left[\begin{array}{l} a_{11}b_{11}k_2^2(z_2+a_2)^2 \\ +a_{10}b_{11}k_2(z_2+a_2)(z_2+b_2) \\ +a_{10}b_{10}(z_2+b_2)^2 \end{array} \right] + \\
k_1(z_1-a_1) \left[\begin{array}{l} a_{01}b_{11}k_2^2(z_2+a_2)^2(z_1+b_1) \\ +\left(\begin{array}{c} (a_{11}b_{00}+a_{00}b_{11}+a_{10}b_{01}+a_{01}b_{10})k_2 \\ (z_2+a_2)(z_2+b_2)(z_1+b_1) \end{array} \right) \\ +a_{10}b_{00}(z_2+b_2)^2(z_1+b_1) \end{array} \right] + \\
\left[\begin{array}{l} a_{01}b_{01}k_2^2(z_2+a_2)^2(z_1+b_1)^2 \\ + a_{01}b_{00}k_2(z_2+a_2)(z_2+b_2)(z_1+b_1)^2 + \\ a_{00}b_{00}(z_2+b_2)^2(z_1+b_1)^2 \end{array} \right]
\end{aligned}
$$

which is a 2-D digital highpass filter transfer function.

3.3 Classification of 2-D Highpass Filter

The 2-D highpass filters are classified into four sets and each set is further classified into four cases. The classification of the four sets are formed based on the coefficients of the CFE and the classification of the four cases involved in each set is based on the coefficients of the generalized bilinear transformation. The same four sets as discussed in Chapter 2 will be considered here and they are given in eqns.(2.24), (2.25), (2.26) and (2.27) respectively. Also the same four cases in each set as discussed in chapter 2 will be considered here with the exception of b_1 and b_2 values set to -1 as shown below.

Case 1:

$a_1 = a_2 \quad , \quad k_1 \neq k_2 \quad , \quad b_1 = b_2 = -1$

Case 2:

$a_1 \neq a_2 \quad , \quad k_1 = k_2 \quad , \quad b_1 = b_2 = -1$

Case 3:

$a_1 \neq a_2 \quad , \quad k_1 \neq k_2 \quad , \quad b_1 = b_2 = -1$

Case 4:

$a_1 = a_2 \quad , \quad k_1 = k_2 \quad , \quad b_1 = b_2 = -1$

The values of a_1 and a_2 vary from 0 to 1 and the values of k_1 and k_2 are greater than 0.

3.4 Frequency Responses of 2-D Digital Highpass Filter

Eqn.(3.1) gives the transfer function of the 2-D digital highpass filter. To investigate the manner in which each coefficient of the generalized bilinear transformation affects the magnitude response of the resulting 2-D highpass filter, we change the values of some of the coefficients or fix some of the coefficients to specific values.

Let us consider the transfer function coefficients and the bilinear transformation coefficients to be unity i.e., $a_1 = 1$, $a_2 = 1$, $b_1 = 1$, $b_2 = 1$, $k_1 = 1$, $k_2 = 1$, $a_{00} = 1$, $a_{10} = 1$, $a_{01} = 1$, $a_{11} = 1$, $b_{00} = 1$, $b_{10} = 1$, $b_{01} = 1$, $b_{11} = 1$. Under this condition, the 3-D

amplitude-frequency response and contour plots of the 2-D digital highpass filter are shown in Fig. 3.1.

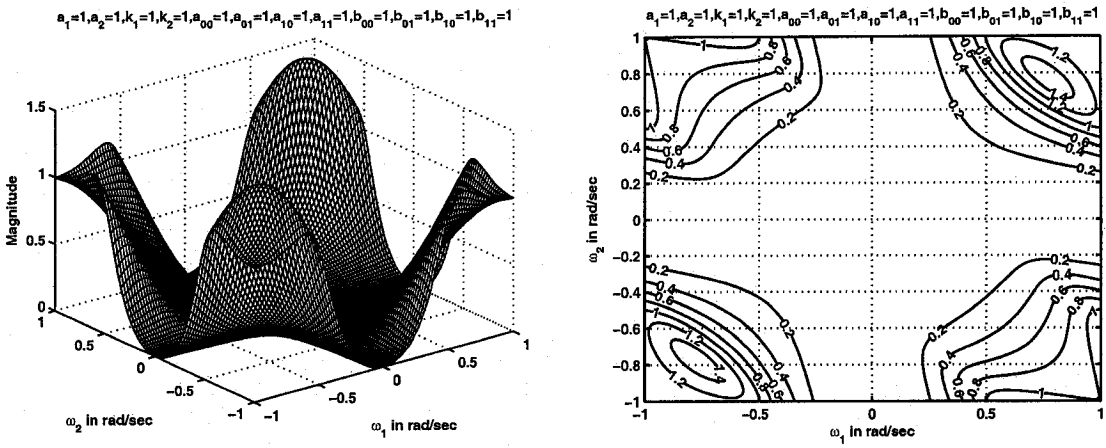

Figure 3.1: 3-D amplitude-frequency response and contour response of 2-D digital high pass filter when all the coefficients are unity

It is observed that there are ripples in the passband of the contour response of 2-D highpass filter. The ripples can be removed by reducing the values of a_1 and a_2 by a small fraction i.e., from 1 to 0.75 as will be later seen in Fig. 3.15 (b).

3.4.1 Frequency Response of 2-D digital Highpass Filters in Set 1

In this section, we study the manner in which all the four cases in set 1 affect the frequency response behavior of the resulting 2-D digital highpass filter. In this set, the values of all the coefficients of the CFE are considered to be the same, i.e.,

$$a_{00} = a_{01} = a_{10} = a_{11} = b_{00} = b_{01} = b_{10} = b_{11} \tag{3.2}$$

Different contour plots are obtained by varying the values of a_1, a_2, k_1 and k_2.

In this set, it is observed in all the four cases that the coefficients k_1, k_2 affect the stopband width and the coefficients a_1, a_2 affect the gain of the amplitude-frequency response. As k_1 and k_2 values are increased, the stopband width of the 2-D highpass filter

increases and also the magnitude of the contour response decreases. As a_1 and a_2 values are increased, the magnitude of the amplitude-frequency response of the 2-D highpass filter increases and also the stopband width increases. Overall, the cut-off frequencies are changed when k_1, k_2, a_1 and a_2 values are increased. It can be noticed that there is rounding of contour edges for higher values of k_1 and k_2. In this set, there are ripples in the contour response for smaller values of k_1 and k_2 and for larger values of a_1 and a_2. In all the four cases, it can be observed that the contours in the first and third quadrant of the contour response are mirror images of one another, and the contours in the second and fourth quadrant of the contour response are mirror images of one another.

3.4.1.1 Case 1:

In this case,

$$a_1 = a_2 \quad , \quad k_1 \neq k_2 \quad , \quad b_1 = b_2 = -1$$

As discussed above, the coefficients k_1, k_2 affect the stopband width of the 2-D digital highpass filter. As can be seen, in Fig. 3.2 (a), (b), (c) and Fig. 3.3 (a), there is a gradual decrease in the stopband width as the values of the coefficients k_1, k_2 are decreased from 2, 10 to 0.25, 0.5 respectively for the same values of $a_1 = a_2 = 0.25$. At the same time, there is also an increase in the magnitude of the contour response from 0.018 to 0.7 for the same.

The coefficients a_1 and a_2 affect the gain of the amplitude-frequency response as discussed in the above section. In Fig. 3.2 (c), Fig. 3.4 (a) and Fig. 3.5 (b), as a_1 and a_2 values are increased from 0.25 to 0.75, for the same values of $k_1 = 0.25$, $k_2 = 1$, the magnitude of the contour response increases from 0.55 to 0.8. In addition, the stopband width increases for the same.

It can be seen that for lower values of k_1, k_2, (i.e., when one of the k_1, k_2 values is less than 0.5) or for higher values of a_1 and a_2, (i.e., when $a_1 = a_2 \geq 0.5$), ripples are present on

the second and fourth quadrants and also it can also be observed that the magnitude of the second and fourth quadrants are slightly greater than that of the first and third quadrants.

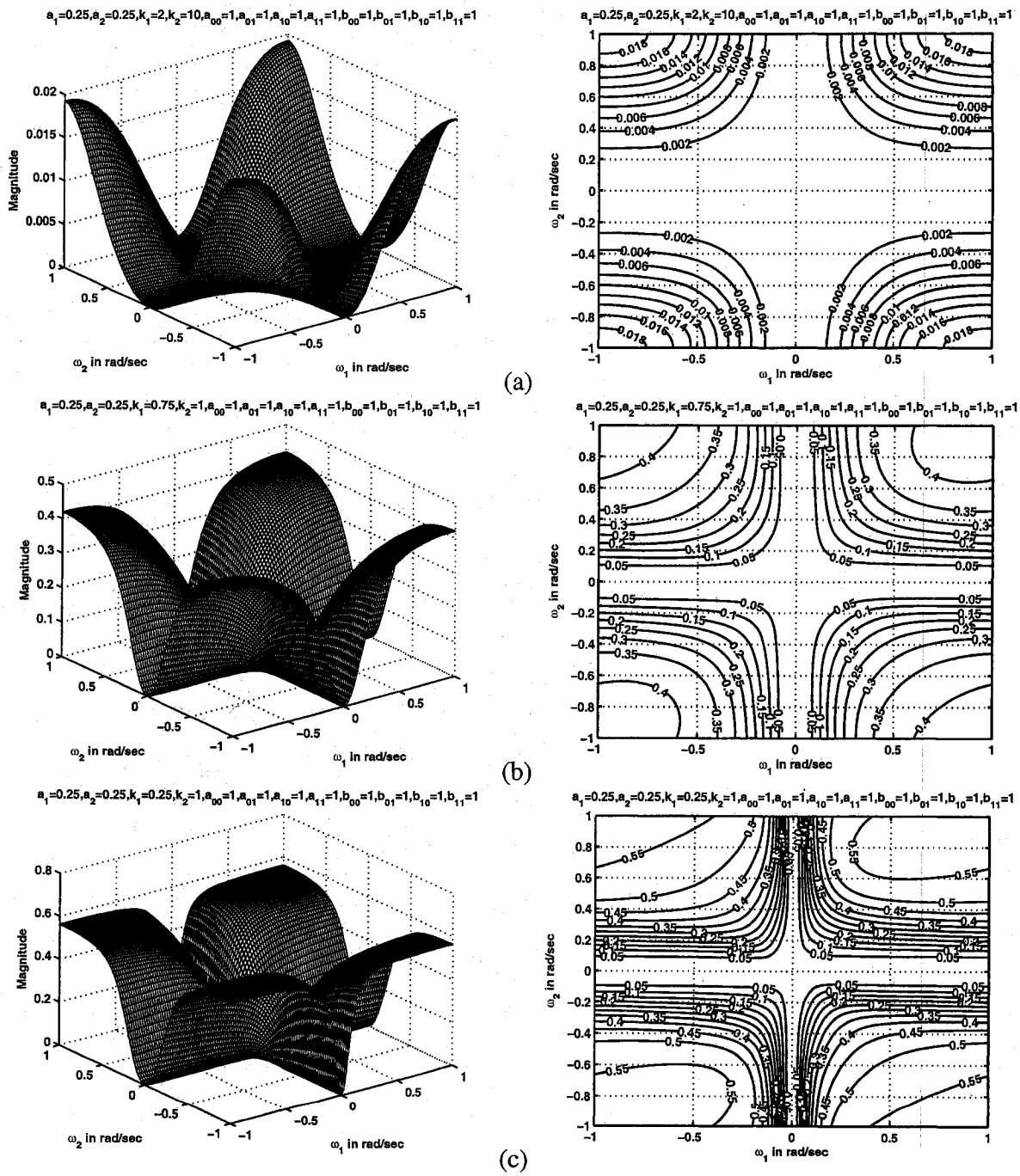

Figure 3.2: 3-D amplitude-frequency response and contour response of the 2-D digital highpass filter in case 1 of set 1 (when $a_1 = a_2 = 0.25$)

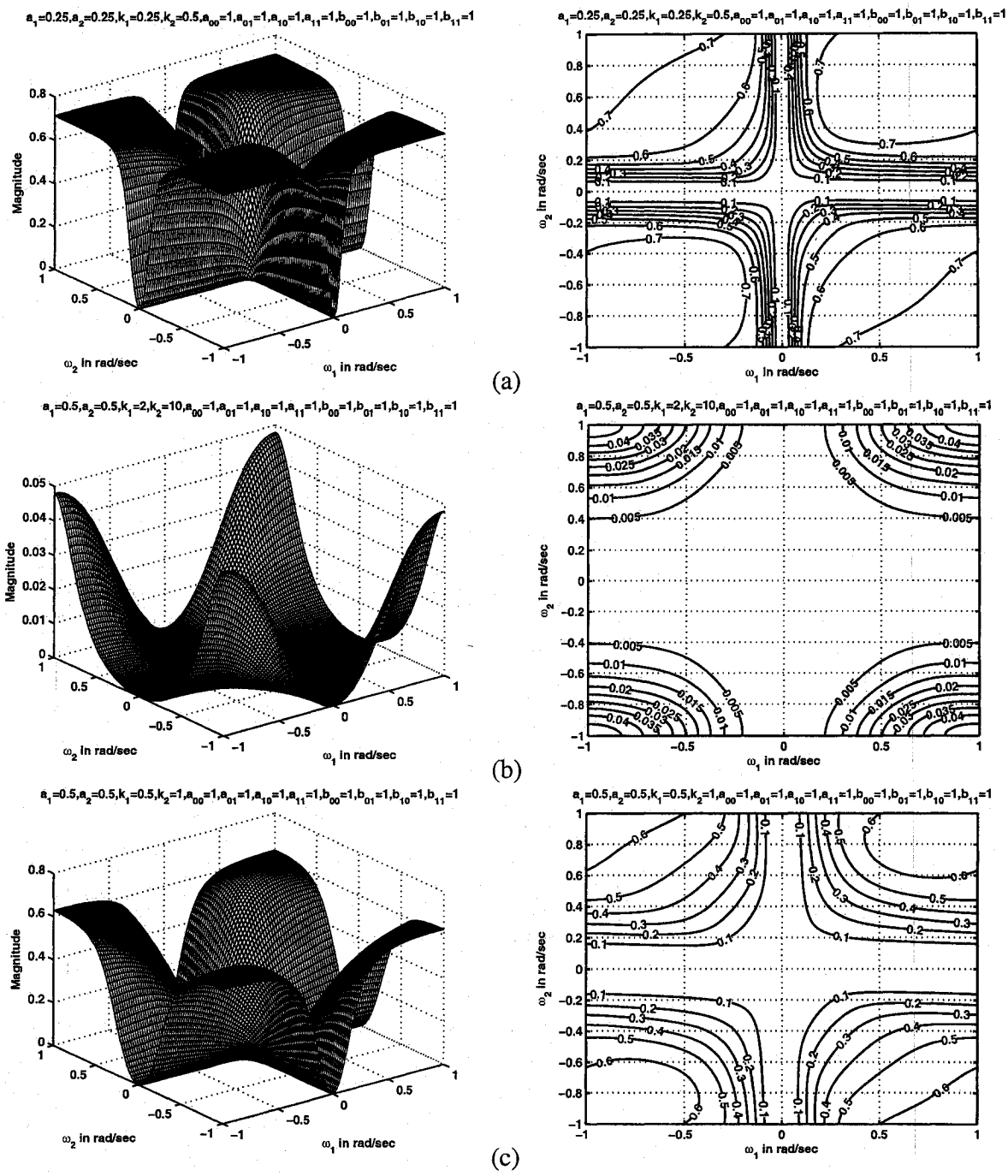

Figure 3.3: 3-D amplitude-frequency response and contour response of the 2-D digital highpass filter in case 1 of set 1 (when $a_1 = a_2 = 0.25,\ 0.5$)

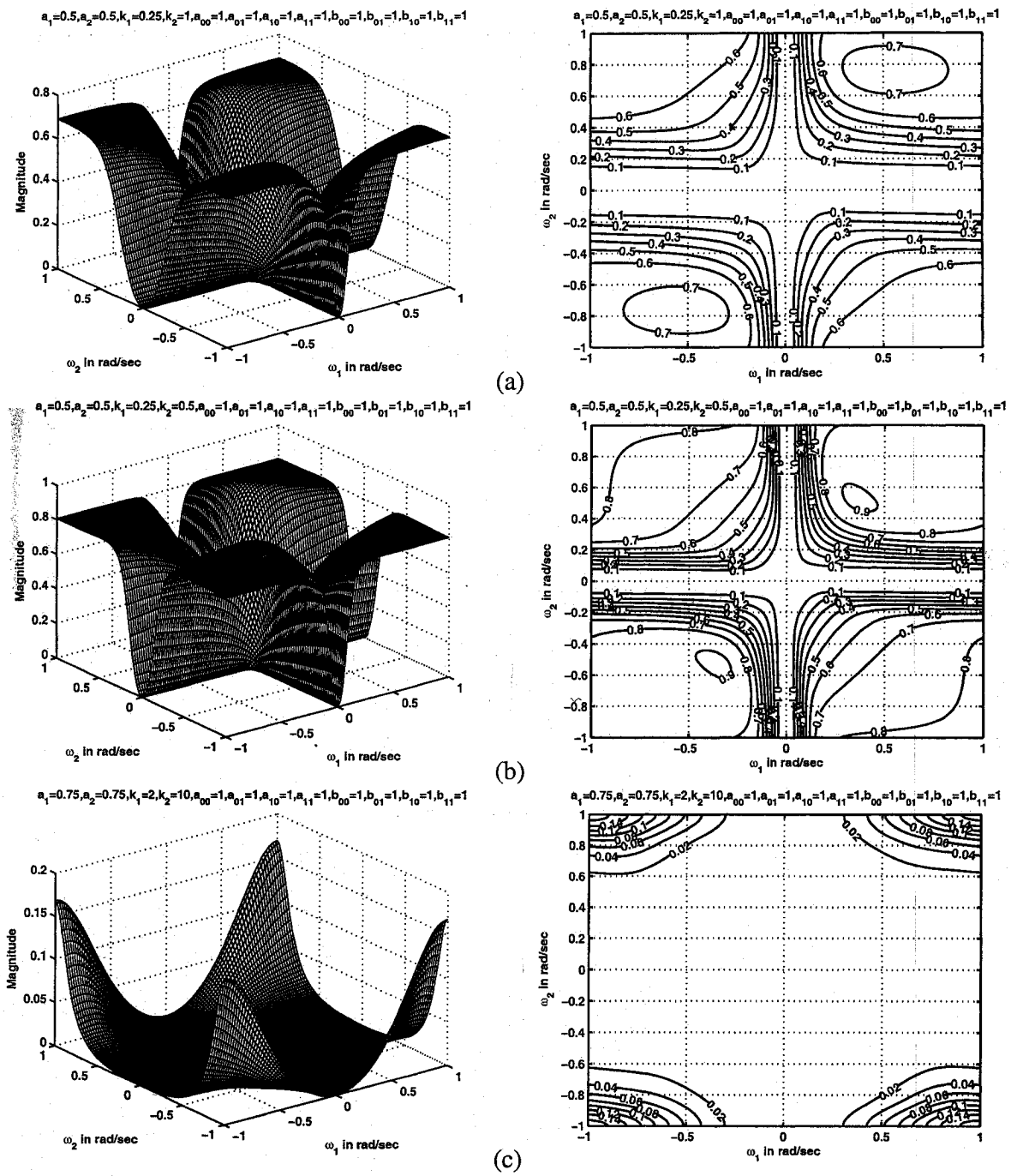

Figure 3.4: 3-D amplitude-frequency response and contour response of the 2-D digital highpass filter in case 1 of set 1 (when $a_1 = a_2 = 0.5,\ 0.75$)

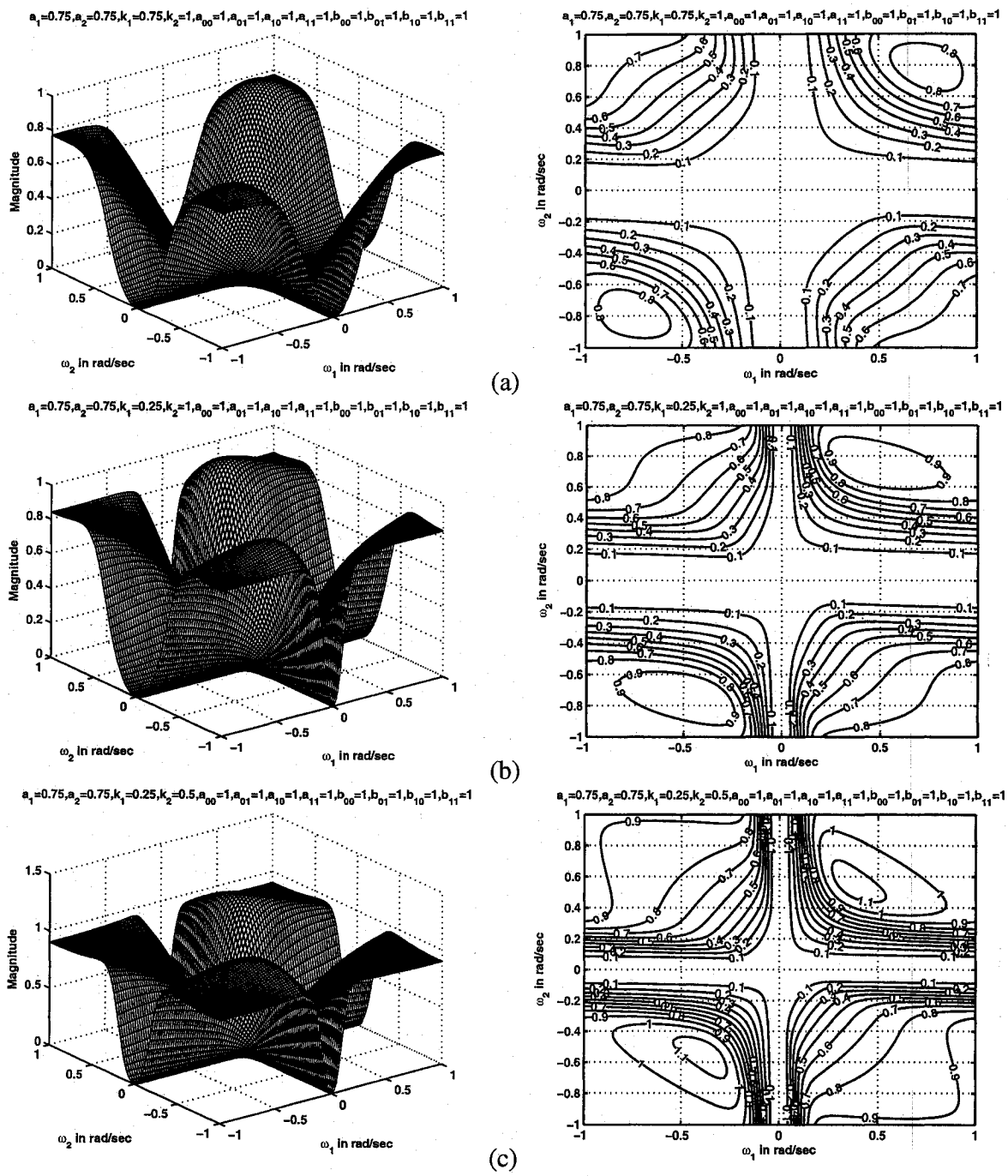

Figure 3.5: 3-D amplitude-frequency response and contour response of the 2-D digital highpass filter in case 1 of set 1 (when $a_1 = a_2 = 0.75$)

3.4.1.2 Case 2:

In this case,

$$a_1 \neq a_2 \quad , \quad k_1 = k_2 \quad , \quad b_1 = b_2 = -1$$

The coefficients k_1 and k_2 affect the stopband width of the 2-D digital highpass filter. When Fig. 3.6 (a), (c) , Fig. 3.7 (c) and Fig. 3.8 (b) are considered, there is a gradual increase in the stopband width as the values of k_1 and k_2 are increased from 0.5 to 5 for the same values of $a_1 = 0.25$, $a_2 = 0.5$. At the same time, there is also a decrease in the magnitude of the contour response for the same.

The coefficients a_1 and a_2 affect the gain of the amplitude-frequency response as discussed in the above section. In Fig. 3.6 (c), Fig. 3.7 (a), (b), as a_1 and a_2 values are increased from 0.25, 0.5 to 0.5, 0.75 respectively, it is observed that the magnitude of the contour response increases from 0.5 to 0.7 for the same values of $k_1 = k_2 = 0.75$. Also, the stopband width increases for the same.

It can be noticed that the contours in the first and third quadrants are mirror images of one another and the contours in the second and fourth quadrants are mirror images of one another. For very low vaues of k_1 and k_2, i.e., when $k_1 = k_2 < 0.75$, there are ripples in the contour response for all values of a_1 and a_2 and also the magnitude of the contours on the second and fourth quadrants is slightly greater than that of the first and third quadrants. It can be observed that there is rounding of contour edges for higher values of k_1 and k_2 as shown in Fig. 3.8 (b).

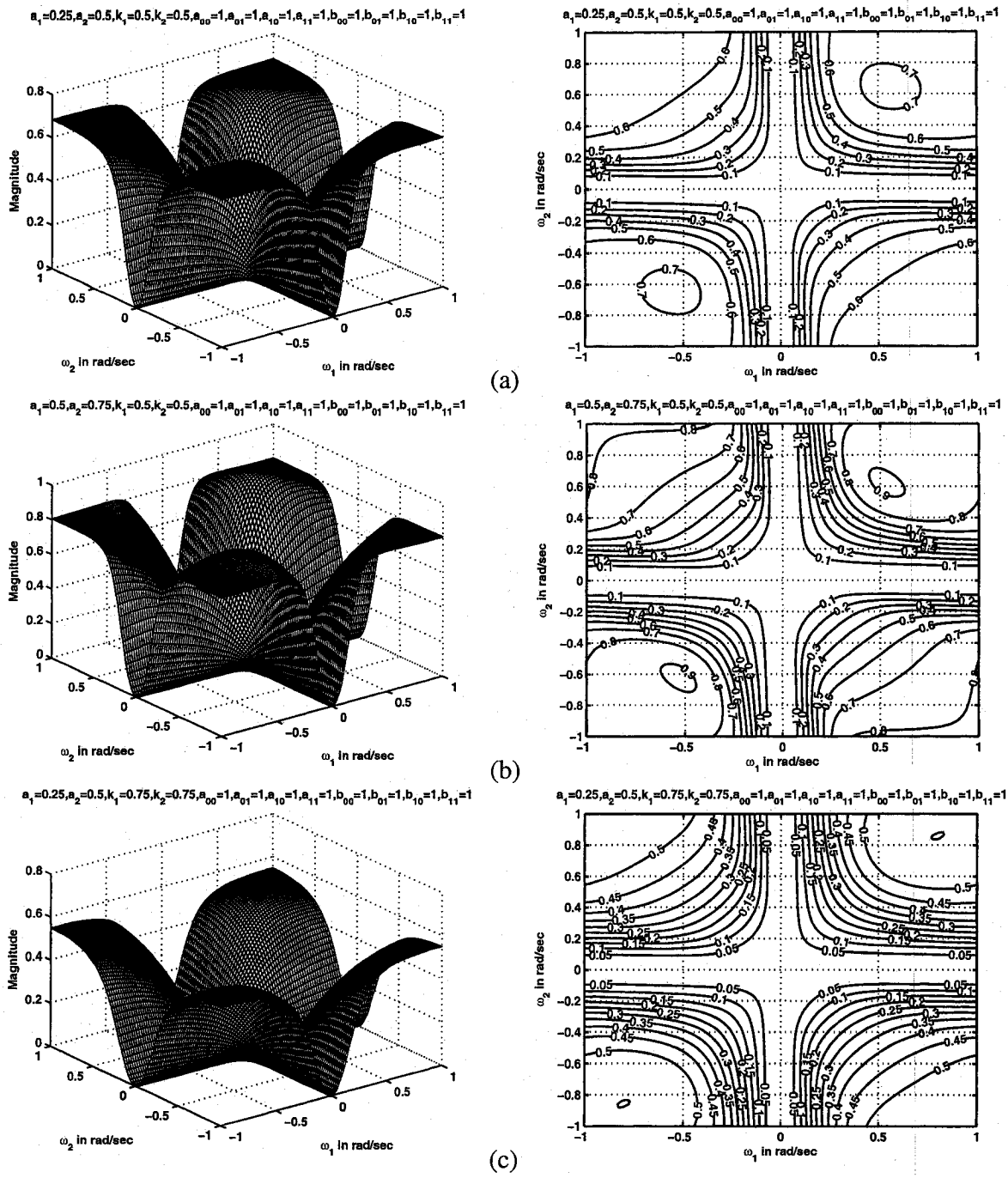

Figure 3.6: 3-D amplitude-frequency response and contour response of the 2-D digital highpass filter in case 2 of set 1 (when $k_1 = k_2 = 0.5,\ 0.75$)

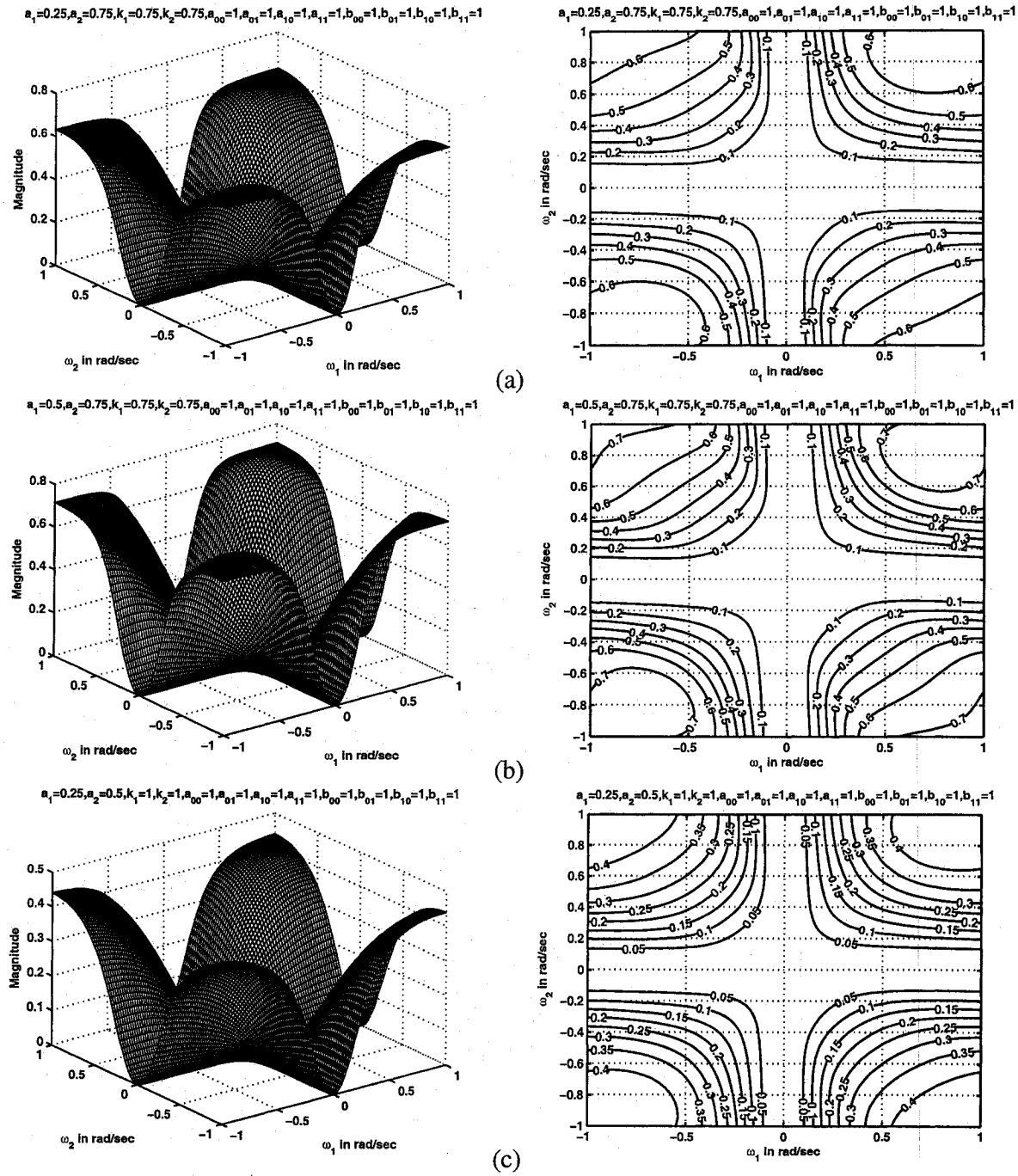

Figure 3.7: 3-D amplitude-frequency response and contour response of the 2-D digital highpass filter in case 2 of set 1 (when $k_1 = k_2 = 0.75,\ 1$)

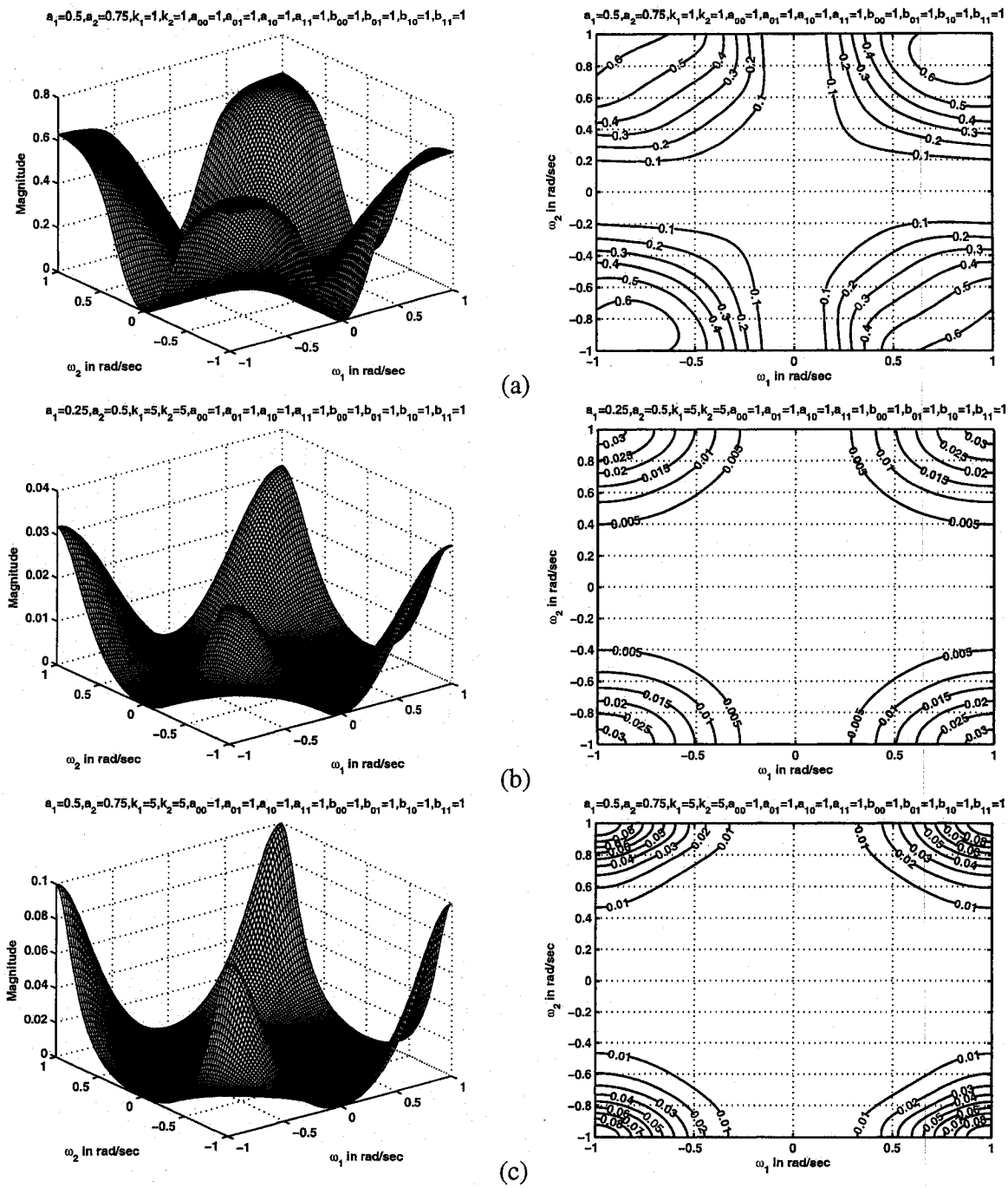

Figure 3.8: 3-D amplitude-frequency response and contour response of the 2-D digital highpass filter in case 2 of set 1 (when $k_1 = k_2 = 1, 5$)

3.4.1.3 Case 3:

In this case,

$$a_1 \neq a_2 \quad , \quad k_1 \neq k_2 \quad , \quad b_1 = b_2 = -1$$

The coefficients k_1 and k_2 affect the stopband width of the 2-D highpass filter. For example, in Fig. 3.9 (a), (c), Fig. 3.10 (b), Fig. 3.11 (b), Fig. 3.12 (a), there is a gradual increase in the stopband width, as the values of k_1 and k_2 are increased from 0.25, 0.5 to 2, 10 respectively for the same values of $a_1 = 0.25$, $a_2 = 0.5$. At the same time, there is also a decrease in the magnitude of the contour response from 0.8 to 0.03 for the same.

The coefficients a_1 and a_2 affect the gain of the amplitude-frequency response as discussed in the above section. In Fig. 3.10 (b), (c) and Fig. 3.11 (a), as a_1 and a_2 values are increased from 0.25, 0.5 to 0.5, 0.75 respectively, for the same values of $k_1 = 0.5$, $k_2 = 1$, the magnitude of the contour response increases from 0.55 to 0.7. Also, there is an increase in the stopband width for the same values.

It can be noticed that the contours in the first and third quadrant are mirror images of one another and the contours in the second and fourth quadrant are mirror images of one another. In this case, as $a_1 \neq a_2$ and $k_1 \neq k_2$, ripples in the contour response occur when a_1 *or* $a_2 \geq 0.5$ or when one of the k_1 *or* $k_2 \leq 0.5$ and also the magnitude of the contours on the second and fourth quadrant is slightly greater than that of the first and third quadrants. It can be noticed that there is rounding of contour edges for higher values of k_1 and k_2 as shown in Fig. 3.12 (a), (b).

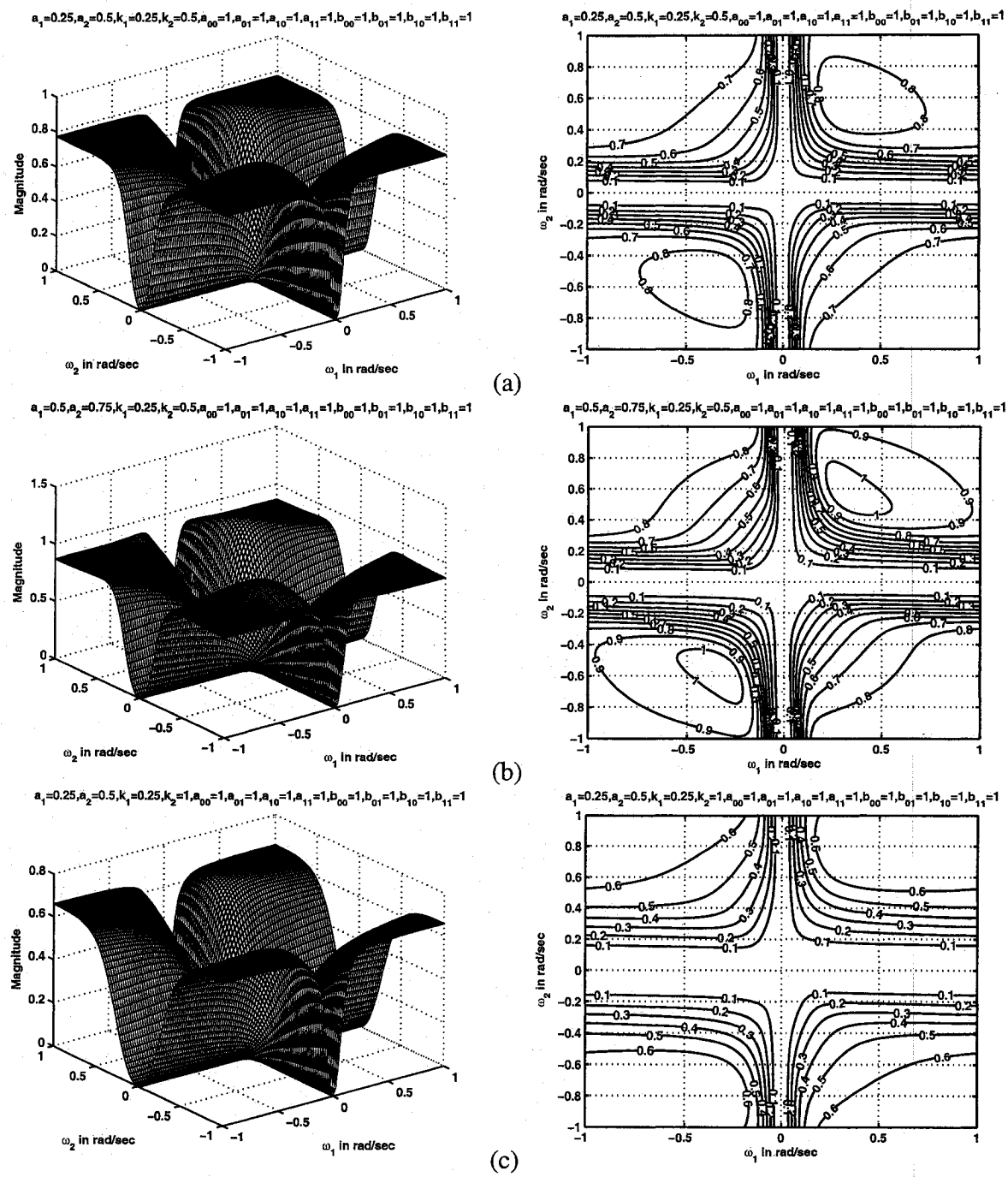

Figure 3.9: 3-D amplitude-frequency response and contour response of the 2-D digital highpass filter in case 3 of set 1 (when $k_1 = 0.25$, $k_2 = 0.5$, 1)

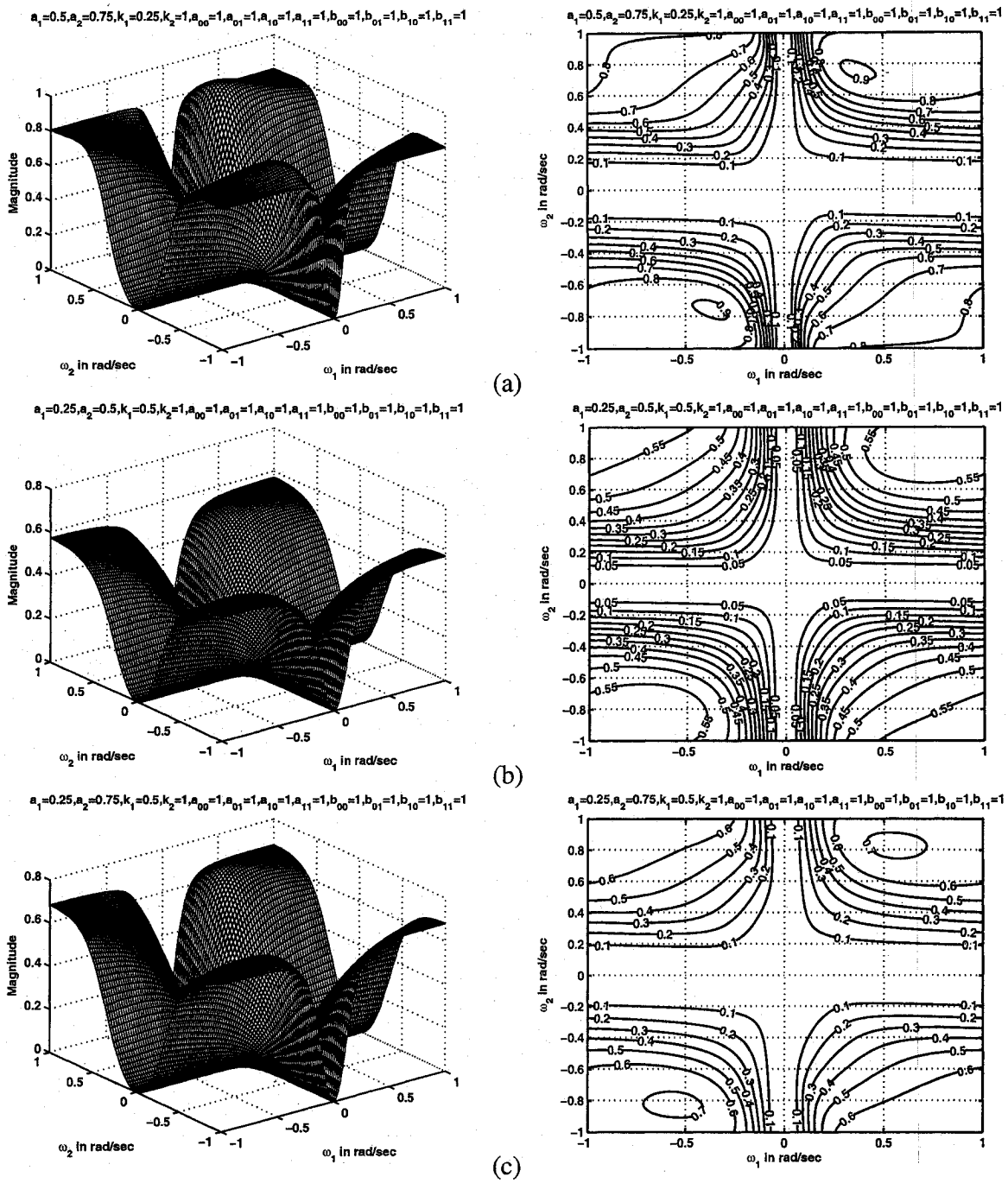

Figure 3.10: 3-D amplitude-frequency response and contour response of the 2-D digital highpass filter in case 3 of set 1 (when $k_1 = 0.25,\ 0.5,\ k_2 = 1$)

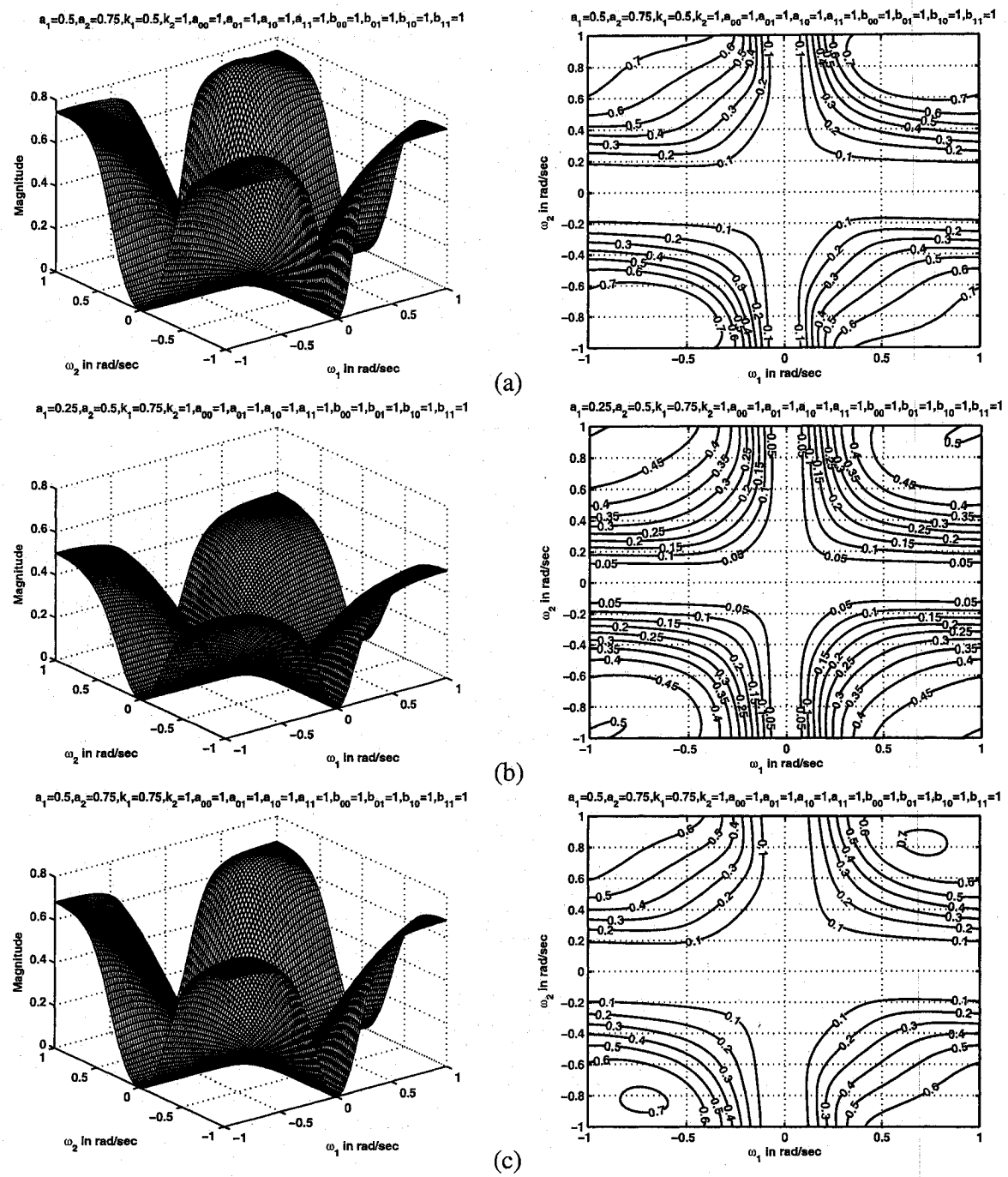

Figure 3.11: 3-D amplitude-frequency response and contour response of the 2-D digital highpass filter in case 3 of set 1 (when $k_1 = 0.5,\ 0.75,\ k_2 = 1$)

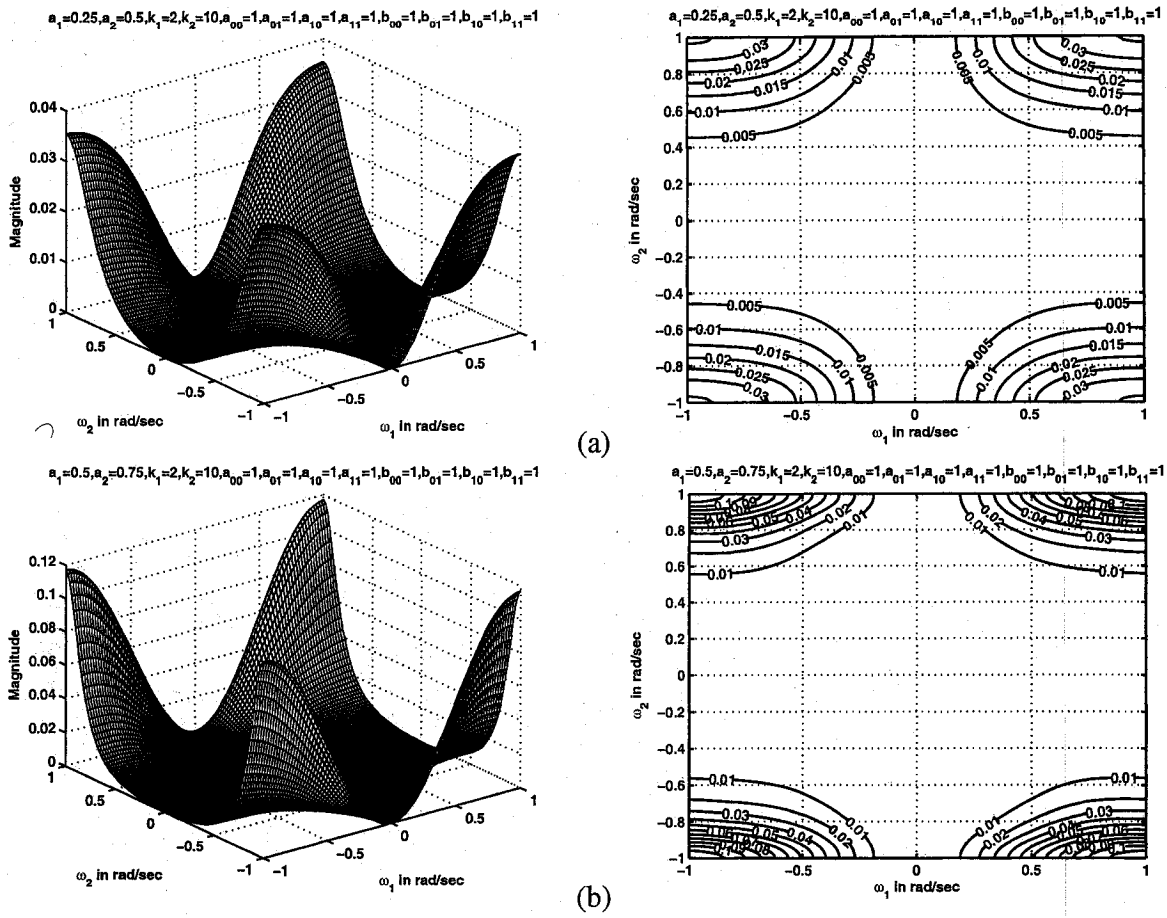

Figure 3.12: 3-D amplitude-frequency response and contour response of the 2-D digital highpass filter in case 3 of set 1 (when $k_1 = 2$, $k_2 = 10$)

3.4.1.4 Case 4:

In this case,

$$a_1 = a_2 \quad , \quad k_1 = k_2 \quad , \quad b_1 = b_2 = -1$$

The coefficients k_1 and k_2 affect the stopband width of the 2-D highpass filter. In Fig. 3.13 (a), Fig. 3.14 (b) and Fig. 3.15 (a), (c), there is a gradual increase in the stopband width as the values of k_1 and k_2 are increased from 0.25 to 5 for the same values of $a_1 = a_2 = 0.25$. At the same time, there is also a decrease in the magnitude of the contour

response for the same.

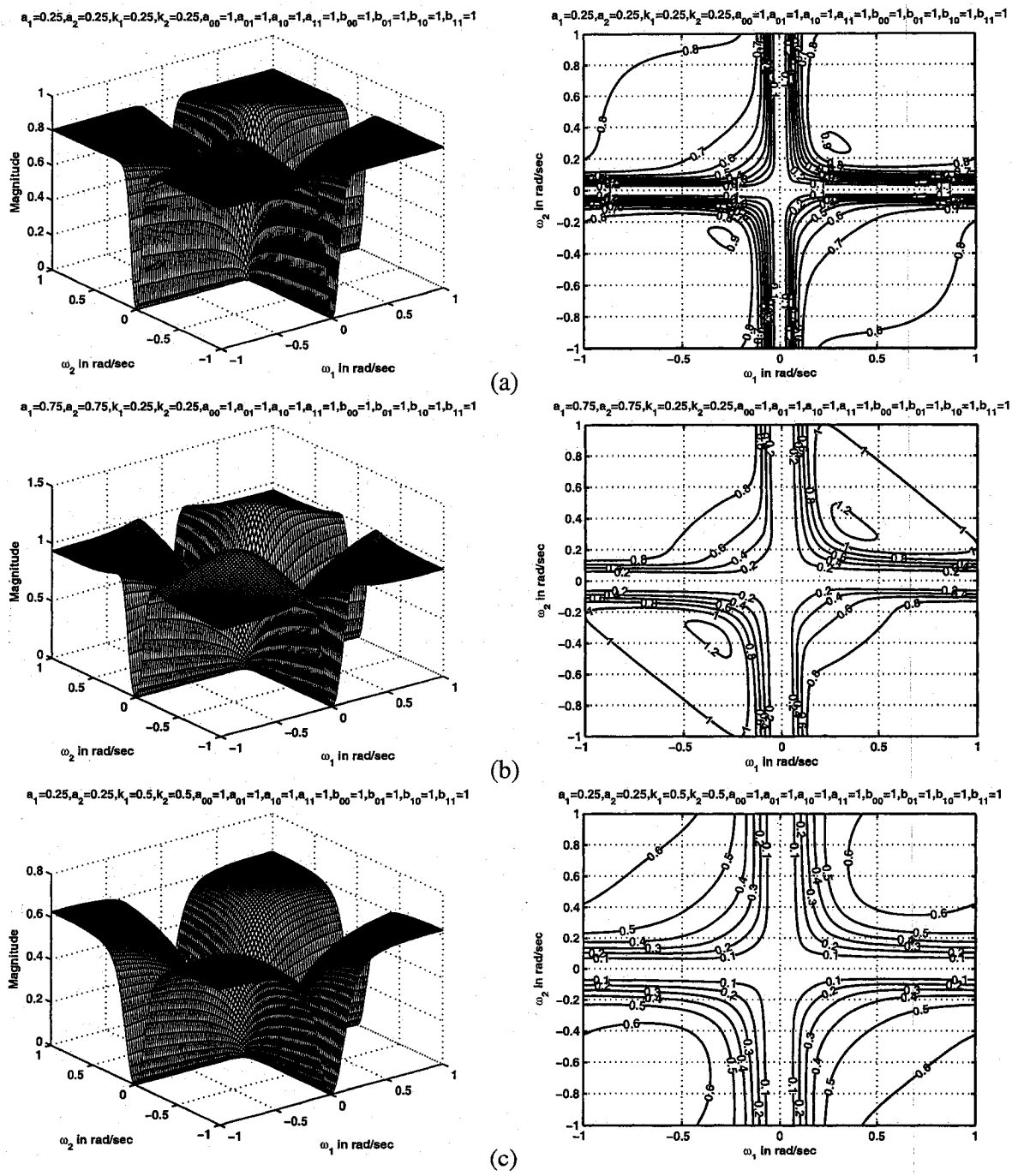

Figure 3.13: 3-D amplitude-frequency response and contour response of the 2-D digital highpass filter in case 4 of set 1 (when $k_1 = k_2 = 0.25,\ 0.5$)

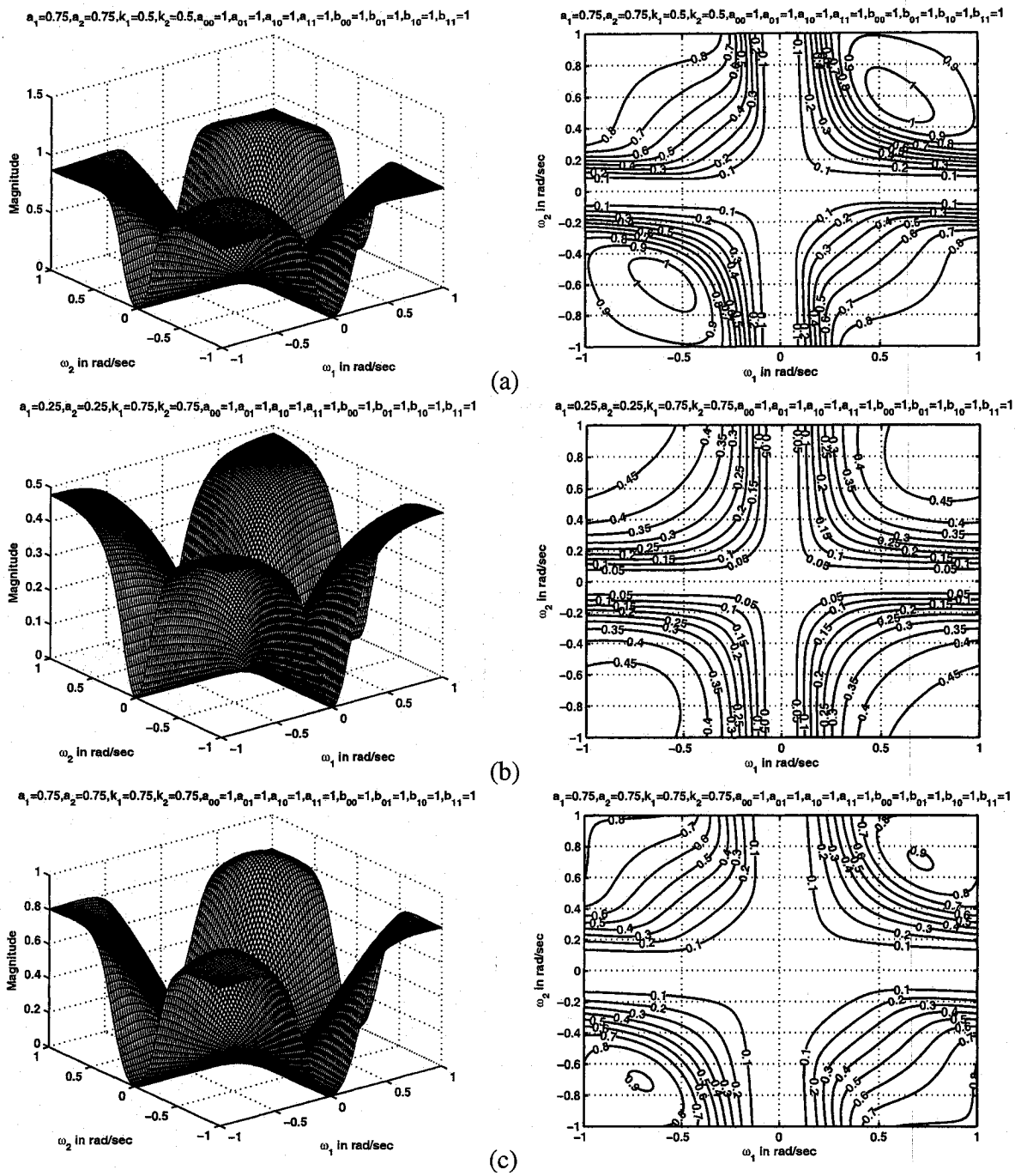

Figure 3.14: 3-D amplitude-frequency response and contour response of the 2-D digital highpass filter in case 4 of set 1 (when $k_1 = k_2 = 0.5,\ 0.75$)

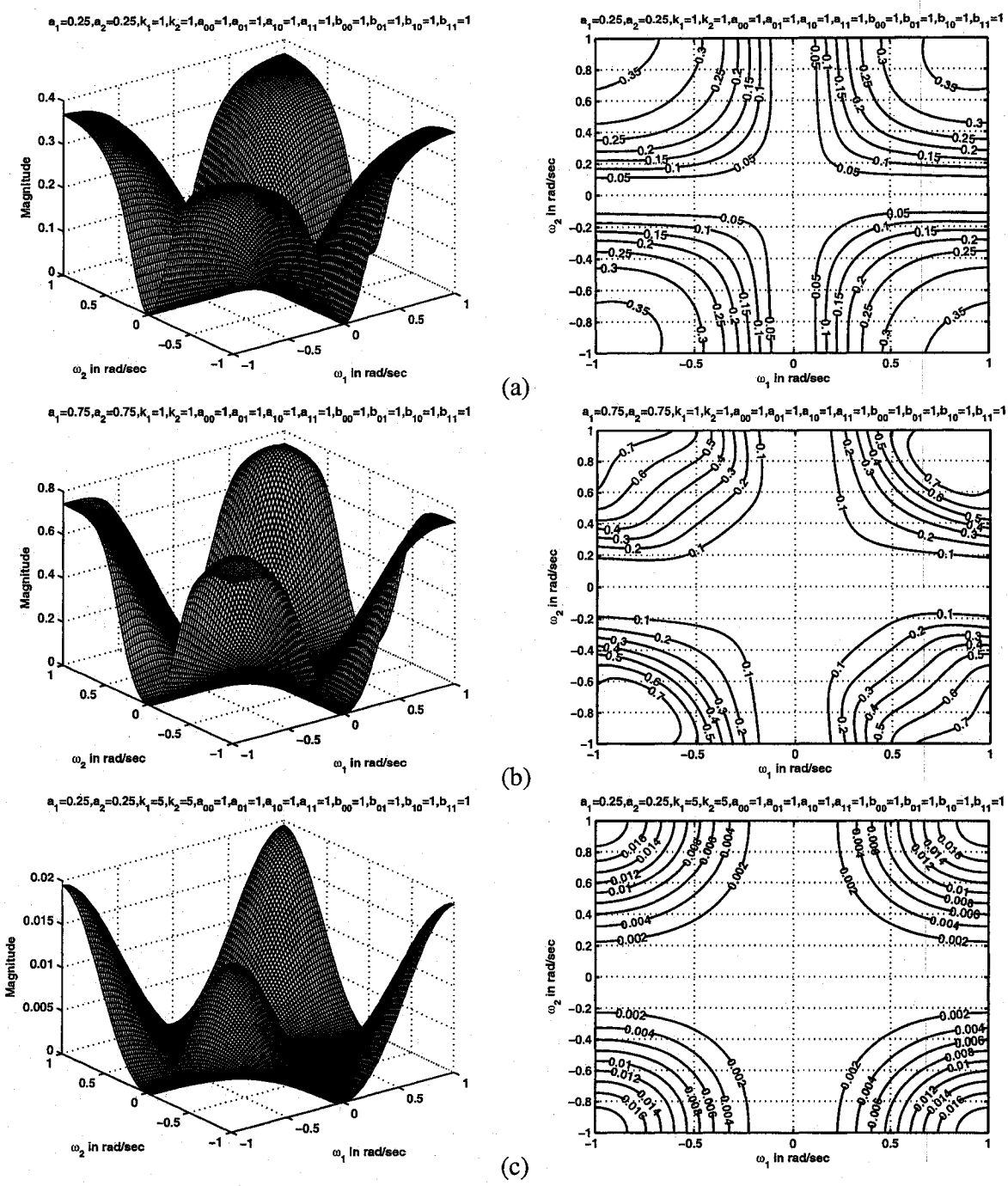

Figure 3.15: 3-D amplitude-frequency response and contour response of the 2-D digital highpass filter in case 4 of set 1 (when $k_1 = k_2 = 1, 5$)

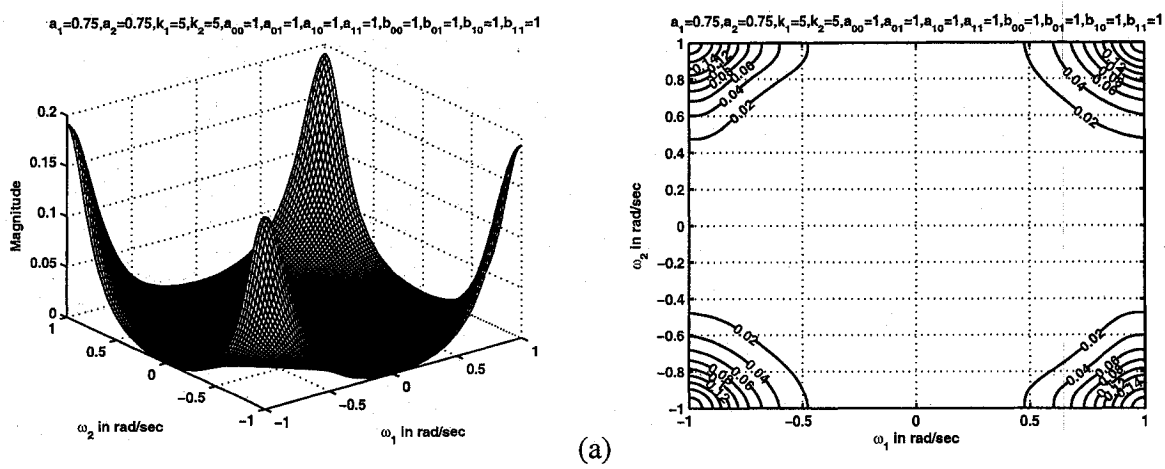

(a)

Figure 3.16: 3-D amplitude-frequency response and contour response of the 2-D digital highpass filter in case 4 of set 1 (when $k_1 = k_2 = 5$)

The coefficients a_1 and a_2 affect the gain of the amplitude-frequency response. In Fig. 3.15 (a), (b), as a_1 and a_2 values are increased from 0.25 to 0.75 respectively, for the same values of $k_1 = k_2 = 1$, the magnitude of the contour response increases from 0.35 to 0.7.

It can be noticed that the contours in the first and third quadrant are mirror images of one another and the contours in the second and fourth quadrant are mirror images of one another. There are ripples in the contour response for values of a_1 and a_2 greater than 0.5 or for values of k_1 and k_2 less than 0.5 as shown in Fig. 3.13 (a), (b) and in Fig. 3.14 (a), (c) and also the magnitude of the contours in the second and fourth quadrant is slightly greater than that of the first and third quadrants. When $k_1 = k_2 \geq 1$, there are no ripples in the contour response even for greater values of a_1 and a_2. It can be noticed that there is rounding of contour edges for higher values of k_1 and k_2 as shown in Fig. 3.15 (c).

3.4.2 Frequency Response of 2-D High Pass Filters in Set 2

In this set,

$$\begin{aligned} a_{00} &= a_{01} = a_{10} = a_{11} \\ b_{00} &= b_{01} = b_{10} = b_{11} \end{aligned} \tag{3.3}$$

When the above combination of coefficients are substituted in eqn.(3.1), the resulting transfer function is the same as the one used in set 1, as the transfer function does not depend on the coefficients of the CFE. It only depends on the coefficients of the generalized bilinear transformation. Hence the responses for set 2 is the same as that of set 1.

3.4.3 Frequency Response of 2-D High Pass Filters in Set 3

In this section, we study the manner in which all the four cases in set 3 affect the frequency response behavior of the resulting 2-D highpass filter. Also, we compare the frequency responses in this set with that of the responses in set 1. Here, we have,

$$\begin{aligned} a_{00} &= a_{11} \\ a_{01} &= a_{10} \\ b_{00} &= b_{11} \\ b_{01} &= b_{10} \end{aligned} \tag{3.4}$$

Different contour plots are obtained by varying the values of a_1, a_2, k_1 and k_2.

Similar to set 1, in set 3, it is observed in all the four cases that the coefficients k_1, k_2 affect the stopband width and the coefficients a_1, a_2 affect the gain of the amplitude-frequency response. As k_1 and k_2 values are increased, the stopband width of the 2-D highpass filter increases and the magnitude of the amplitude frequency response also decreases. As a_1 and a_2 values are increased, the magnitude of the amplitude-frequency response of the 2-D highpass filter increases and the stopband width increases. Overall, the cut-off frequencies of the 2-d highpass filters change when k_1, k_2, a_1 and a_2 values are

increased. Also, it can be noticed that there is rounding of contour edges for higher values of k_1 and k_2.

It can be observed that there are not many ripples in the contour response when compared to set 1 except under few circumstances which shall be dealt later in this section. Also the magnitude of the contour response is low when compared to set 1 for the same values of k_1, k_2, a_1 and a_2. The amplitude-frequency responses are more or less similar to set 1 for all values of a_1 and a_2, when k_1, $k_2 > 1$. It can be noticed that the contours in the first and third quadrant are mirror images of one another and the contours in the second and fourth quadrant are mirror images of one another.

3.4.3.1 Case 1:

In this case,

$$a_1 = a_2 \quad , \quad k_1 \neq k_2 \quad , \quad b_1 = b_2 = -1$$

It is observed that the coefficients k_1 and k_2 affect the stopband width and the coefficients a_1 and a_2 affect the gain of the amplitude-frequency response. As k_1 and k_2 values are increased, the stopband width of the 2-D highpass filter increases and the magnitude of the amplitude-frequency response decreases. As a_1 and a_2 values are increased, the magnitude of the amplitude-frequency response of the 2-D highpass filter increases and the stopband width increases. Overall, the cut-off frequencies of the 2-D highpass filter changes when k_1, k_2, a_1 and a_2 values are increased.

In this case, there are no ripples in the contour response of the 2-D highpass filter for all values of k_1, k_2, a_1 and a_2. The magnitude of the contour responses in this case of set 3 is lower than that of the contour responses in case 1 of set 1 for the same values of k_1, k_2, a_1 and a_2. It is noted that, the magnitude of the contour response in Fig. 3.3 (a) is 0.7 whereas the magnitude for the same values in Fig. 3.18 (a) is 0.5. The edges of the contours are

sharper for values of $k_1,\ k_2 \leq 0.5$.

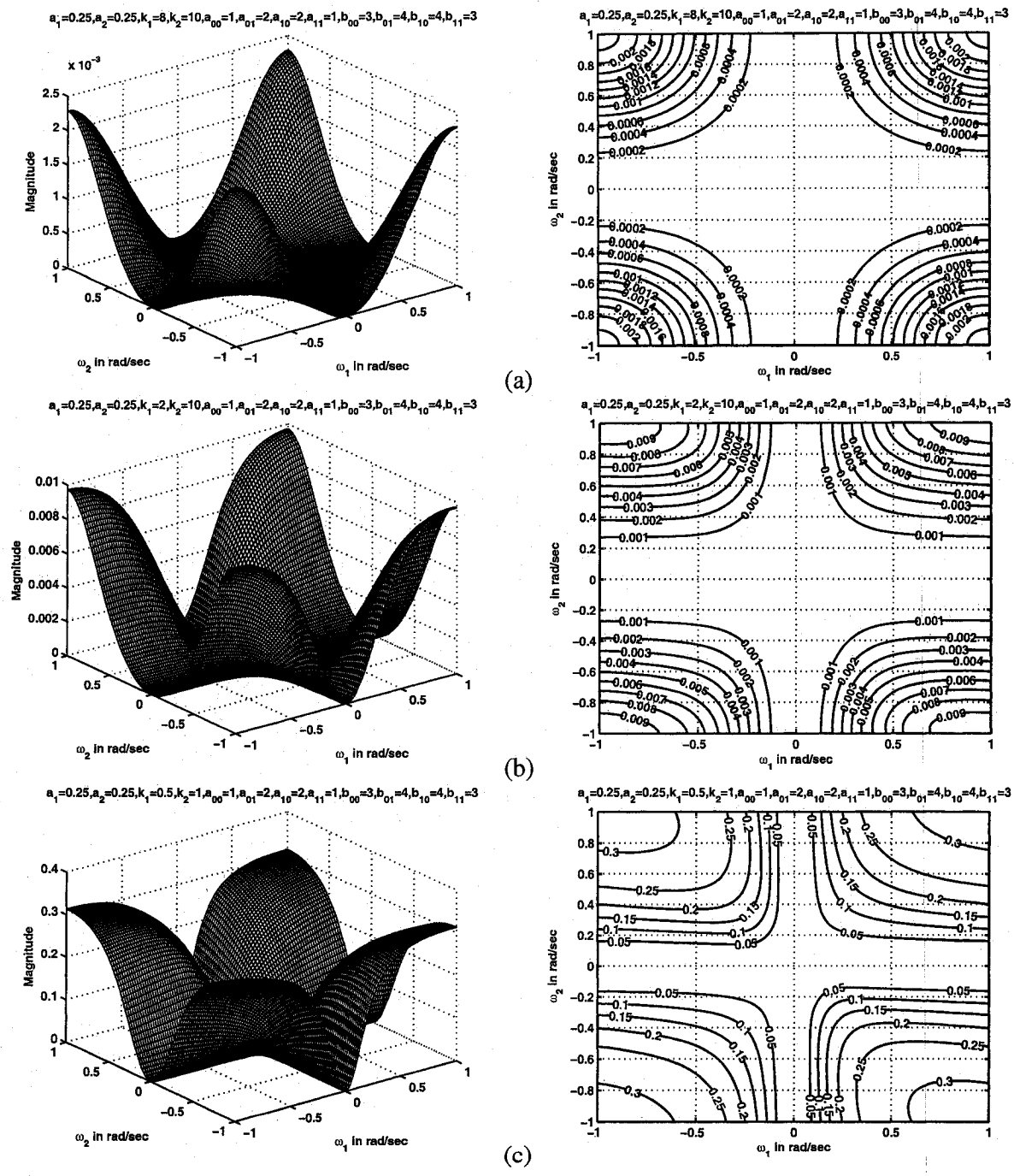

Figure 3.17: 3-D amplitude-frequency response and contour response of the 2-D digital highpass filter in case 1 of set 3 (when $a_1 = a_2 = 0.25$)

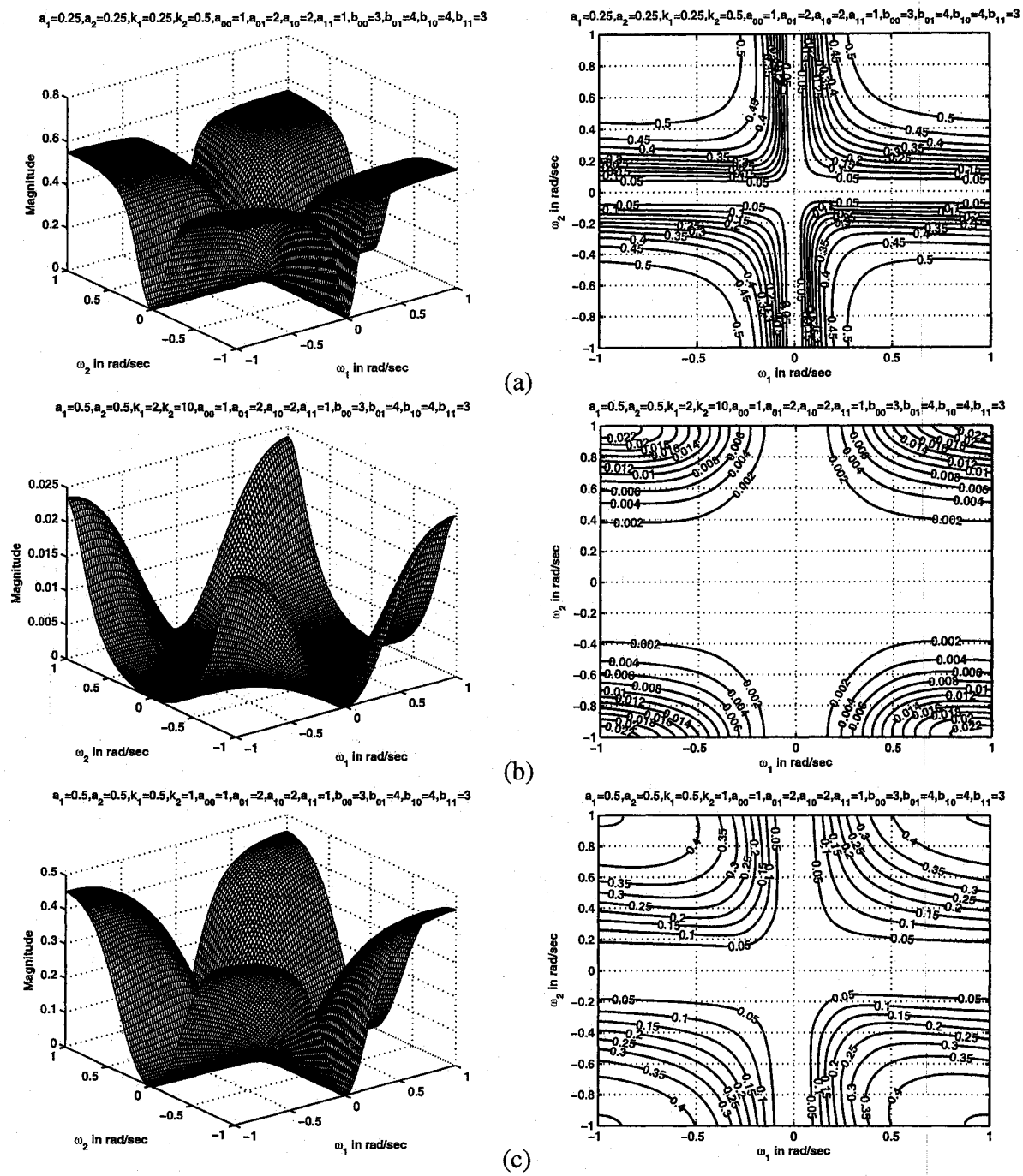

Figure 3.18: 3-D amplitude-frequency response and contour response of the 2-D digital highpass filter in case 1 of set 3 (when $a_1 = a_2 = 0.25,\ 0.5$)

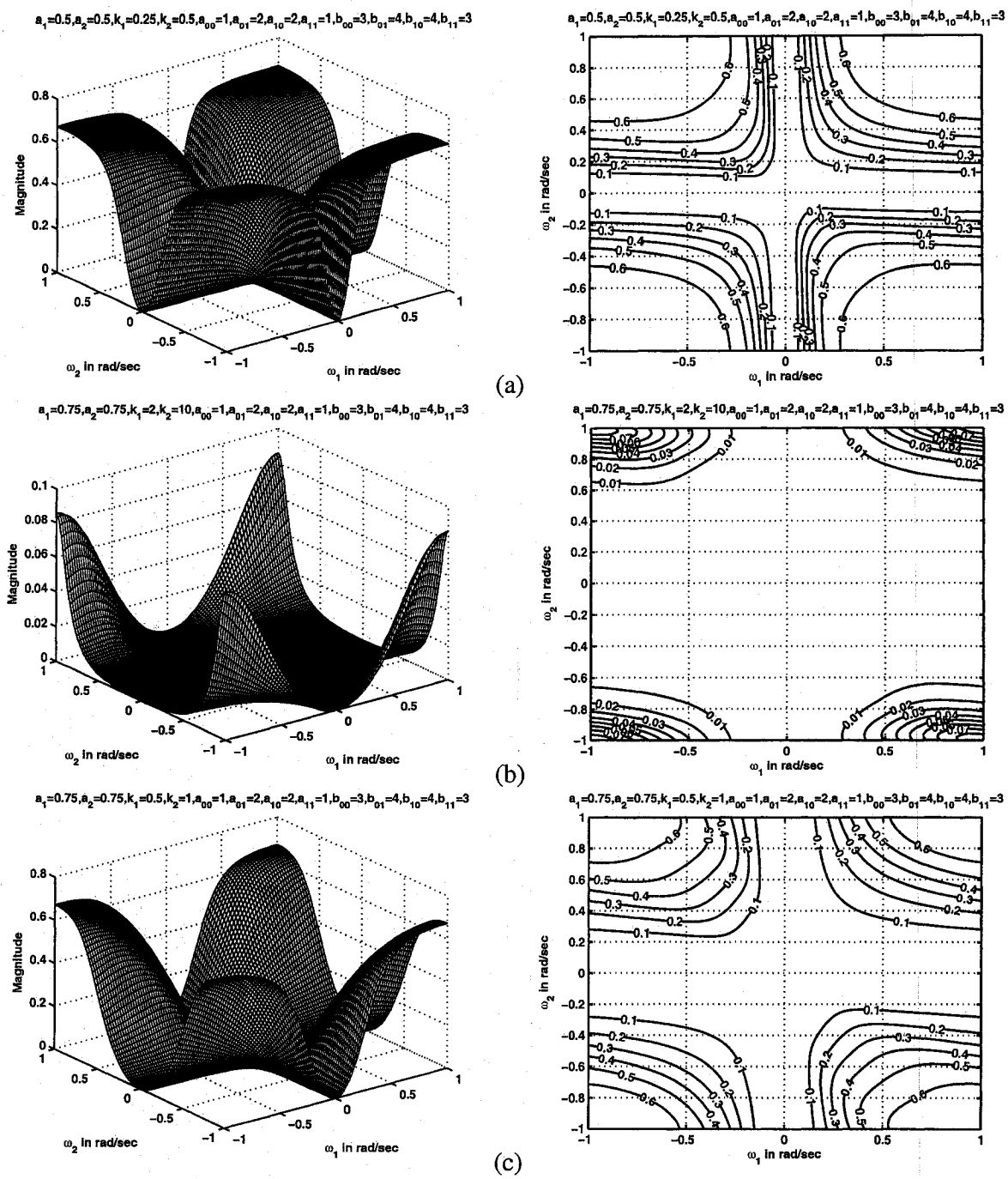

Figure 3.19: 3-D amplitude-frequency response and contour response of the 2-D digital highpass filter in case 1 of set 3 (when $a_1 = a_2 = 0.5,\ 0.75$)

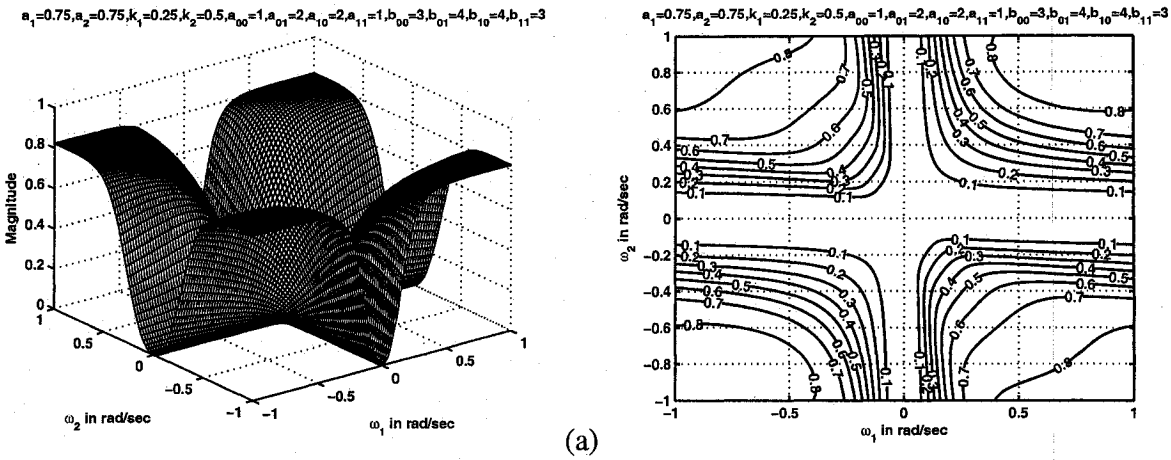

(a)

Figure 3.20: 3-D amplitude-frequency response and contour response of the 2-D digital highpass filter in case 1 of set 3 (when $a_1 = a_2 = 0.75$)

It can be noticed that there is rounding of contour edges for higher values of k_1 and k_2. In Fig. 3.17 (a), (b), (c) and Fig. 3.18 (a), the contour response changes from nearly circular to square when the values of k_1, k_2 are decreased from 8, 10 to 0.25, 0.5 respectively. Also, it can be observed that the passband width of the contour response is greater in this case of set 3 than that of the case 1 in set 1 for higher values of k_1 and k_2. It is noted that, the passband width is greater in Fig. 3.17 (b) of set 3 than that of the passband width in Fig. 3.2 (a) of case 1 in set 1. It can also be noticed that the contours in the first and third quadrants are mirror images of one another and the contours in the second and fourth quadrants are mirror images of one another.

3.4.3.2 Case 2:

In this case,

$$a_1 \neq a_2 \quad , \quad k_1 = k_2 \quad , \quad b_1 = b_2 = -1$$

It is observed that the coefficients k_1 and k_2 affect the stopband width and the coefficients a_1 and a_2 affect the gain of the amplitude-frequency response. As k_1 and k_2 values

are increased, the stopband width of the 2-D highpass filter increases and the magnitude of the amplitude-frequency response decreases. As a_1 and a_2 values are increased, the magnitude of the amplitude-frequency response of the 2-D highpass filter increases and the stopband width increases. Overall, the cut-off frequencies of the 2-D highpass filter are changed when k_1, k_2, a_1 and a_2 values are increased.

In this case, there are ripples in the passband of the contour response for values of k_1 and k_2 as low as 0.25 and for values of $a_1 = 0.5$, $a_2 = 1$ as seen in Fig. 3.22 (a). In additon, the ripples in the passband occur for values of $k_1 = k_2 = 0.5$ and for values of $a_1 = 0.75$, $a_2 = 1$ as seen in Fig. 3.23 (b) and also the magnitude of the contours in the second and fourth quadrant is slightly greater than that of the first and third quadrants. The magnitude of the contour response is lower than that of the magnitude in case 2 of set 1 for the same values of k_1, k_2, a_1 and a_2. In Fig. 3.7 (c), the magnitude of the contour response is 0.4 whereas the magnitude for the same values of k_1, k_2, a_1 and a_2 in Fig. 3.24 (b) is 0.25.

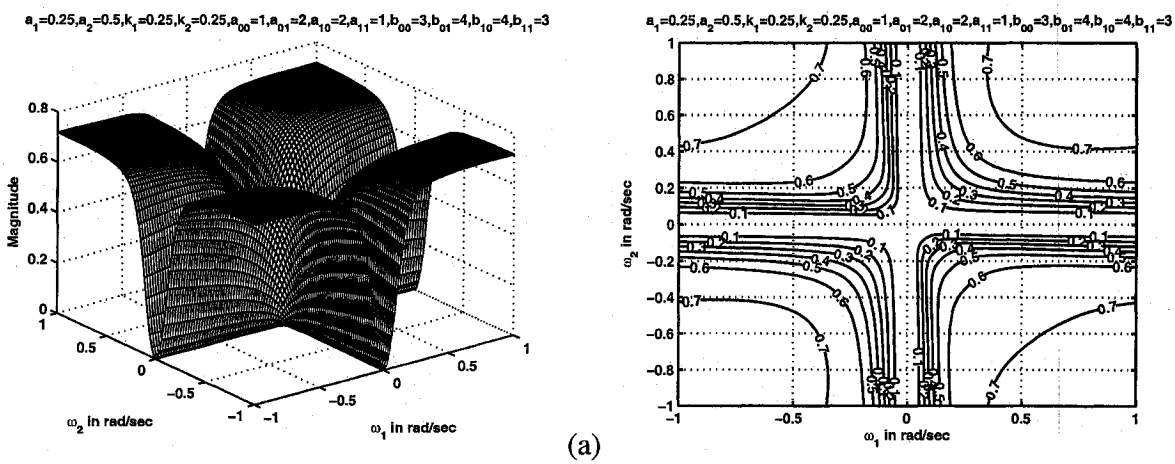

(a)

Figure 3.21: 3-D amplitude-frequency response and contour response of the 2-D digital highpass filter in case 2 of set 3 (when $k_1 = k_2 = 0.25$)

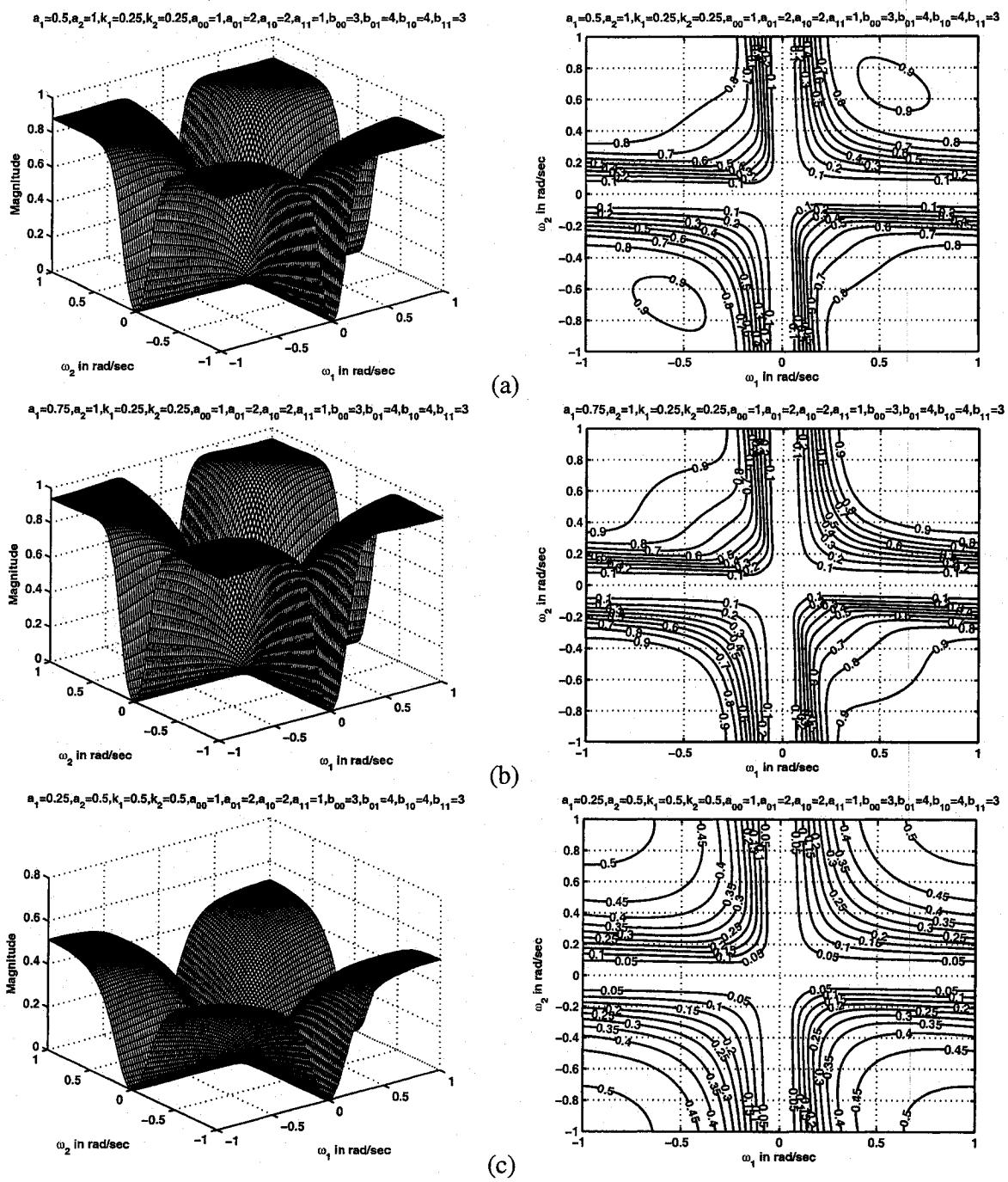

Figure 3.22: 3-D amplitude-frequency response and contour response of the 2-D digital highpass filter in case 2 of set 3 (when $k_1 = k_2 = 0.25,\ 0.5$)

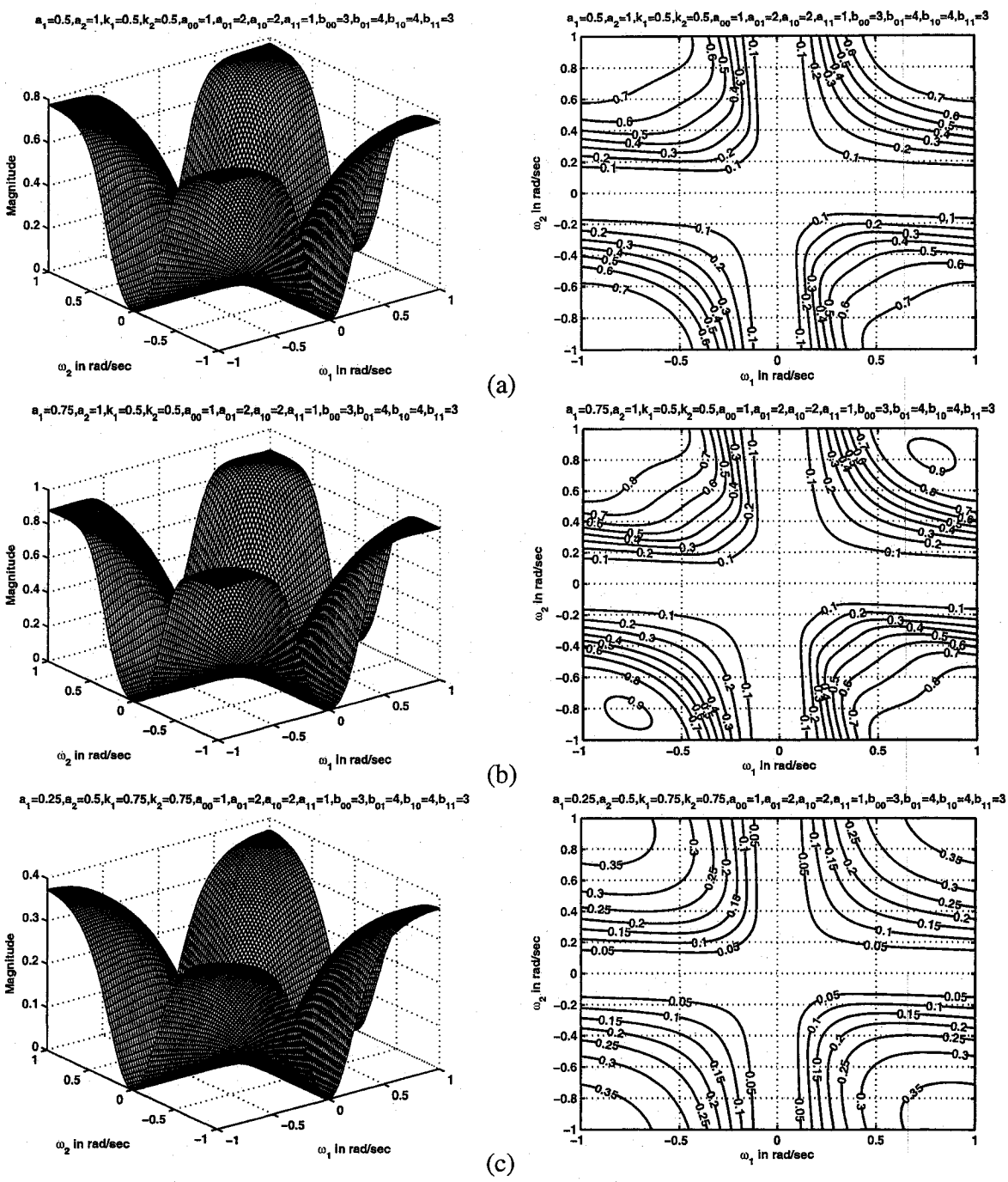

Figure 3.23: 3-D amplitude-frequency response and contour response of the 2-D digital highpass filter in case 2 of set 3 (when $k_1 = k_2 = 0.5, 0.75$)

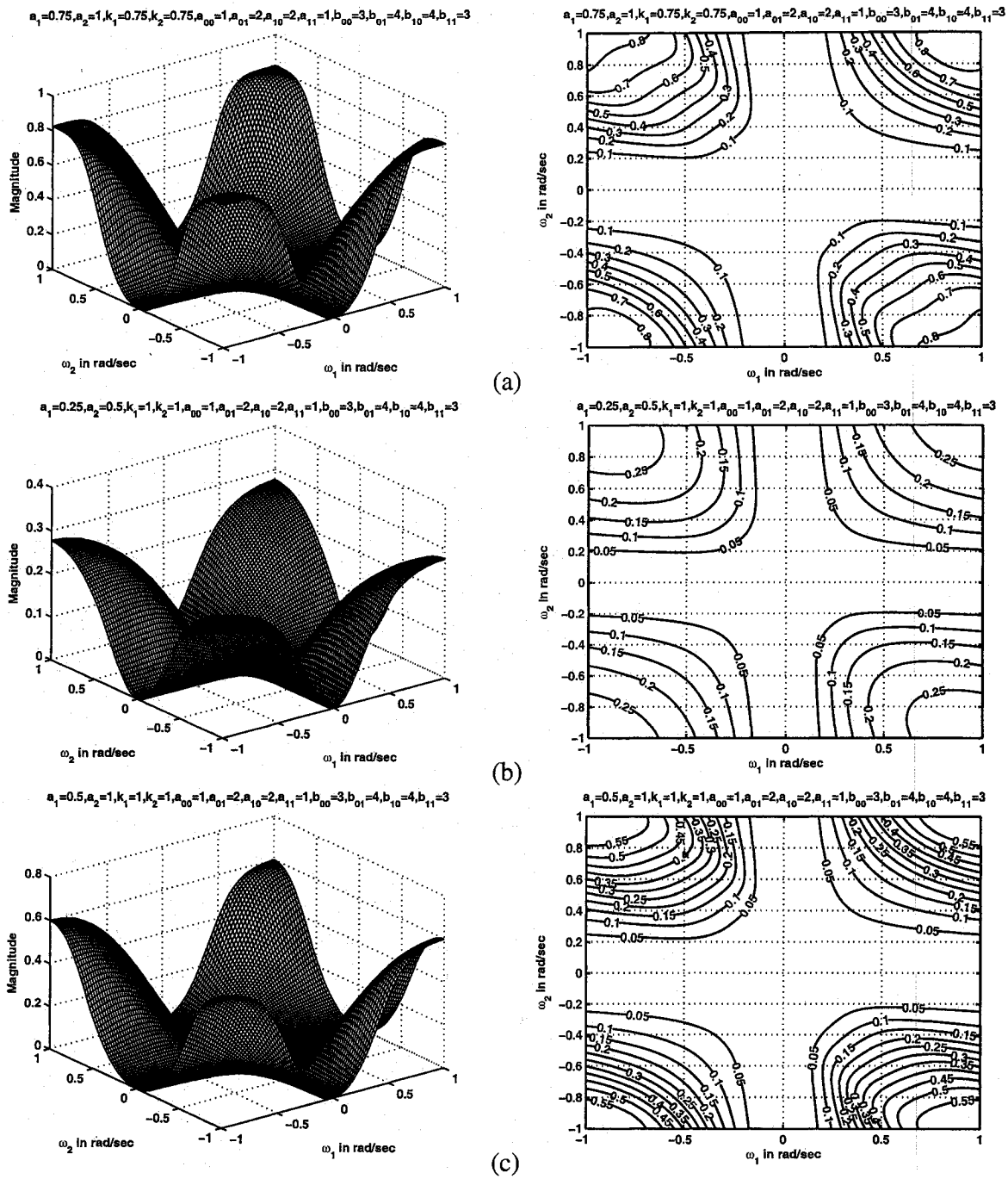

Figure 3.24: 3-D amplitude-frequency response and contour response of the 2-D digital highpass filter in case 2 of set 3 (when $k_1 = k_2 = 0.75,\ 1$)

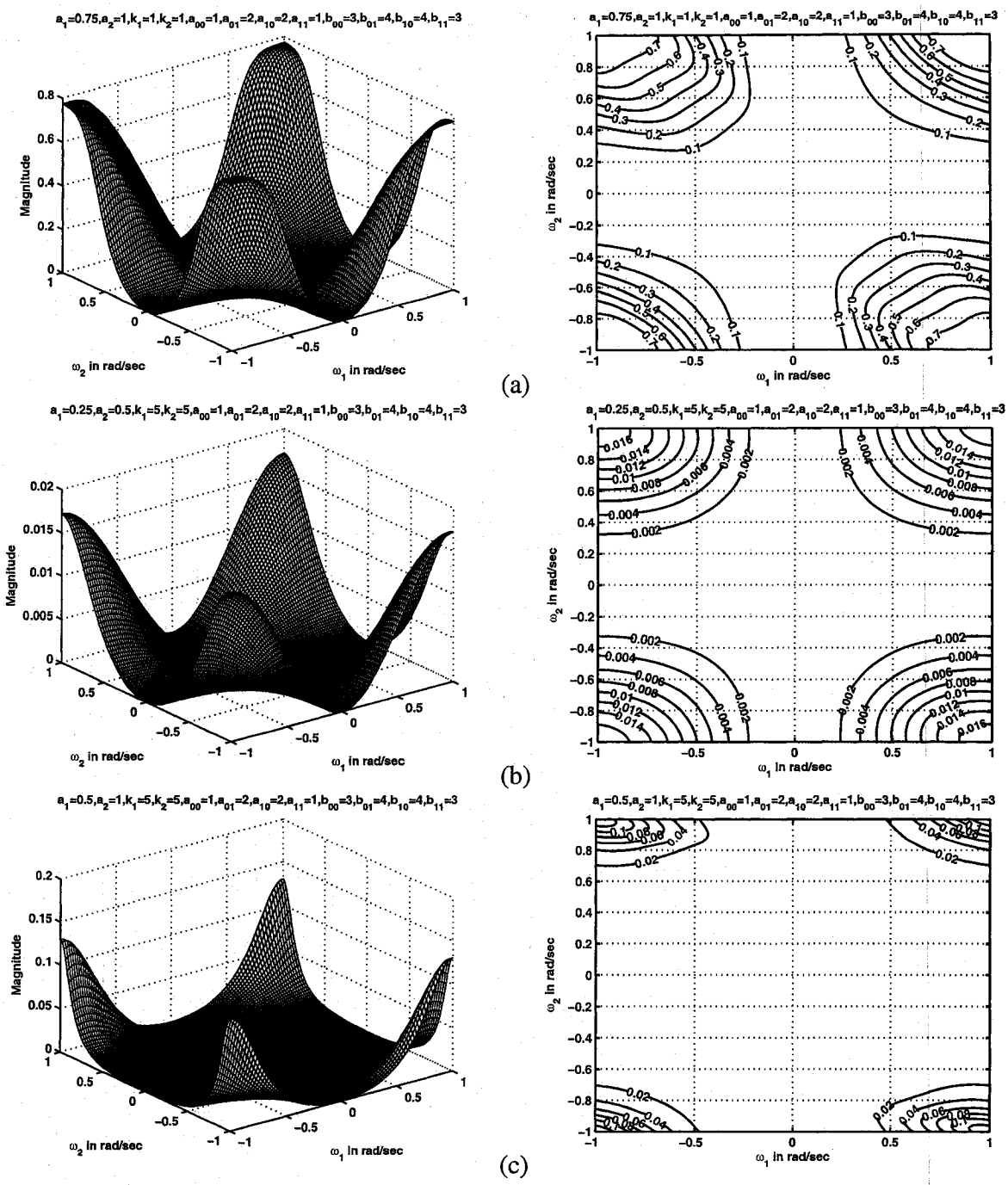

Figure 3.25: 3-D amplitude-frequency response and contour response of the 2-D digital highpass filter in case 2 of set 3 (when $k_1 = k_2 = 1, 5$)

3.4.3.3 Case 3:

In this case,

$$a_1 \neq a_2 \quad , \quad k_1 \neq k_2 \quad , \quad b_1 = b_2 = -1$$

It is observed in this case that the coefficients k_1 and k_2 affect the stopband width and the coefficients a_1 and a_2 affect the gain of the amplitude-frequency response. As k_1 and k_2 values are increased, the stopband width of the 2-D highpass filter increases and the magnitude of the amplitude-frequency response also decreases. As a_1 and a_2 values are increased, the magnitude of the amplitude-frequency response of the 2-D highpass filter increases and the stopband width increases. Overall, the cut-off frequencies of the 2-D highpass filter changes when k_1, k_2, a_1 and a_2 values are increased.

In this case, there are ripples in the passband of the contour response when the values of k_1 and k_2 are as low as 0.25 and 0.5 respectively and the values of a_1 and a_2 are 0.5 and 1 respectively as shown in Fig. 3.26 (b). In addition, it is observed that there are ripples in the passband when the values of k_1 and k_2 are 0.5 and 1 respectively and the values of a_1 and a_2 are 0.75 and 1 respectively as shown in Fig. 3.27 (c). The magnitude of the contour response in this case is lower than that of the magnitude in case 3 of set 1 for the same values of k_1, k_2, a_1 and a_2. In Fig. 3.10 (b), the magnitude of the contour response in case 3 of set 1 is 0.55 whereas the magnitude in Fig. 3.27 (a) is 0.35. The magnitude of the contours in the second and fourth quadrant is slightly greater than that of the contours in the first and third quadrants.

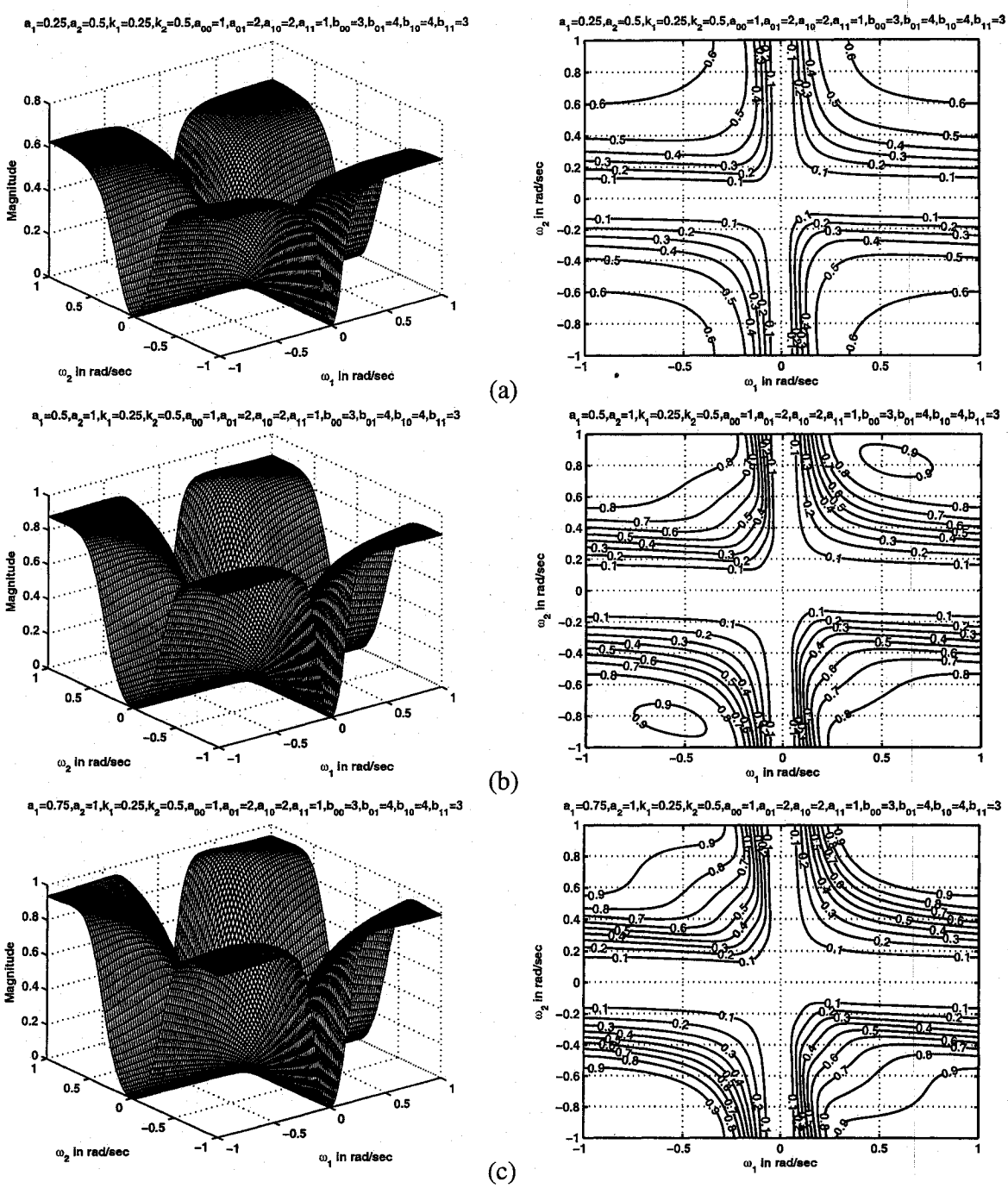

Figure 3.26: 3-D amplitude-frequency response and contour response of the 2-D digital highpass filter in case 3 of set 3 (when $k_1 = 0.25$, $k_2 = 0.5$)

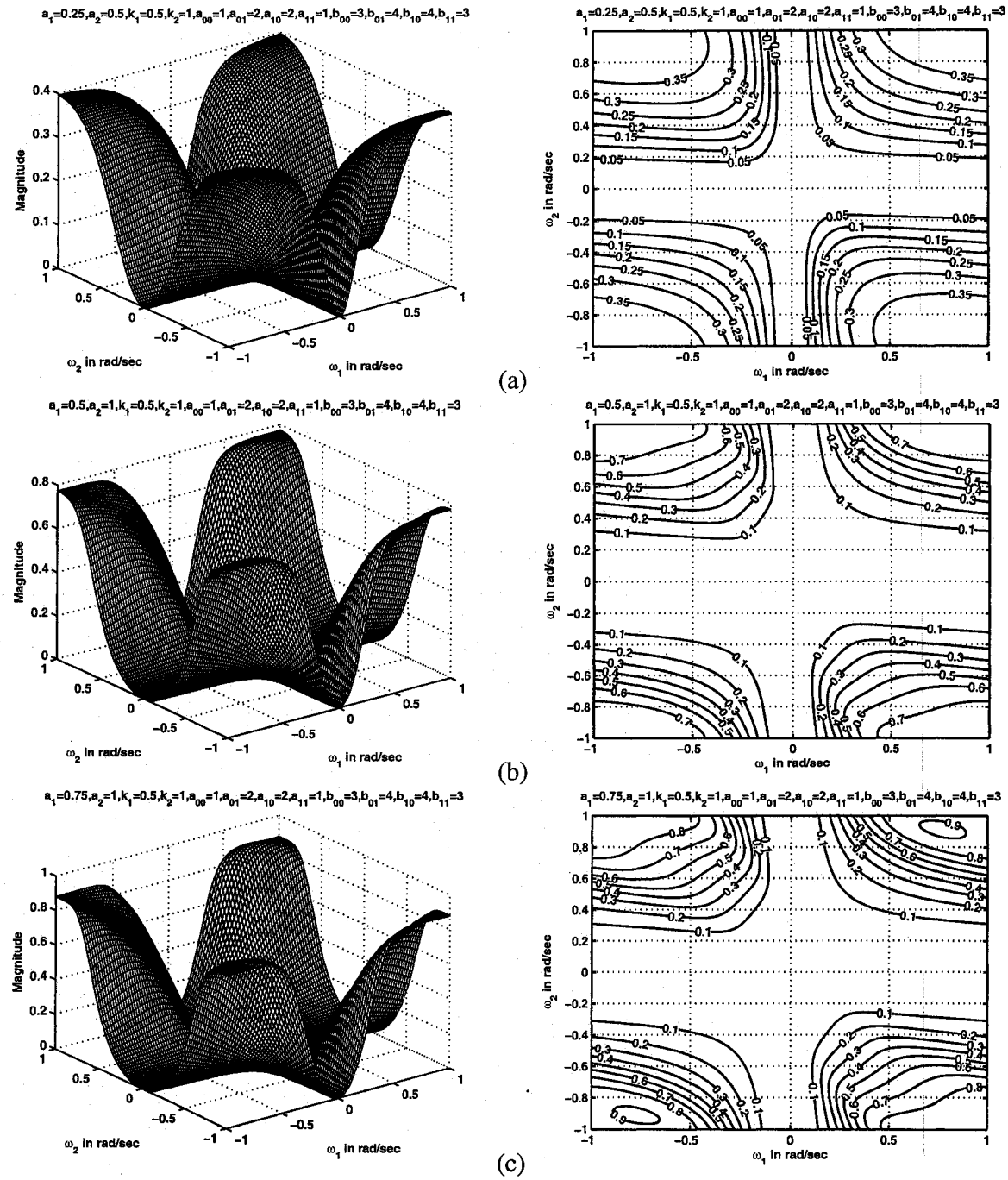

Figure 3.27: 3-D amplitude-frequency response and contour response of the 2-D digital highpass filter in case 3 of set 3 (when $k_1 = 0.5,\ k_2 = 1$)

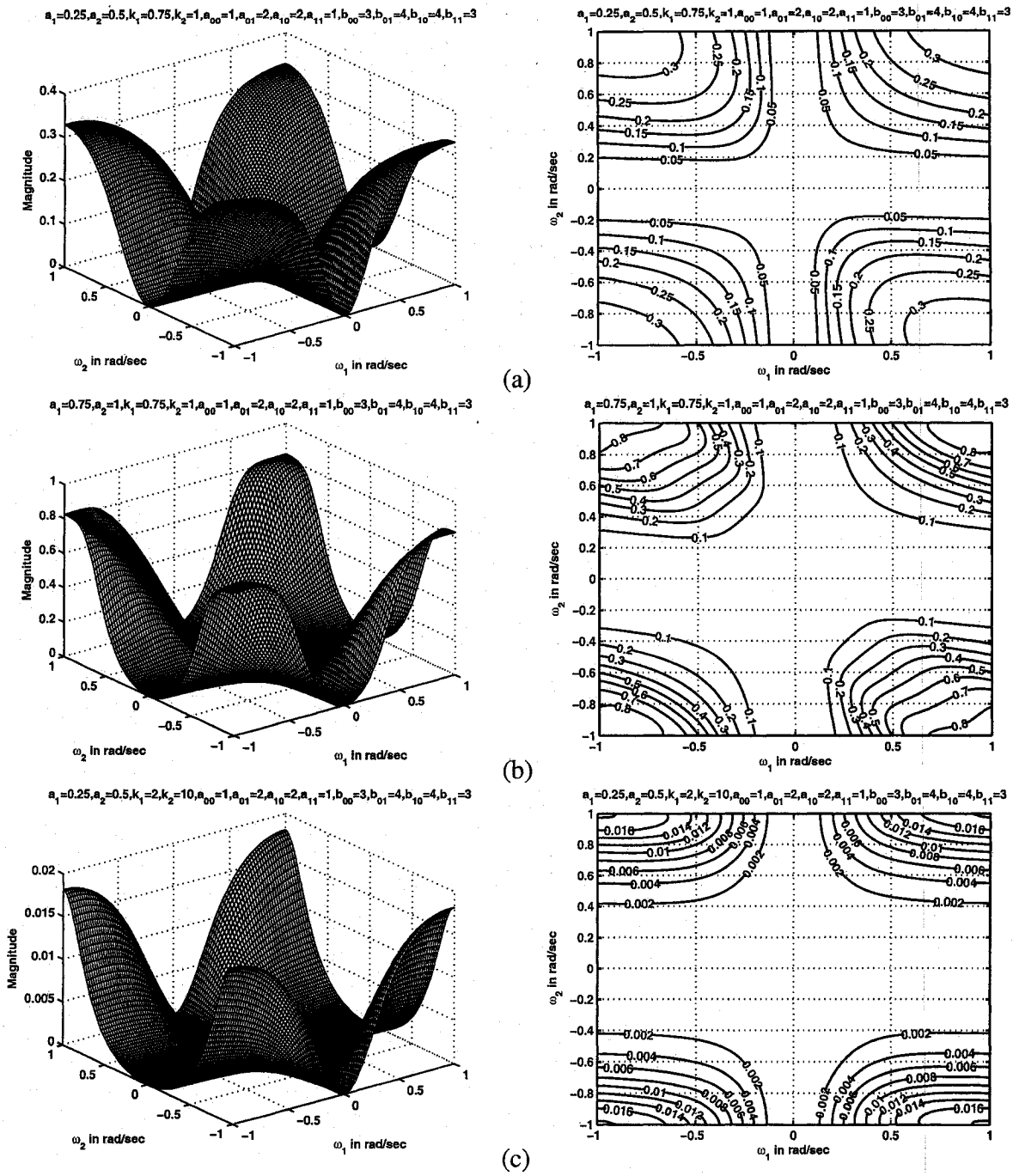

Figure 3.28: 3-D amplitude frequency response and contour response of the 2-D digital highpass filter in case 3 of set 3 (when $k_1 = 0.75,\ 2,\ k_2 = 1,\ 10$)

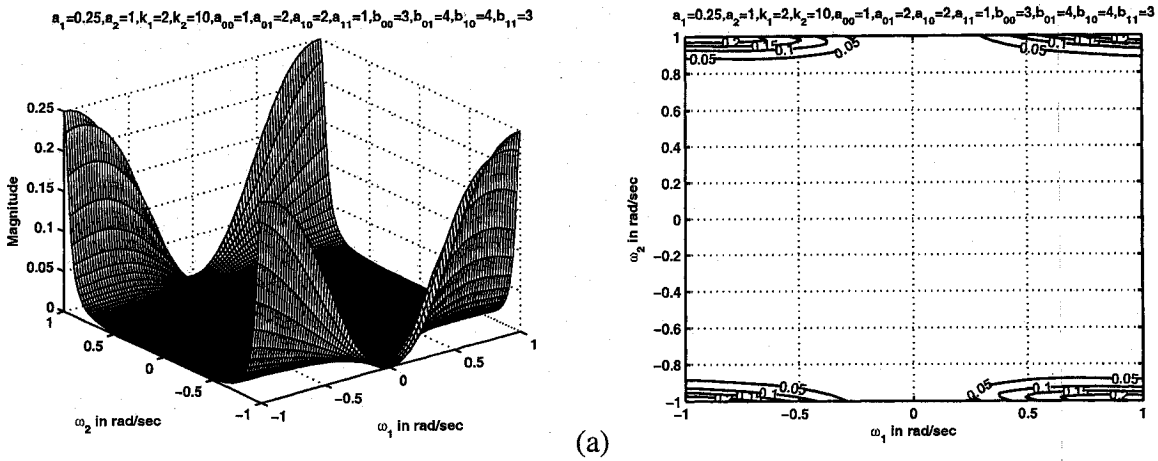

(a)

Figure 3.29: 3-D amplitude-frequency response and contour response of the 2-D digital highpass filter in case 3 of set 3 (when $k_1 = 2$, $k_2 = 10$)

3.4.3.4 Case 4:

In this case,

$$a_1 = a_2 \quad , \quad k_1 = k_2 \quad , \quad b_1 = b_2 = -1$$

It is observed that the coefficients k_1 and k_2 affect the stopband width and the coefficients a_1 and a_2 affect the gain of the amplitude-frequency response. As k_1 and k_2 values are increased, the stopband width of the 2-D highpass filter increases and the magnitude of the amplitude-frequency response also decreases. As a_1 and a_2 values are increased, the magnitude of the amplitude-frequency response of the 2-D highpass filter increases and the stopband width increases. Overall, the cut-off frequencies of the 2-D highpass filter changes when k_1, k_2, a_1 and a_2 values are increased.

In this case, there are ripples in the passband of the contour response for the values of $k_1 = k_2 = 0.25$ and for values of $a_1 = a_2 \geq 0.75$ as seen in Fig. 3.30 (b) and the magnitude of the contours of the second and fourth quadrant is slightly greater than that of the first and third quadrants. The magnitude of the contour response in this case is lower than that of the magnitude in case 4 of set 1 for the same values of k_1, k_2, a_1 and a_2. In Fig. 3.13

(c), the magnitude of the contour response of case 3 in set 1 is 0.6 whereas the magnitude in Fig. 3.30 (a) is 0.4. When the values of $k_1 = k_2 > 1$, the contour responses are more circular in nature as shown in Fig. 3.32 (c) and in Fig. 3.33 (a).

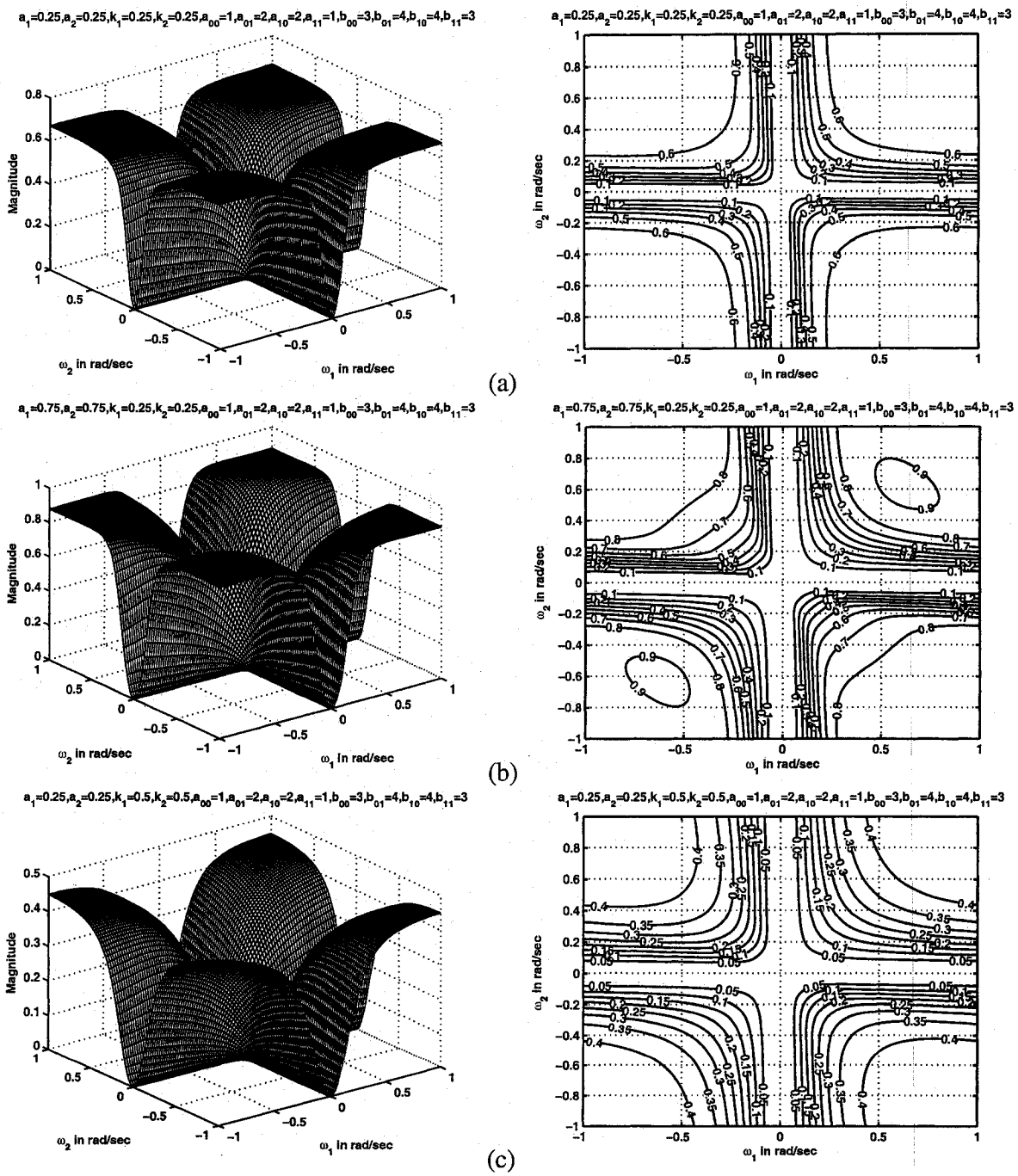

Figure 3.30: 3-D amplitude-frequency response and contour response of the 2-D digital highpass filter in case 4 of set 3 (when $k_1 = k_2 = 0.25,\ 0.5$)

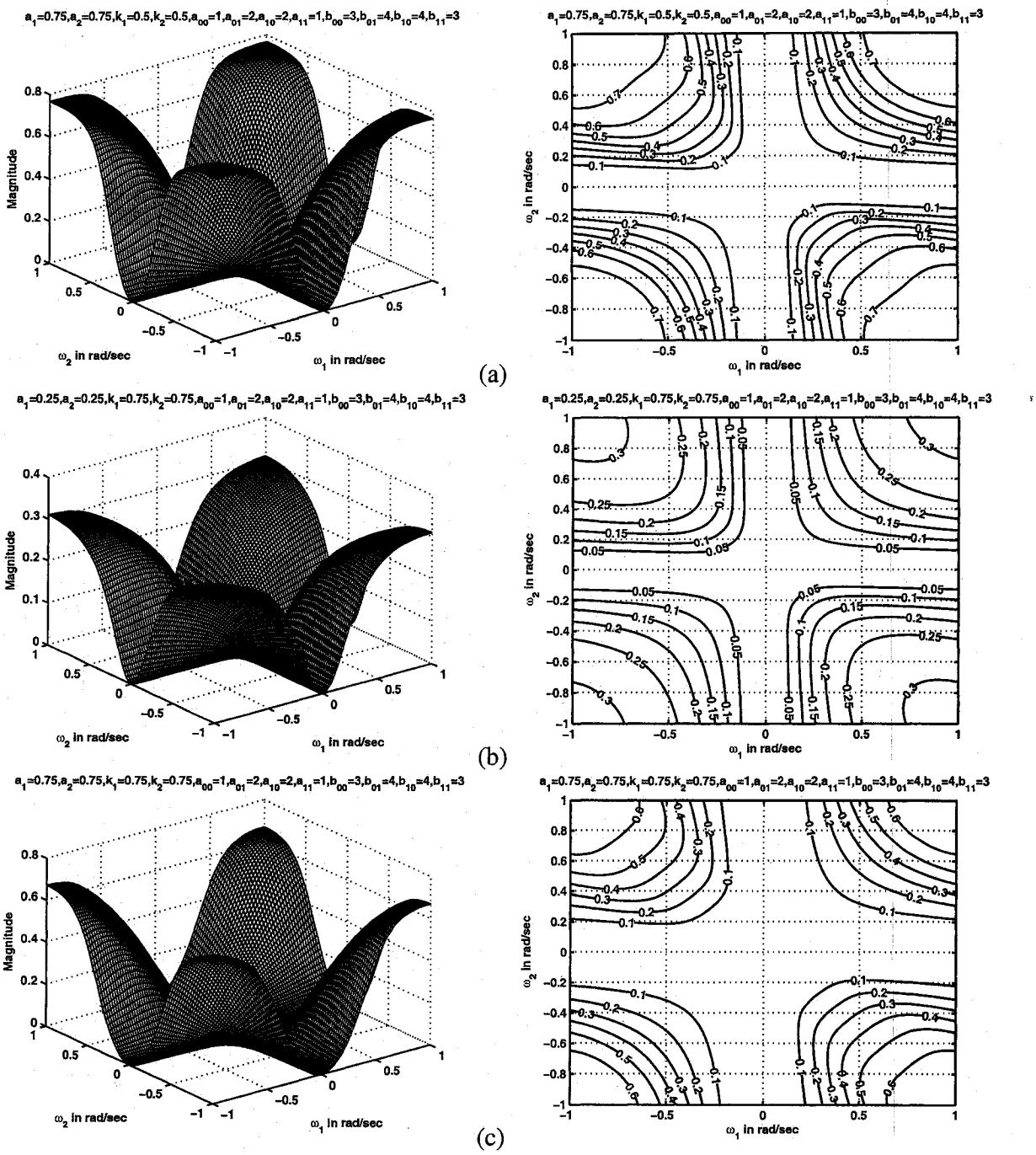

Figure 3.31: 3-D amplitude-frequency response and contour response of the 2-D digital highpass filter in case 4 of set 3 (when $k_1 = k_2 = 0.5,\ 0.75$)

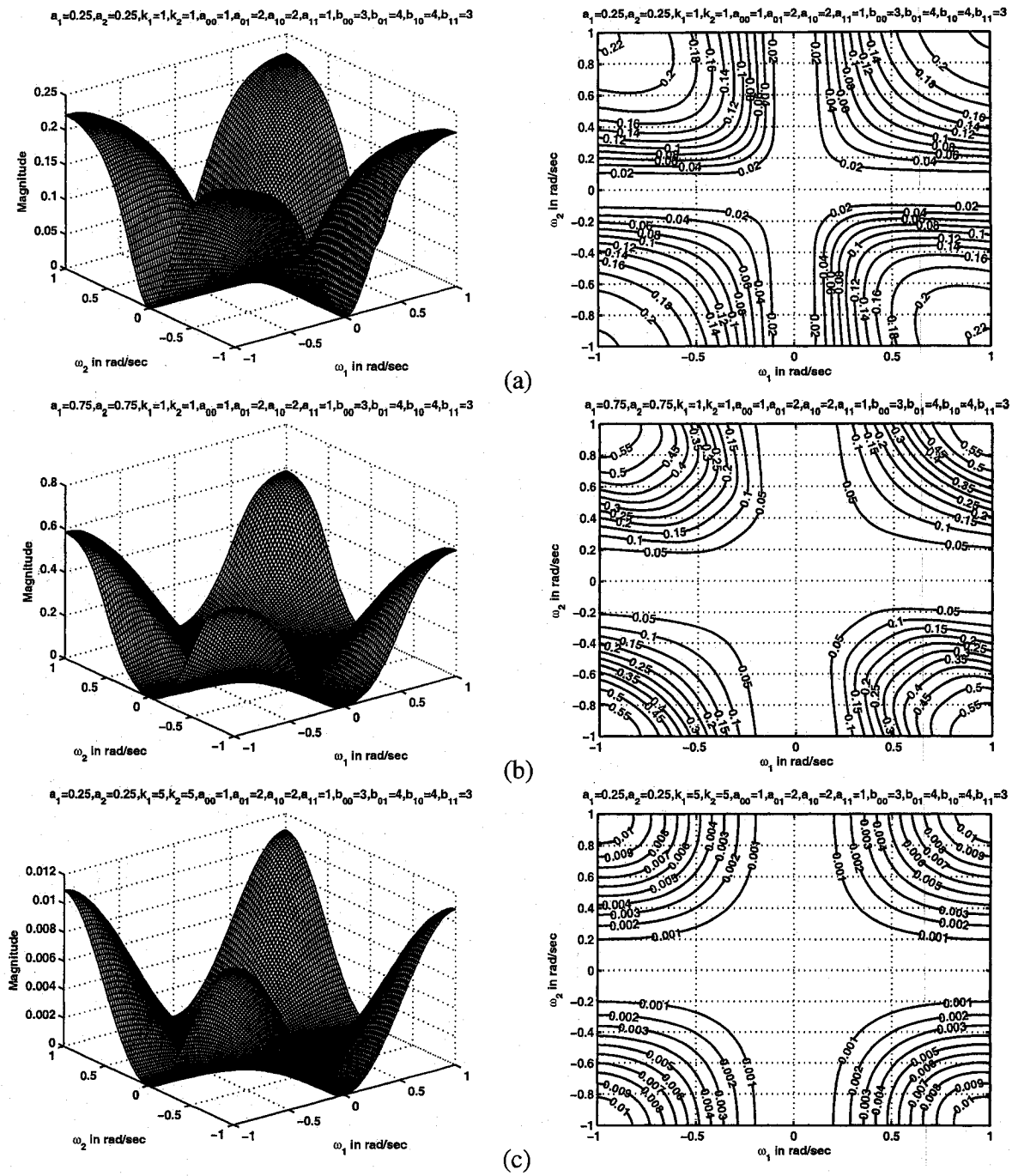

Figure 3.32: 3-D amplitude-frequency response and contour response of the 2-D digital highpass filter in case 4 of set 3 (when $k_1 = k_2 = 1, 5$)

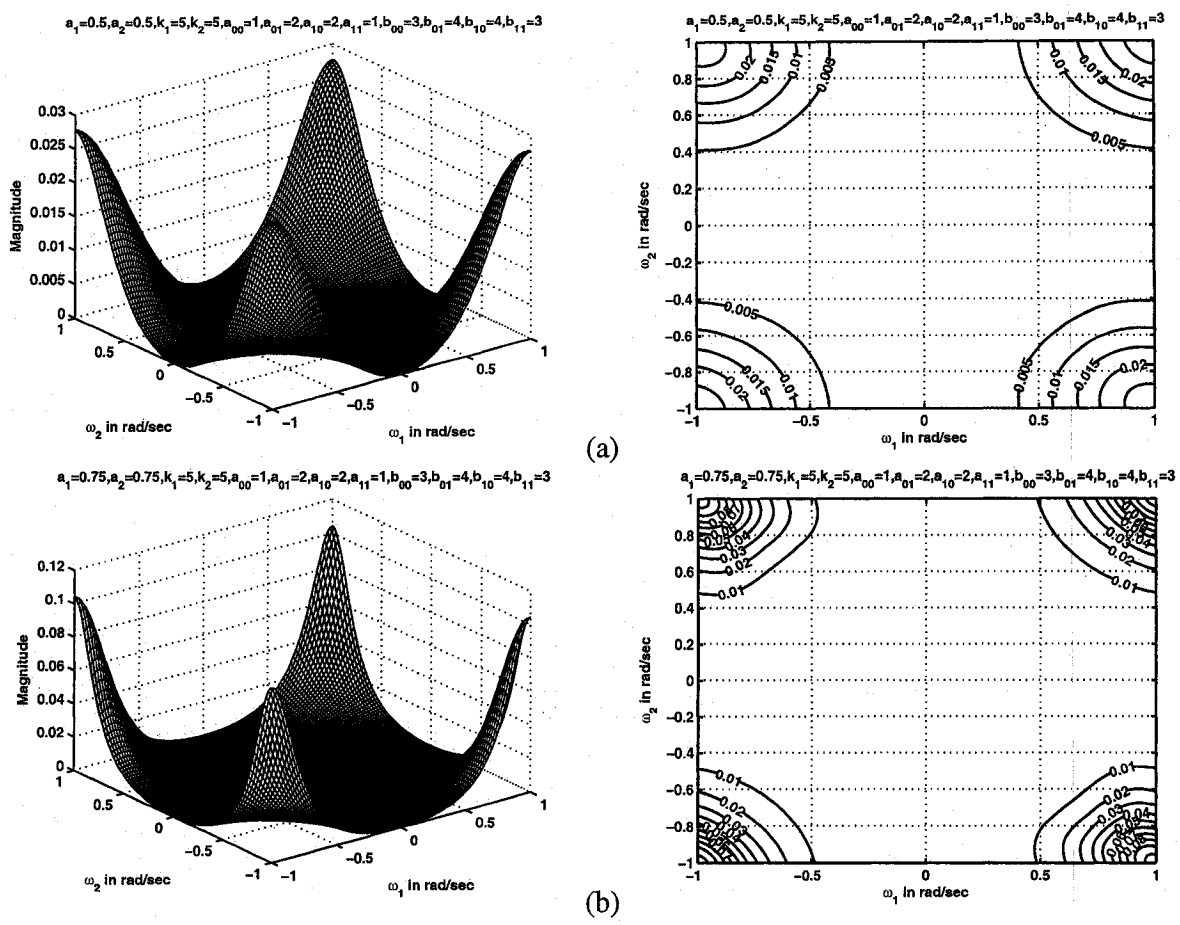

Figure 3.33: 3-D amplitude-frequency response and contour response of the 2-D digital highpass filter in case 4 of set 3 (when $k_1 = k_2 = 5$)

3.4.4 Frequency Response of 2-D High Pass Filters in Set 4

In this section, we study the manner in which all the four cases in set 4 affect the frequency response behavior of the resulting 2-D highpass filter. In this set,

$$a_{00} \neq a_{01} \neq a_{10} \neq a_{11} \neq b_{00} \neq b_{01} \neq b_{10} \neq b_{11} \tag{3.5}$$

Different contour plots are obtained by varying the values of k_1, k_2, a_1 and a_2.

Similar to set 3, it is observed in all the four cases that the coefficients k_1 and k_2 affect the stopband width and the coefficients a_1 and a_2 affect the gain of the amplitude-frequency response. As k_1 and k_2 values are increased, the stopband width of the 2-D highpass filter increases and the magnitude of the amplitude-frequency response also decreases. As a_1 and a_2 values are increased, the magnitude of the amplitude-frequency response of the 2-D highpass filter increases and the stopband width increases. Overall, the cut-off frequencies of the 2-D highpass filter changes when k_1, k_2, a_1 and a_2 values are increased.

In set 4, the responses are similar to that of set 3. But the passband width is smaller in the contour responses of set 4 when compared to that of set 3. Also the magnitude of the contour response is low when compared to set 3 for the same values of k_1, k_2, a_1 and a_2. It can be noticed that the contours in the first and third quadrant are mirror images of one another and the contours in the second and fourth quadrant are mirror images of one another.

3.4.4.1 Case 1:

In this case,

$$a_1 = a_2 \qquad k_1 \neq k_2 \qquad b_1 = b_2 = -1$$

It is observed that the coefficients k_1 and k_2 affect the stopband width and the coefficients a_1 and a_2 affect the gain of the amplitude-frequency response. As k_1 and k_2 values

are increased, the stopband width of the 2-D highpass filter increases and the magnitude of the amplitude-frequency response also decreases. As a_1 and a_2 values are increased, the magnitude of the amplitude-frequency response of the 2-D highpass filter increases and the stopband width increases. Overall, the cut-off frequencies of the 2-D highpass filter changes when k_1, k_2, a_1 and a_2 values are increased.

In this case, the contour responses are similar to that of the responses in case 1 of set 3, except that there are ripples in the contour response for values of $a_1 = a_2 = 0.75$ and for values of k_1 and k_2 to be 0.25 and 0.5 respectively as shown in Fig. 3.37 (c) and the magnitude of the contours of the second and fourth quadrant is slightly greater than that of the first and third quadrants. The stopband width of the contour response in this case of set 4 is larger than the stopband width in case 1 of set 3. In Fig. 3.34 (a),the stopband width is larger than the stopband width in Fig. 3.17 (b) of case 1 of set 3 for the same values of k_1, k_2, a_1 and a_2. The magnitude of the contour response in this case is slightly lower than that of the magnitude in case 1 of set 3 for the same values of k_1, k_2, a_1 and a_2. The magnitude of the contour response in Fig. 3.17 (c) of case 1 in set 3 is 0.3 whereas the magnitude in Fig. 3.35 (b) is 0.25.

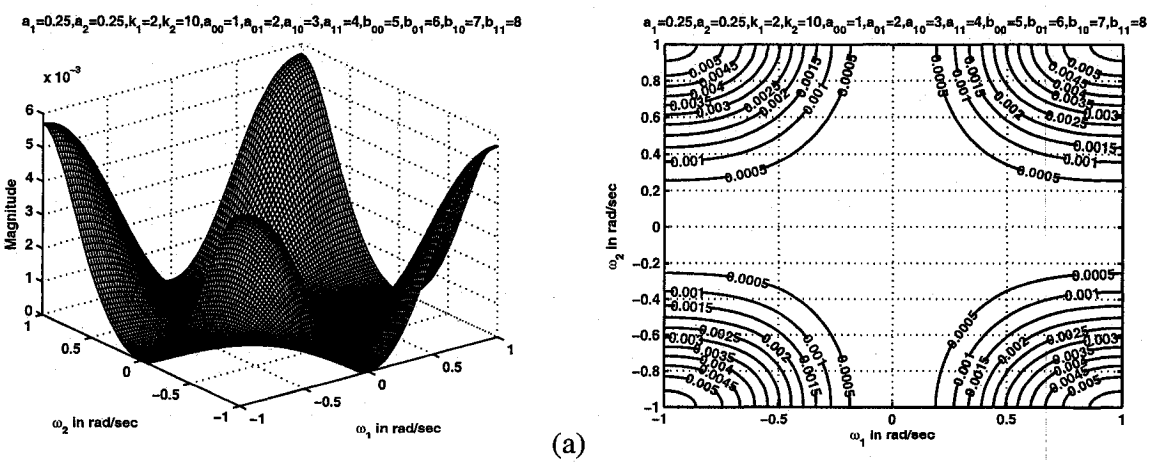

(a)

Figure 3.34: 3-D amplitude-frequency response and contour response of the 2-D digital highpass filter in case 1 of set 4 (when $a_1 = a_2 = 0.25$)

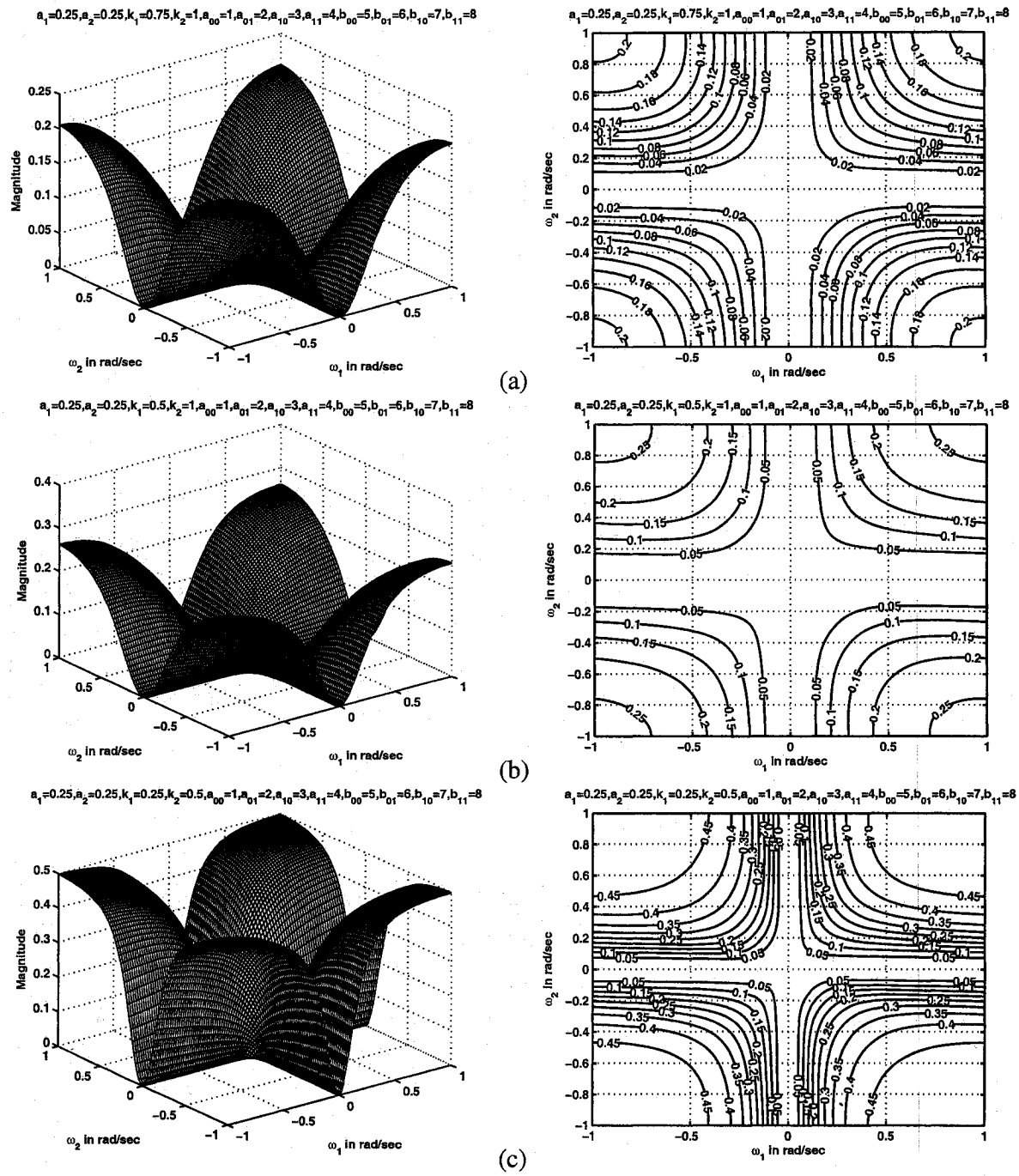

Figure 3.35: 3-D amplitude-frequency response and contour response of the 2-D digital highpass filter in case 1 of set 4 (when $a_1 = a_2 = 0.25$)

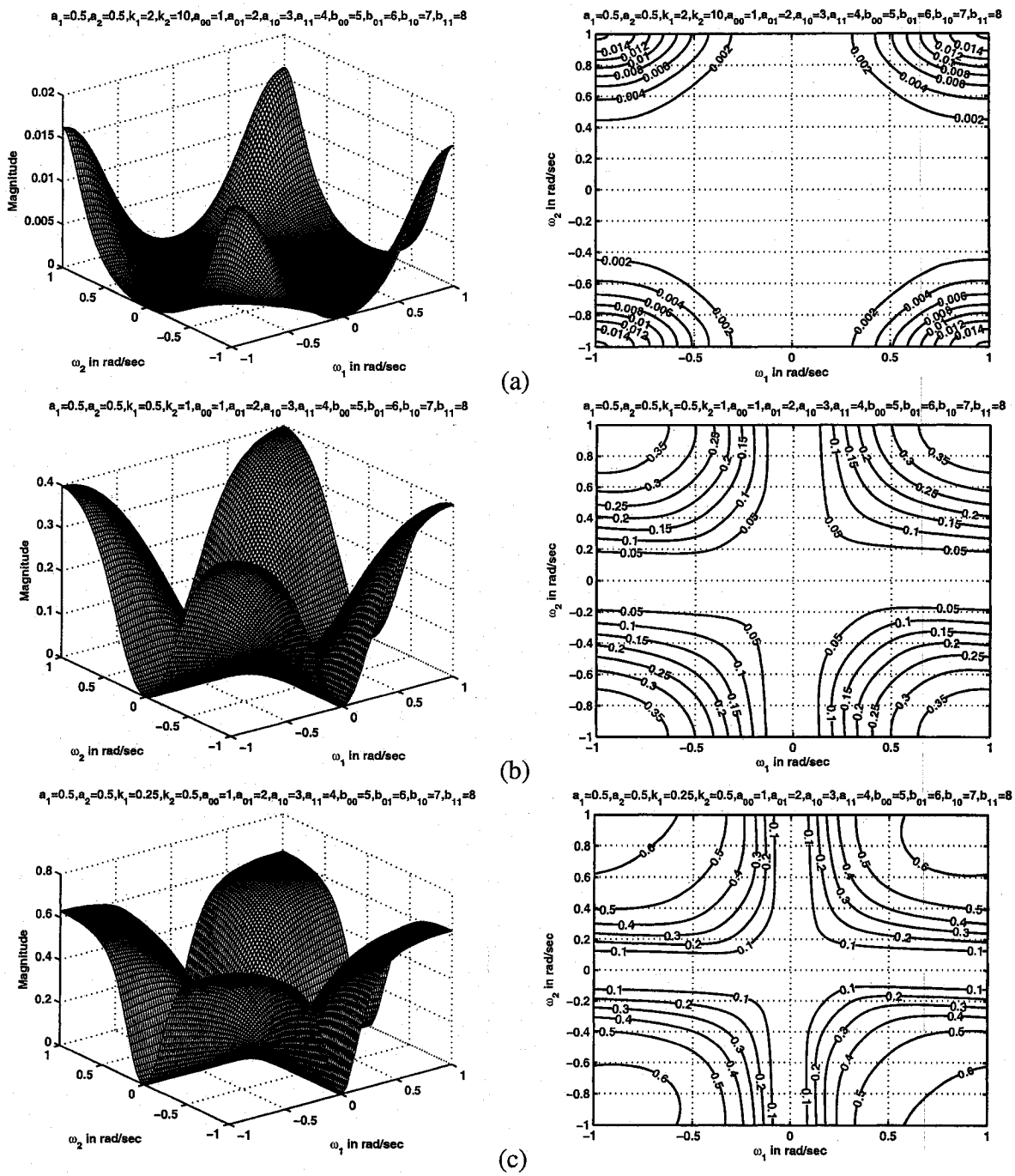

Figure 3.36: 3-D amplitude-frequency response and contour response of the 2-D digital highpass filter in case 1 of set 4 (when $a_1 = a_2 = 0.5$)

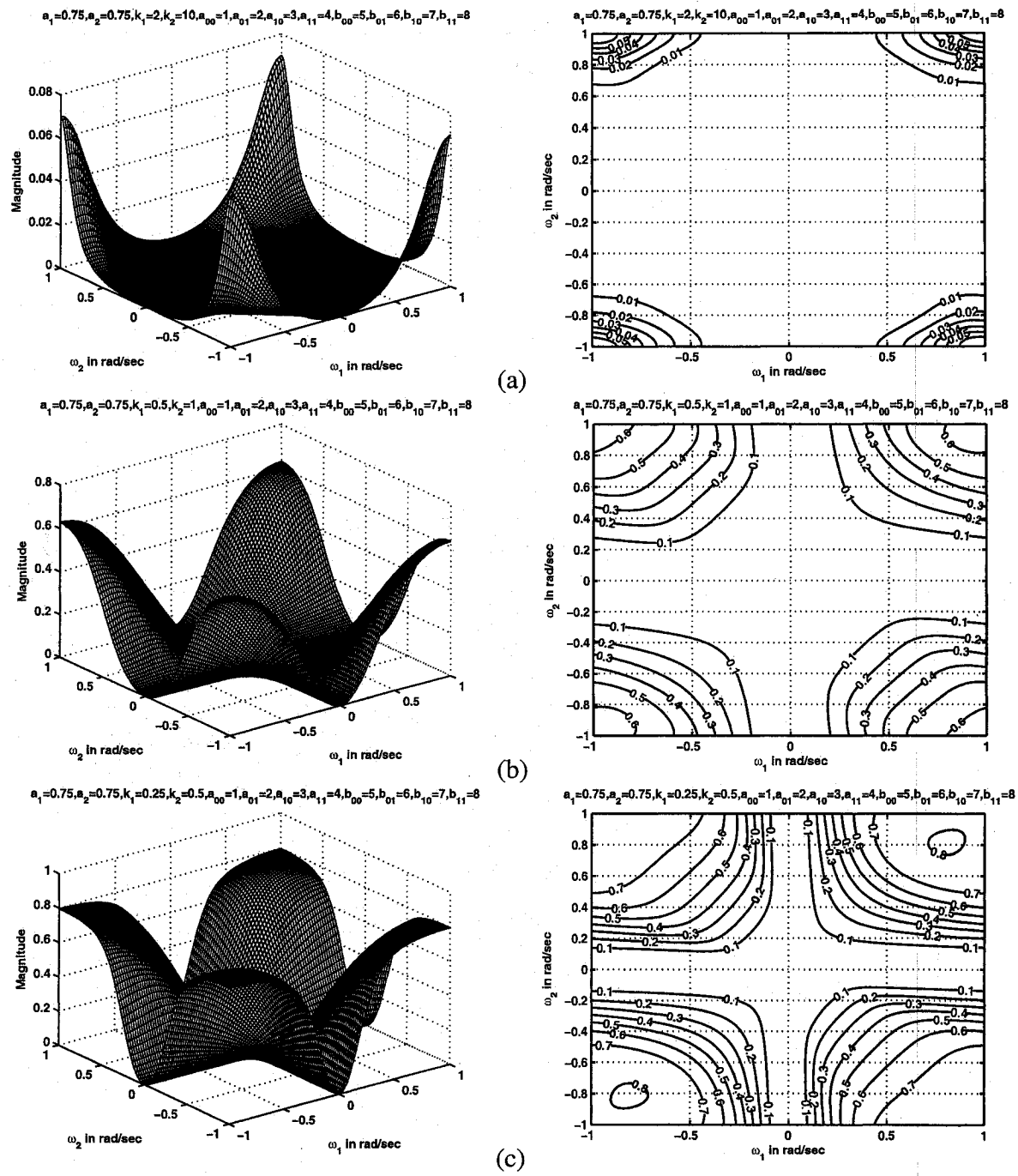

Figure 3.37: 3-D amplitude-frequency response and contour response of the 2-D digital highpass filter in case 1 of set 4 (when $a_1 = a_2 = 0.75$)

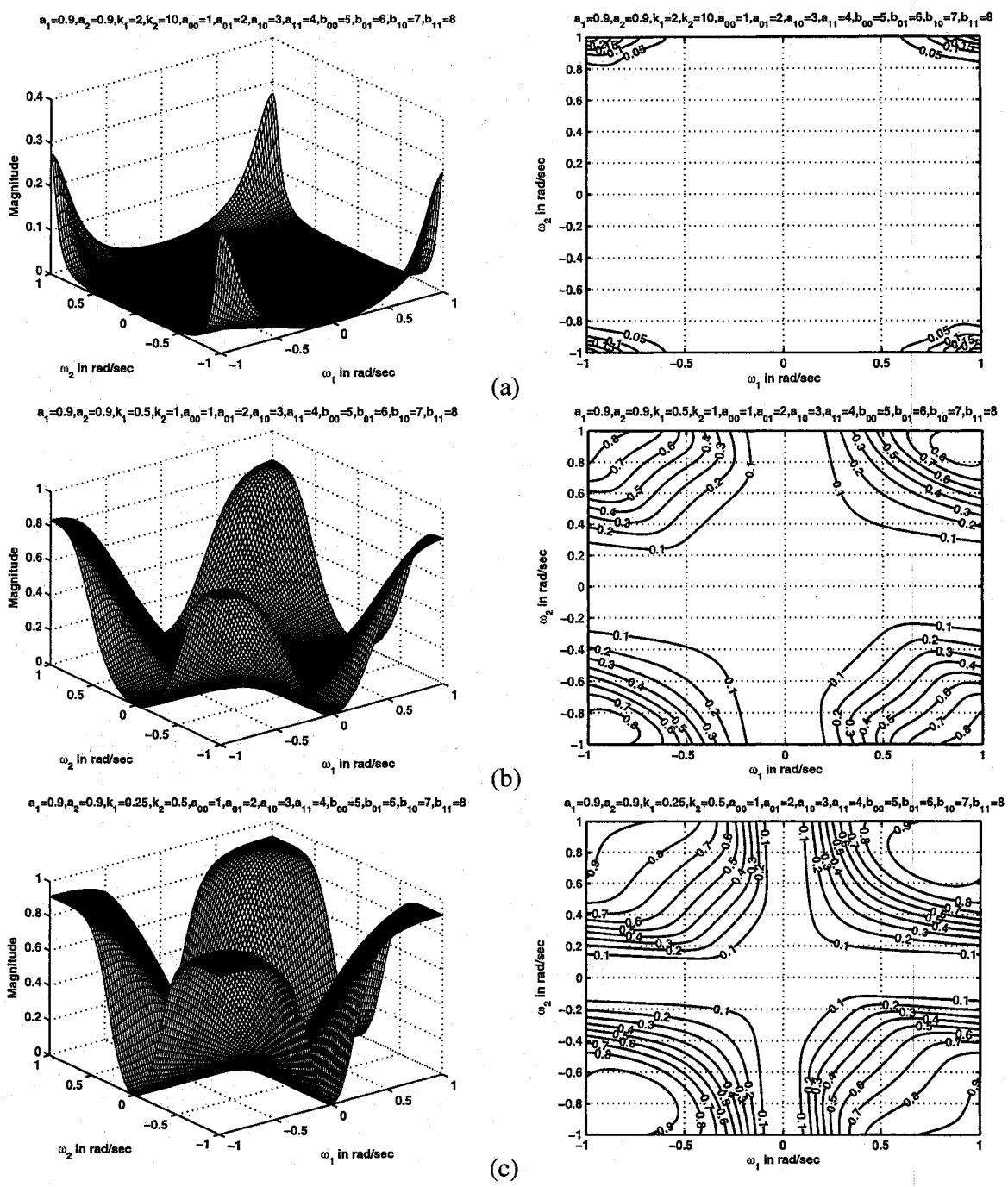

Figure 3.38: 3-D amplitude-frequency response and contour response of the 2-D digital highpass filter in case 1 of set 4 (when $a_1 = a_2 = 0.9$)

3.4.4.2 Case 2:

In this case,

$$a_1 \neq a_2 \quad , \quad k_1 = k_2 \quad , \quad b_1 = b_2 = -1$$

It is observed that the coefficients k_1 and k_2 affect the stopband width and the coefficients a_1 and a_2 affect the gain of the amplitude-frequency response. As k_1 and k_2 values are increased, the stopband width of the 2-D highpass filter increases and the magnitude of the amplitude-frequency response also decreases. As a_1 and a_2 values are increased, the magnitude of the amplitude-frequency response of the 2-D highpass filter increases and the stopband width increases. Overall, the cut-off frequencies of the 2-D highpass filter changes when k_1, k_2, a_1 and a_2 values are increased.

In this case, there are ripples in the passband of the contour response for values of $a_1 = 0.75$, $a_2 = 0.9$ and $k_1 = k_2 = 0.25$ as shown in Fig. 3.39 (c). The magnitude of the contour response in case 2 of set 4 is lower than that of the contour responses in case 2 of set 3 for the same values of k_1, k_2, a_1 and a_2. As can be observed, the magnitude of the contour response in Fig. 3.21 (a) of case 2 in set 3 is 0.7 whereas the magnitude for the same values in Fig. 3.39 (a) is 0.6. The stopband width of the contour response in case 2 of set 4 is larger than the stopband width in case 2 of set 3. As an example, the stopband in Fig. 3.40 (a) of set 4 is larger than the stopband in Fig. 3.22 (a) of set 3.

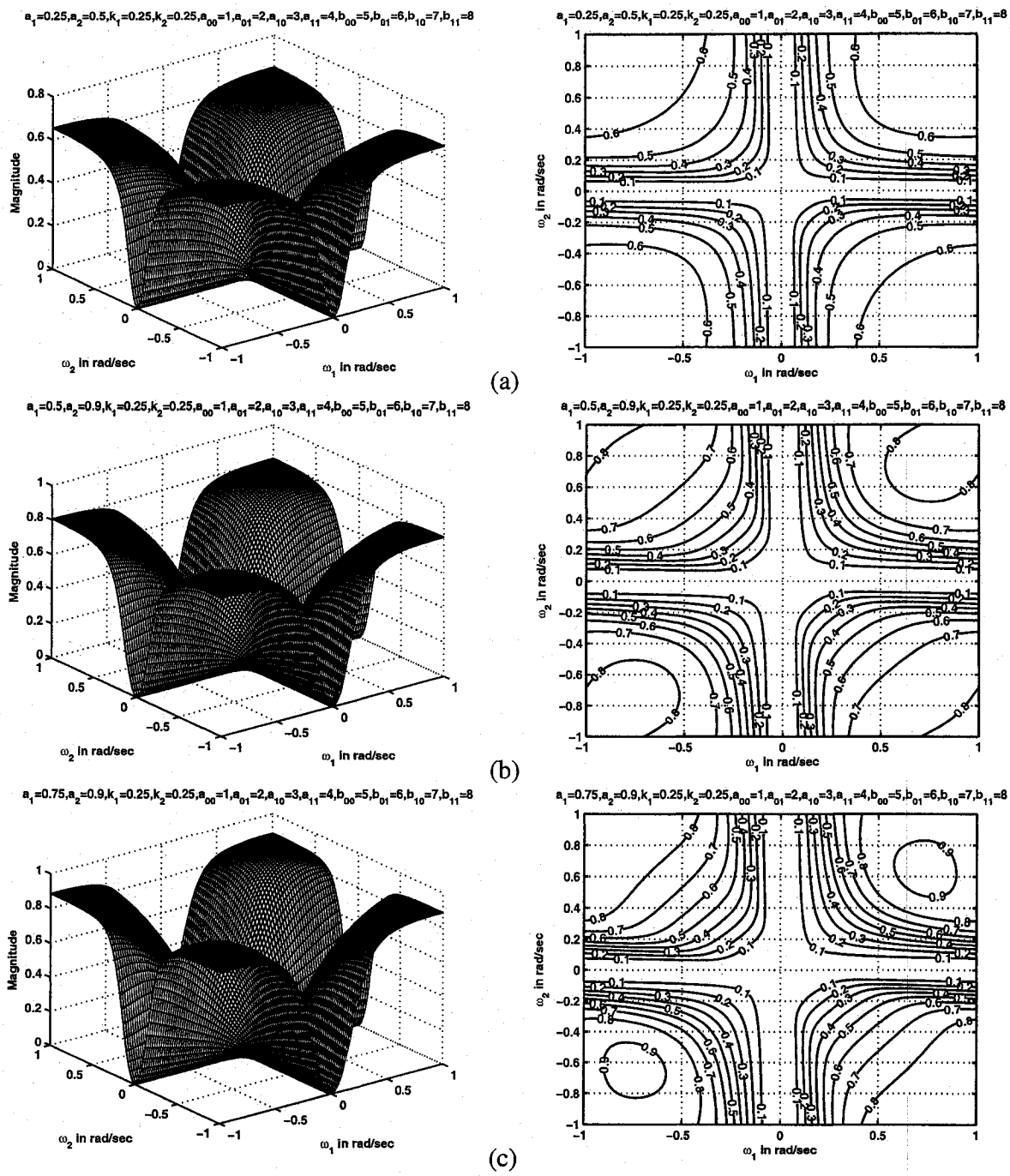

Figure 3.39: 3-D amplitude-frequency response and contour response of the 2-D digital highpass filter in case 2 of set 4 (when $k_1 = k_2 = 0.25$)

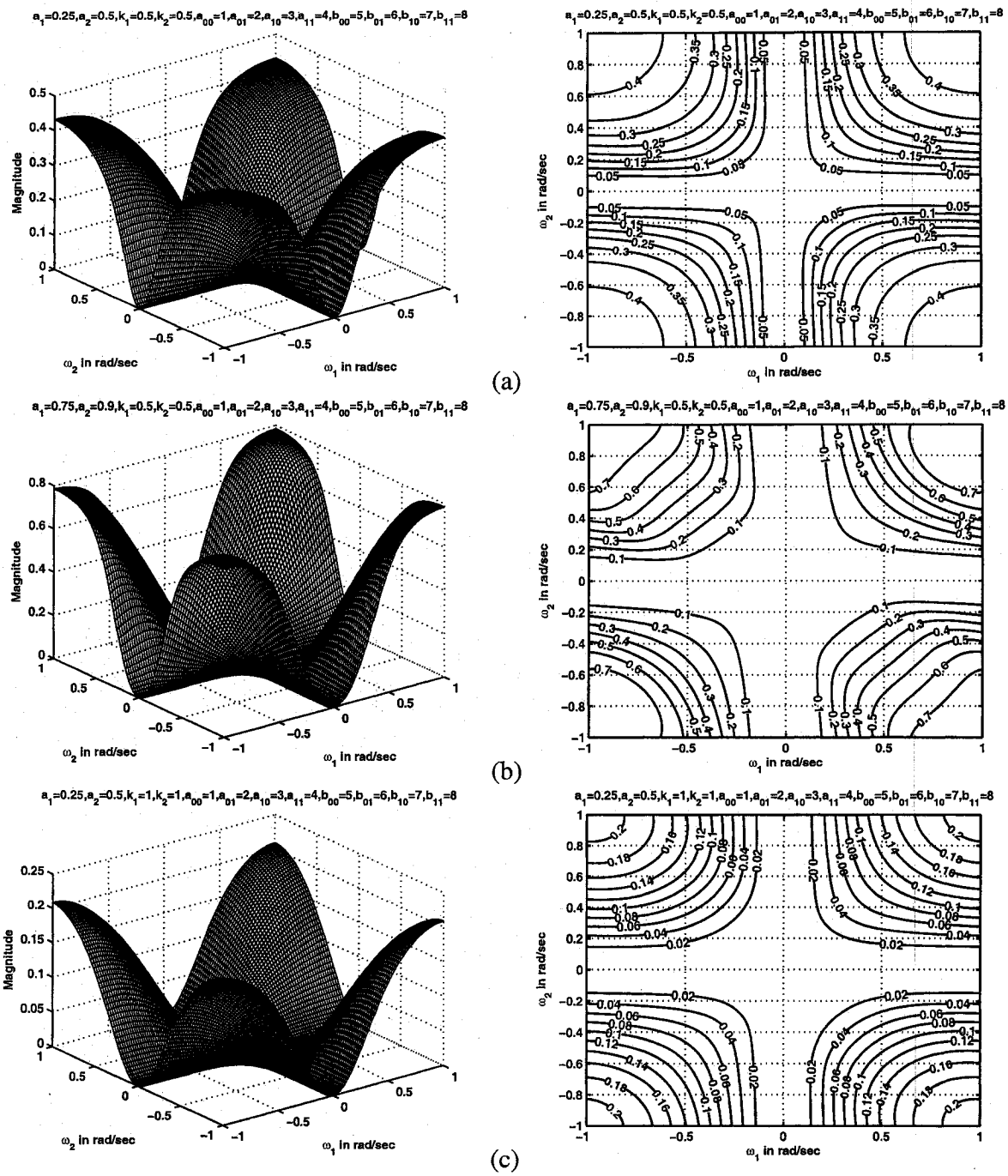

Figure 3.40: 3-D amplitude-frequency response and contour response of the 2-D digital highpass filter in case 2 of set 4 (when $k_1 = k_2 = 0.5,\ 1$)

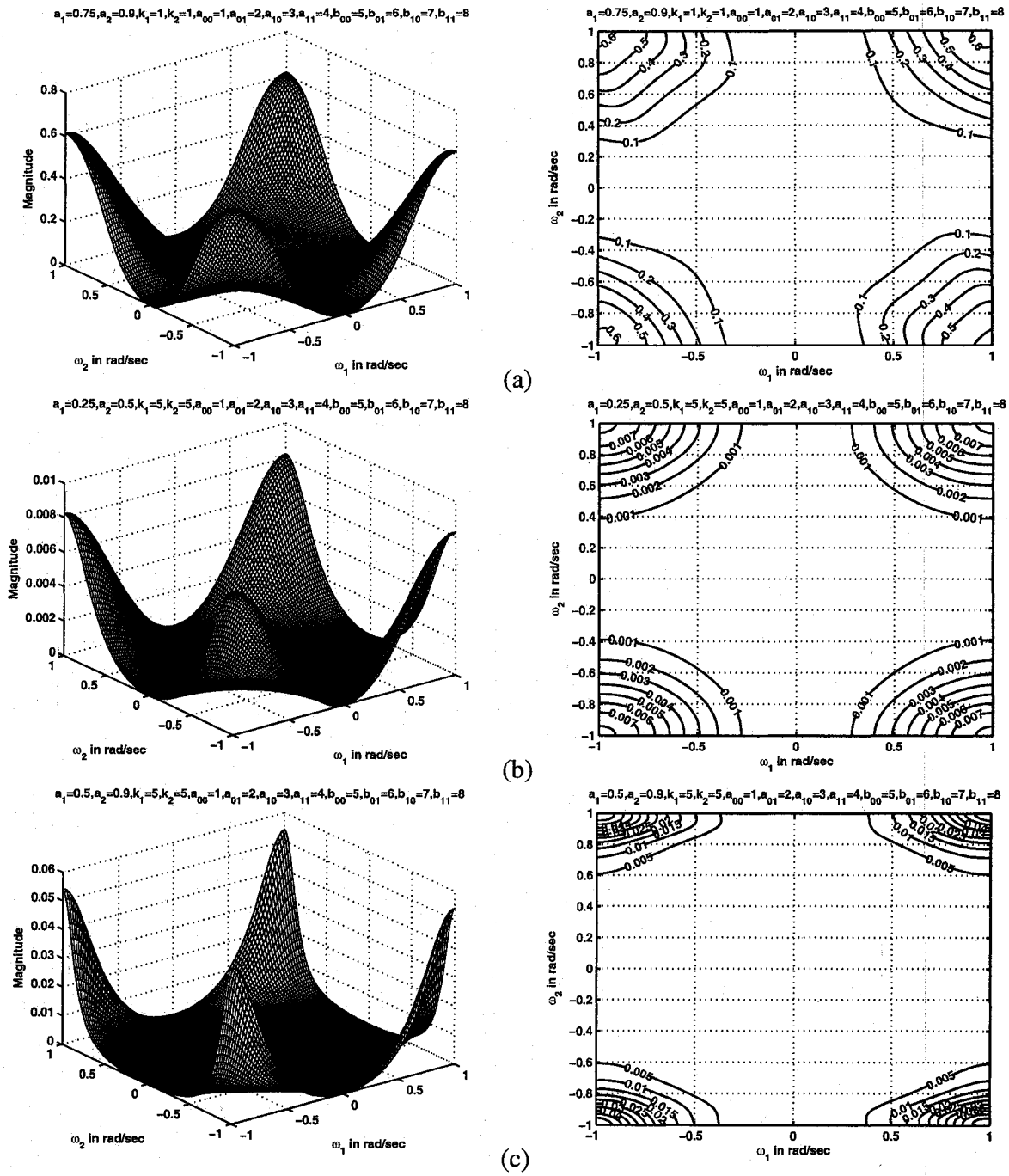

Figure 3.41: 3-D amplitude-frequency response and contour response of the 2-D digital highpass filter in case 2 of set 4 (when $k_1 = k_2 = 1, 5$)

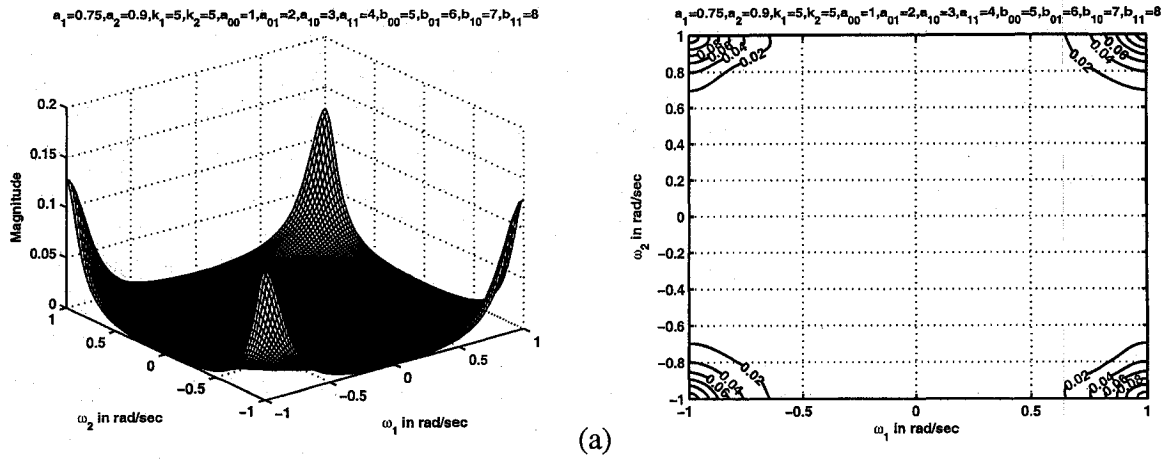

(a)

Figure 3.42: 3-D amplitude-frequency response and contour response of the 2-D digital highpass filter in case 2 of set 4 (when $k_1 = k_2 = 5$)

3.4.4.3 Case 3:

In this case,

$$a_1 \neq a_2 \quad , \quad k_1 \neq k_2 \quad , \quad b_1 = b_2 = -1$$

It is observed that the coefficients k_1 and k_2 affect the stopband width and the coefficients a_1 and a_2 affect the gain of the amplitude-frequency response. As k_1 and k_2 values are increased, the stopband width of the 2-D highpass filter increases and the magnitude of the amplitude-frequency response also decreases. As a_1 and a_2 values are increased, the magnitude of the amplitude-frequency response of the 2-D highpass filter increases and the stopband width increases. Overall, the cut-off frequencies of the 2-D highpass filter changes when k_1, k_2, a_1 and a_2 values are increased.

In this case, there are no ripples in the contour response of the 2-D highpass filter for all values of k_1, k_2, a_1 and a_2. The magnitude of the contour response is slightly lower than that of the contour responses in case 3 of set 3 for the same values of k_1, k_2, a_1 and a_2. The magnitude of the contour response in Fig. 3.45 (a) in case 3 of set 4 is 0.25 whereas the magnitude for the same values in Fig. 3.28 (a) in case 3 of set 3 is 0.3. The stopband width

of the contour response in this case of set 4 is larger than the stopband width in case 3 of set 3. In Fig. 3.45 (a), the stopband width is larger than the stopband width in Fig. 3.28 (a) of set 3 for same values of k_1, k_2, a_1 and a_2.

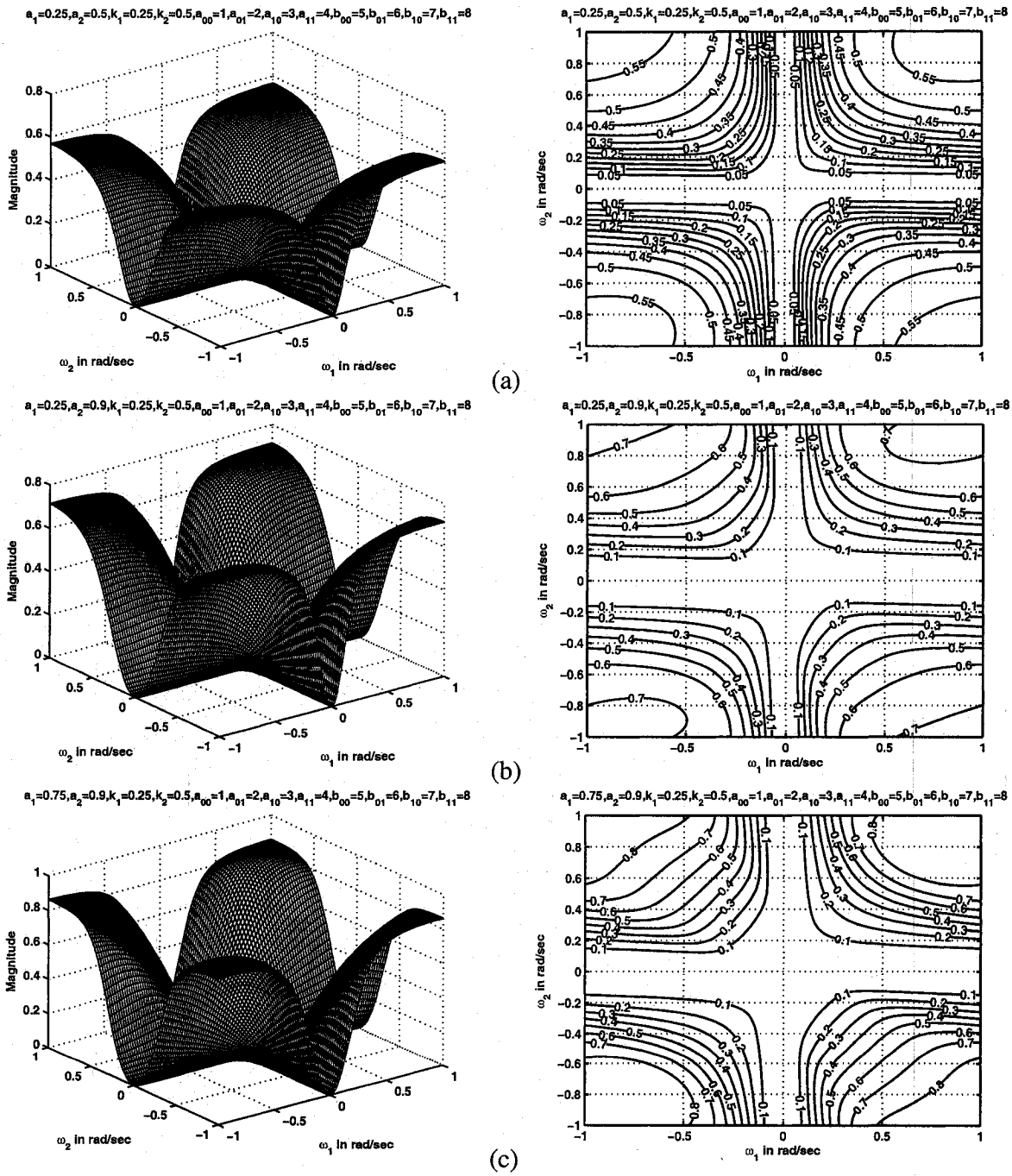

Figure 3.43: 3-D amplitude-frequency response and contour response of the 2-D digital highpass filter in case 3 of set 4 (when $k_1 = 0.25$, $k_2 = 0.5$)

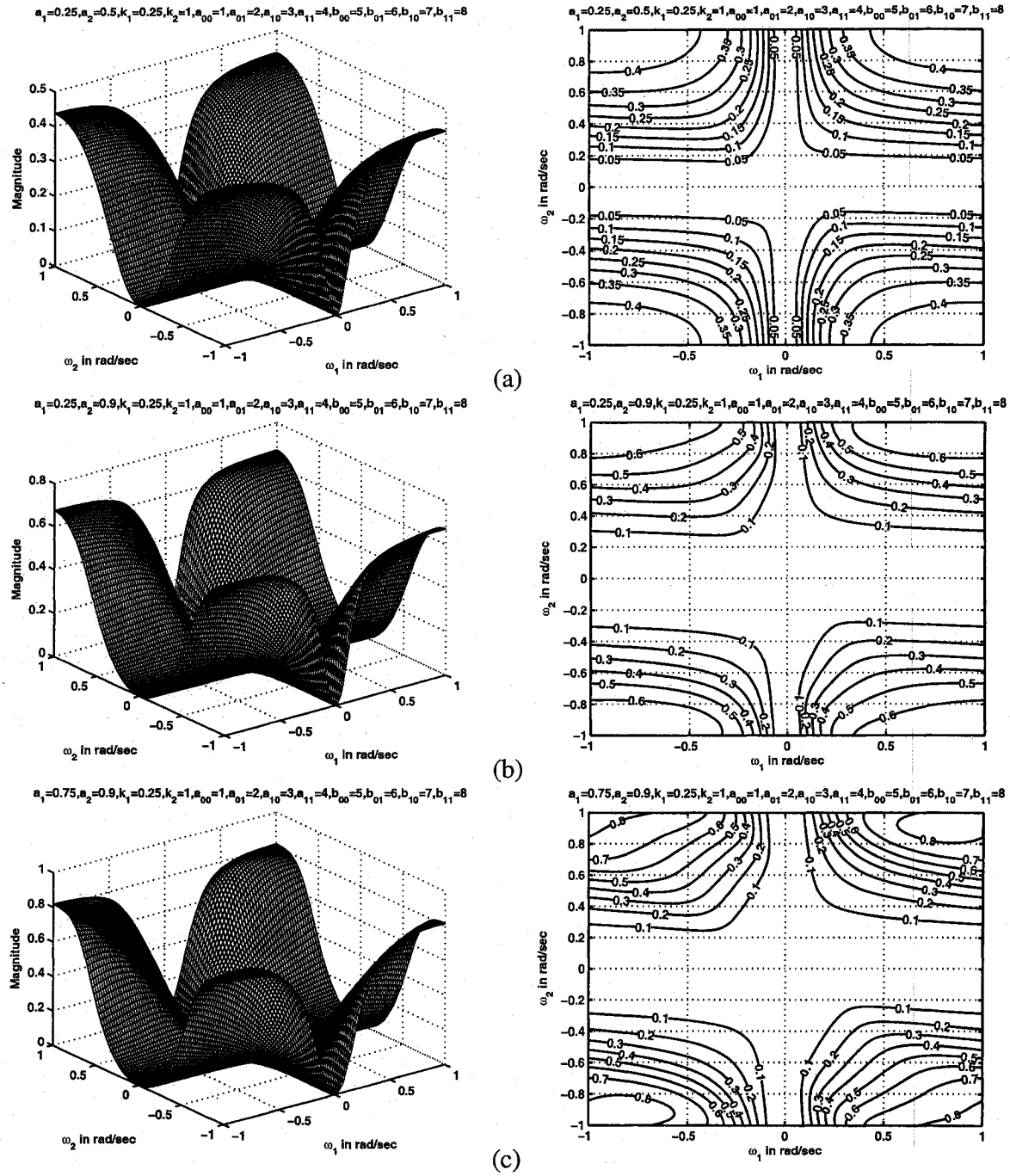

Figure 3.44: 3-D amplitude-frequency response and contour response of the 2-D digital highpass filter in case 3 of set 4 (when $k_1 = 0.25$, $k_2 = 1$)

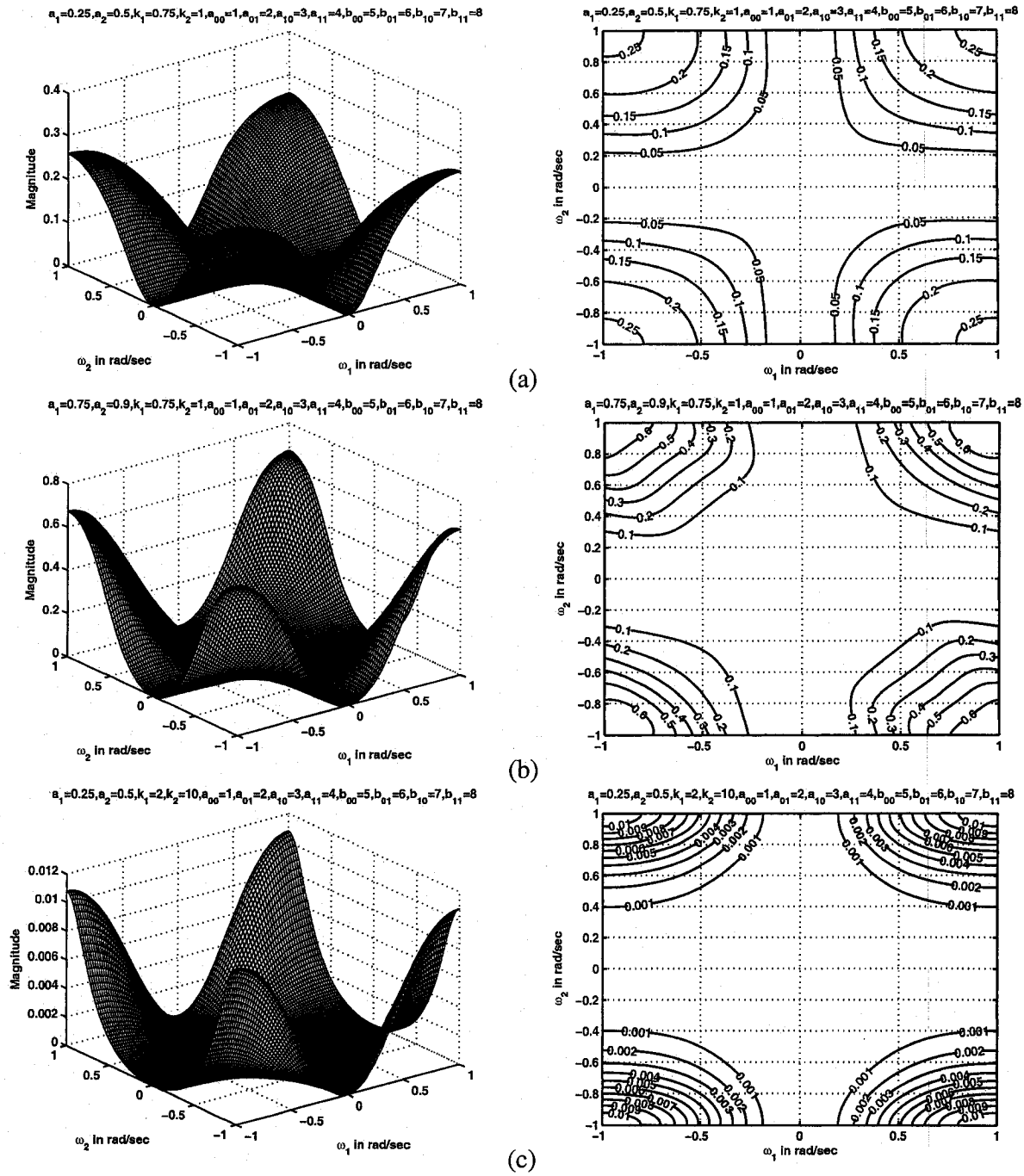

Figure 3.45: 3-D amplitude-frequency response and contour response of the 2-D digital highpass filter in case 3 of set 4 (when $k_1 = 0.75,\ 2,\ k_2 = 1,\ 10$)

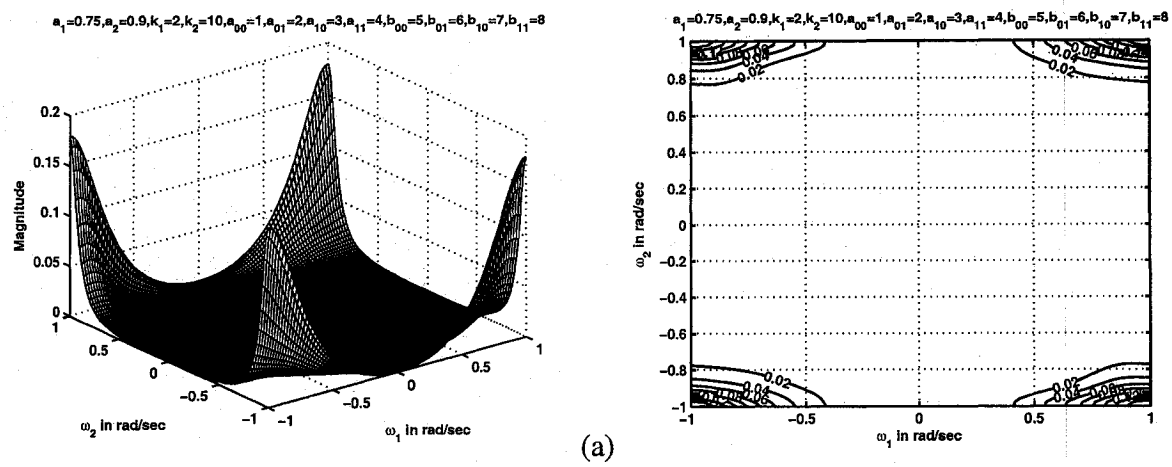

(a)

Figure 3.46: 3-D amplitude-frequency response and contour response of the 2-D digital highpass filter in case 3 of set 4 (when $k_1 = 2$, $k_2 = 10$)

3.4.4.4 Case 4:

In this case,

$$a_1 = a_2 \quad , \quad k_1 = k_2 \quad , \quad b_1 = b_2 = -1$$

It is observed that the coefficients k_1 and k_2 affect the stopband width and the coefficients a_1 and a_2 affect the gain of the amplitude-frequency response. As k_1 and k_2 values are increased, the stopband width of the 2-D highpass filter increases and the magnitude of the amplitude-frequency response decreases. As a_1 and a_2 values are increased, the magnitude of the amplitude-frequency response of the 2-D highpass filter increases and the stopband width increases. Overall, thecut-off frequencies of the 2-D highpass filter changes when k_1, k_2, a_1 and a_2 values are increased.

The ripples in the passband of the contour response in case 4 of set 3 for the values of $k_1 = k_2 = 0.25$ and for values of$a_1 = a_2 \geq 0.75$ as shown in Fig. 3.30 (b), disappear in case 4 of set 4 as shown in Fig. 3.47 (b). Also, in this case, there are ripples in the passband of the contour response for the values of $k_1 = k_2 = 0.5$ and for values of $a_1 = a_2 = 0.9$ as shown in Fig. 3.48 (b).

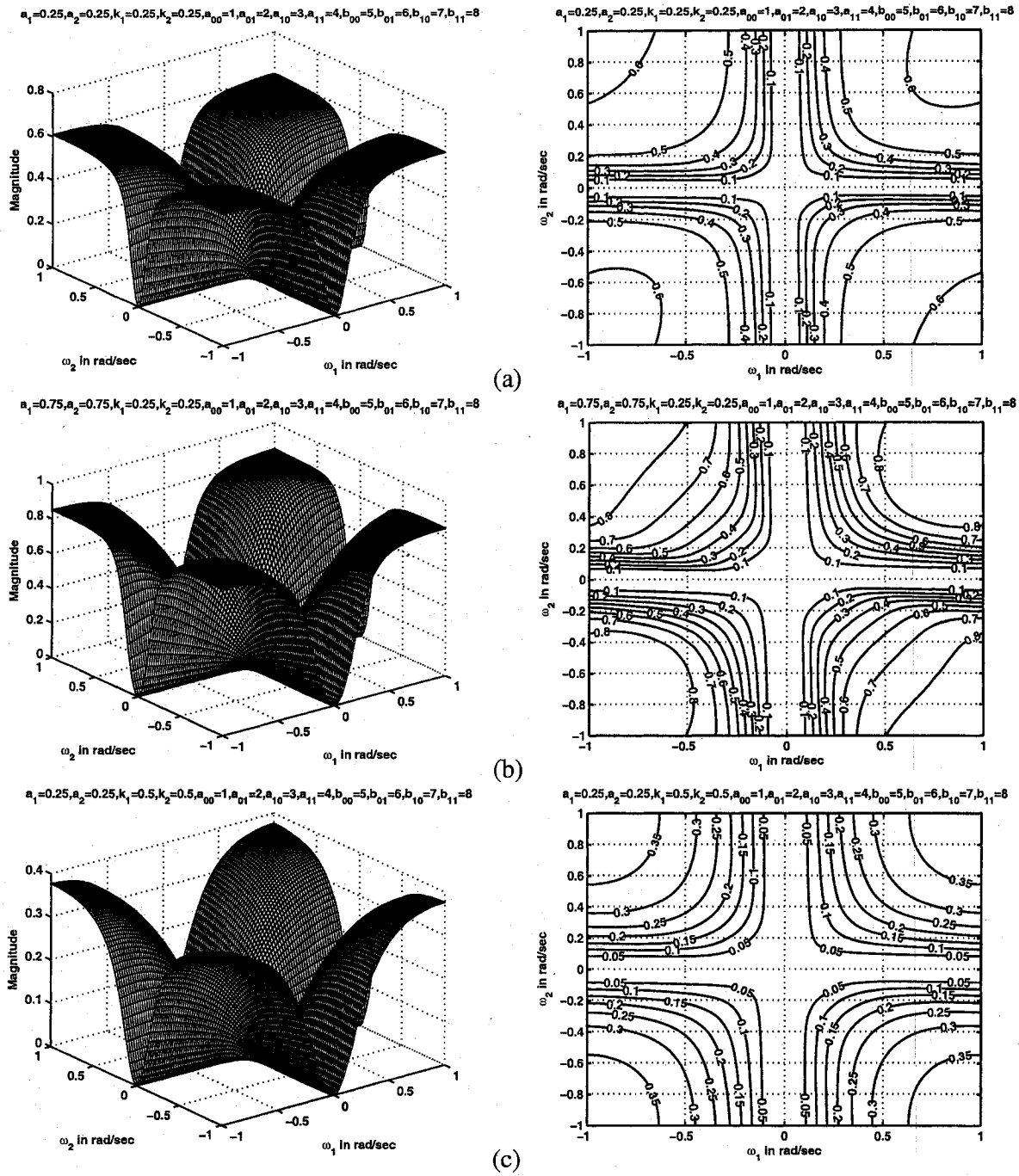

Figure 3.47: 3-D amplitude-frequency response and contour response of the 2-D digital highpass filter in case 4 of set 4 (when $k_1 = k_2 = 0.25$)

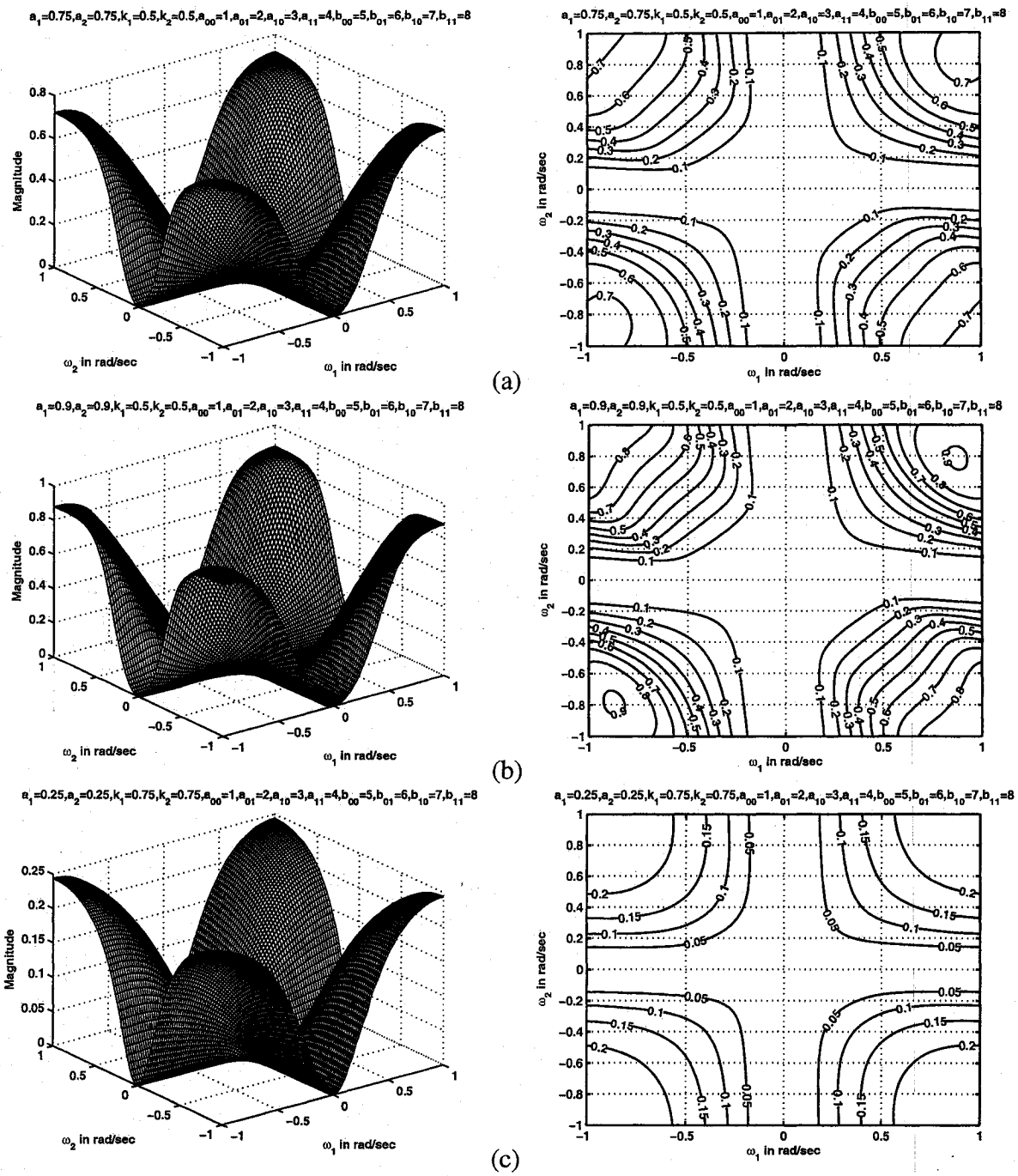

Figure 3.48: 3-D amplitude-frequency response and contour response of the 2-D digital highpass filter in case 4 of set 4 (when $k_1 = k_2 = 0.5,\ 0.75$)

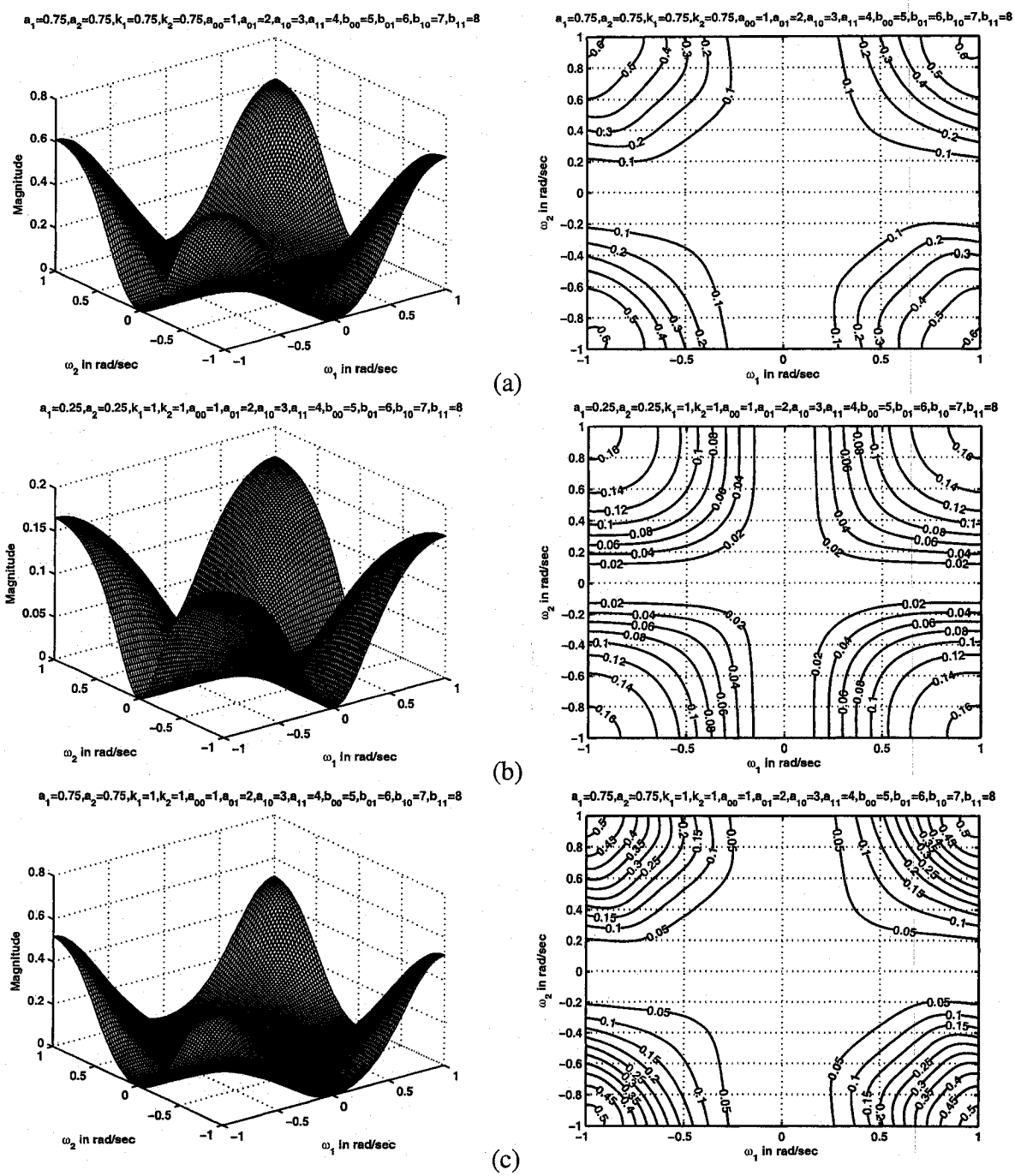

Figure 3.49: 3-D amplitude-frequency response and contour response of the 2-D digital highpass filter in case 4 of set 4 (when $k_1 = k_2 = 0.75,\ 1$)

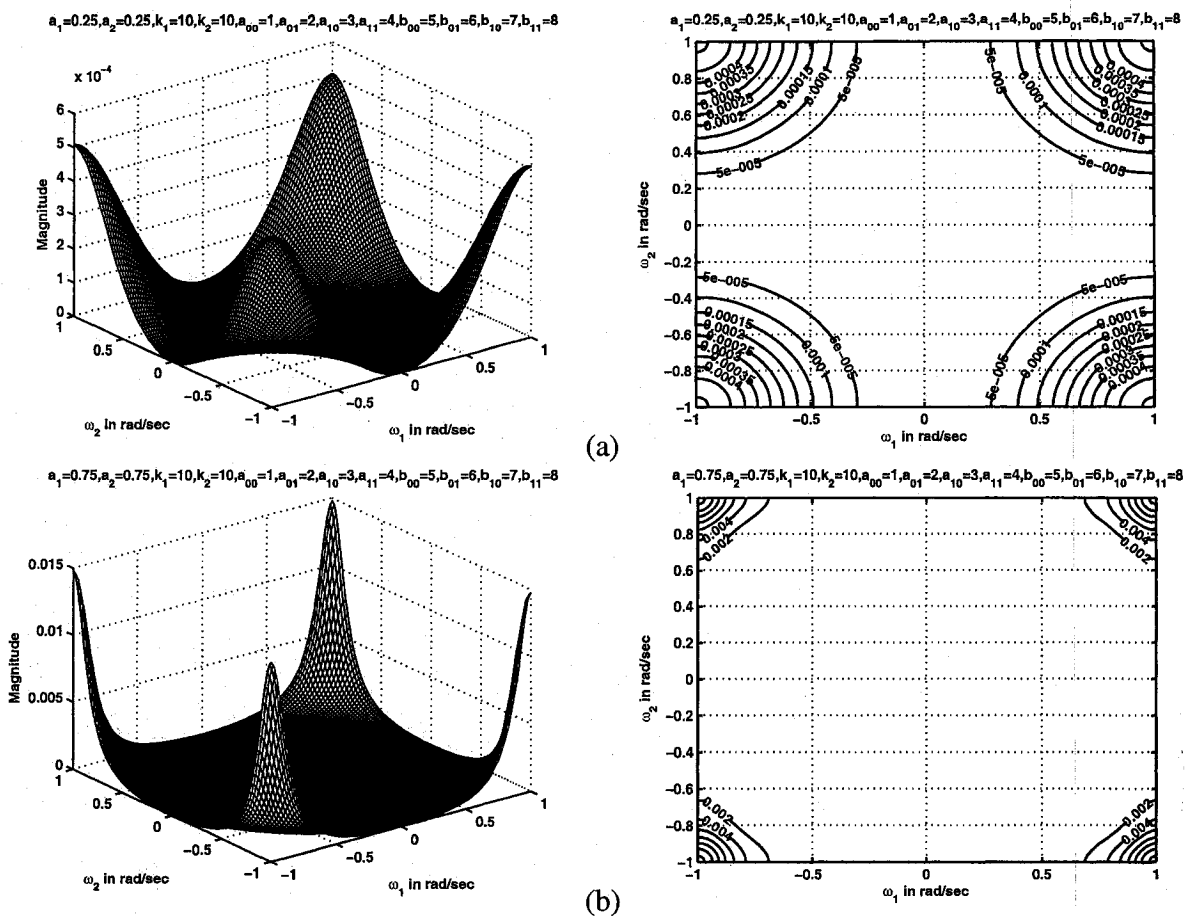

Figure 3.50: 3-D amplitude-frequency response and contour response of the 2-D digital highpass filter in case 4 of set 4 (when $k_1 = k_2 = 10$)

The magnitude of the contour response in this case of set 4 is slightly lower than that of the contour responses in case 4 of set 3 for the same values of k_1, k_2, a_1 and a_2. The magnitude of the contour response in Fig. 3.31 (b) of case 4 in set 3 is 0.3 whereas the magnitude of the contour response in Fig. 3.48 (c) of case 4 in set 4 is 0.2. The stopband width of the contour response in this case of set 4 is larger than that of the stopband width in case 4 of set 3. The stopband width of Fig. 3.48 (c) in this case of set 4 is much larger than the stopband width of 3.31 (b) of case 4 in set 3 for the same values of k_1, k_2, a_1 and a_2.

3.5 Summary

It is observed in all the four cases that the coefficients k_1 and k_2 affect the stopband width and the coefficients a_1 and a_2 affect the gain of the amplitude-frequency response. As k_1 and k_2 values are increased, the stopband width of the 2-D highpass filter increases, i.e., the cut-off frequencies are changed and the magnitude of the amplitude-frequency response decreases. As a_1 and a_2 values are increased, the magnitude of the amplitude-frequency response of the 2-D highpass filter increases and the stopband width increases. Overall, the cut-off frequencies of the 2-D highpass filter changes when k_1, k_2, a_1 and a_2 values are changed. It can be noticed that there is rounding of contour edges for higher values of k_1 and k_2. Also, the contours in the first and third quadrants are mirror images of one another and the contours in the second and fourth quadrants are mirror images of one another. In all the cases, values of k_1 and k_2 upto 10 have been studied. Higher values are not reported because the responses exhibit a tendency to repeat themselves.

In set 1, there are ripples in the contour response for smaller values of k_1 and k_2 (i.e., when k_1, $k_2 \leq 0.75$) and for larger values of a_1 and a_2 (i.e., when a_1, $a_2 \geq 0.75$). In case 1, it can be seen that for lower values of k_1, k_2, (i.e., when one of the k_1, k_2 values is less than 0.5) or for higher values of a_1 and a_2, (i.e., when $a_1 = a_2 \geq 0.5$), ripples are present on the second and fourth quadrants. In case 2, for very low vaues of k_1 and k_2, i.e., when $k_1 = k_2 < 0.75$, there are ripples in the contour response for all values of a_1 and a_2. In case 3, as $a_1 \neq a_2$ and $k_1 \neq k_2$, ripples in the contour response occur when a_1 *or* $a_2 \geq 0.5$ or when one of the k_1 *or* $k_2 \leq 0.5$. In case 4, there are ripples in the contour response for values of a_1 and a_2 greater than 0.5 or for values of k_1 and k_2 less than 0.5.

An important obervation to be noted is that the responses for set 2 is the same as that of set 1. This is because of the resulting transfer function for set 2 is the same as the one used in set 1 as the transfer function does not depend on the coefficients of the VSHP polynomial.It only depends on the coefficients of the bilinear transformation.

In set 3, it can be observed that there are not many ripples in the contour response when

compared to set 1 except under few circumstances which was dealt in detail in Sec.3.4.3. Also the magnitude of the contour response is low when compared to set 1 for the same values of k_1, k_2, a_1 and a_2. The amplitude-frequency responses are more or less similar to set 1 for all values of a_1 and a_2 when k_1, $k_2 > 1$. In case 1, there are no ripples in the contour response of the 2-D highpass filter for all values of k_1, k_2, a_1 and a_2. In case 2, there are ripples in the passband of the contour response for values of k_1 and k_2 as low as 0.25 and for values of $a_1 = 0.5$, $a_2 = 1$. Also, the ripples in the passband occur for values of $k_1 = k_2 = 0.5$ and for values of $a_1 = 0.75$, $a_2 = 1$. In case 3, there are ripples in the passband of the contour response when the values of k_1 and k_2 are as low as 0.25 and 0.5 respectively and the values of a_1 and a_2 are 0.5 and 1. In addition, it is observed that there are ripples in the passband when the values of k_1 and k_2 are 0.5 and 1 respectively and the values of a_1 and a_2 are 0.75 and 1 respectively. In case 4, there are ripples in the passband of the contour response for the values of $k_1 = k_2 = 0.25$ and for values of $a_1 = a_2 \geq 0.75$.

In set 4, the responses are similar to that of set 3. But the stopband width is larger in the contour responses of set 4 when compared to that of set 3. Also the magnitude of the contour response is low when compared to set 3 for the same values of k_1, k_2, a_1 and a_2. In case 1, there are ripples in the contour response for values of $a_1 = a_2 = 0.75$ and for values of k_1 and k_2 to be 0.25 and 0.5 respectively. In case 2, there are ripples in the passband of the contour response for values of $a_1 = 0.75$, $a_2 = 0.9$ and $k_1 = k_2 = 0.25$. In case 3, there are no ripples in the contour response of the 2-D highpass filter for all values of k_1, k_2, a_1 and a_2. In case 4, there are ripples in the passband of the contour response for the values of $k_1 = k_2 = 0.5$ and for values of $a_1 = a_2 = 0.9$.

Chapter 4

Two Dimensional Bandpass Filters from the CFE

4.1 Introduction

There are various ways to obtain bandpass filters from lowpass filters. A common method is by using lowpass filter and highpass filter combinations. By cascading 2-D digital lowpass and highpass filters, we can obtain bandpass filters, provided that the passband of both the filters overlap. In this section, we will study 2-D digital bandpass filters by using the lowpass and highpass filter transfer functions proposed in chapters 2 and 3 respectively.

In Sec. 4.2, we will generate 2-D digital bandpass filters. In Sec. 4.3, we shall discuss about the classification of bandpass filters. In Sec. 4.4, each set in particular is considered and the effect of the coefficients of the filter on the amplitude-frequency response will be studied. Sec. 4.5 gives the summary and discussions of the results contained in this chapter.

4.2 Generation of 2-D digital Bandpass Filter

The 2-D analog and digital lowpass filter proposed in Chapter 2 are given by eqn.(2.20) and eqn.(2.23). The 2-D digital highpass filter proposed in Chapter 3 is given by eqn.(3.2). By

cascading the 2-D digital lowpass and highpass filters, we can get combinational 2-D digital bandpass filter. For the resulting 2-D digital bandpass filter to be stable, it is required that $k_i > 0$ and $0 \leq a_i \leq 1$. Mathematically, $H(z_1, z_2)_{BPF} = H(z_1, z_2)_{LPF} * H(z_1, z_2)_{HPF}$.

4.3 Classification of 2-D Bandpass Filter

The 2-D bandpass filters are classified into four sets and each set is further classified into four cases. The classification of four sets is formed based on the coefficients of the CFE and the classification of four cases involved in each set is based on the coefficients of the generalized bilinear transformation.

4.3.1 The four types of sets

The different sets are formed based on the coefficients of the transfer function, i.e., eqn.(2.20). The values of a_1 and a_2 vary between 0 and 1 and the values of k_1 and k_2 are greater than 0. The same sets as used in Chapters 2 and 3 will be used here and they are given below:

In **set 1**, the values of all the coefficients of the transfer function are the same, i.e

$$a_{00} = a_{01} = a_{10} = a_{11} = b_{00} = b_{01} = b_{10} = b_{11} \tag{4.1}$$

Different magnitude and contour plots are obtained by varying the values of a_1, a_2, k_1 and k_2.

In **set 2**,

$$\begin{aligned} a_{00} &= a_{01} = a_{10} = a_{11} \\ b_{00} &= b_{01} = b_{10} = b_{11} \end{aligned} \tag{4.2}$$

Different magnitude and contour plots are obtained by varying the values of a_1, a_2, k_1 and k_2.

In **set 3**,

$$\begin{aligned} a_{00} &= a_{11} \\ a_{01} &= a_{10} \\ b_{00} &= b_{11} \\ b_{01} &= b_{10} \end{aligned} \tag{4.3}$$

Different magnitude and contour plots are obtained by varying the values of a_1, a_2, k_1 and k_2 .

In **set 4**,

$$a_{00} \neq a_{01} \neq a_{10} \neq a_{11} \neq b_{00} \neq b_{01} \neq b_{10} \neq b_{11} \tag{4.4}$$

Different magnitude and contour plots are obtained by varying the values of a_1, a_2, k_1 and k_2.

4.3.2 The different cases involved in the 4 sets

There are four different cases involved in each set. The four cases are formed based on the coefficients of the generalized bilinear transformation i.e., a_1, a_2, k_1 and k_2. The same cases as used in Chapters 2 and 3 will be used here and are given below:

Case 1: $a_1 = a_2$, $k_1 \neq k_2$

Case 2: $a_1 \neq a_2$, $k_1 = k_2$

Case 3: $a_1 \neq a_2$, $k_1 \neq k_2$

Case 4: $a_1 = a_2$, $k_1 = k_2$

4.4 Frequency Responses of 2-D Digital Bandpass Filter

By cascading the 2-D digital lowpass and highpass filters, we can get combinational 2-D digital bandpass filters. To investigate the manner in which each coefficient of the CFE and the generalized bilinear transformation affects the magnitude response of the resulting

2-D bandpass filter, we change the value of some of the coefficients or fix some of the coefficients to specific values.

Let us consider the filter coefficients and the bilinear transformation coefficients to be unity i.e., $a_1 = 1$, $a_2 = 1$, $k_1 = 1$, $k_2 = 1$, $a_{00} = 1$, $a_{10} = 1$, $a_{01} = 1$, $a_{11} = 1$, $b_{00} = 1$, $b_{10} = 1$, $b_{01} = 1$, $b_{11} = 1$. Under this condition, the 3-D amplitude-frequency response and contour response of the 2-D digital bandpass filter are shown in Fig. 4.1.

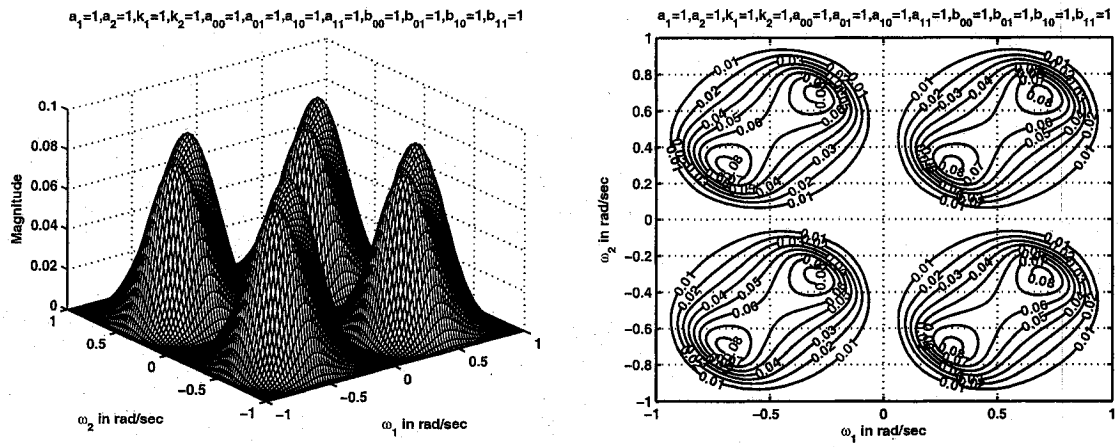

Figure 4.1: 3-D amplitude-frequency response and contour response of 2-D digital bandpass filter when all the coefficients are unity

The ripples in the passband can be removed by reducing the values of a_1 and a_2 by a small fraction i.e from 1 to 0.75 as seen in Fig. 4.16 (a) of case 4 in set 4. As discussed in Chapters 2 and 3, it is important to note that a normalizing constant has to be added to normalize the frequency response.

4.4.1 Frequency Response of 2-D Bandpass Filters in Set 1

In this section, we study the manner in which all the four cases in set 1 affect the frequency response behavior of the resulting 2-D bandpass filter. In this set, the values of all the coefficients are considered to be the same i.e.,

$$a_{00} = a_{01} = a_{10} = a_{11} = b_{00} = b_{01} = b_{10} = b_{11} \tag{4.5}$$

Different contour plots are obtained by varying the values of a_1, a_2, k_1 and k_2.

In this set, it is observed in all the four cases that the coefficients k_1, k_2 affect the passband width and the coefficients a_1, a_2 affect the gain of the amplitude-frequency response. As k_1 and k_2 values are increased, the passband width of the 2-D bandpass filter decreases and the magnitude of the contour response also decreases. Only in cases 1 and 3, as $k_1 \neq k_2$, the passband width of the 2-D digital bandpass filter increases and decreases periodically and the magnitude of the contour response decreases. As a_1 and a_2 values are increased, the magnitude of the amplitude-frequency response of the 2-D bandpass filter increases and the passband width decreases. It can be noticed that there is rounding of contour edges for higher values of k_1 and k_2. It can be also observed that the first and third quadrants of the contour response of the 2-D bandpass filters have the same passband width and magnitude whereas the second and fourth quadrants of the contour response have the same passband width and magnitude.

4.4.1.1 Case 1

In this case,

$$a_1 = a_2 \quad , \quad k_1 \neq k_2$$

As discussed above, the coefficients k_1 and k_2 affect the passband width of the 2-D

bandpass filter. In Fig. 4.2 (a), (b), (c) and Fig. 4.3 (a), there is a gradual decrease in the passband width as the values of k_1 and k_2 are increased from 0.25, 0.5 to 2, 10 respectively for the same values of $a_1 = a_2 = 0.25$. Further increase in the values of k_1 and k_2 result in gradual increase in the passband width. In Fig. 4.3 (b), it can be seen that the passband width increases when the values of k_1 and k_2 are increased to 8, 10 respectively. The passband width increases and decreases periodically for different values of k_1 and k_2. At the same time, there is also a decrease in the magnitude of the contour response for the same.

The coefficients a_1 and a_2 affect the gain of the amplitude-frequency response as discussed in the above section. In Fig. 4.2 (a), Fig. 4.3 (c) and Fig. 4.5 (b), as a_1 and a_2 values are increased from 0.25 to 0.75, for the same values of $k_1 = 0.25$, $k_2 = 0.5$, the magnitude of the contour response increases. There are ripples in the passband of the 2-D bandpass filters when the values of $a_1 = a_2 \geq 0.75$ and when the values of k_1, k_2 are less than 0.5. Also, the magnitude of the contours on the second and fourth quadrants for this particular set of values is twice that of the magnitude of the contours in the first and third quadrants as seen in Fig. 4.5 (b).

It can be noticed that the contours in the first and third quadrants are mirror images of one another and the contours in the second and fourth quadrants are mirror images of one another. Also the magnitude of the contours in the second and fourth quadrants is greater than the magnitude of the contours in the first and third quadrants.

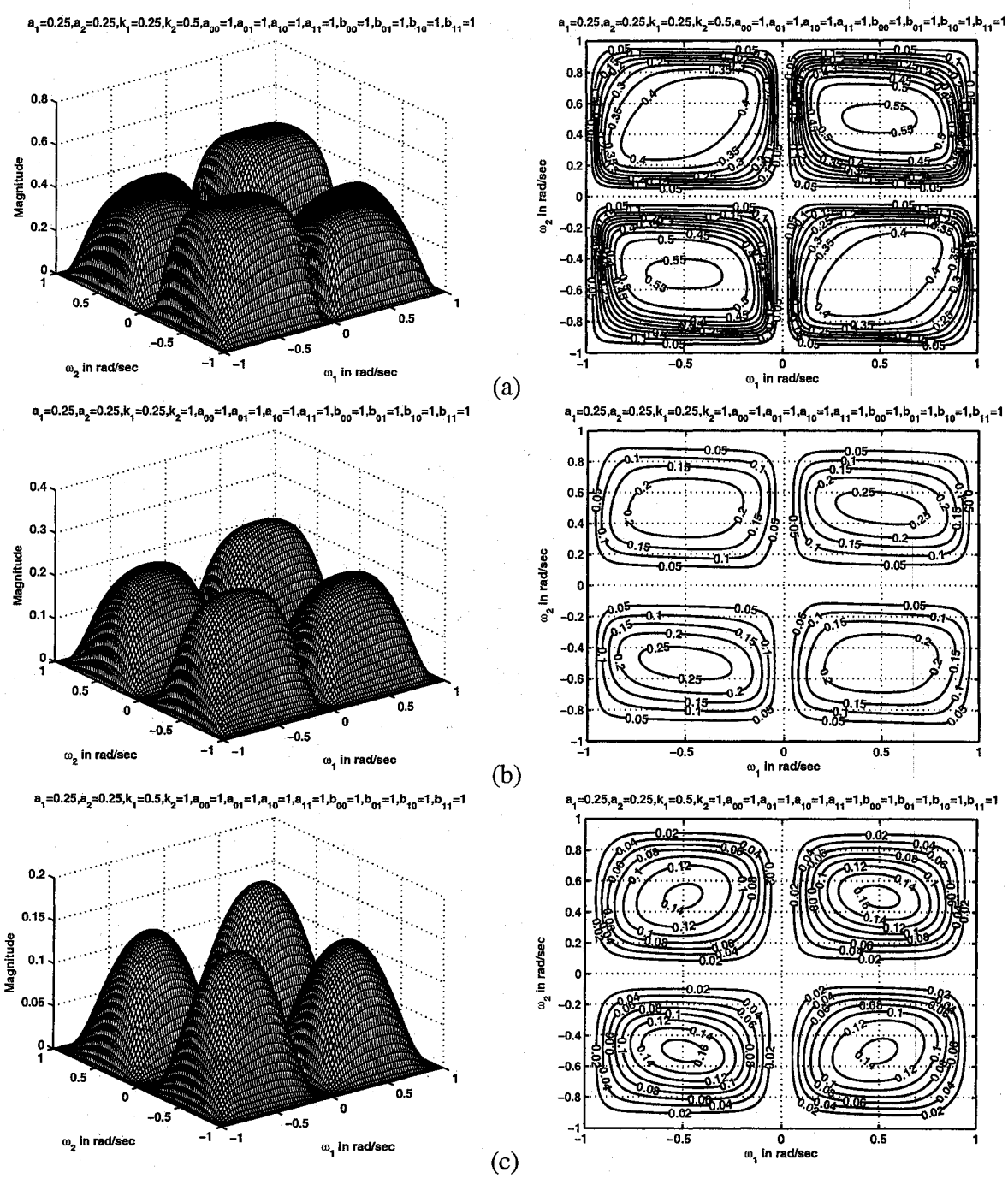

Figure 4.2: 3-D amplitude-frequency response and contour response of 2-D digital band-pass filter in case 1 of set 1 (when $a_1 = a_2 = 0.25$)

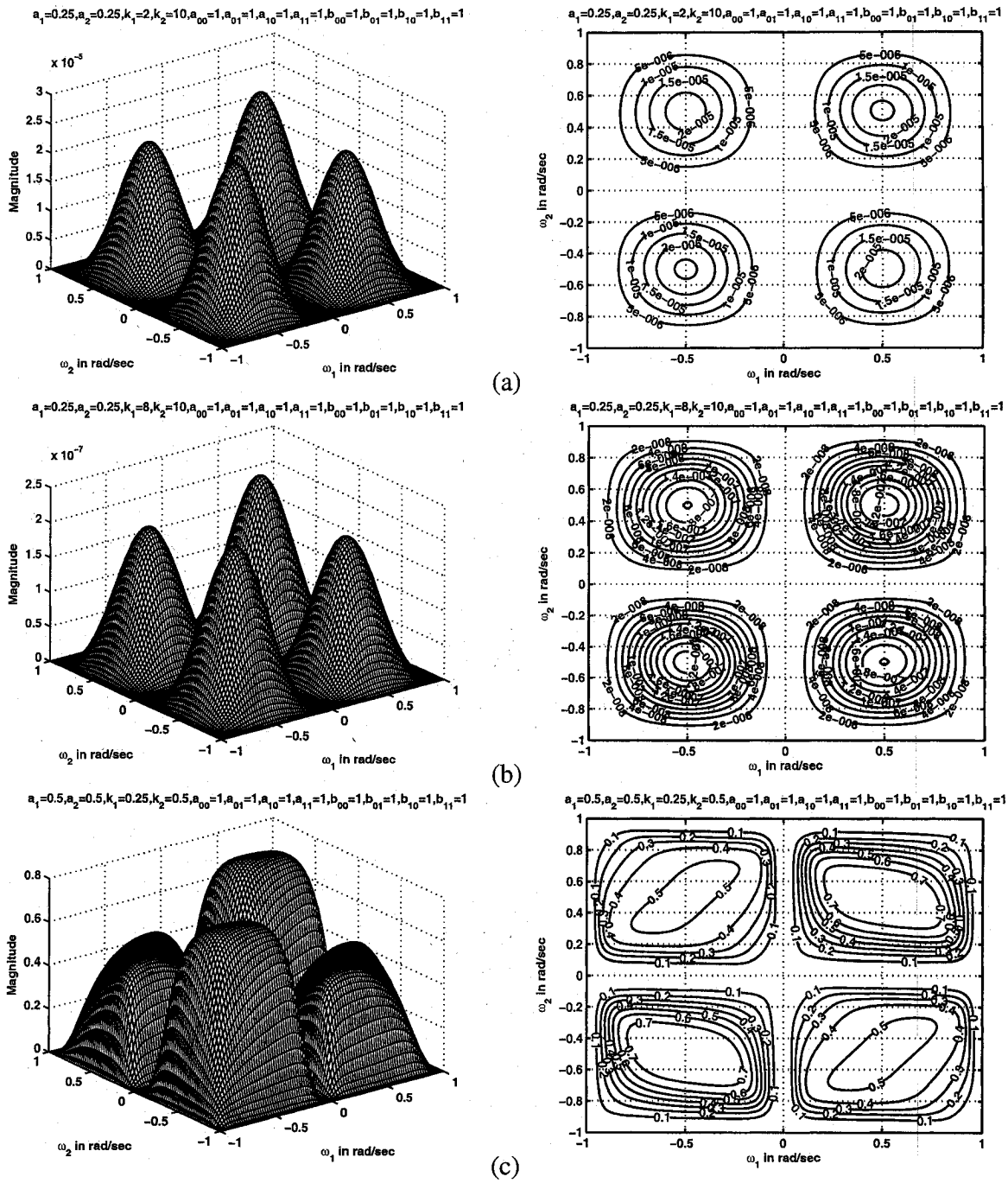

Figure 4.3: 3-D amplitude-frequency response and contour response of 2-D digital band-pass filter in case 1 of set 1 (when $a_1 = a_2 = 0.25,\ 0.5$)

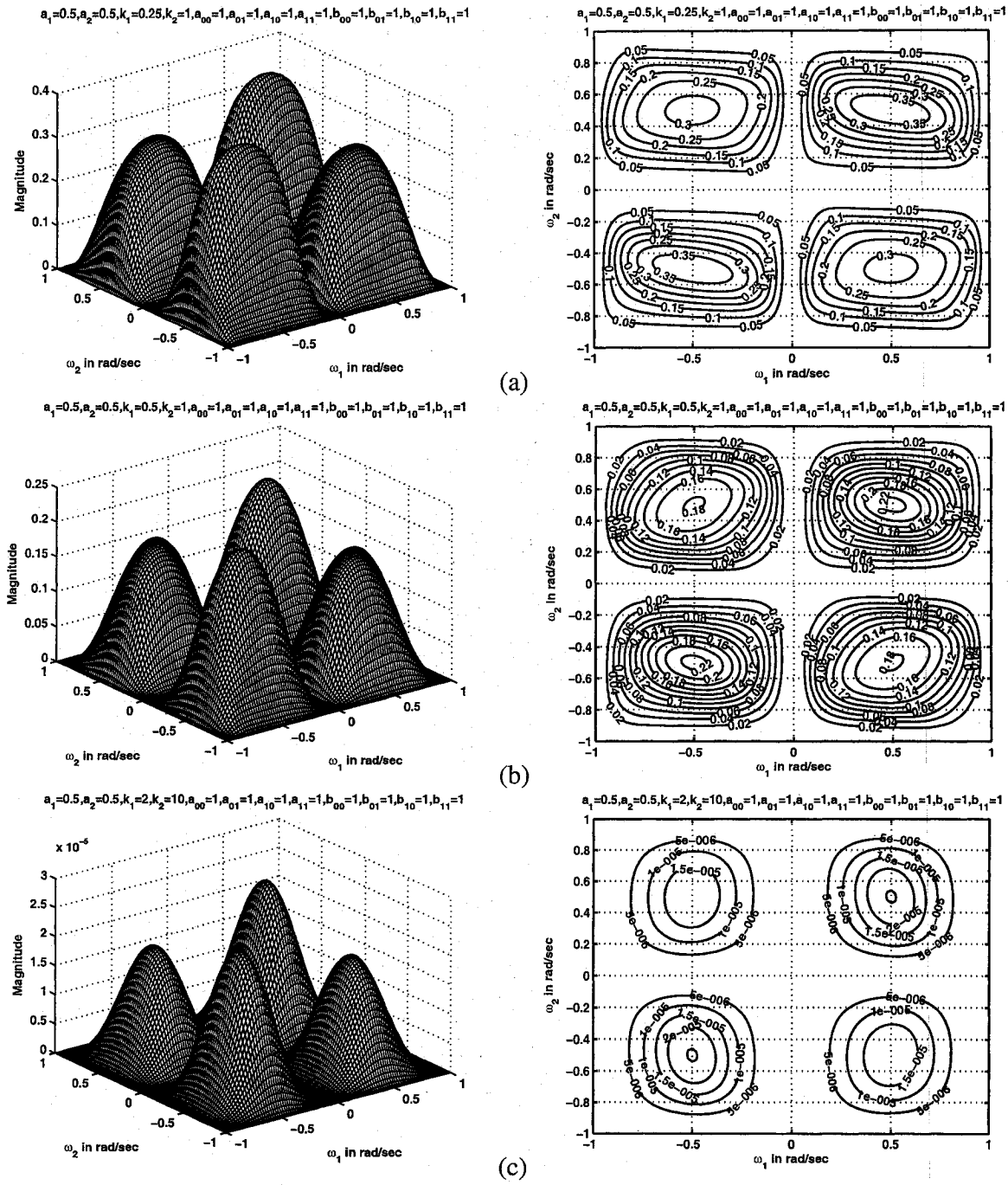

Figure 4.4: 3-D amplitude-frequency response and contour response of 2-D digital band-pass filter in case 1 of set 1 (when $a_1 = a_2 = 0.5$)

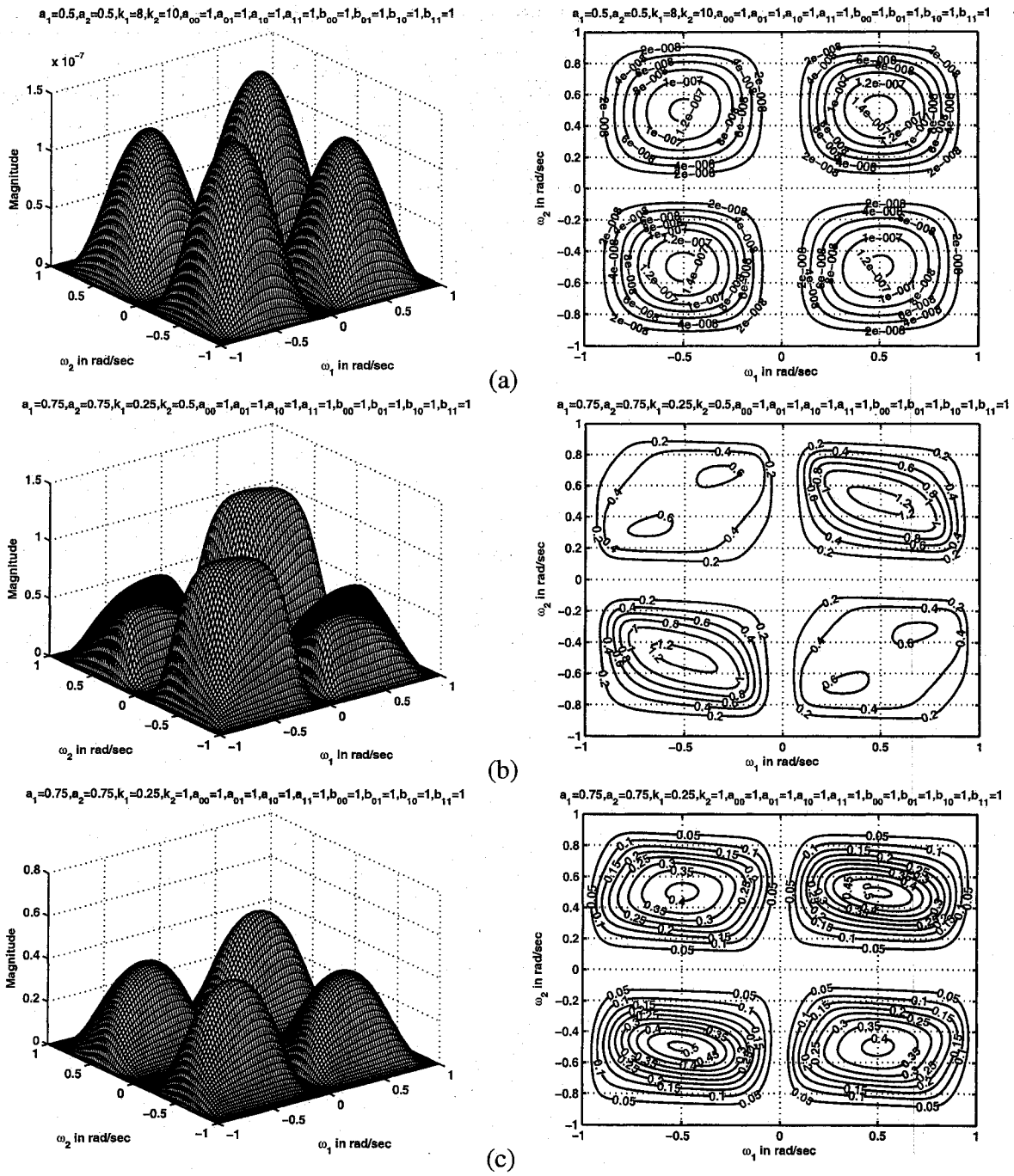

Figure 4.5: 3-D amplitude-frequency response and contour response of 2-D digital band-pass filter in case 1 of set 1 (when $a_1 = a_2 = 0.5,\ 0.75$)

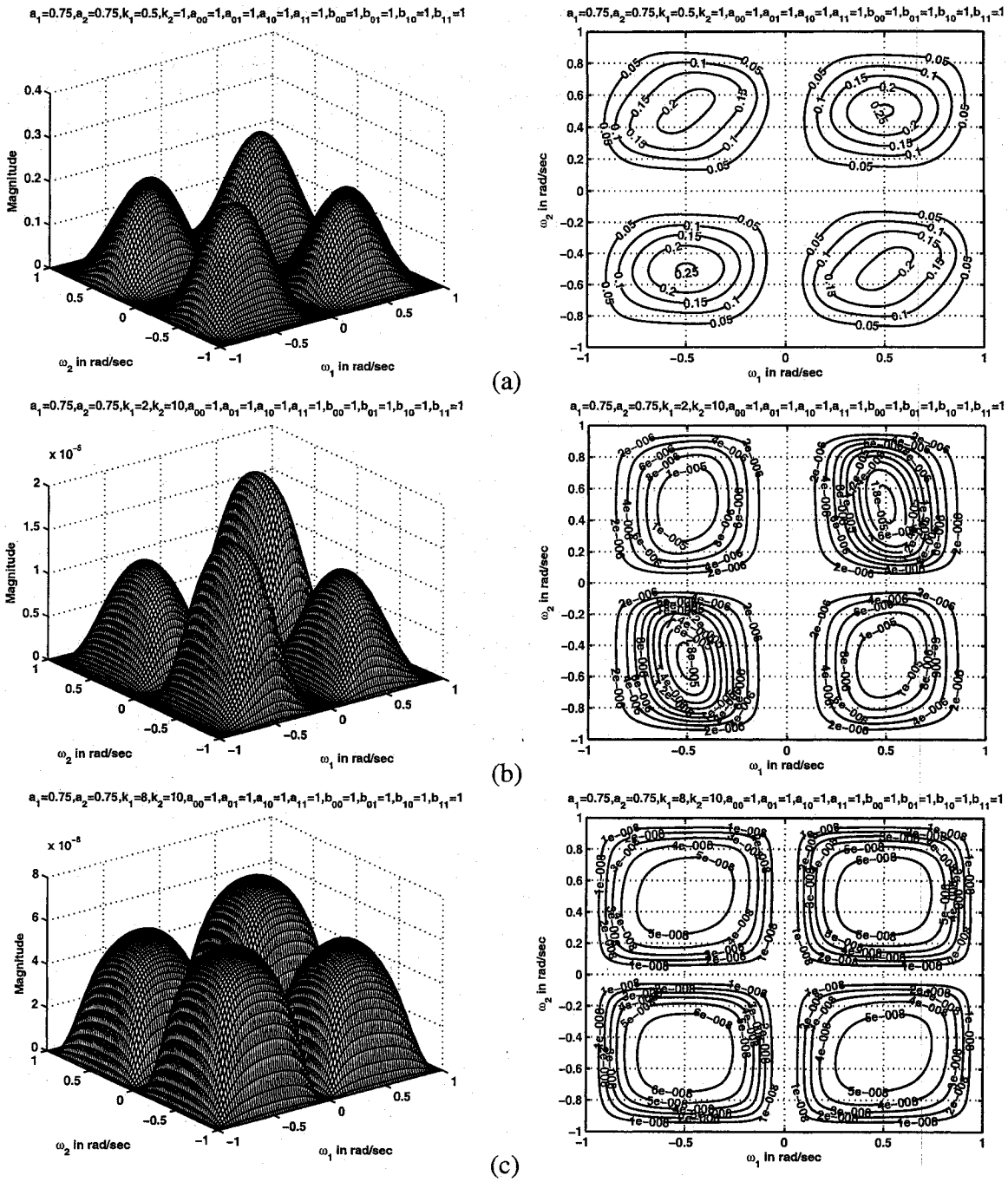

Figure 4.6: 3-D amplitude-frequency response and contour response of 2-D digital band-pass filter in case 1 of set 1 (when $a_1 = a_2 = 0.75$)

4.4.1.2 Case 2

In this case,

$$a_1 \neq a_2 \quad , \quad k_1 = k_2$$

The coefficients k_1 and k_2 affect the passband width of the 2- D bandpass filter. For example, in Fig. 4.7 (a), (c) , Fig. 4.8 (b) and Fig. 4.9 (a), there is a gradual decrease in the passband width, as the values of k_1 and k_2 are increased from 0.25 to 5 for the same values of $a_1 = 0.25$, $a_2 = 0.5$. At the same time, there is also a decrease in the magnitude of the contour response for the same.

The coefficients a_1 and a_2 affect the gain of the amplitude-frequency response as discussed in the above section. In Fig. 4.7 (a), (b), as a_1 and a_2 values are increased from 0.25, 0.5 to 0.5, 0.75 respectively, for the same values of $k_1 = k_2 = 0.25$, the magnitude of the contour response increases. Also, there are ripples in the contour response for all values of a_1 and a_2 till $k_1 = k_2 \leq 0.25$.

It can be noticed that the contours in the first and third quadrants are mirror images of one another and the contours in the second and fourth quadrants are mirror images of one another. Also the magnitude of the contours in the second and fourth quadrants is greater than the magnitude of the contours in the first and third quadrants.

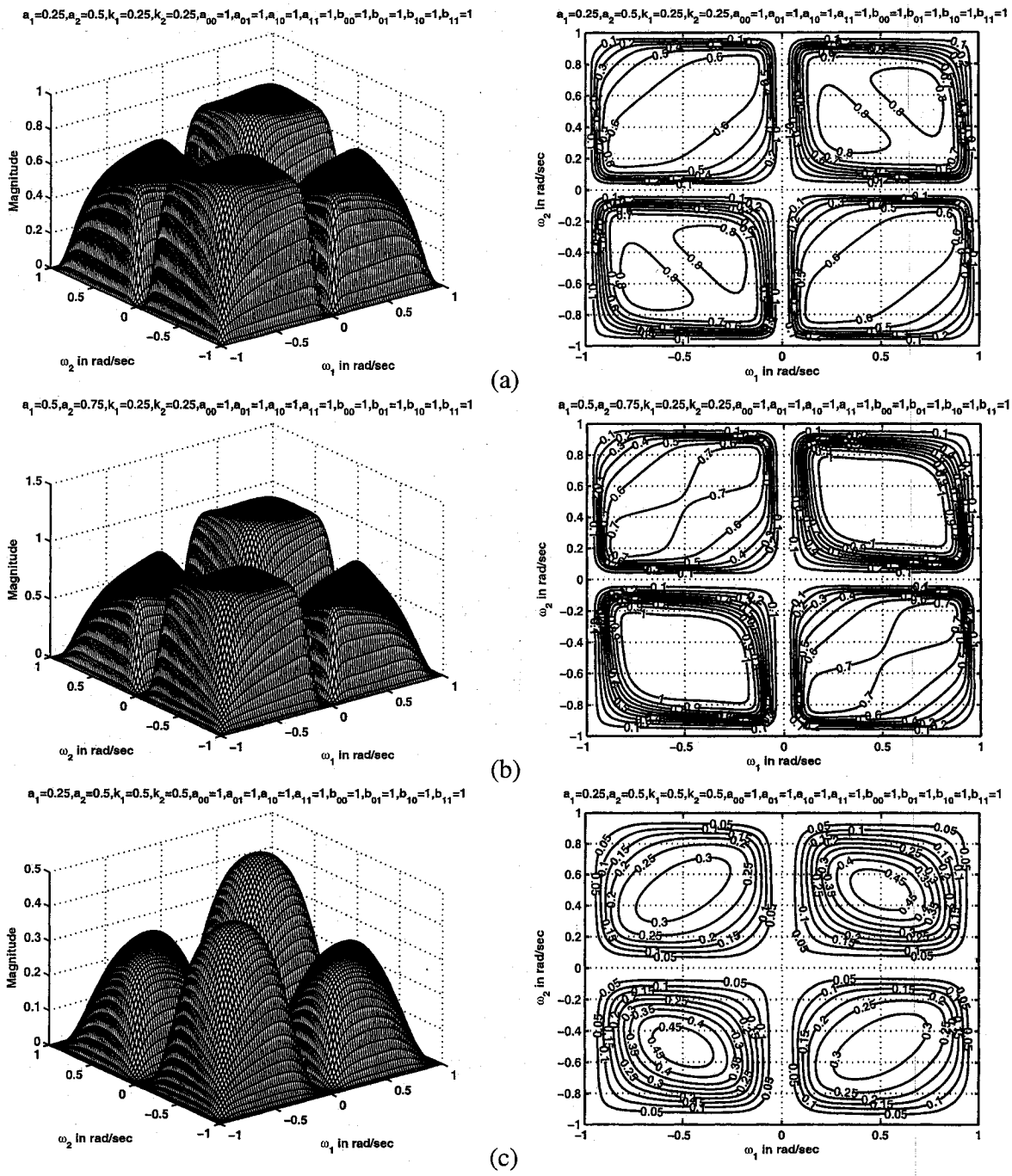

Figure 4.7: 3-D amplitude-frequency response and contour response of 2-D digital band-pass filter in case 2 of set 1 (when $k_1 = k_2 = 0.25,\ 0.5$)

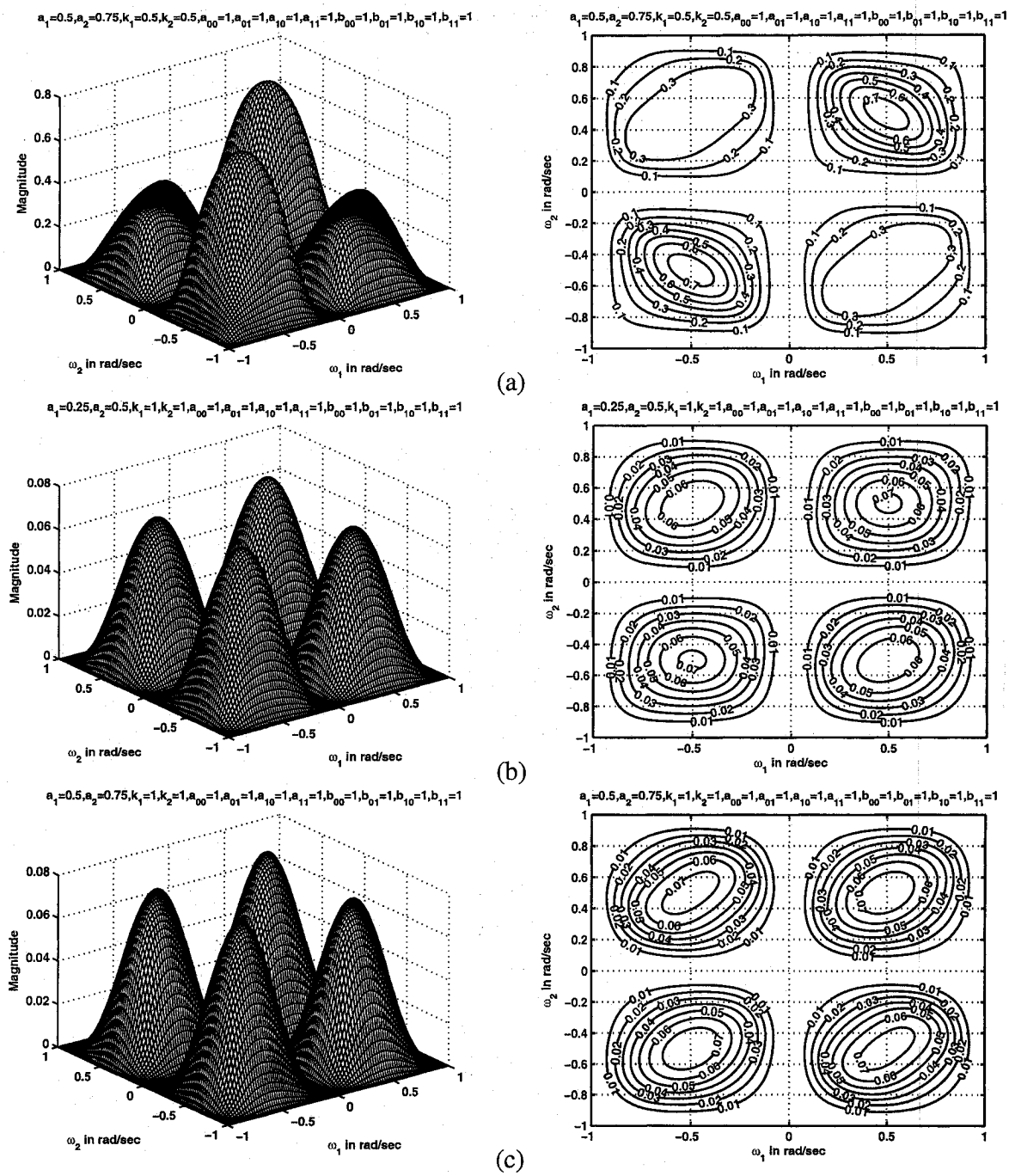

Figure 4.8: 3-D amplitude-frequency response and contour response of 2-D digital band-pass filter in case 2 of set 1 (when $k_1 = k_2 = 0.5,\ 1$)

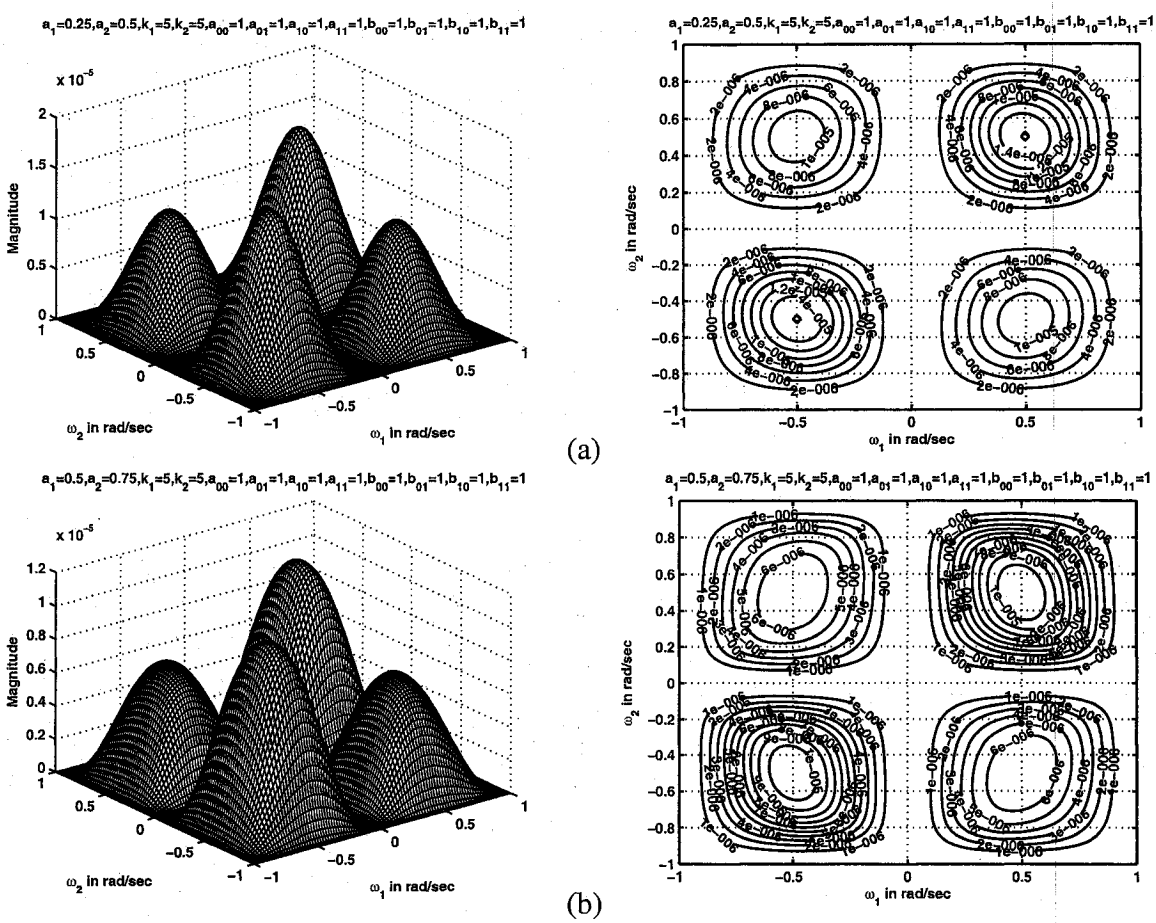

Figure 4.9: 3-D amplitude-frequency response and contour response of 2-D digital bandpass filter in case 2 of set 1 (when $k_1 = k_2 = 5$)

4.4.1.3 Case 3

In this case,

$$a_1 \neq a_2 \quad , \quad k_1 \neq k_2$$

The coefficients k_1 and k_2 affect the passband width of the 2-D bandpass filter. In Fig. 4.10 (b), Fig. 4.11 (a), (c) and Fig. 4.12 (b), there is a gradual decrease in the passband width as the values of k_1 and k_2 are increased from $k_1 = 0.25$, $k_2 = 0.5$ to $k_1 = 2$, $k_2 = 10$ for the same values of $a_1 = 0.5$, $a_2 = 0.75$.

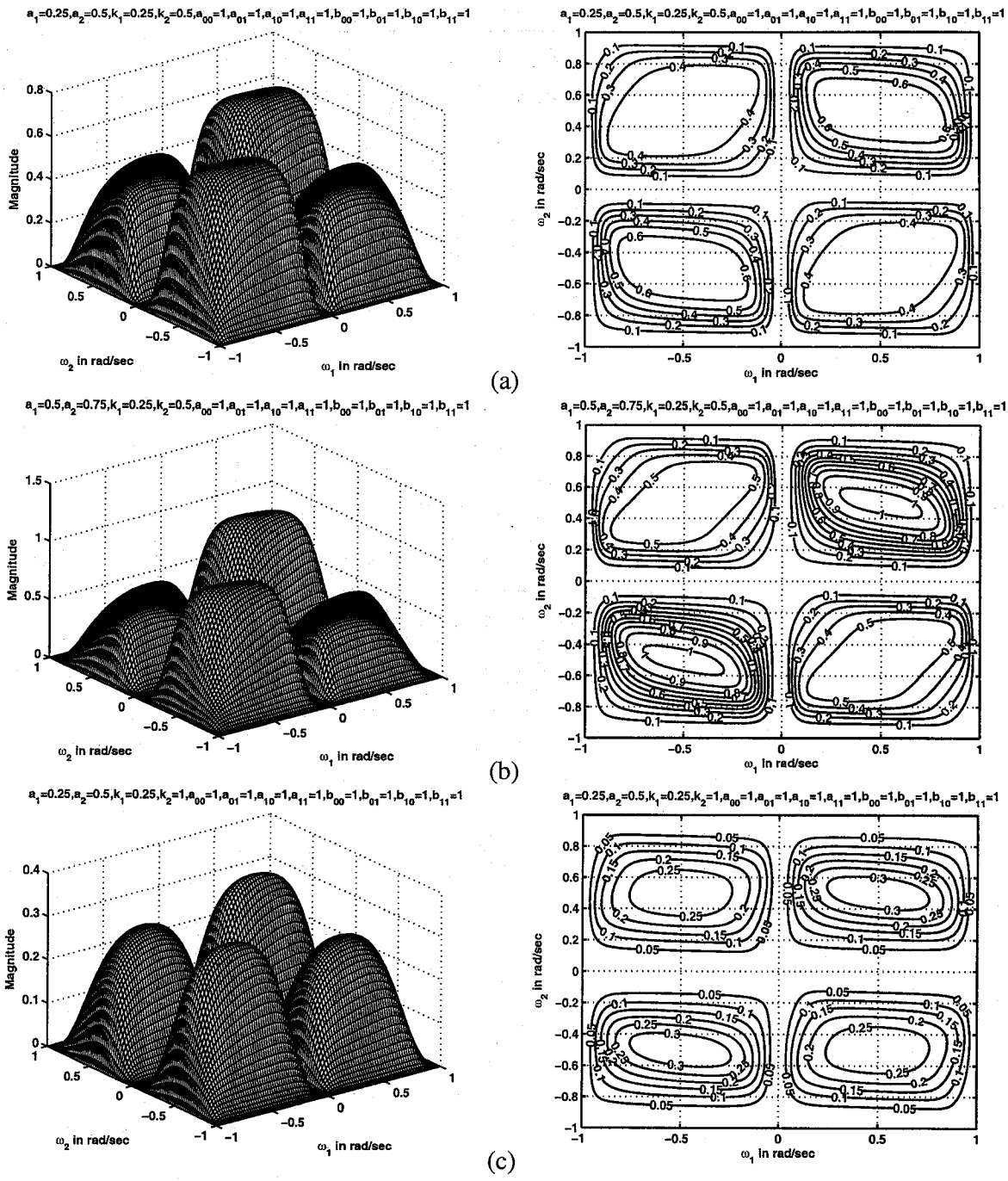

Figure 4.10: 3-D amplitude-frequency response and contour response of 2-D digital band-pass filter in case 3 of set 1 (when $k_1 = 0.25$, $k_2 = 0.5,\ 1$)

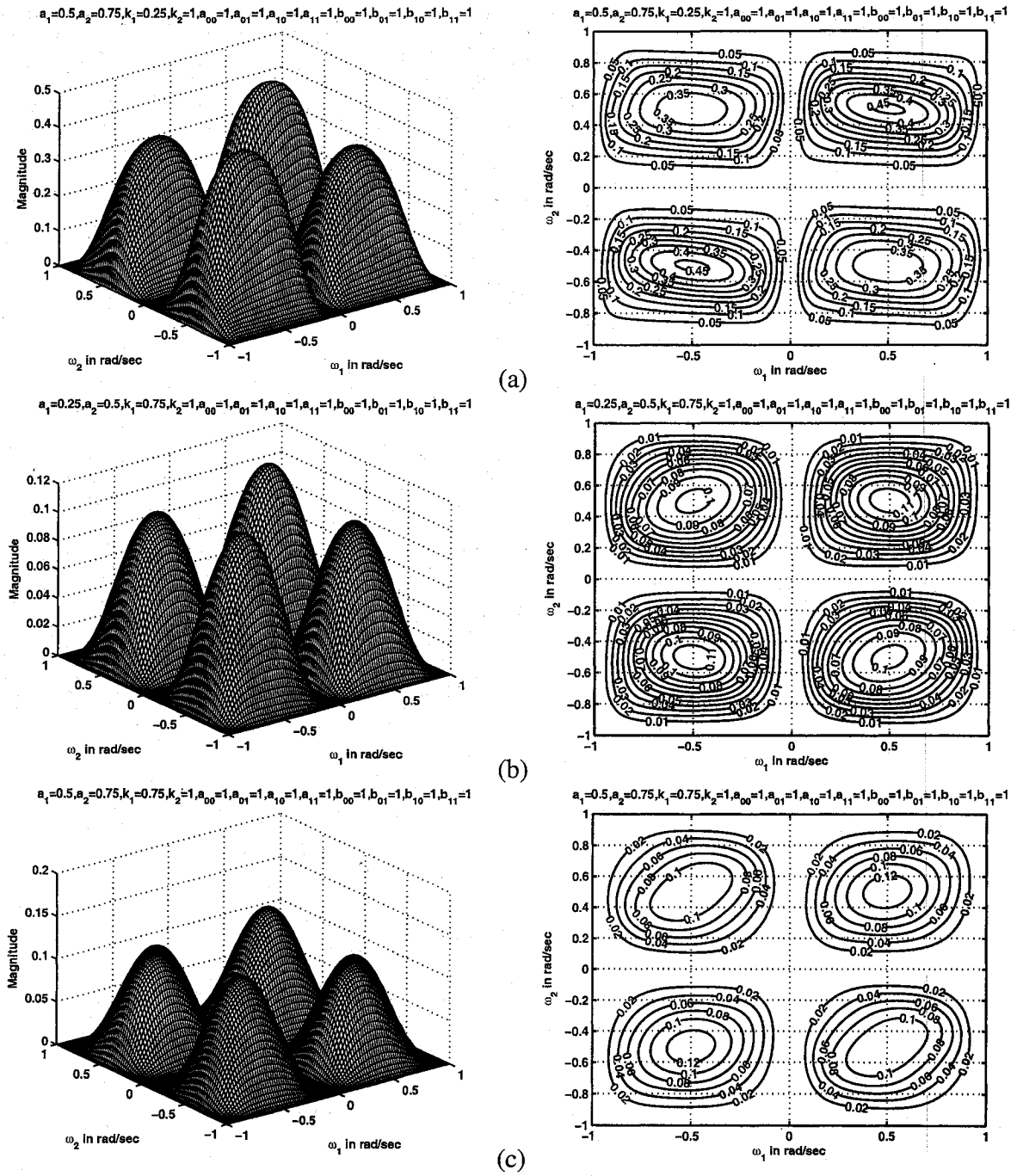

Figure 4.11: 3-D amplitude-frequency response and contour response of 2-D digital band-pass filter in case 3 of set 1 (when $k_1 = 0.25,\ 0.75,\ k_2 = 1$)

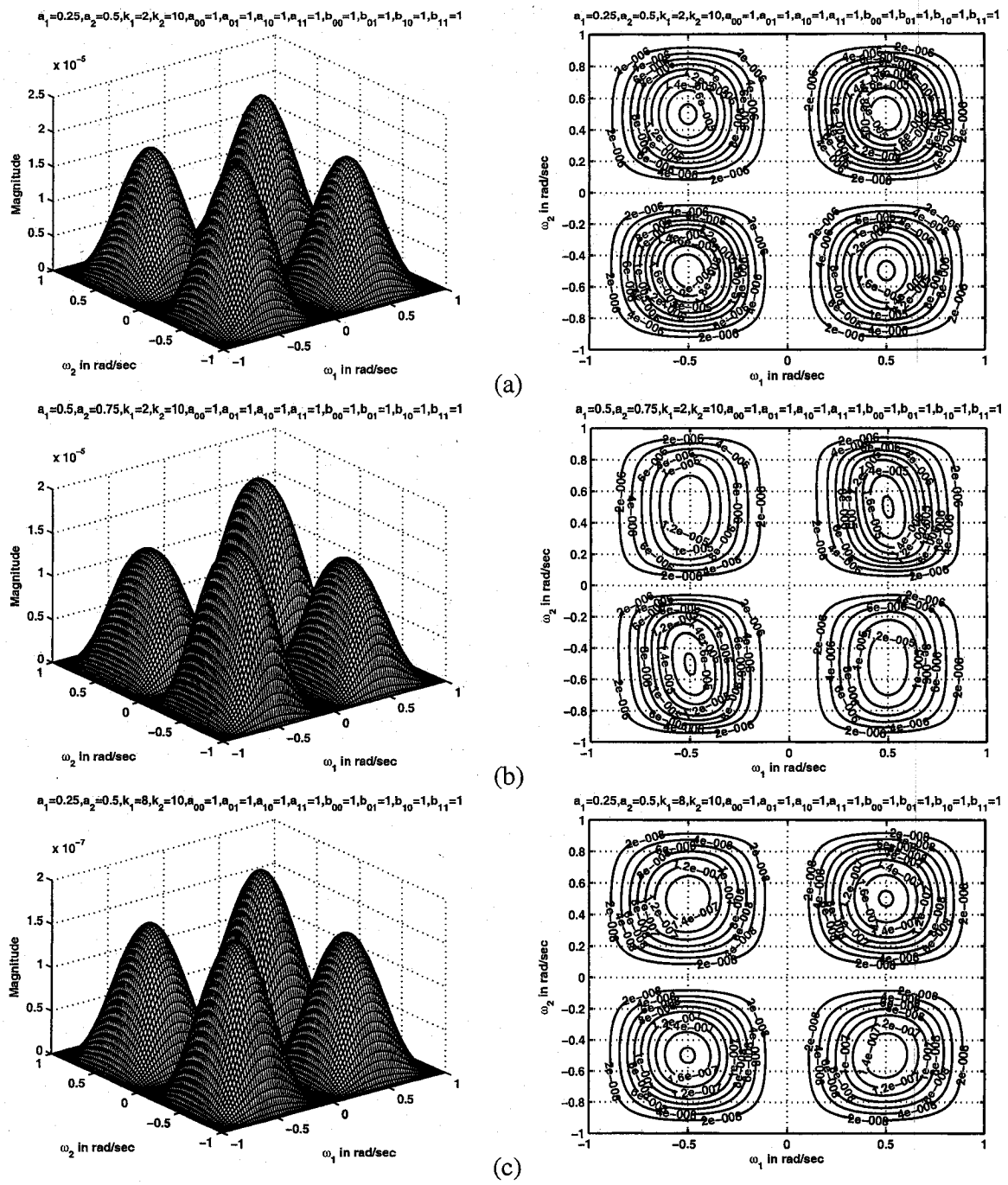

Figure 4.12: 3-D amplitude-frequency response and contour response of 2-D digital band-pass filter in case 3 of set 1 (when $k_1 = 2,\ 8,\ k_2 = 10$)

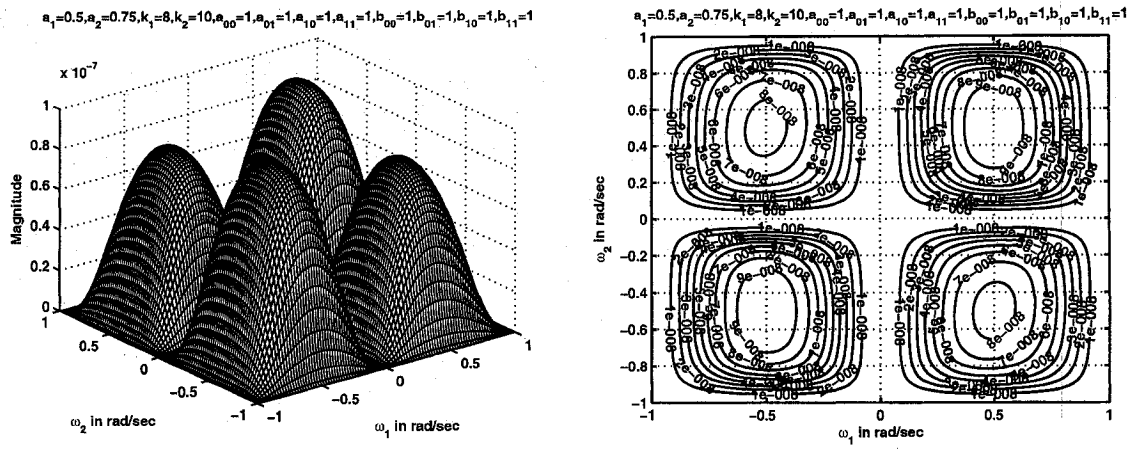

Figure 4.13: 3-D amplitude-frequency response and contour response of 2-D digital band-pass filter in case 3 of set 1 (when $k_1 = 8$, $k_2 = 10$)

Further increase in the values of k_1 and k_2 result in gradual increase of the passband width. In Fig. 4.13, it can be seen that the passband width increases when the values of k_1 and k_2 are increased to 8, 10 respectively. The passband width increases and decreases periodically for different values of k_1 and k_2. At the same time, there is also a decrease in the magnitude of the contour response for the same.

The coefficients a_1 and a_2 affect the gain of the amplitude-frequency response as discussed in the above section. In Fig.4.10 (a), (b), as a_1 and a_2 values are increased from 0.25, 0.5 to 0.5, 0.75 respectively, for the same values of $k_1 = 0.25$, $k_2 = 0.5$, the magnitude of the contour response increases. There are no ripples in the passband of the contour response for all values of a_1, a_2, k_1 and k_2.

It can be noticed that the contours in the first and third quadrants are mirror images of one another and the contours in the second and fourth quadrants are mirror images of one another. Also the magnitude of the contours in the second and fourth quadrants is greater than the magnitude of the contours in the first and third quadrants. For very low values of k_1 and k_2 (k_1, $k_2 \leq 0.5$), the magnitude of the contours in the second and fourth quadrants is nearly twice than that of the magnitude of the contours in the first and third quadrants.

4.4.1.4 Case 4

In this case,

$$a_1 = a_2 \quad , \quad k_1 = k_2$$

The coefficients k_1 and k_2 affect the passband width of the 2-D bandpass filter. In Fig. 4.14 (a), Fig. 4.15 (a) , Fig. 4.16 (a), (c) and Fig. 4.17 (b), there is a gradual decrease in the passband width as the values of k_1 and k_2 are increased from 0.25 to 5 for the same values of $a_1 = a_2 = 0.25$. At the same time, there is also a decrease in the magnitude of the contour response for the same.

The coefficients a_1 and a_2 affect the gain of the amplitude-frequency response. In Fig. 4.14 (a), (b), (c), as a_1 and a_2 values are increased from 0.25 to 0.75 respectively, for the same values of $k_1 = k_2 = 0.25$, the magnitude of the contour response increases. There are ripples in the contour response for values of a_1 and a_2 greater than 0.5 and for values of k_1, $k_2 \leq 0.5$ as shown in Figs. 4.14 (b), (c) and 4.15 (c).

It can be noticed that the contours in the first and third quadrants are mirror images of one another and the contours in the second and fourth quadrants are mirror images of one another. Also, the magnitude of the contours in the second and fourth quadrants is greater than the magnitude of the contours in the first and third quadrants.

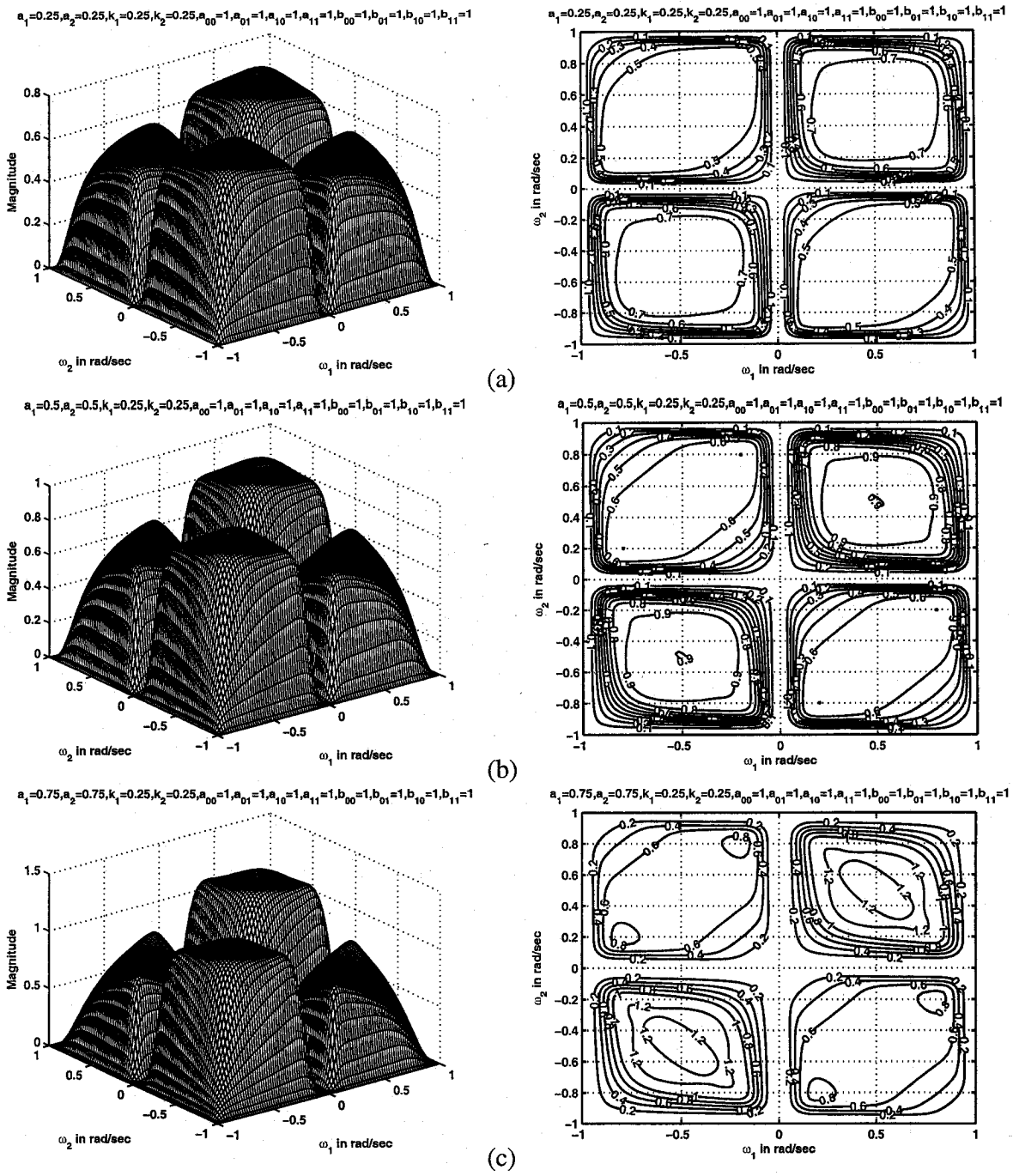

Figure 4.14: 3-D amplitude-frequency response and contour response of 2-D digital band-pass filter in case 4 of set 1 (when $k_1 = k_2 = 0.25$)

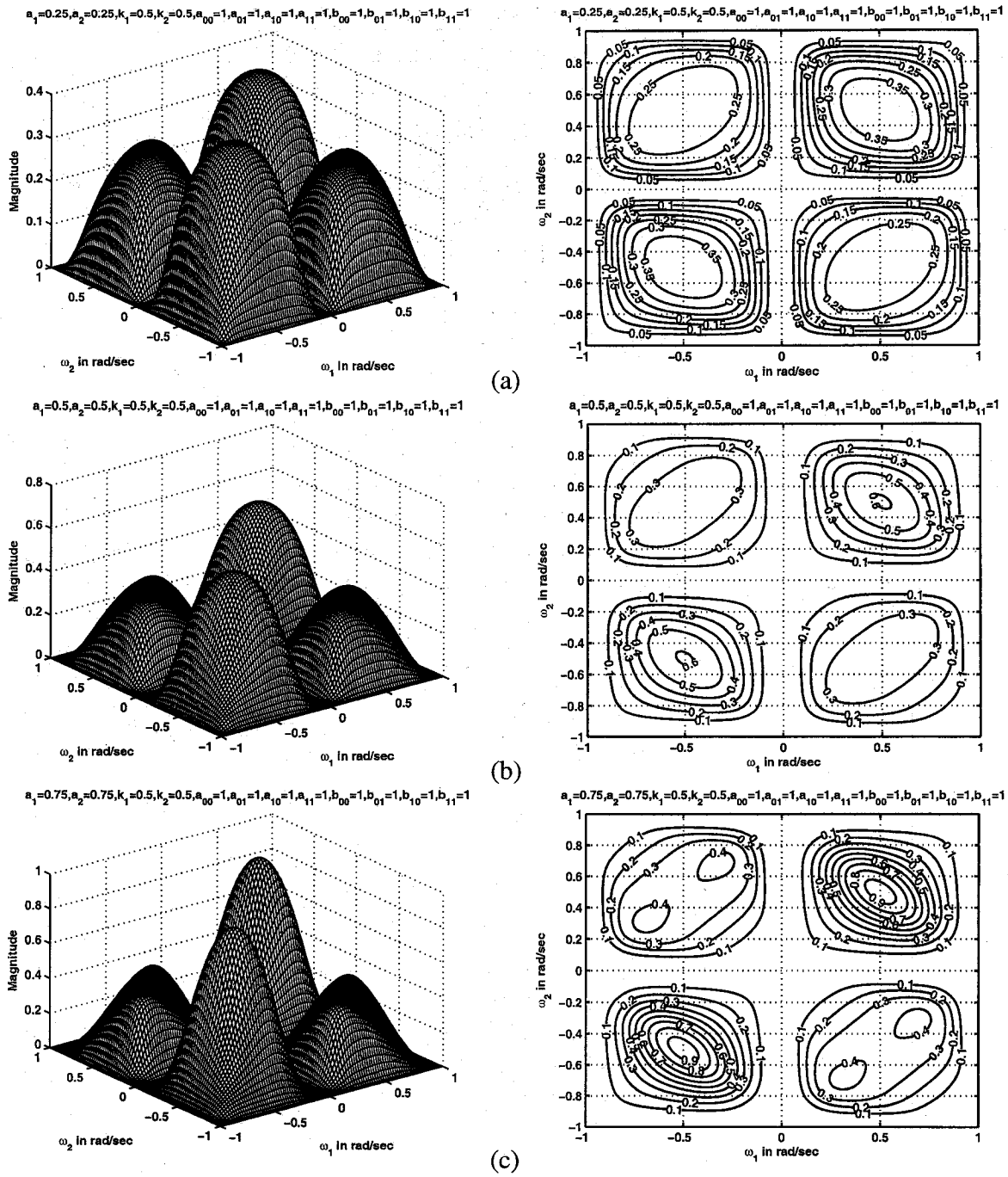

Figure 4.15: 3-D amplitude-frequency response and contour response of 2-D digital band-pass filter in case 4 of set 1 (when $k_1 = k_2 = 0.5$)

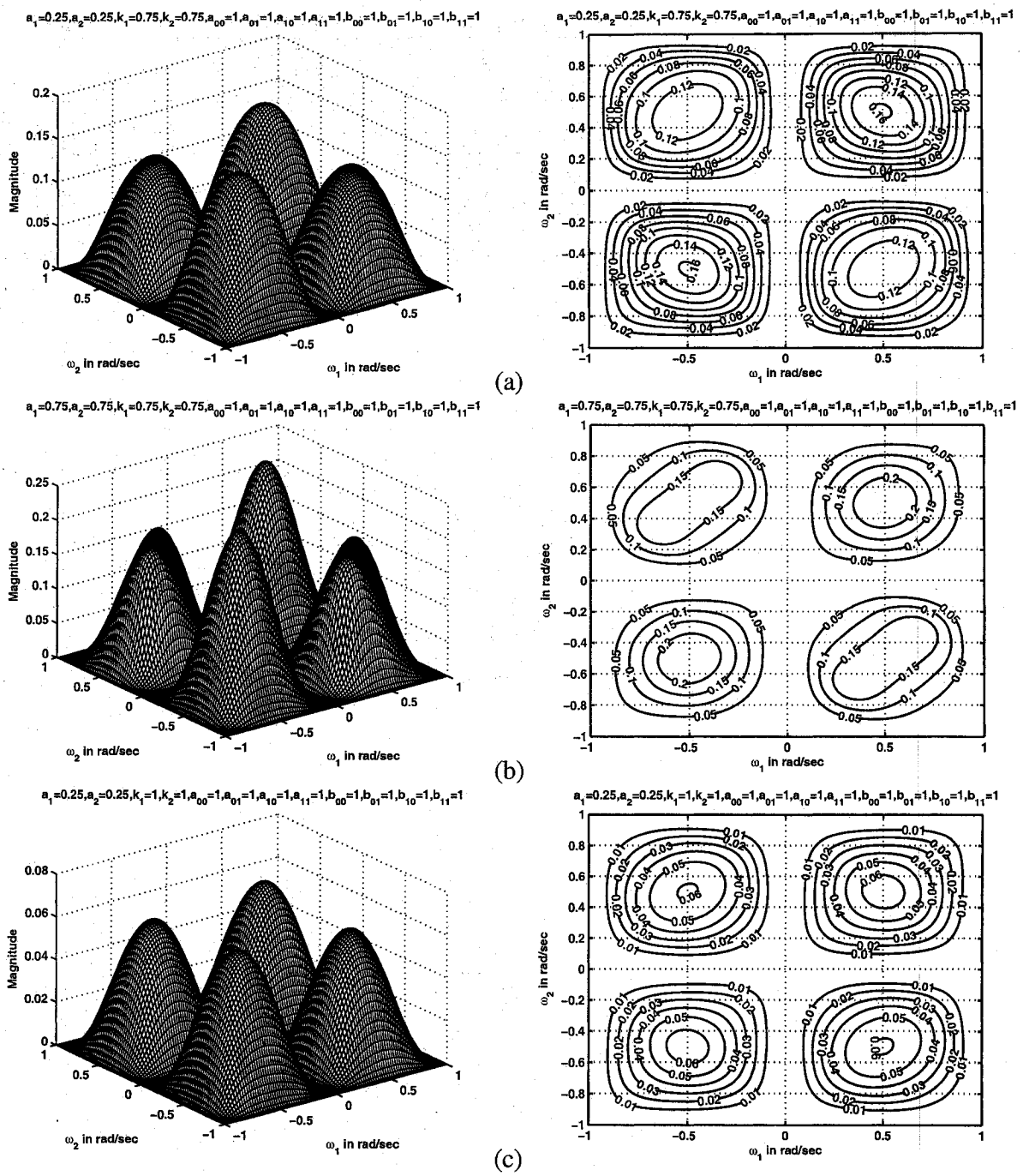

Figure 4.16: 3-D amplitude-frequency response and contour response of 2-D digital band-pass filter in case 4 of set 1 (when $k_1 = k_2 = 0.75,\ 1$)

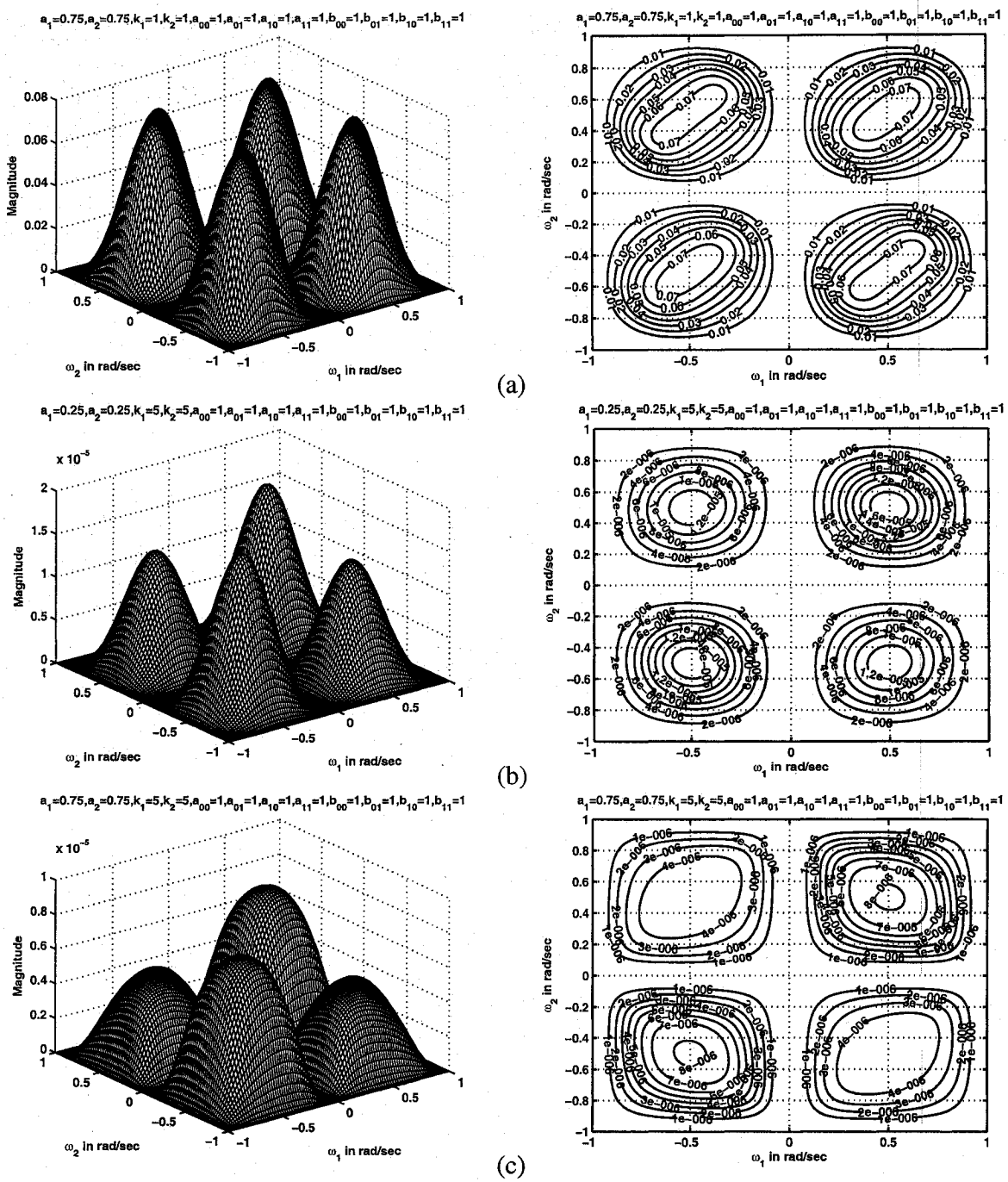

Figure 4.17: 3-D amplitude-frequency response and contour response of 2-D digital band-pass filter in case 4 of set 1 (when $k_1 = k_2 = 1, 5$)

4.4.2 Frequency Response of 2-D Bandpass Filters in Set 2

In this set,

$$\begin{aligned} a_{00} &= a_{01} = a_{10} = a_{11} \\ b_{00} &= b_{01} = b_{10} = b_{11} \end{aligned} \tag{4.6}$$

When the above combination of coefficients are substituted in the transfer function of bandpass filter, the resulting transfer function is the same as the one used in set 1 as the transfer function does not depend on the coefficients of the CFE. It only depends on the coefficients of the bilinear transformation. Hence the frequency response of 2-D bandpass filters in set 2 is the same as that of set 1.

4.4.3 Frequency Response of 2-D Bandpass Filters in Set 3

In this section, we study the manner in which all the four cases in set 3 affect the frequency response behavior of the resulting 2-D bandpass filter. In this set,

$$\begin{aligned} a_{00} &= a_{11} \\ a_{01} &= a_{10} \\ b_{00} &= b_{11} \\ b_{01} &= b_{10} \end{aligned} \tag{4.7}$$

Different contour plots are obtained by varying the values of a_1, a_2, k_1 and k_2.

Similar to set 1, in set 3, it is observed in all the four cases, the coefficients k_1 and k_2 affect the passband width and the coefficients a_1 and a_2 affect the gain of the amplitude-frequency response. As k_1 and k_2 values are increased, the passband width of the 2-D bandpass filter decreases and the magnitude of the contour response also decreases. Only in cases 1 and 3, as $k_1 \neq k_2$, the passband width of the 2-D digital bandpass filter increases and decreases periodically and the magnitude of the contour response decreases. As a_1 and a_2 values are increased, the magnitude of the amplitude-frequency response of the 2-D

bandpass filter increases and the passband width decreases. It can be noticed that there is rounding of contour edges for higher values of k_1 and k_2.

It can be observed that the contours in the first and third quadrants are mirror images of one another and the contours in the second and fourth quadrants are mirror images of one another. Also the magnitude of the contours in the second and fourth quadrants is smaller than the magnitude of the contours in the first and third quadrants unlike in set 1 where the magnitude of the contours in the second and fourth quadrants is higher than the magnitude of the contours in the first and third quadrants.

It can be observed that there are no ripples in the contour response in all the four cases. Also, the magnitude of the contour response is low when compared to set 1 for the same values of a_1, a_2, k_1 and k_2.

4.4.3.1 Case 1

In this case,

$$a_1 = a_2 \quad , \quad k_1 \neq k_2$$

It is observed in this case that the coefficients k_1 and k_2 affect the passband width and the coefficients a_1 and a_2 affect the gain of the amplitude-frequency response. As k_1 and k_2 values are increased, the passband width of the 2-D digital bandpass filter increases and decreases periodically and the magnitude of the contour response decreases. In Fig. 4.19 (a), (b), (c) and Fig. 4.20 (a), there is a gradual decrease in the passband width as the values of k_1 and k_2 are increased from 0.25, 0.5 to 2, 10 respectively for the same values of $a_1 = a_2 = 0.25$. Further increase in the values of k_1 and k_2 result in gradual increase in the passband width. In Fig. 4.20 (b), it can be seen that the passband width increases when the values of k_1 and k_2 are increased to 8, 10 respectively. As a_1 and a_2 values are increased, the magnitude of the amplitude-frequency response of the 2-D bandpass filter

increases and the passband width decreases.

In this case, there are no ripples in the contour response for all values of a_1, a_2, k_1 and k_2. The magnitude of the contour responses is lower than that of the contour responses in case 1 of set 1 for the same values of a_1, a_2, k_1 and k_2. The magnitude of the contour response in Fig. 4.18 (a) is lower than that of Fig. 4.2 (a) for the same values of $a_1 = a_2 = 0.25$, $k_1 = 0.25$ and $k_2 = 0.5$. Also, it can be observed that the passband width of the contour response is greater in this case of set 3 than that of case 1 in set 1 for higher values of k_1 and k_2. For example, the passband width in Fig. 4.18 (c) of set 3 is greater than that of the passband width in Fig. 4.3 (a) of case 1 in set 1.

For certain values of a_1, a_2, k_1 and k_2, i.e., when one of the k_1, $k_2 = 1$ and $a_1 = a_2 \geq 0.5$, the magnitude of the contours in the second and fourth quadrants drops to a minimum value when compared to the contours in the first and third quadrants as shown in Fig. 4.19 (c) and Fig. 4.21 (a).

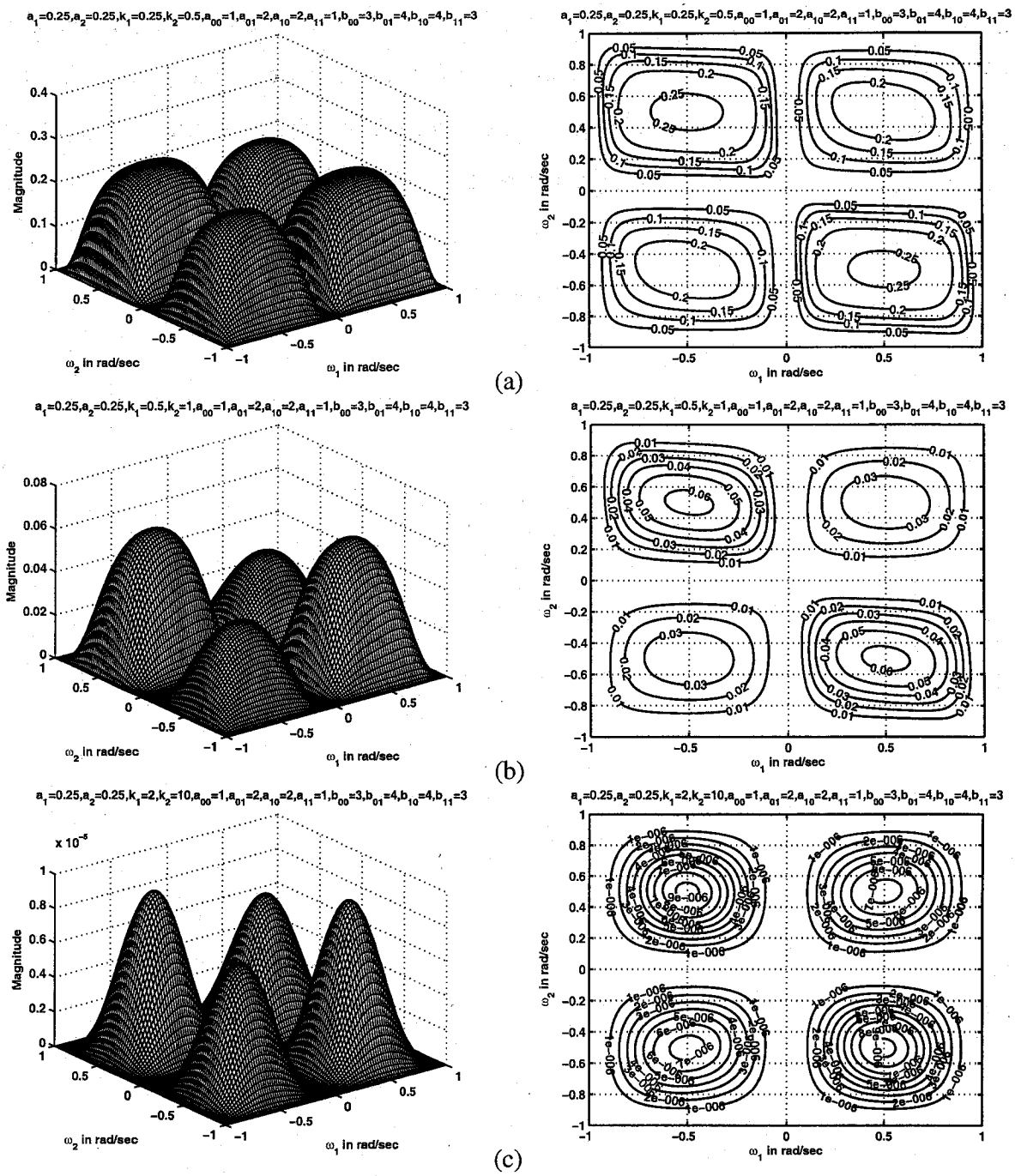

Figure 4.18: 3-D amplitude-frequency response and contour response of 2-D digital band-pass filter in case 1 of set 3 (when $a_1 = a_2 = 0.25$)

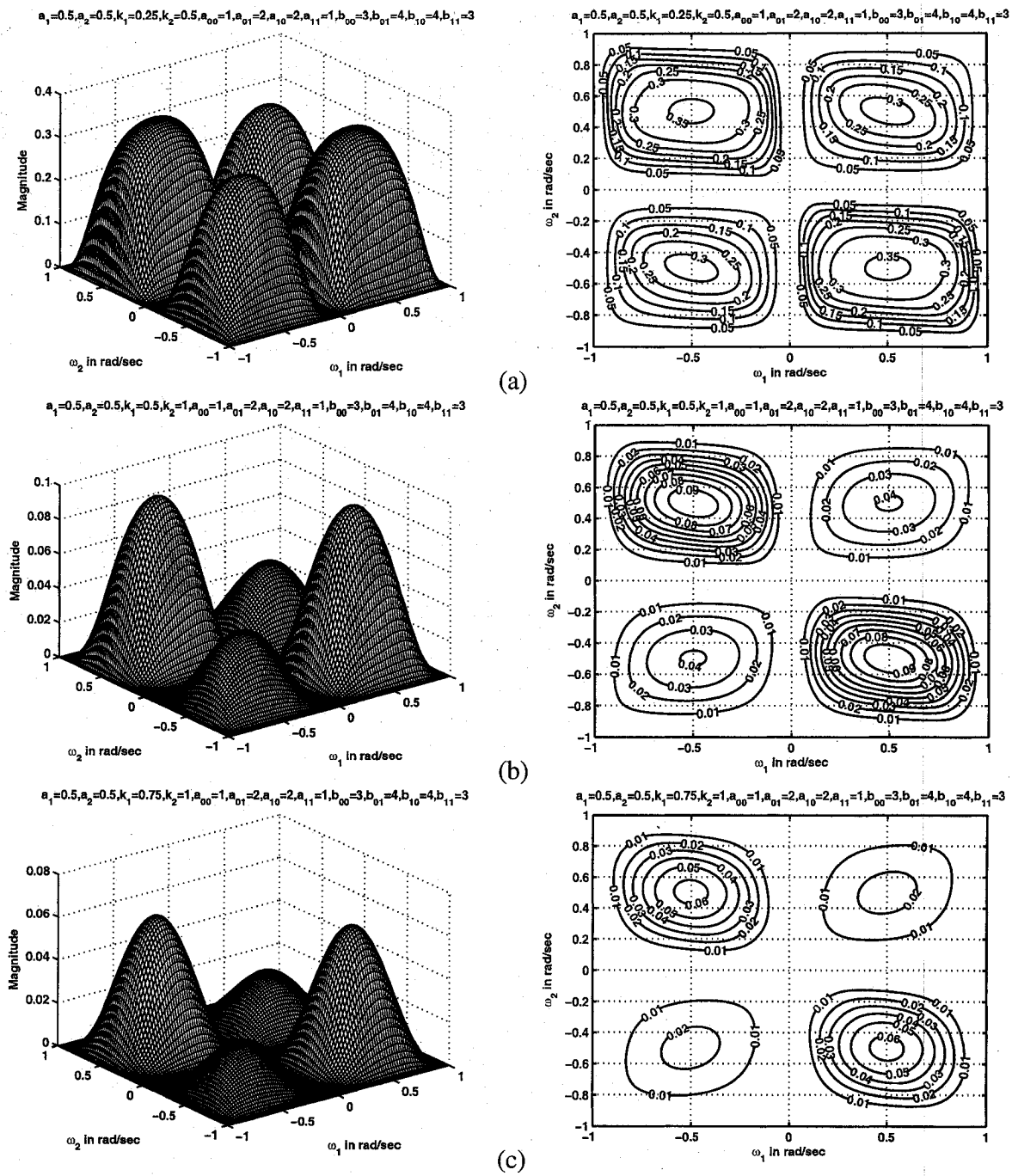

Figure 4.19: 3-D amplitude-frequency response and contour response of 2-D digital band-pass filter in case 1 of set 3 (when $a_1 = a_2 = 0.5$)

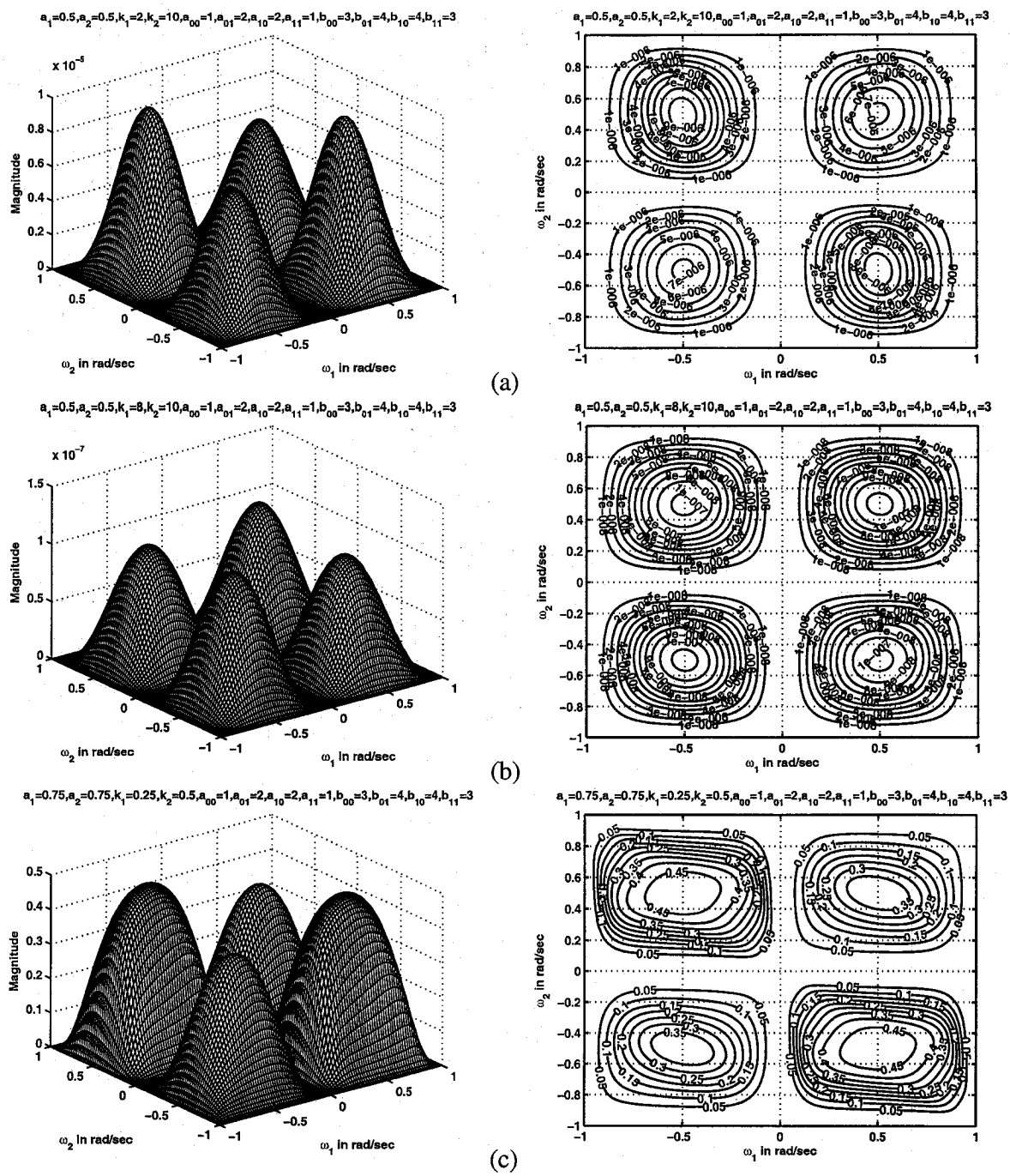

Figure 4.20: 3-D amplitude-frequency response and contour response of 2-D digital band-pass filter in case 1 of set 3 (when $a_1 = a_2 = 0.5, 0.75$)

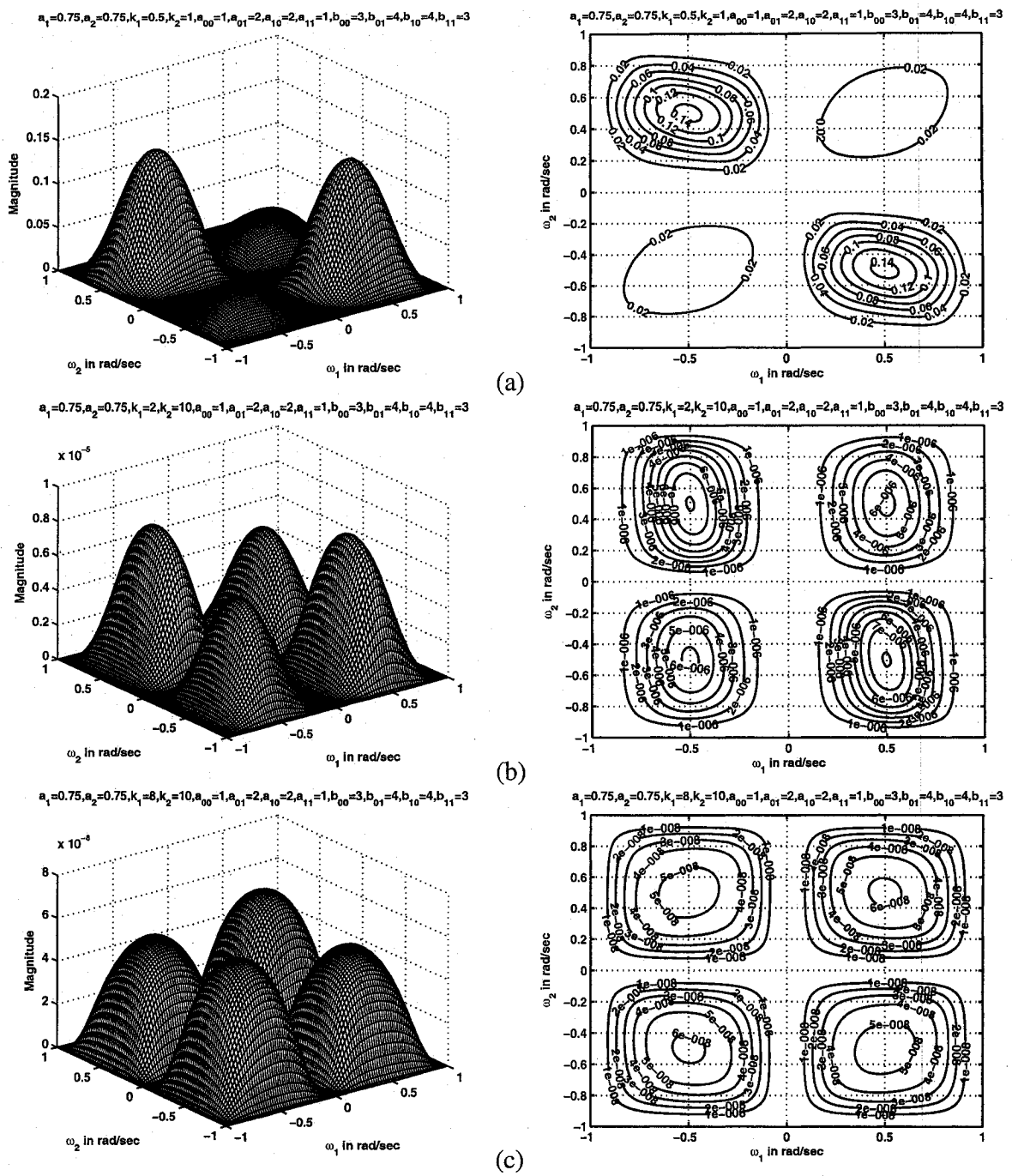

Figure 4.21: 3-D amplitude-frequency response and contour response of 2-D digital band-pass filter in case 1 of set 3 (when $a_1 = a_2 = 0.75$)

4.4.3.2 Case 2

In this case,

$$a_1 \neq a_2 \quad , \quad k_1 = k_2$$

It is observed in this case that the coefficients k_1 and k_2 affect the passband width and the coefficients a_1 and a_2 affect the gain of the amplitude-frequency response. As k_1 and k_2 values are increased, the passband width of the 2-D bandpass filter decreases and the magnitude of the contour response also decreases. As a_1 and a_2 values are increased, the magnitude of the amplitude-frequency response of the 2-D bandpass filter increases and the passband width decreases.

In this case, there are no ripples in the passband of the contour response even when the values of k_1 and k_2 are as low as 0.25 unlike in case 2 of set 1 as shown in Fig. 4.22 (a). The magnitude of the contour response is smaller than that of the magnitude in case 2 of set 1 for the same values of a_1, a_2, k_1 and k_2. The magnitude of the contour response in Fig. 4.22 (c) is smaller than the magnitude in Fig. 4.7 (c) of case 2 in set 1, for the same values of $a_1 = 0.25$, $a_2 = 0.5$, $k_1 = k_2 = 0.5$. In addition, the passband width of the contour response is slightly smaller than that of the passband width in case 2 of set 1 for the same values of a_1, a_2, k_1 and k_2.

For smaller values of k_1 and k_2, i.e., when $k_1 = k_2 = 0.25$, the magnitude of the contours in the second and fourth quadrants is greater than or equal to the magnitude of the contours in the first and third quadrants. But for values of $0.25 < k_1, k_2 \leq 1$, the magnitude of the contours in the second and fourth quadrants is less than the magnitude of the contours in the first and third quadrants as shown in Fig. 4.22 and Fig. 4.23. For further higher values of k_1 and k_2, the magnitude of the contours in the second and fourth quadrants is greater than or equal to the magnitude of the contours in the first and third quadrants as shown in Fig. 4.24 (b), (c). It can be noticed that the contours in the first and

third quadrants are mirror images of one another and the contours in the second and fourth quadrants are mirror images of one another.

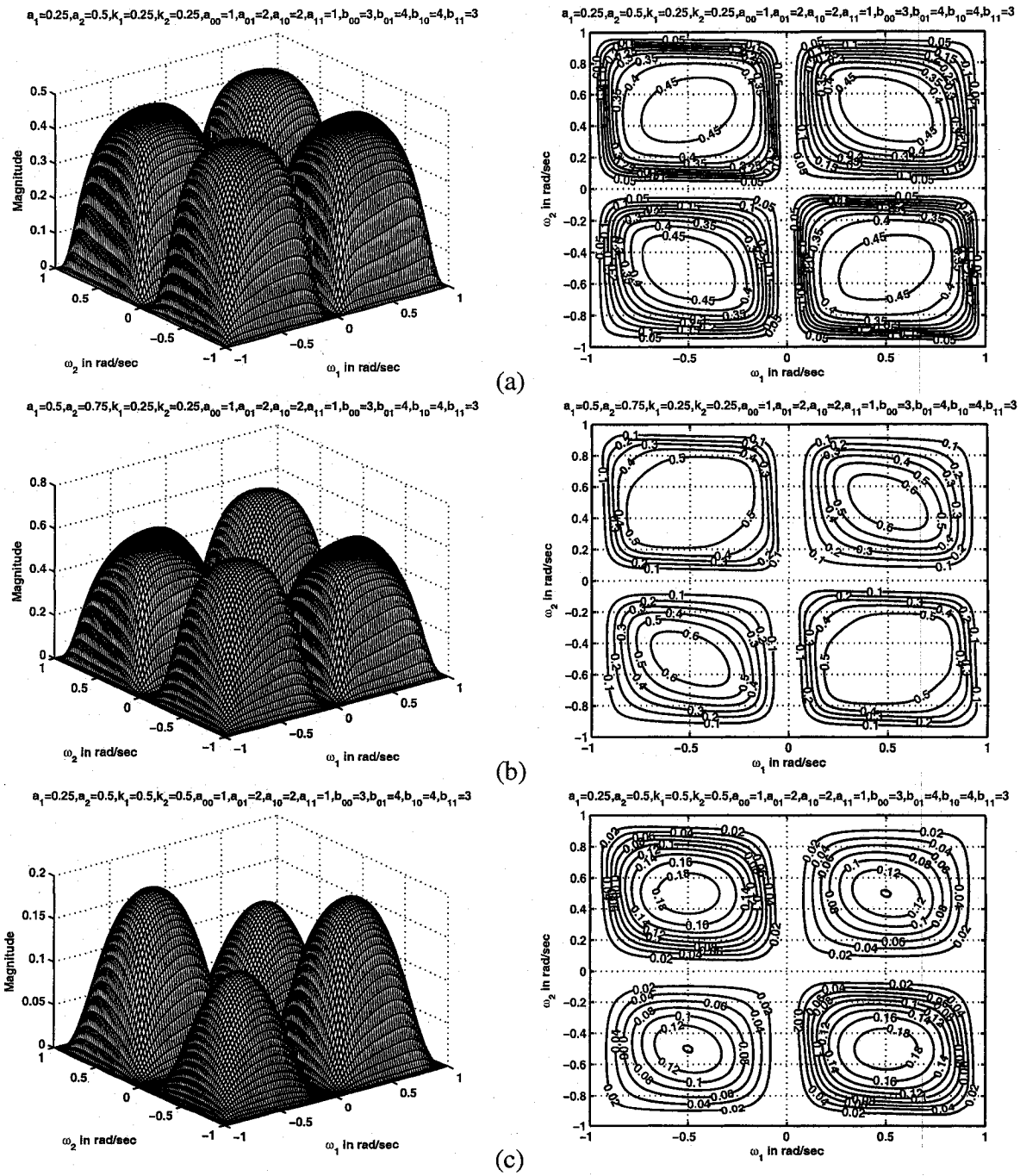

Figure 4.22: 3-D amplitude-frequency response and contour response of 2-D digital band-pass filter in case 2 of set 3 (when $k_1 = k_2 = 0.25,\ 0.5$)

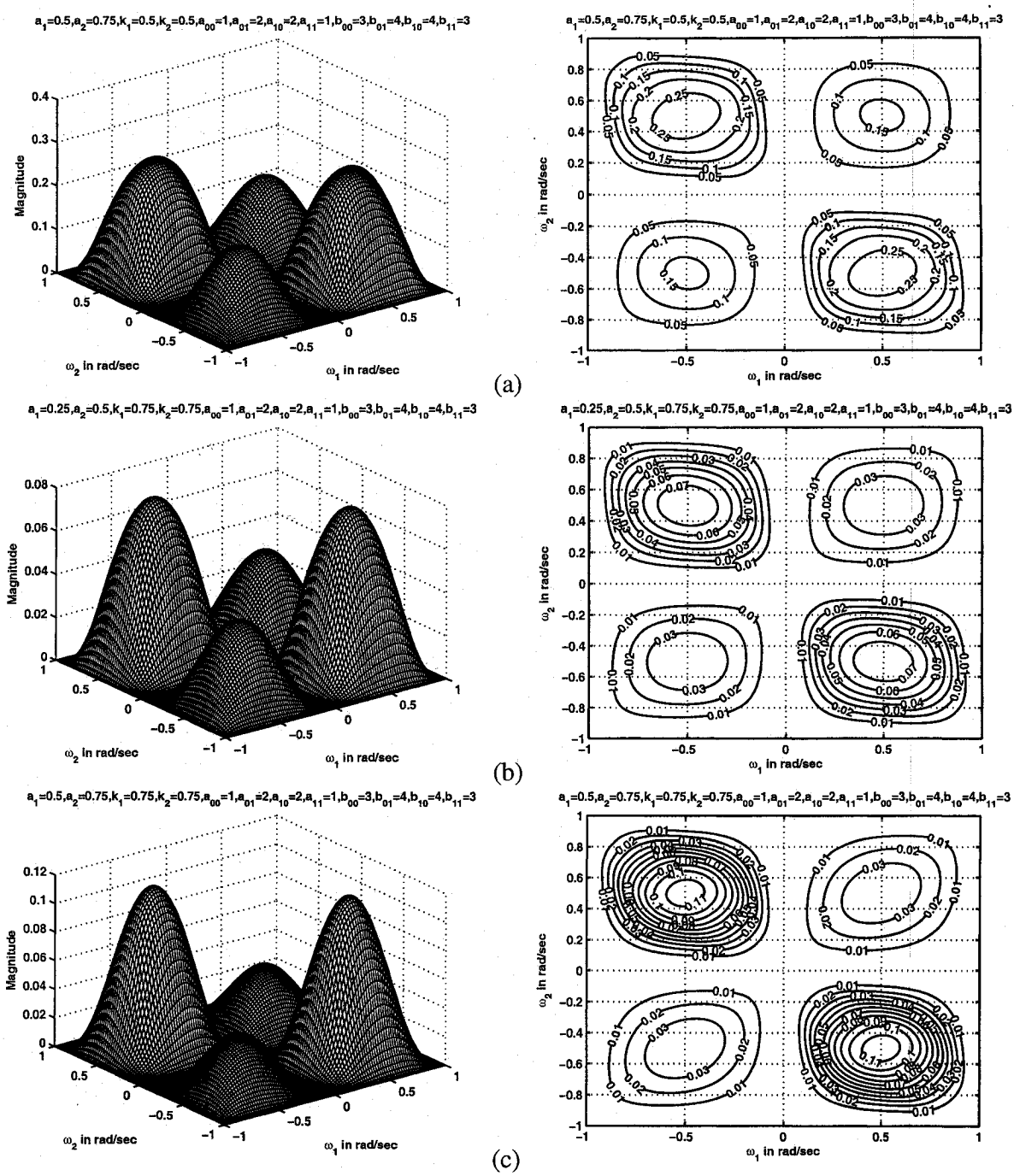

Figure 4.23: 3-D amplitude-frequency response and contour response of 2-D digital band-pass filter in case 2 of set 3 (when $k_1 = k_2 = 0.5,\ 0.75$)

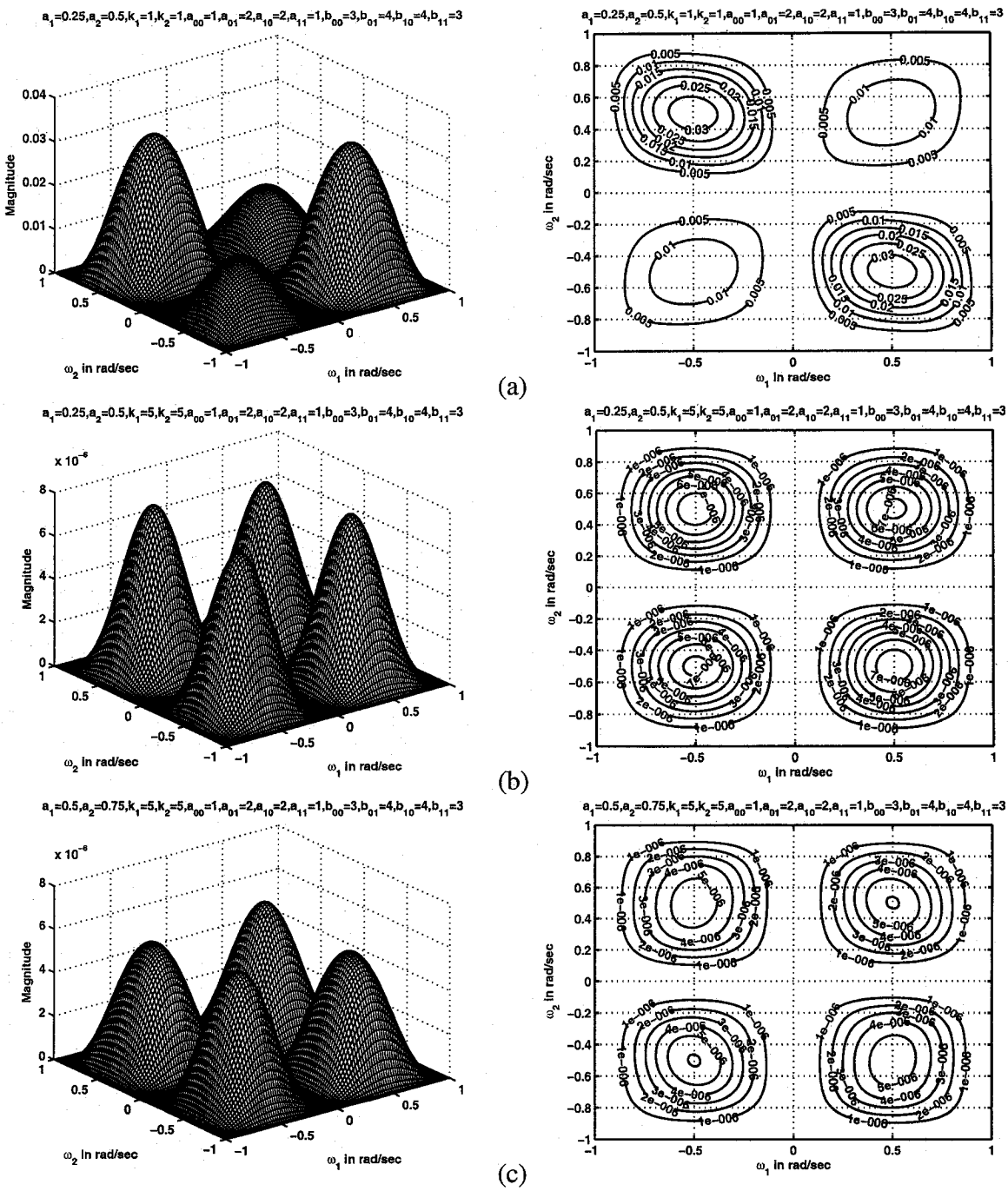

Figure 4.24: 3-D amplitude-frequency response and contour response of the 2-D digital bandpass filter in case 2 of set 3 (when $k_1 = k_2 = 1, 5$)

4.4.3.3 Case 3

In this case,

$$a_1 \neq a_2 \quad , \quad k_1 \neq k_2$$

It is observed in this case that the coefficients k_1 and k_2 affect the passband width and the coefficients a_1 and a_2 affect the gain of the amplitude-frequency response. As k_1 and k_2 values are increased, the passband width of the 2-D digital bandpass filter increases and decreases periodically and the magnitude of the contour response decreases. In Fig. 4.25 (a), (c) and Fig. 4.26 (b), Fig. 4.27 (a), there is a gradual decrease in the passband width as the values of k_1 and k_2 are increased from 0.25, 0.5 to 2, 10 respectively for the same values of $a_1 = a_2 = 0.25$. Further increase in the values of k_1 and k_2 result in gradual increase in the passband width. In Fig. 4.27 (c), it can be seen that the passband width increases when the values of k_1 and k_2 are increased to 8, 10 respectively. As a_1 and a_2 values are increased, the magnitude of the amplitude-frequency response of the 2-D bandpass filter increases and the passband width decreases.

The magnitude of the contour response is smaller than that of the magnitude in case 3 of set 1 for the same values of a_1, a_2, k_1 and k_2. For example, the magnitude of the contour response in Fig. 4.25 (a) is smaller than the magnitude of the contour response in Fig. 4.10 (a) of case 3 in set 1 for the same values of $a_1 = 0.25$, $a_2 = 0.5$, $k_1 = 0.25$, $k_2 = 0.5$.

In addition, the magnitude of the contours in the second and fourth quadrant is smaller than the magnitude of the contours in the first and third quadrant unlike in case 3 of set 1 where the magnitude of the contours in the first and third quadrant is smaller than the magnitude of the contours in the second and fourth quadrant. For values of k_1, $k_2 \leq 1$, as the values of k_1 and k_2 increases from 0.25, 0.5 to 0.75, 1 respectively, the magnitude of the contours in the second and fourth quadrant decreases gradually as shown in Fig. 4.25 (b), Fig. 4.26 (a) and (c) for the same values of $a_1 = 0.5$, $a_2 = 0.75$.

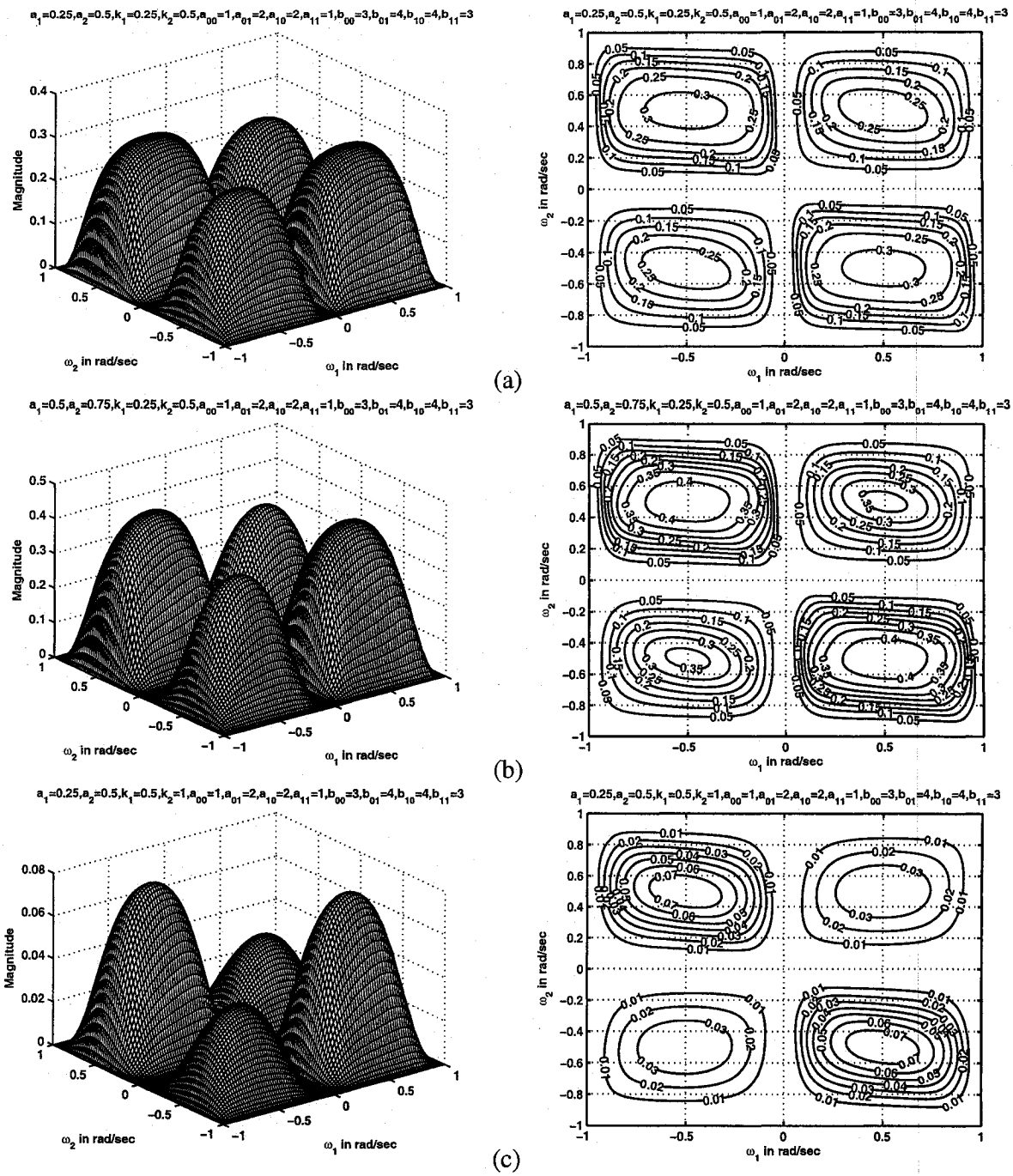

Figure 4.25: 3-D amplitude-frequency response and contour response of 2-D digital band-pass filter in case 3 of set 3 (when $k_1 = 0.25,\ 0.5,\ k_2 = 0.5,\ 1$)

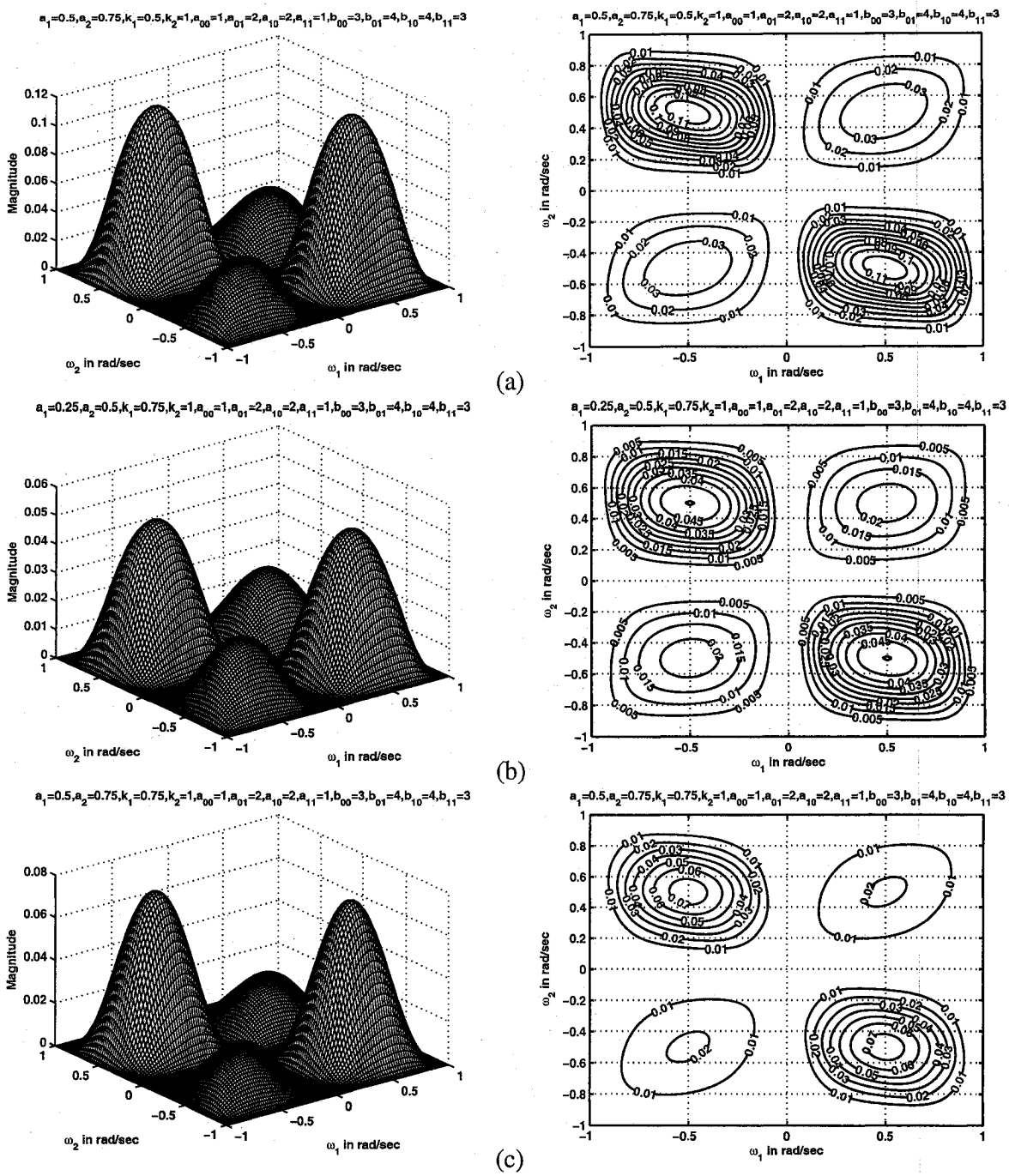

Figure 4.26: 3-D amplitude-frequency response and contour response of 2-D digital band-pass filter in case 3 of set 3 (when $k_1 = 0.5,\ 0.75,\ k_2 = 1$)

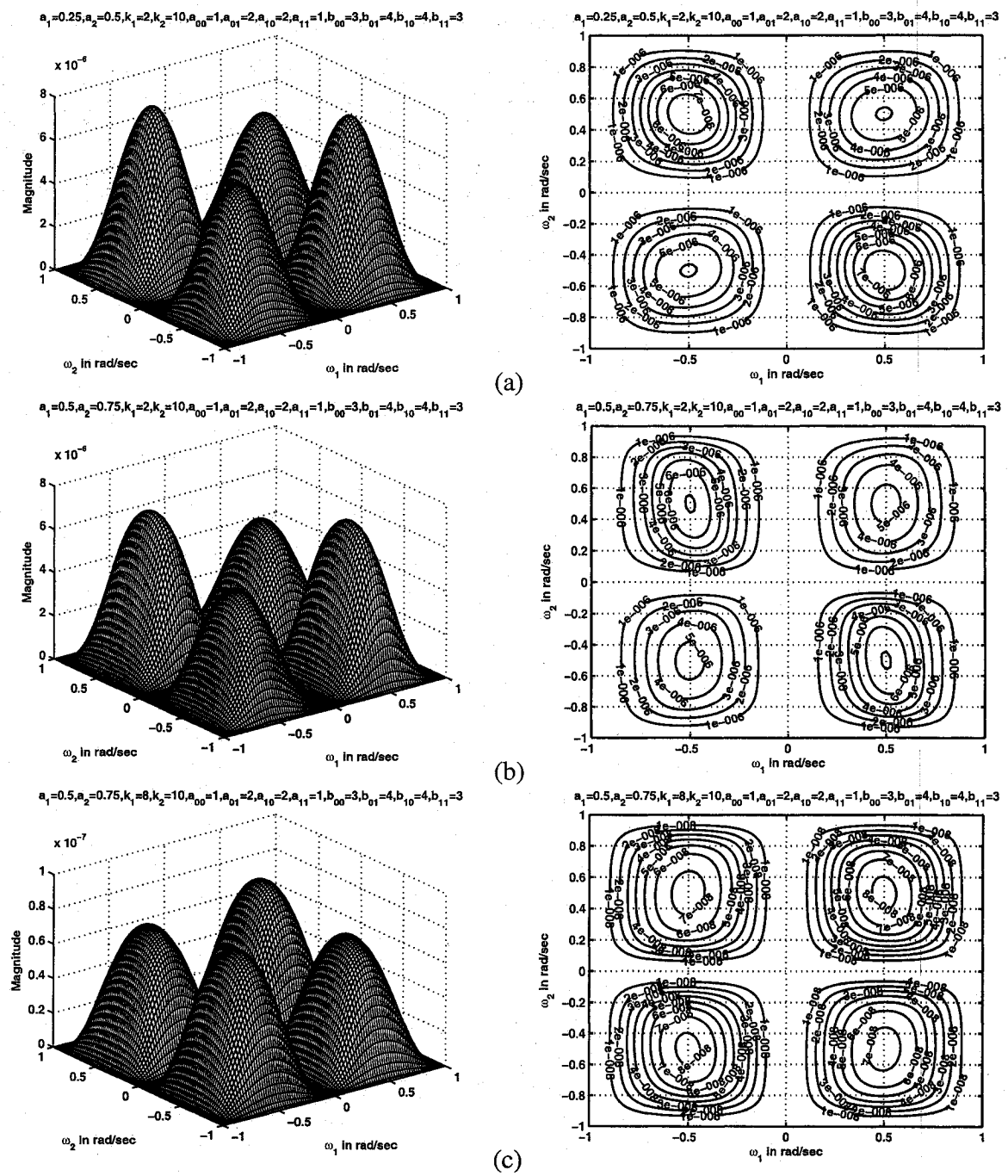

Figure 4.27: 3-D amplitude-frequency response and contour response of 2-D digital band-pass filter in case 3 of set 3 (when $k_1 = 2,\ 8,\ k_2 = 10$)

4.4.3.4 Case 4

In this case,

$$a_1 = a_2 \quad , \quad k_1 = k_2$$

It is observed in this case that the coefficients k_1 and k_2 affect the passband width and the coefficients a_1 and a_2 affect the gain of the amplitude-frequency response. As k_1 and k_2 values are increased, the passband width of the 2-D bandpass filter decreases and the magnitude of the contour response also decreases. As a_1 and a_2 values are increased, the magnitude of the amplitude-frequency response of the 2-D bandpass filter increases and the passband width decreases.

The magnitude of the contour response is lower than that of the magnitude in case 4 of set 1 for the same values of a_1, a_2, k_1 and k_2. The magnitude of the contour response in Fig. 4.28 (c) is smaller than the magnitude of the contour response in Fig. 4.15 (a) of case 4 in set 1 for the same values of $k_1 = k_2 = 0.5$, $a_1 = a_2 = 0.25$.

It can be noticed that the contours in the first and third quadrants are mirror images of one another and the contours in the second and fourth quadrants are mirror images of one another. For smaller values of k_1 and k_2, i.e., when $k_1 = k_2 = 0.25$, the magnitude of the contours in the second and fourth quadrants is greater than or equal to the magnitude of the contours in the first and third quadrants. But for values of $0.25 < k_1, k_2 \leq 1$, the magnitude of the contours in the second and fourth quadrants gradually decreases. At one stage, the contours in the second and fourth quadrants totally disappears. In Fig. 4.30 (b), (c), it can be noticed that the magnitude of the contours in the second and fourth quadrants gradually decreases and in Fig. 4.31 (a), the contours in the second and fourth quadrants totally disappears for the same values of $a_1 = a_2 = 0.9$.

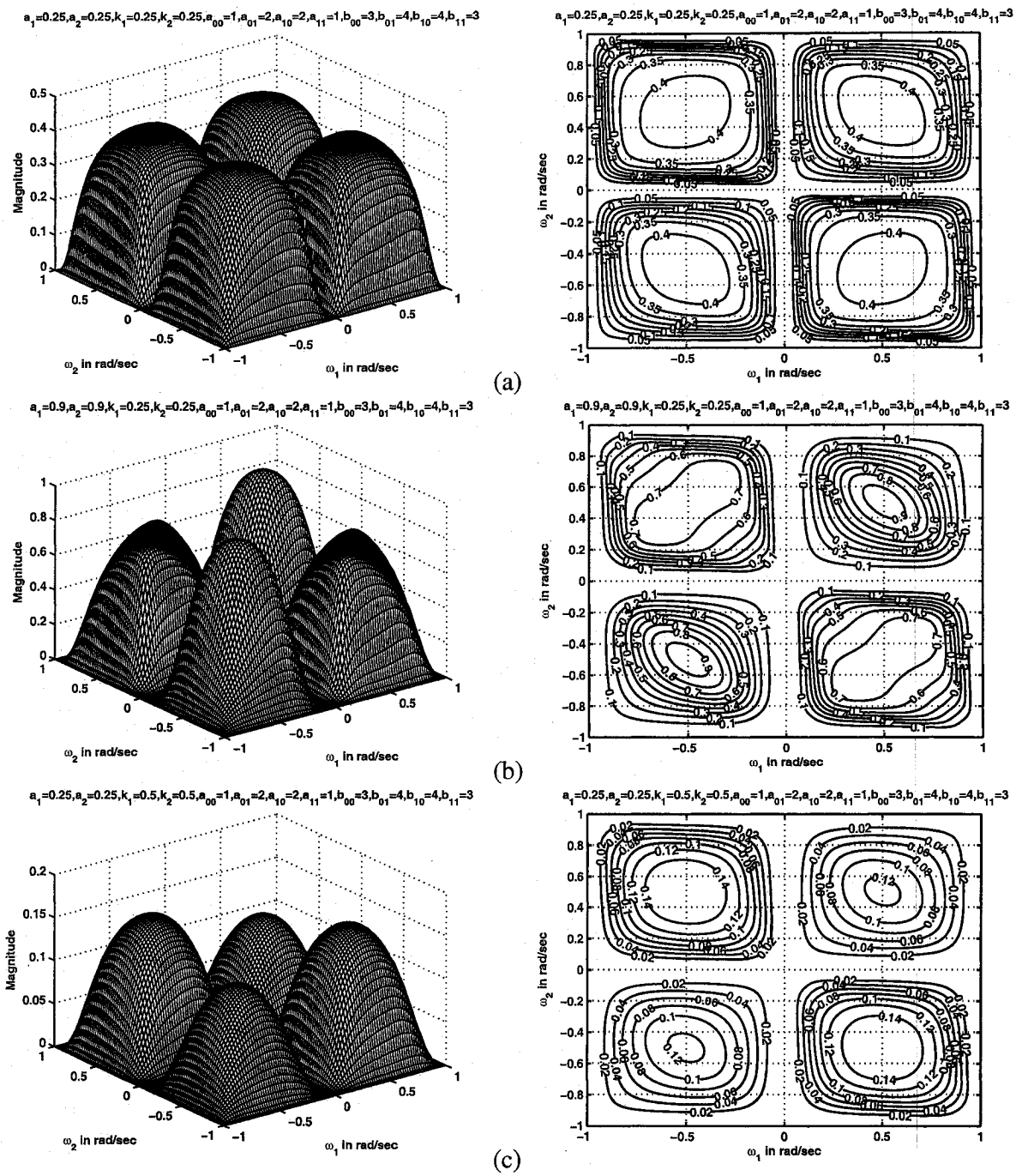

Figure 4.28: 3-D amplitude-frequency response and contour response of 2-D digital band-pass filter in case 4 of set 3 (when $k_1 = k_2 = 0.25,\ 0.5$)

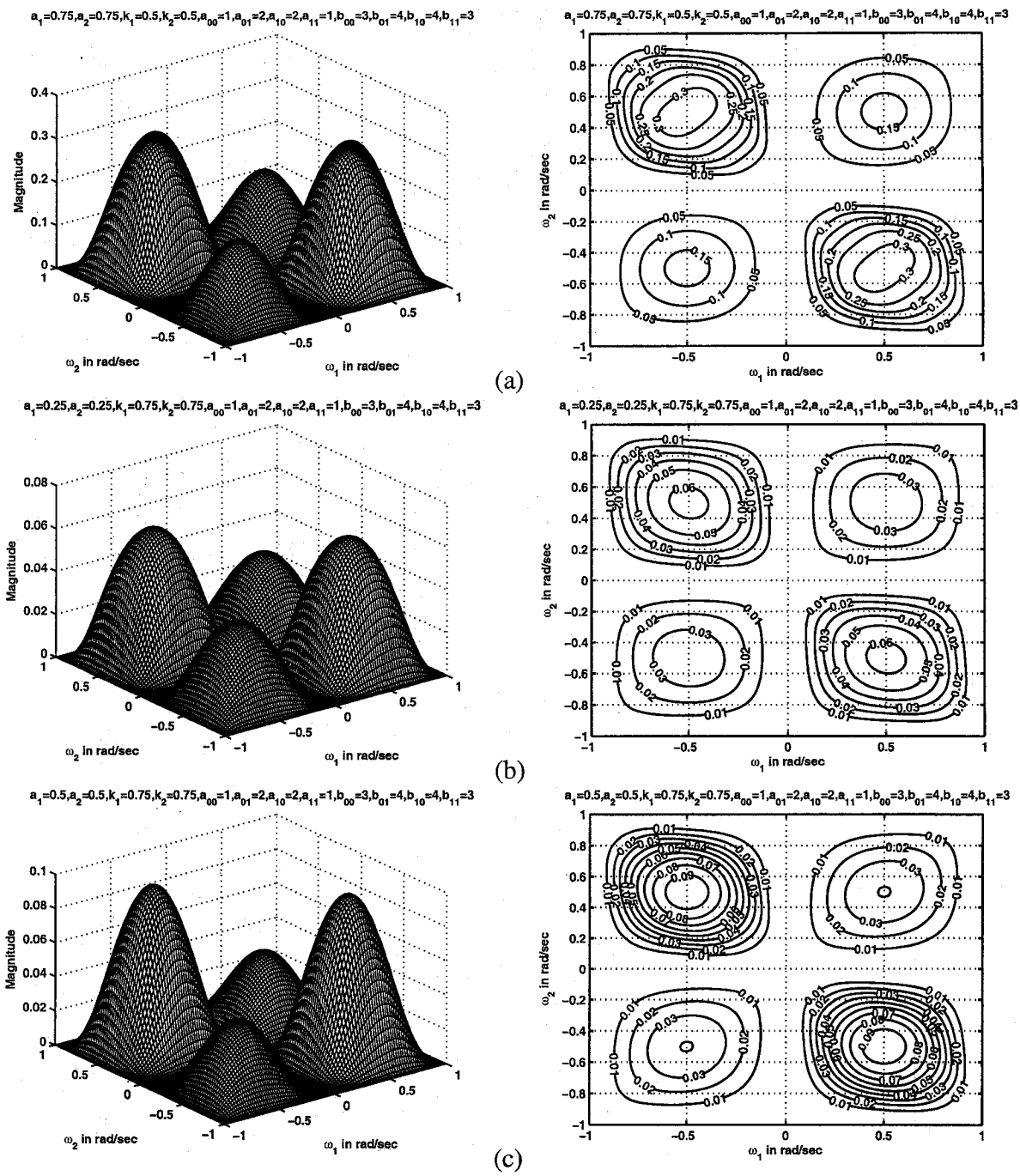

Figure 4.29: 3-D amplitude-frequency response and contour response of 2-D digital band-pass filter in case 4 of set 3 (when $k_1 = k_2 = 0.5,\ 0.75$)

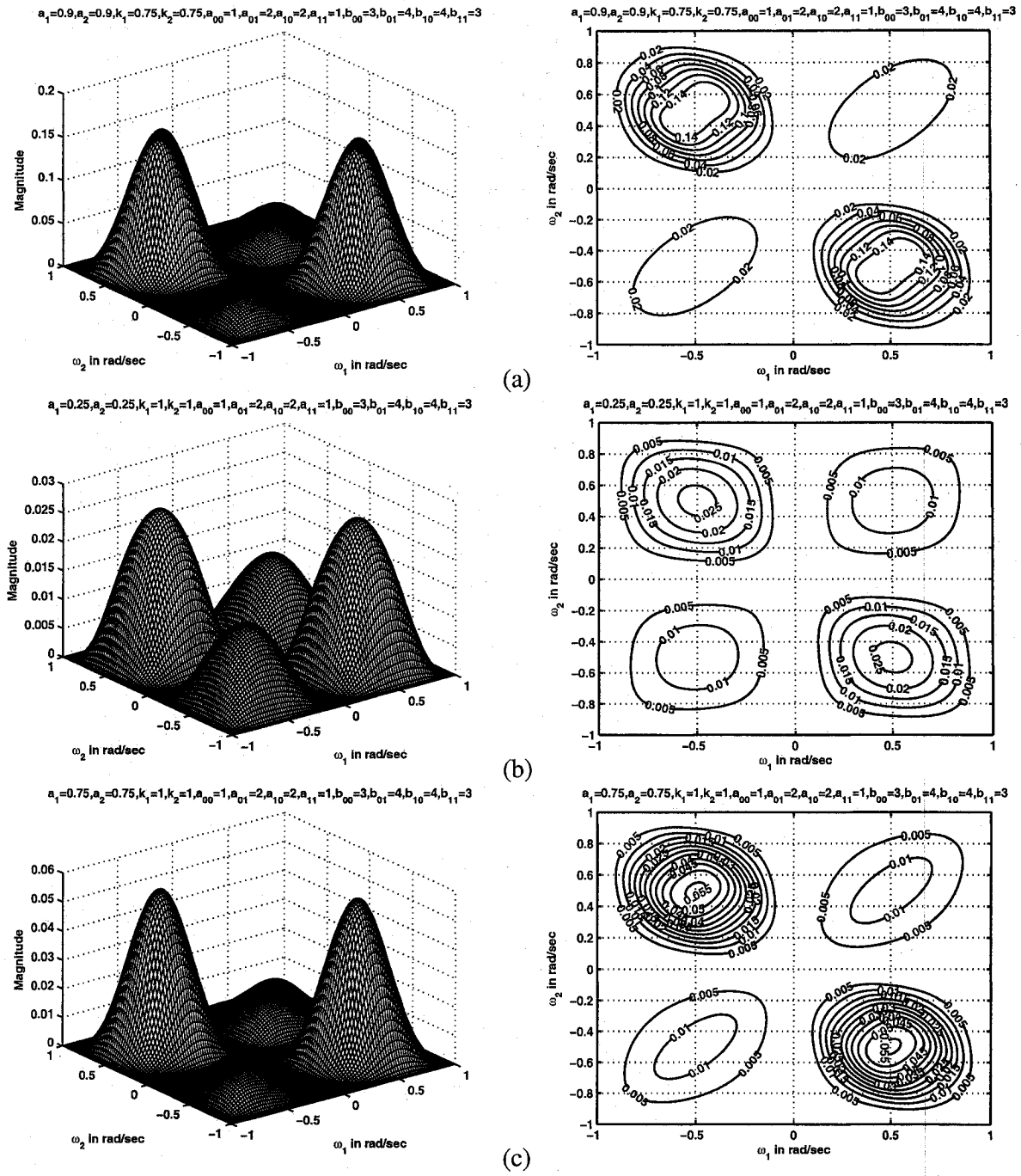

Figure 4.30: 3-D amplitude-frequency response and contour response of 2-D digital band-pass filter in case 4 of set 3 (when $k_1 = k_2 = 0.75,\ 1$)

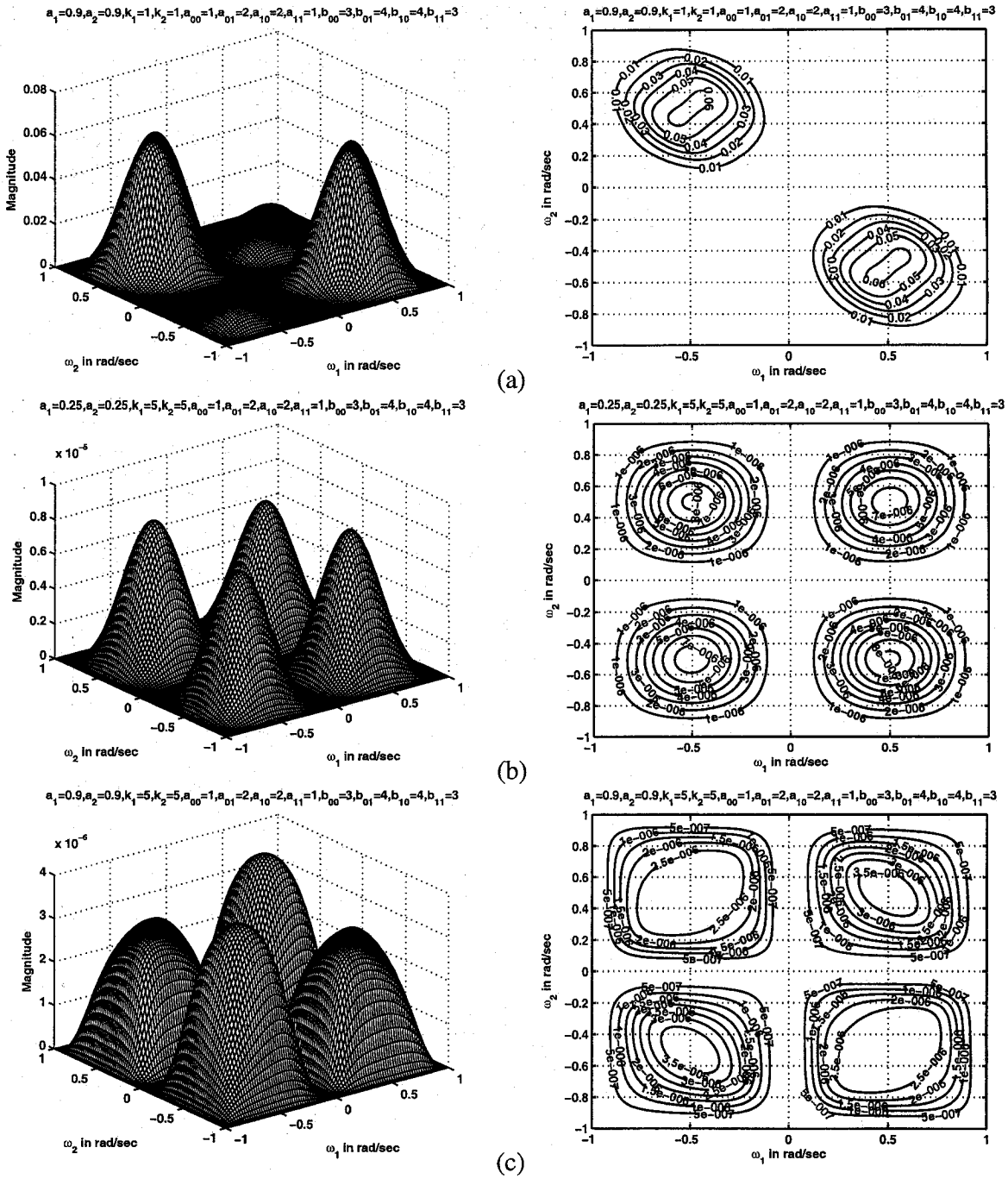

Figure 4.31: 3-D amplitude-frequency response and contour response of the 2-D digital bandpass filter in case 4 of set 3 (when $k_1 = k_2 = 1, 5$)

4.4.4 Frequency Response of 2-D Bandpass Filters in Set 4

In this section, we study the manner in which all the four cases in set 4 affect the frequency response behavior of the resulting 2-D band pass filter. In this set,

$$a_{00} \neq a_{01} \neq a_{10} \neq a_{11} \neq b_{00} \neq b_{01} \neq b_{10} \neq b_{11} \tag{4.8}$$

Different contour plots are obtained by varying the values of a_1, a_2, k_1 and k_2.

Similar to set 3, it is observed in all the four cases that the coefficients k_1 and k_2 affect the passband width and the coefficients a_1 and a_2 affect the gain of the amplitude-frequency response. As k_1 and k_2 values are increased, the passband width of the 2-D bandpass filter decreases and the magnitude of the contour response also decreases. Only in cases 1 and 3, as $k_1 \neq k_2$, the passband width of the 2-D digital bandpass filter increases and decreases periodically and the magnitude of the contour response decreases. As a_1 and a_2 values are increased, the magnitude of the amplitude-frequency response of the 2-D bandpass filter increases and the passband width decreases. It can be noticed that there is rounding of contour edges for higher values of k_1 and k_2.

It can be noticed that the contours in the first and third quadrants are mirror images of one another and the contours in the second and fourth quadrants are mirror images of one another. Also the magnitude of the contours in the second and fourth quadrants is lower than the magnitude of the contours in the first and third quadrants unlike in set 1 where the magnitude of the contours in the second and fourth quadrants is higher than the magnitude of the contours in the first and third quadrants.

In set 4, the magnitude of the contour response is smaller when compared to that of set 3 for the same values of a_1, a_2, k_1 and k_2.

4.4.4.1 Case 1

In this case,

$$a_1 = a_2 \quad , \quad k_1 \neq k_2$$

It is observed in this case that the coefficients k_1 and k_2 affect the passband width and the coefficients a_1 and a_2 affect the gain of the amplitude-frequency response. As k_1 and k_2 values are increased, the passband width of the 2-D digital bandpass filter increases and decreases periodically and the magnitude of the contour response decreases. In Fig. 4.33 (a), (b), (c) and Fig. 4.34 (a), there is a gradual decrease in the passband width as the values of k_1 and k_2 are increased from 0.25, 0.5 to 2, 10 respectively for the same values of $a_1 = a_2 = 0.5$. Further increase in the values of k_1 and k_2 result in gradual increase in the passband width. In Fig. 4.34 (b), it can be seen that the passband width increases when the values of k_1 and k_2 are increased to 8, 10 respectively. As a_1 and a_2 values are increased, the magnitude of the amplitude-frequency response of the 2-D bandpass filter increases and the passband width decreases.

In this case, the magnitude of the contour response is lower than that of the magnitude in case 1 of set 3 for the same values of a_1, a_2, k_1 and k_2. For example, the magnitude of the contour response in Fig. 4.32 (a) is lower than the magnitude in Fig. 4.18 (c) of case 1 in set 3 for the same values of $a_1 = a_2 = 0.25$, $k_1 = 0.25$ and $k_2 = 0.5$. The edges of the contours are sharper for values of k_1, $k_2 \leq 0.5$. It can be noticed that there is rounding of contour edges for larger values of k_1 and k_2.

It can be noticed that the contours in the first and third quadrant are mirror images of one another and the contours in the second and fourth quadrant are mirror images of one another. Similar to set 3, the magnitude of the contours in the second and fourth quadrant is lower than that of the magnitude in the first and third quadrant . Also, it can be noticed that the magnitude of the contours in all the four quadrants is the same for values of $k_1 = 0.25$ and $k_2 = 0.5$ as shown in Fig. 4.32 (a), Fig. 4.33 (a) and Fig. 4.34 (b).

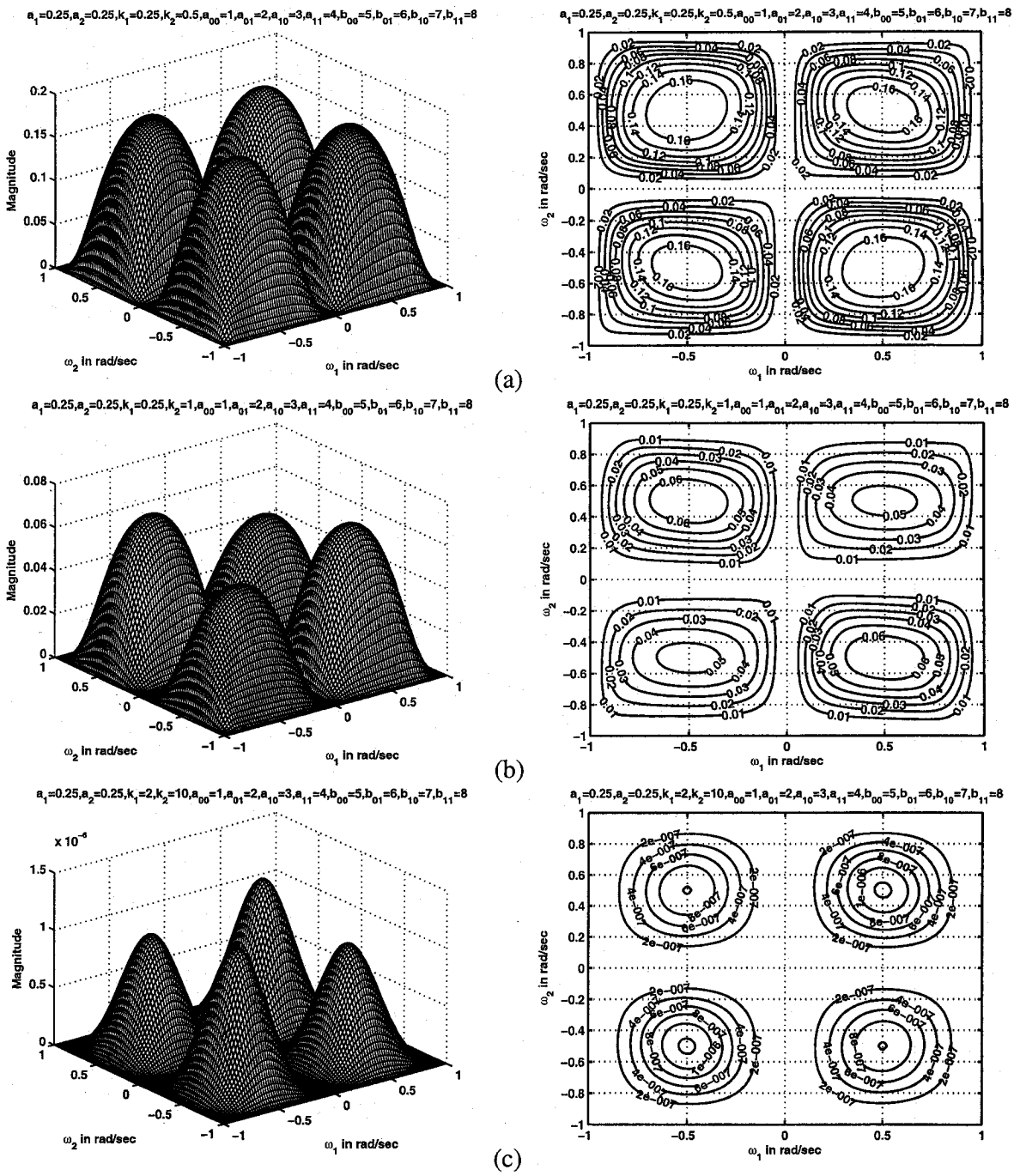

Figure 4.32: 3-D amplitude-frequency response and contour response of 2-D digital band-pass filter in case 1 of set 4 (when $a_1 = a_2 = 0.25$)

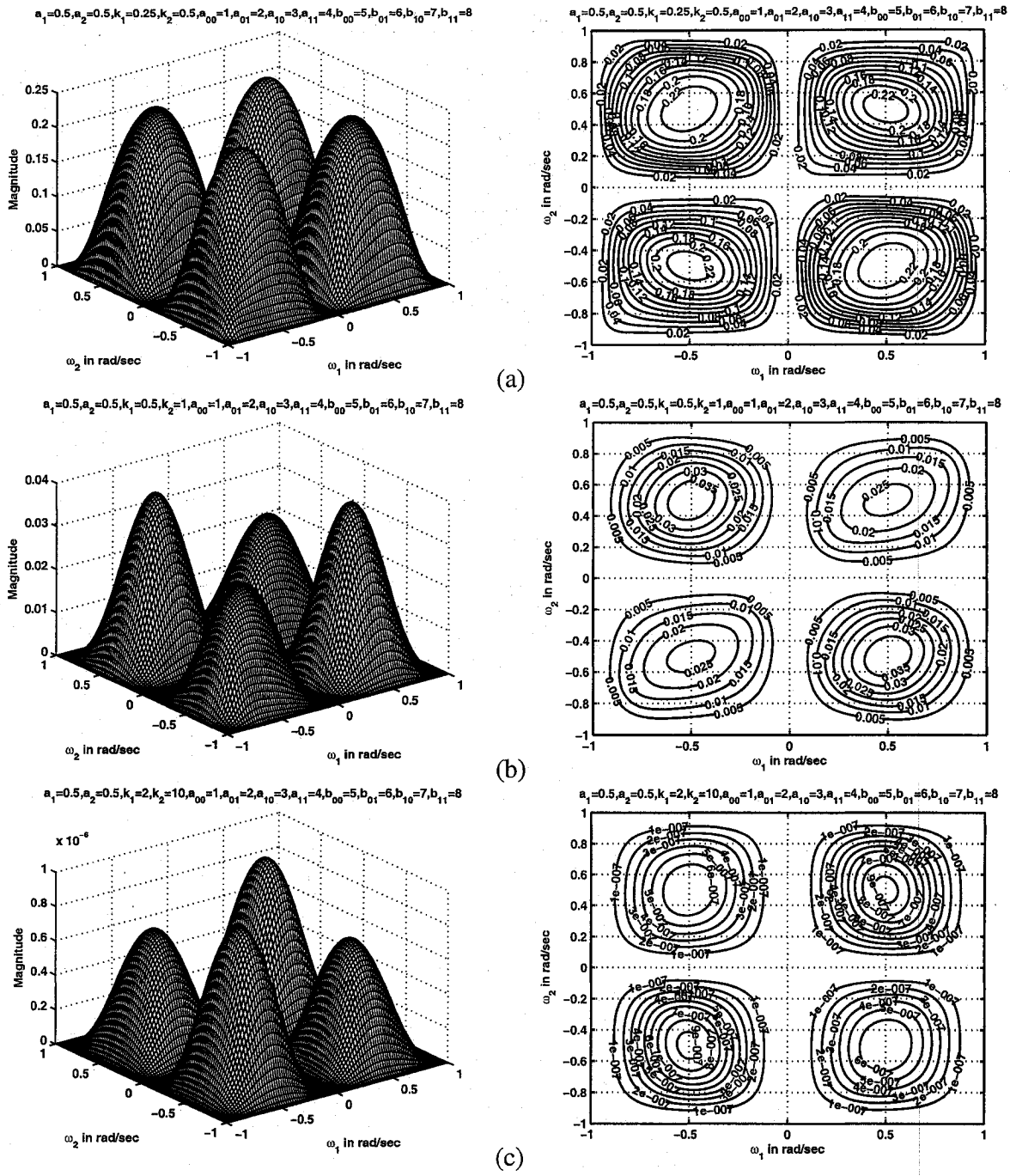

Figure 4.33: 3-D amplitude-frequency response and contour response of the 2-D digital bandpass filter in case 1 of set 4 (when $a_1 = a_2 = 0.5$)

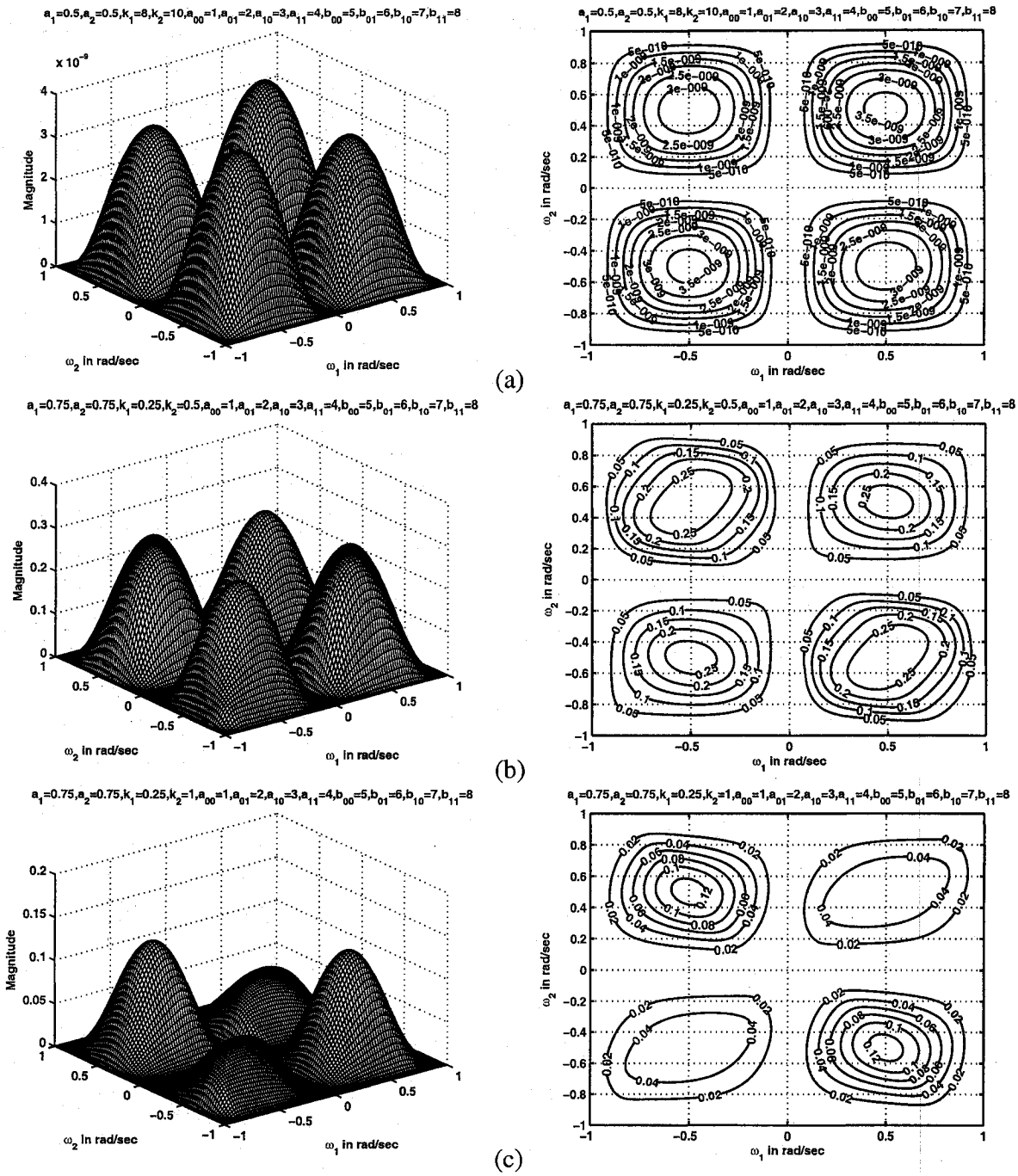

Figure 4.34: 3-D amplitude-frequency response and contour response of 2-D digital band-pass filter in case 1 of set 4 (when $a_1 = a_2 = 0.75$)

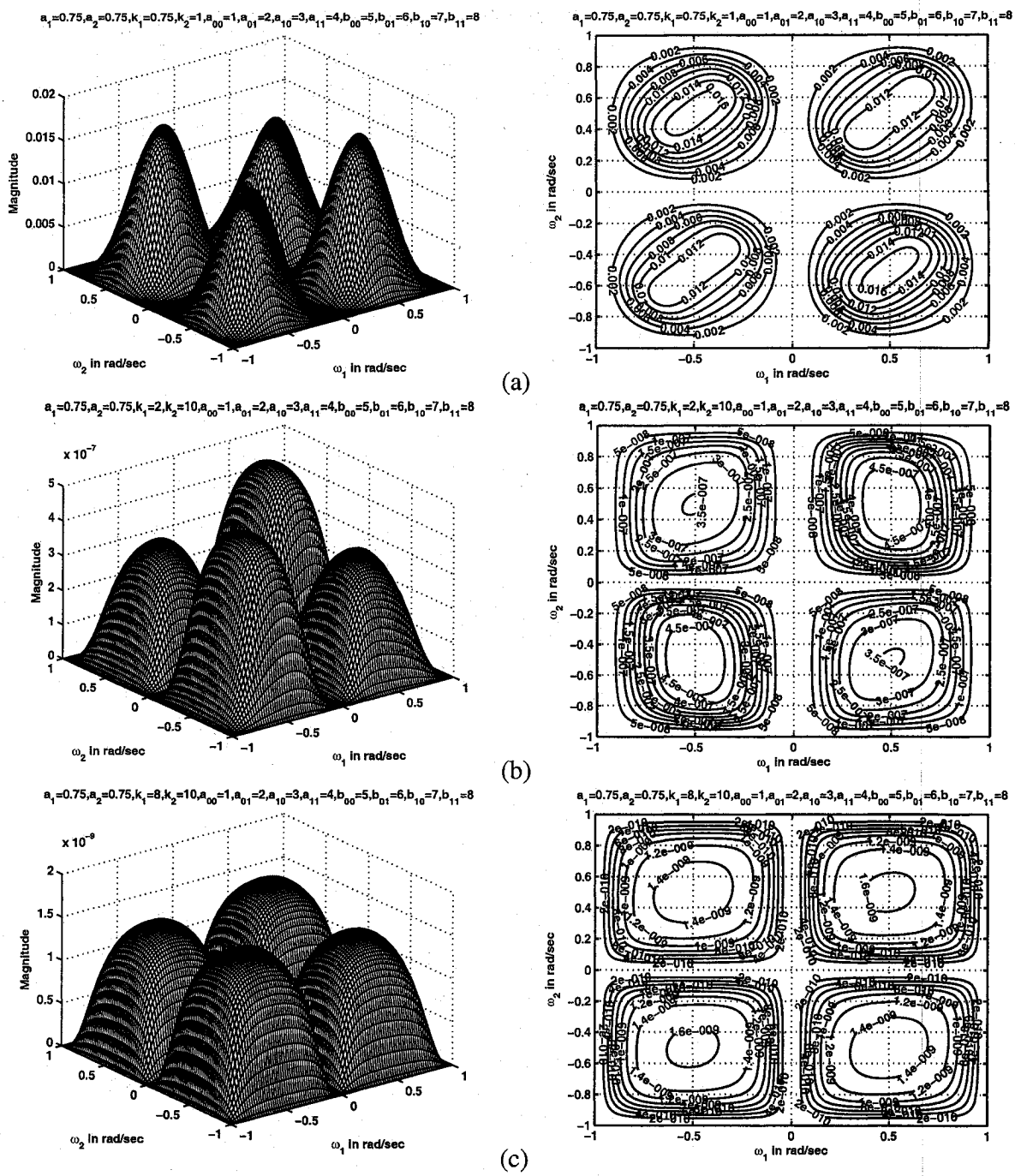

Figure 4.35: 3-D amplitude-frequency response and contour response of 2-D digital band-pass filter in case 1 of set 4 (when $a_1 = a_2 = 0.75$)

4.4.4.2 Case 2

In this case,

$$a_1 \neq a_2 \quad , \quad k_1 = k_2$$

It is observed in this case that the coefficients k_1 and k_2 affect the passband width and the coefficients a_1 and a_2 affect the gain of the amplitude-frequency response. As k_1 and k_2 values are increased, the passband width of the 2-D bandpass filter decreases and the magnitude of the contour response also decreases. As a_1 and a_2 values are increased, the magnitude of the amplitude-frequency response of the 2-D bandpass filter increases and the passband width decreases.

The magnitude of the contour response is smaller than that of the magnitude in case 2 of set 3 for the same values of a_1, a_2, k_1 and k_2. The magnitude of the contour response in Fig. 4.36 (a) is smaller than the magnitude in Fig. 4.22 (a) of case 2 in set 3 for the same values of $k_1 = k_2 = 0.25$, $a_1 = 0.25$ and $a_2 = 0.5$.

For smaller values of k_1 and k_2, i.e., when $k_1 = k_2 = 0.25$, the magnitude of the contours in the second and fourth quadrants is greater than the magnitude of the contours in the first and third quadrants. But for values of $0.25 < k_1, k_2 \leq 1$, the magnitude of the contours in the second and fourth quadrants is less than the magnitude of the contours in the first and third quadrants as shown in Fig. 4.37 (a), (b), (c) and Fig. 4.38 (a). For higher values of k_1 and k_2, the magnitude of the contours in the second and fourth quadrants is greater than the magnitude of the contours in the first and third quadrants as shown in Fig. 4.38 (b), (c). It can be noticed that the contours in the first and third quadrants are mirror images of one another and the contours in the second and fourth quadrants are mirror images of one another.

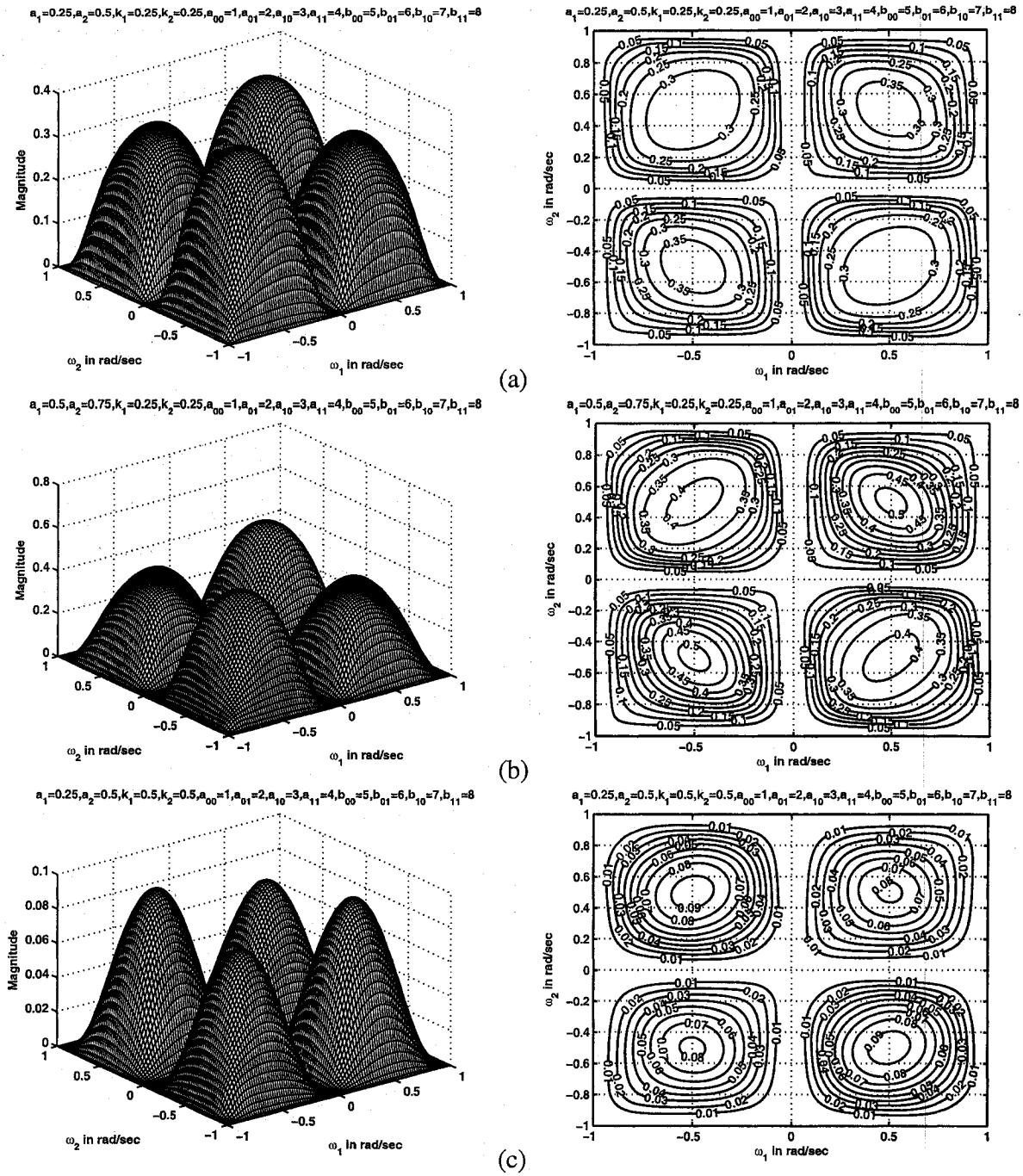

Figure 4.36: 3-D amplitude-frequency response and contour response of 2-D digital band-pass filter in case 2 of set 4 (when $k_1 = k_2 = 0.25,\ 0.5$)

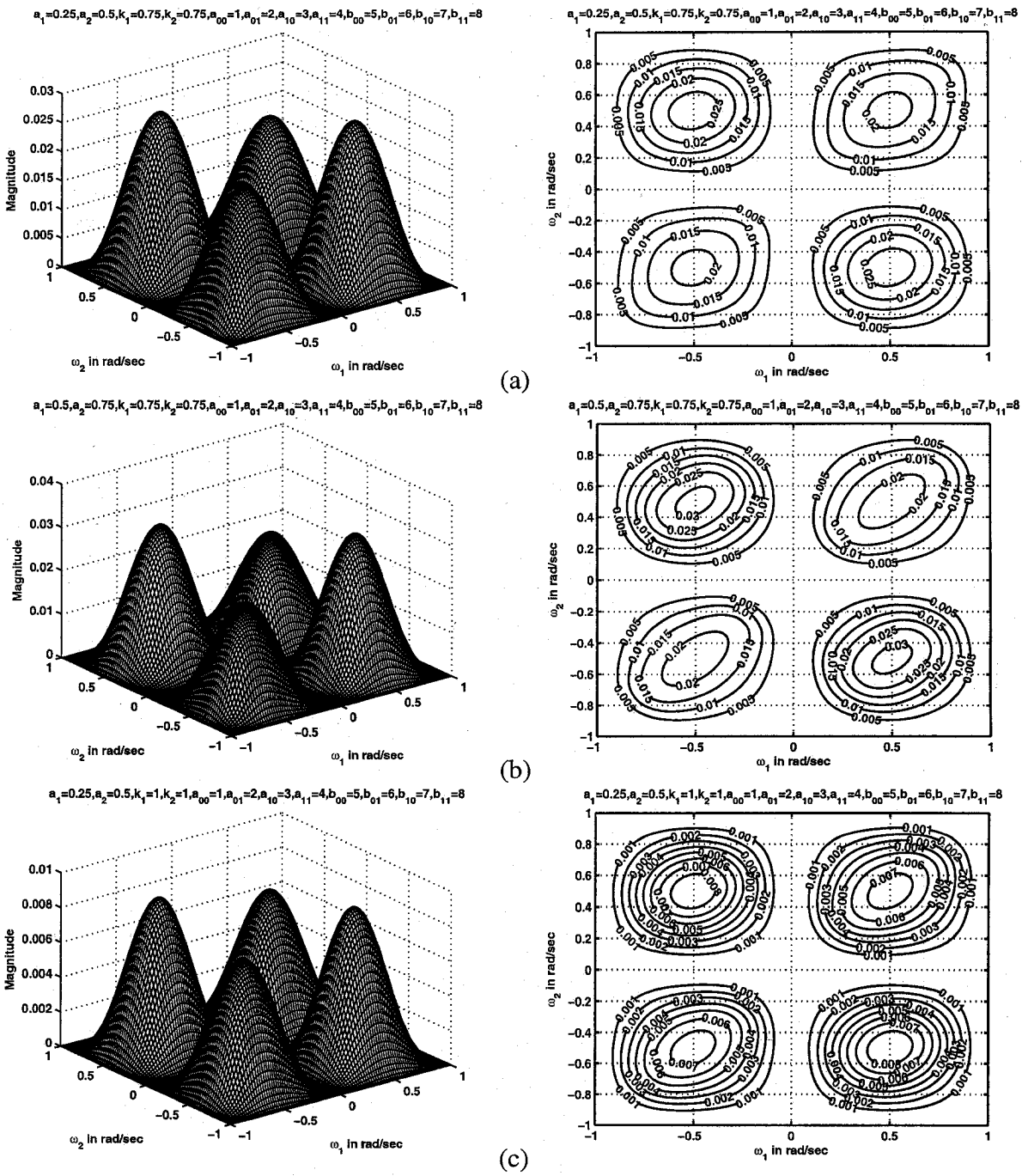

Figure 4.37: 3-D amplitude-frequency response and contour response of 2-D digital band-pass filter in case 2 of set 4 (when $k_1 = k_2 = 0.75,\ 1$)

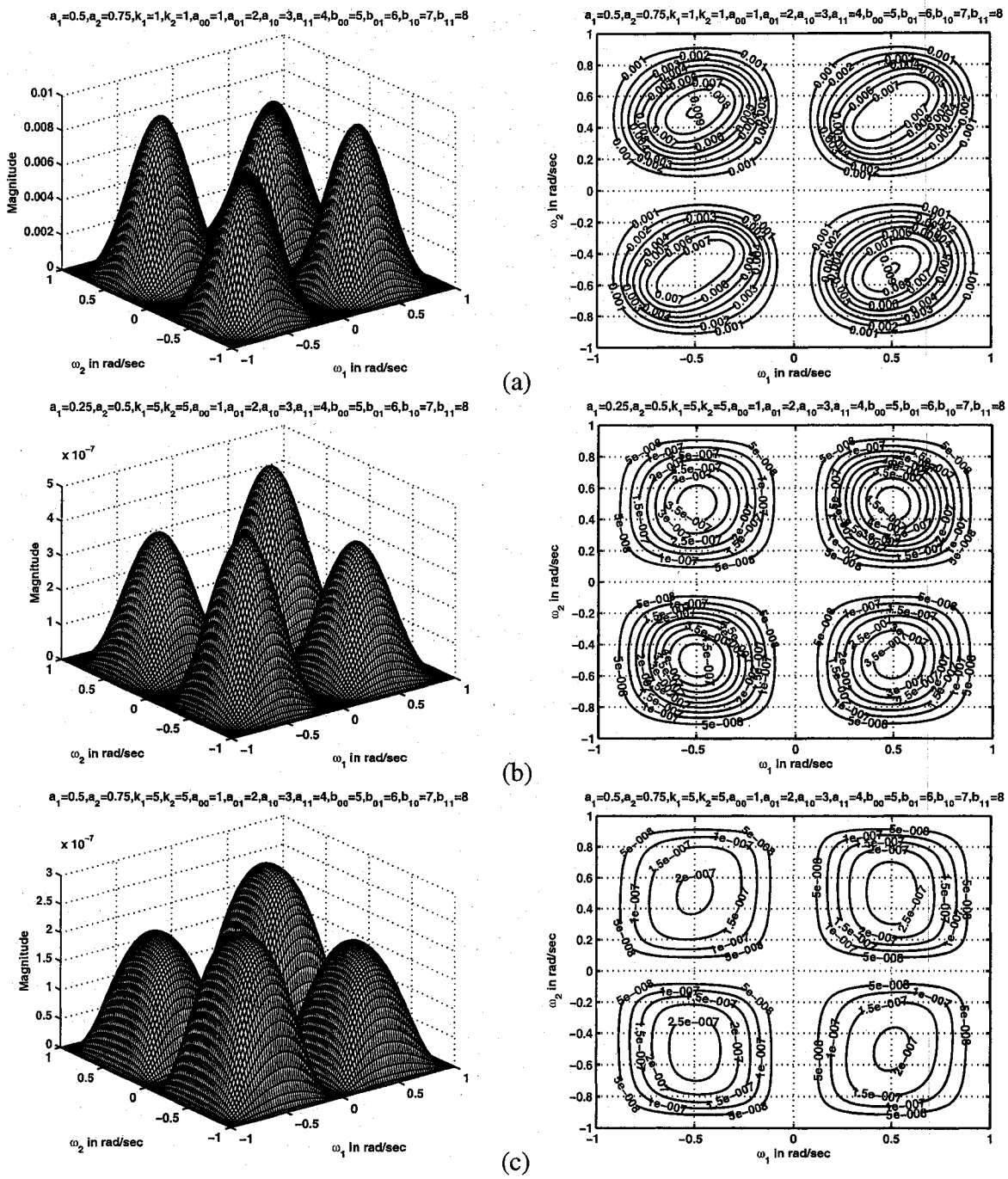

Figure 4.38: 3-D amplitude-frequency response and contour response of 2-D digital band-pass filter in case 2 of set 4 (when $k_1 = k_2 = 1, 5$)

4.4.4.3 Case 3

In this case,

$$a_1 \neq a_2 \quad , \quad k_1 \neq k_2$$

In this case, the coefficients k_1 and k_2 affect the passband width and the coefficients a_1 and a_2 affect the gain of the amplitude-frequency response. As k_1 and k_2 values are increased, the passband width of the 2-D digital bandpass filter increases and decreases periodically and the magnitude of the contour response also decreases. In Fig. 4.39 (b), (c), Fig. 4.40 (b) and Fig. 4.41 (a) there is a gradual decrease in the passband width as the values of k_1 and k_2 are increased from 0.25, 0.5 to 2, 10 respectively for the same values of $a_1 = 0.5; a_2 = 0.75$. Further increase in the values of k_1 and k_2 result in gradual increase in the passband width. In Fig. 4.41 (b) and (c), it can be seen that the passband width increases when the values of k_1 and k_2 are increased to 8, 10 respectively. As a_1 and a_2 values are increased, the magnitude of the amplitude-frequency response of the 2-D bandpass filter increases and the passband width decreases.

The magnitude of the contour response is lower than that of the magnitude in case 3 of set 3 for the same values of a_1, a_2, k_1 and k_2. The magnitude of the contour response in Fig. 4.39 (b) is smaller than the magnitude of the contour response in Fig. 4.25 (b) of case 3 of set 3 for the same values of $k_1 = 0.25$, $k_2 = 0.5$, $a_1 = 0.5$ and $a_2 = 0.75$.

It can be noticed that the contours in the first and third quadrants are mirror images of one another and the contours in the second and fourth quadrants are mirror images of one another. For smaller values of k_1 and k_2 , i.e when $k_1 = 0.25$, $k_2 = 0.5$, the magnitude of the contours in all the four quadrants are the same as shown in Fig. 4.39 (a), (b). But for greater values of $0.25 < k_1, k_2 \leq 1$, the magnitude of the contours in the second and fourth quadrants is less than the magnitude of the contours in the first and third quadrants as shown in Fig. 4.40 (c) and Fig. 4.41 (a). When the values of $k_1, k_2 \geq 1$, the the magnitude

of the contours in the second and fourth quadrants is greater than the magnitude of the contours in the first and third quadrants as shown in Fig. 4.41 (b), (c).

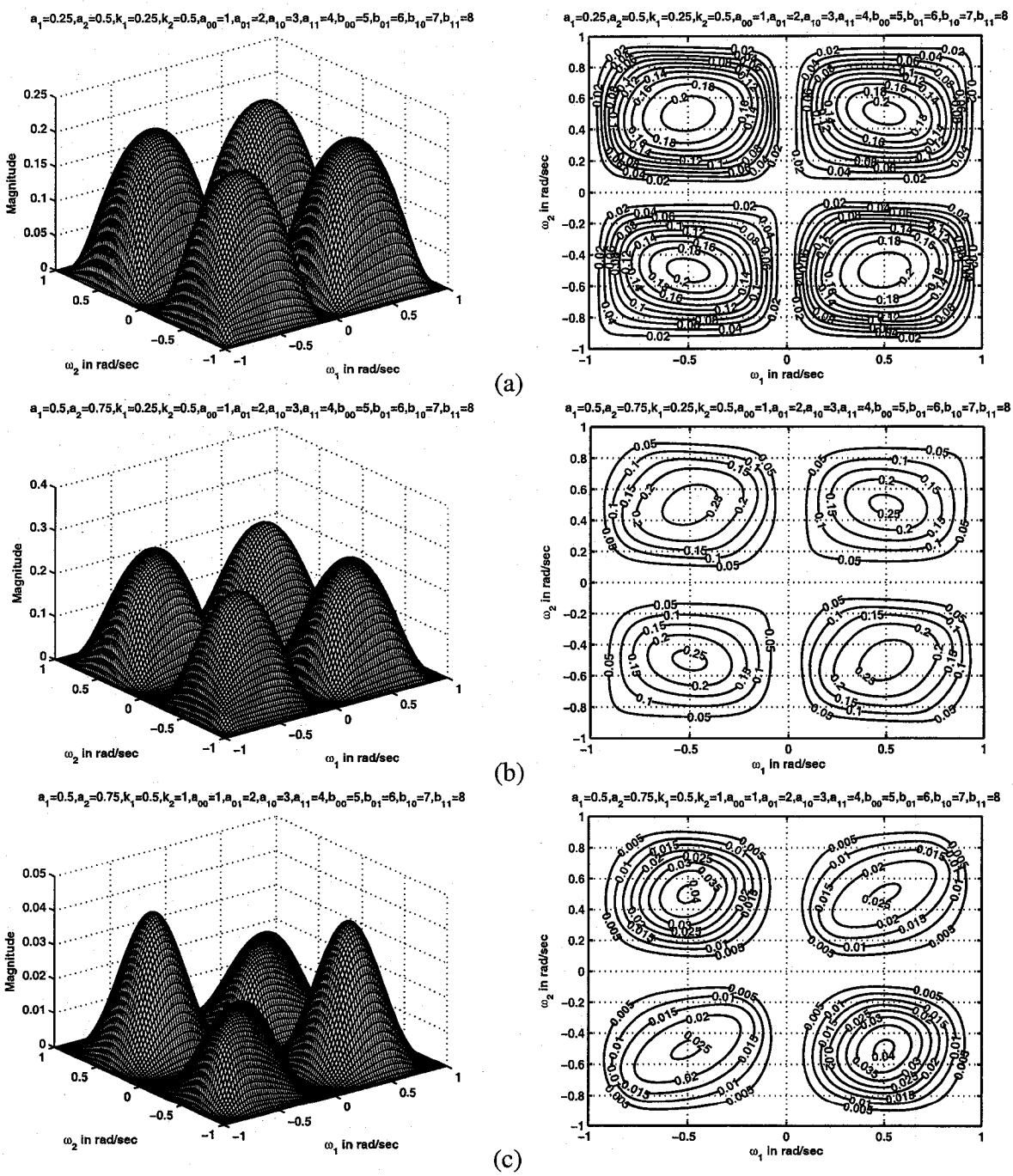

Figure 4.39: 3-D amplitude-frequency response and contour response of 2-D digital band-pass filter in case 3 of set 4 (when $k_1 = 0.25,\ 0.5,\ k_2 = 0.5,\ 1$)

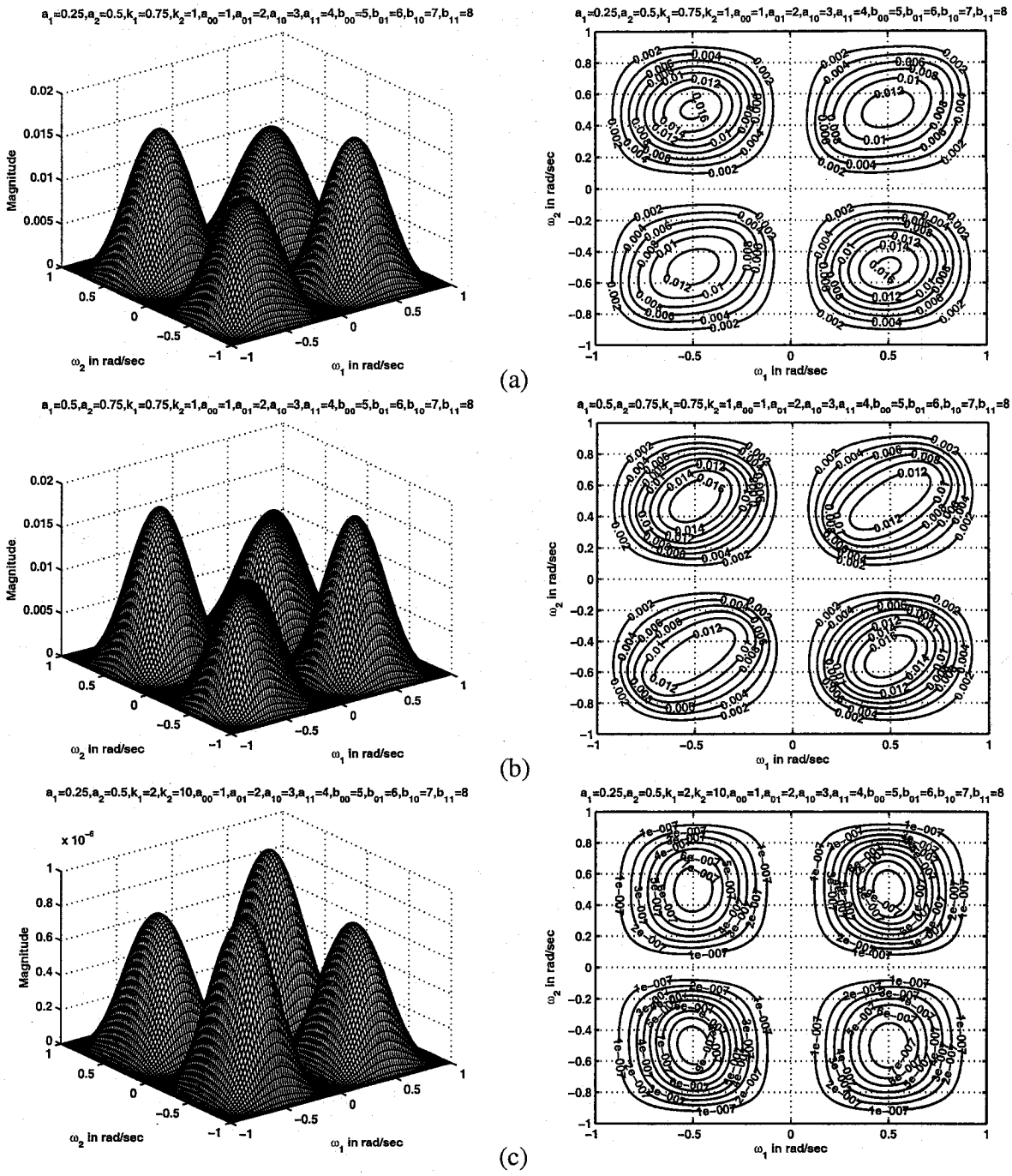

Figure 4.40: 3-D amplitude-frequency response and contour response of 2-D digital band-pass filter in case 3 of set 4 (when $k_1 = 0.75,\ 2,\ k_2 = 1,\ 10$)

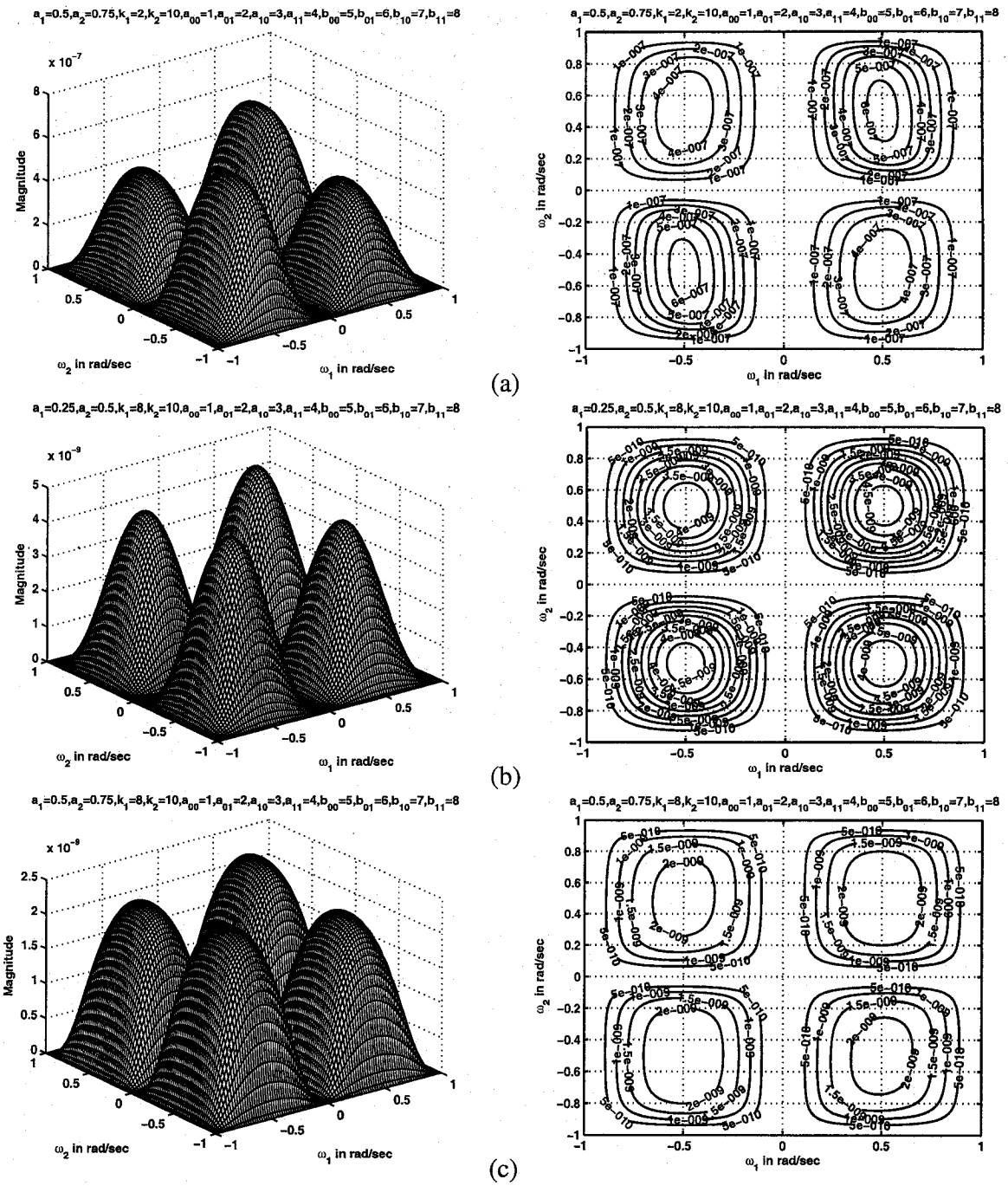

Figure 4.41: 3-D amplitude-frequency response and contour response of 2-D digital band-pass filter in case 3 of set 4 (when $k_1 = 2,\ 8,\ k_2 = 10$)

4.4.4.4 Case 4

In this case,

$$a_1 = a_2 \quad , \quad k_1 = k_2$$

It is observed in this case that the coefficients k_1 and k_2 affect the passband width and the coefficients a_1 and a_2 affect the gain of the amplitude-frequency response. As k_1 and k_2 values are increased, the passband width of the 2-D bandpass filter decreases and the magnitude of the passband also decreases. As a_1 and a_2 values are increased, the magnitude of the amplitude-frequency response of the 2-D bandpass filter increases and the passband width decreases.

The magnitude of the contour response is lower than that of the magnitude in case 4 of set 3 for the same values of a_1, a_2, k_1 and k_2. The magnitude of the contour response in Fig. 4.42 (a) is smaller than the magnitude of the contour response in Fig. 4.28 (a) of case 4 in set 3 for the same values of $k_1 = k_2 = 0.25$ and $a_1 = a_2 = 0.25$.

It can be noticed that the contours in the first and third quadrants are mirror images of one another and the contours in the second and fourth quadrants are mirror images of one another. For smaller values of k_1 and k_2, i.e., when $k_1 = k_2 = 0.25$, the magnitude of the contours in the second and fourth quadrants is greater than or equal to the magnitude of the contours in the first and third quadrants as shown in Fig. 4.42 (a), (b), (c). But for values of $0.25 < k_1,\ k_2 \leq 1$, the magnitude of the contours in the second and fourth quadrants is less when compared to the magnitude of the contours in the first and third quadrants as shown in Fig. 4.43 (a), (b), (c) and Fig. 4.44 (a). For higher values of k_1 and k_2, the magnitude of the contours in the second and fourth quadrants is greater than or equal to the magnitude of the contours in the first and third quadrants as seen in Fig. 4.44 (b), (c).

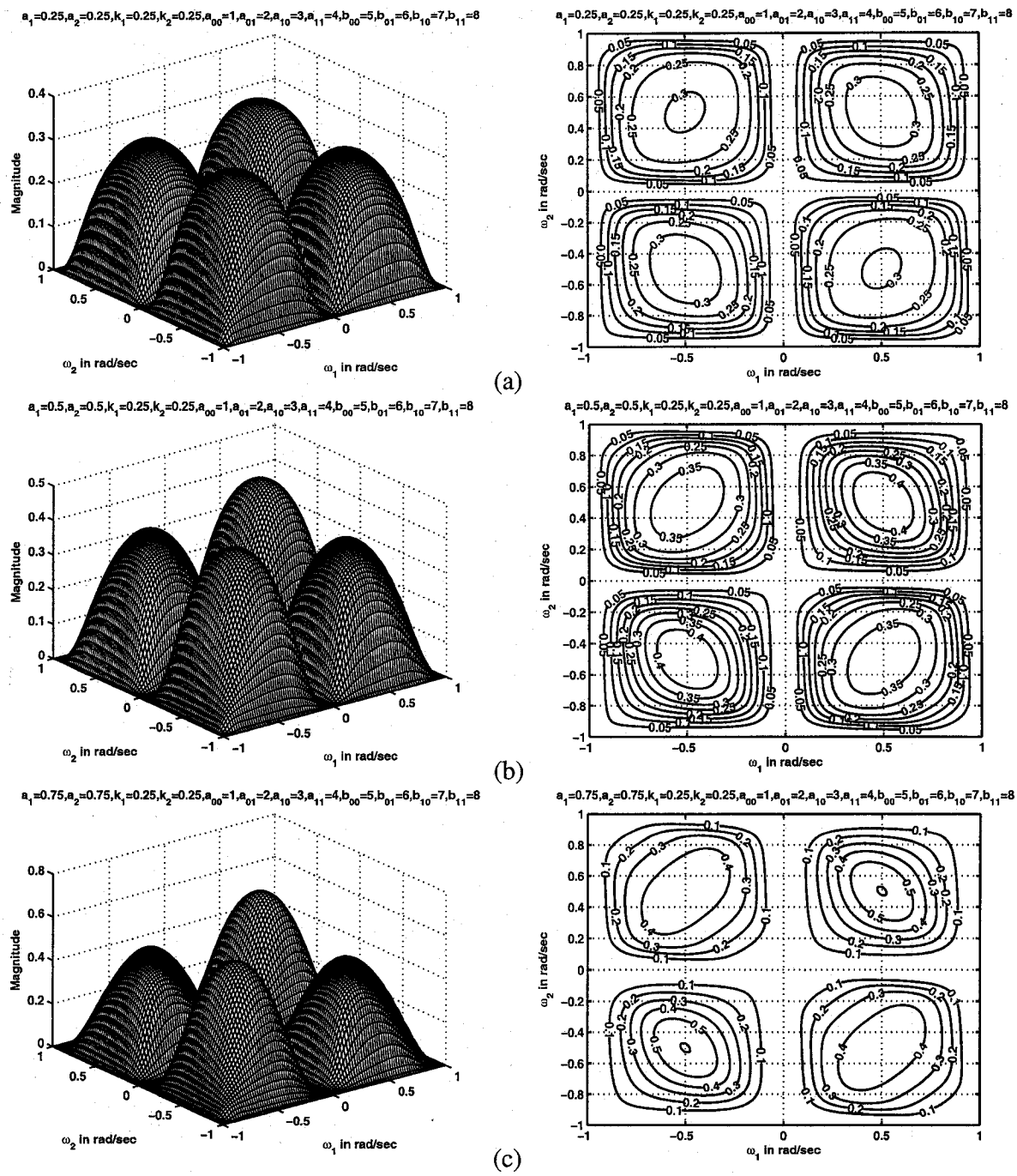

Figure 4.42: 3-D amplitude-frequency response and contour response of 2-D digital band-pass filter in case 4 of set 4 (when $k_1 = k_2 = 0.25$)

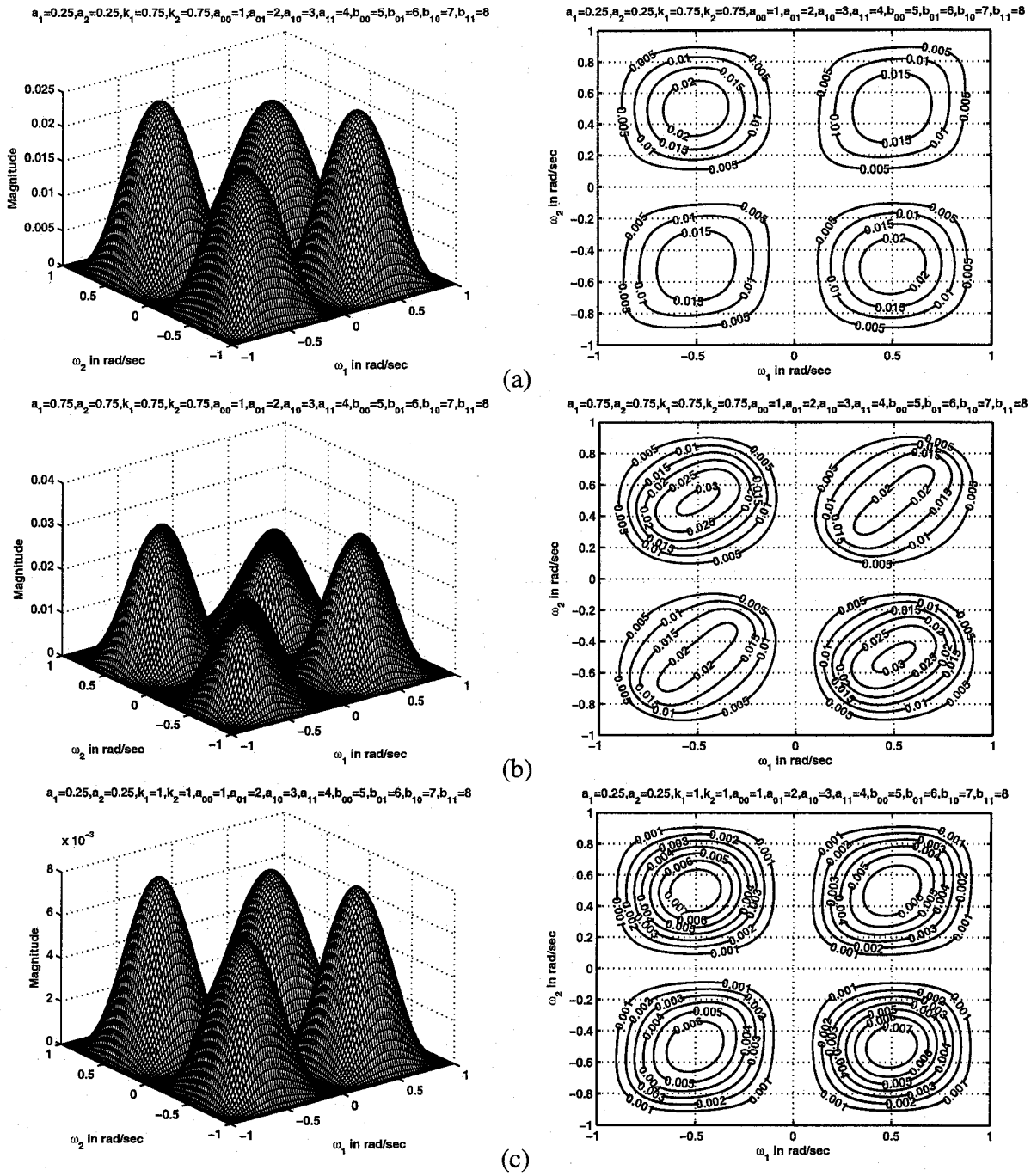

Figure 4.43: 3-D amplitude-frequency response and contour response of 2-D digital band-pass filter in case 4 of set 4 (when $k_1 = k_2 = 0.75,\ 1$)

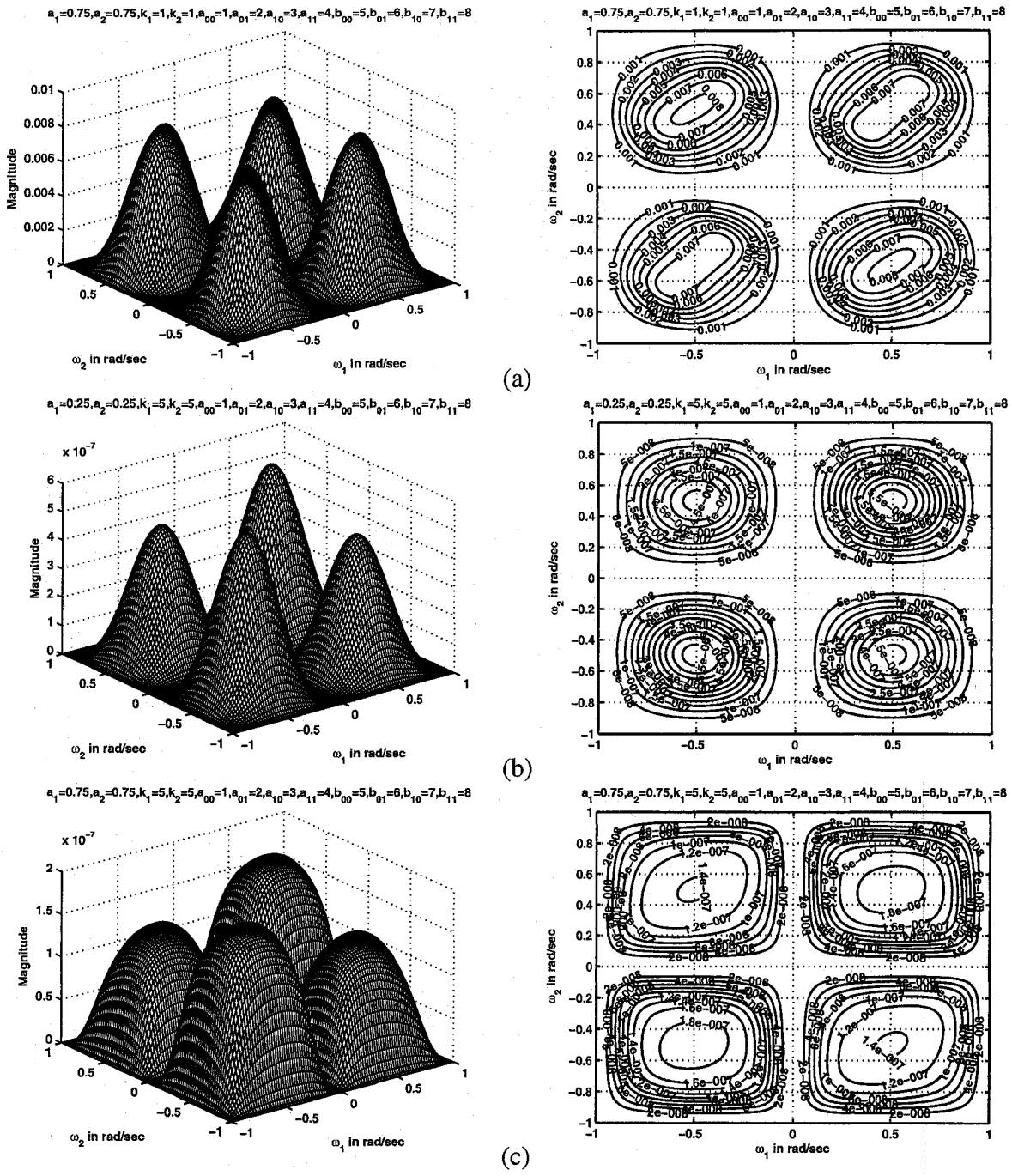

Figure 4.44: 3-D amplitude-frequency response and contour response of 2-D digital band-pass filter in case 4 of set 4 (when $k_1 = k_2 = 1,\ 5$)

4.5 Summary

It is observed in all the four cases that the coefficients k_1, k_2 affect the passband width and the coefficients a_1, a_2 affect the gain of the amplitude-frequency response. As k_1 and k_2 values are increased, the passband width increases and decreases periodically (only for case 1 and case 3) and the magnitude of the contour response decreases. As a_1 and a_2 values are increased, the magnitude of the amplitude-frequency response of the 2-D bandpass filter increases and the passband width decreases. It can be noticed that there is rounding of contour edges for higher values of k_1 and k_2. It can be observed that the first and third quadrants of the contour response of the 2-D bandpass filters have the same passband width and magnitude whereas the second and fourth quadrants of the contour response have the same passband width and magnitude.

In set 1, there are ripples in the contour responses of case 1 when the values of $a_1 = a_2 \geq 0.75$ and when the values of k_1, k_2 are less than 0.5. Also, the magnitude of the contours on the second and fourth quadrants for this particular set of values is twice that of the magnitude of the contours in the first and third quadrants. There are ripples in the contour response of case 2 for all values of a_1 and a_2 till $k_1 = k_2 \leq 0.25$. In case 3, for very low values of k_1 and k_2 (k_1, $k_2 \leq 0.5$), the magnitude of the contours in the second and fourth quadrants is nearly twice than that of the magnitude of the contours in the first and third quadrants. There are no ripples in the passband of the contour response for all values of a_1, a_2, k_1 and k_2. In case 4, there are ripples in the contour response for values of a_1 and a_2 greater than 0.5 and for values of k_1, $k_2 \leq 0.5$. In cases 1 and 3, as k_1 and k_2 values are increased, the passband width increases and decreases periodically. This is because $k_1 \neq k_2$ only in these two cases. The magnitude of the contours in the second and fourth quadrants is greater than the magnitude of the contours in the first and third quadrants.

An important obervation to be noted is that the responses for set 2 is the same as that of set 1. This is because of the resulting transfer function for set 2 is the same as the one used in set 1 as the transfer function does not depend on the coefficients of the CFE. It only

depends on the coefficients of the generalized bilinear transformation.

In set 3, it can be observed that there are no ripples in the contour response in all the four cases, when compared to set 1. Also the magnitude of the contour response is low when compared to set 1 for the same values of a_1, a_2, k_1 and k_2. In cases 1 and 3, it can be observed that the passband width of the contour response is greater than that of cases 1 and 3 in set 1 for higher values of k_1 and k_2. Also the magnitude of the contours in the second and fourth quadrant is lower than the magnitude of the contours in the first and third quadrants unlike in set 1 where the magnitude of the contours in the second and fourth quadrants is higher than the magnitude of the contours in the first and third quadrants. For certain values of a_1, a_2, k_1 and k_2, i.e., when one of the k_1, $k_2 = 1$ and $a_1 = a_2 \geq 0.5$, the magnitude of the contours in the second and fourth quadrants drops to a minimum value when compared to the contours in the first and third quadrants. In cases 2 and 4, for smaller values of k_1 and k_2, i.e., when $k_1 = k_2 = 0.25$, the magnitude of the contours in the second and fourth quadrants are greater than or equal to the magnitude of the contours in the first and third quadrants. But for values of $0.25 < k_1$, $k_2 \leq 1$, the magnitude of the contours in the second and fourth quadrants are less than the magnitude of the contours in the first and third quadrants. For further higher values of k_1 and k_2, the magnitude of the contours in the second and fourth quadrants are greater than or equal to the magnitude of the contours in the first and third quadrants. In case 4, when the values of a_1, a_2, k_1 and k_2 are closer to 1, the contours in the first and third quadrants totally disappears.

In set 4, the magnitude of the contour response is smaller when compared to that of set 3 for the same values of a_1, a_2, k_1 and k_2. Similar to set 3, in cases 1 and 3, the magnitude of the contours in the second and fourth quadrants is lower than that of the magnitude in the first and third quadrants. Also, it can be noticed that the magnitude of the contours in all the four quadrants is the same for values of $k_1 = 0.25$ and $k_2 = 0.5$. In cases 2 and 4, for smaller values of k_1 and k_2, i.e., when $k_1 = k_2 = 0.25$, the magnitude of the contours in the second and fourth quadrants is greater than the magnitude of the contours in the first

and third quadrants. But for values of $0.25 < k_1, k_2 \leq 1$, the magnitude of the contours in the second and fourth quadrants is less than the magnitude of the contours in the first and third quadrants. For higher values of k_1 and k_2, the magnitude of the contours in the second and fourth quadrants is greater than or equal to the magnitude of the contours in the first and third quadrants.

Chapter 5

Generation of 2-D Bandstop Filters from the CFE

5.1 Introduction

In this chapter, 2-D digital bandstop filters are analyzed. There are various ways to obtain bandstop filters. A common method is by using the lowpass filter. The analog lowpass filter is transformed to a bandstop filter which in turn is transformed to a digital filter by using the generalized bilinear transformation. Then the coefficients of the 2-D bandstop filter are varied to analyze their effect in the design of 2-D digital bandstop filters.

In Sec. 5.2, we will generate 2-D digital bandstop filters from the lowpass filters discussed in chapter 2. In Sec. 5.3, we review the classification of bandstop filters. In Sec. 5.4, each set in particular is discussed and the effect of coefficients of the filter on the amplitude-frequency response is analysed. Sec. 5.5 gives the summary and discussions of the results obtained in this chapter.

5.2 Generation of 2-D digital Bandstop Filter

The generation of 2-D lowpass filter is discussed in Sec. 2.3 of Chapter 2. In the case of bandstop filters, the transformation F(s) must map lowpass response to a bandstop response. The result is a banstop filter with the center frequency ω_0 and width B of the band rejected. The transformation used to transform lowpass filter to bandstop filter is [33]

$$s = \frac{Bs}{s^2 + \omega_0^2} \tag{5.1}$$

The lowpass filter transfer function in analog domain is given by eqn.(2.20).

Applying lowpass to bandstop transformation to eqn.(2.20),

$$s_1 \rightarrow \frac{Bs_1}{s_1^2 + \omega_0^2} \tag{5.2}$$

$$s_2 \rightarrow \frac{Bs_2}{s_2^2 + \omega_0^2} \tag{5.3}$$

where $B = 1$ and $\omega_0 = 1$,

the resulting analog bandstop filter transfer function is,

$$H(s_1, s_2) = \frac{a_{00}b_{00}(s_1^2+1)^2(s_2^2+1)^2}{\begin{array}{c} s_1^2[a_{11}b_{11}s_2^2 + a_{10}b_{11}s_2(s_2^2+1) + a_{10}b_{10}(s_2^2+1)^2] + \\ s_1\left[\begin{array}{c} a_{01}b_{11}s_2^2(s_1^2+1) + (a_{11}b_{00} + a_{00}b_{11} + a_{10}b_{01} + a_{01}b_{10})s_2 \\ (s_1^2+1)(s_2^2+1) + a_{10}b_{00}(s_1^2+1)(s_2^2+1)^2 \end{array}\right] + \\ \left[\begin{array}{c} a_{01}b_{01}s_2^2(s_1^2+1)^2 + a_{01}b_{00}s_2(s_1^2+1)^2(s_2^2+1) \\ +a_{00}b_{00}(s_1^2+1)^2(s_2^2+1)^2 \end{array}\right] \end{array}} \tag{5.4}$$

Applying generalized bilinear transformation, i.e., $s_1 \rightarrow k_1\frac{z_1-a_1}{z_1+b1}$, $s_2 \rightarrow k_2\frac{z_2-a_2}{z_2+b_2}$, where $k_1 > 0, k_2 > 0$, $0 \leq a_1 \leq 1$, $0 \leq a_2 \leq 1$ and $b_1 = b_2 = 1$ to the above eqn.(5.4), we get,

$$H(z_1,z_2)=\frac{a_{00}b_{00}(k_1^2\frac{a^2}{c^2}+1)^2(k_2^2\frac{b^2}{d^2}+1)^2}{\begin{array}{l} k_1^2\frac{a^2}{c^2}\left[\begin{array}{c} a_{11}b_{11}k_2^2\frac{b^2}{d^2}+a_{10}b_{11}k_2(\frac{b}{d})(k_2^2\frac{b^2}{d^2}+1)+ \\ a_{10}b_{10}(k_2^2\frac{b^2}{d^2}+1)^2 \end{array}\right]+ \\ k_1(\frac{a}{c})(k_1^2\frac{a^2}{c^2}+1)\left[\begin{array}{c} a_{01}b_{11}k_2^2\frac{b^2}{d^2}+ \\ (a_{11}b_{00}+a_{00}b_{11}+a_{10}b_{01}+a_{01}b_{10})\ k_2(\frac{b}{d})(k_2^2\frac{b^2}{d^2}+1) \\ +a_{10}b_{00}(k_2^2\frac{b^2}{d^2}+1)^2 \end{array}\right]+ \\ (k_1^2\frac{a^2}{c^2}+1)^2\left[\begin{array}{c} a_{01}b_{01}k_2^2\frac{b^2}{d^2}+a_{01}b_{00}k_2(\frac{b}{d})(k_2^2\frac{b^2}{d^2}+1)+ \\ a_{00}b_{00}(k_2^2\frac{b^2}{d^2}+1)^2 \end{array}\right] \end{array}} \tag{5.5}$$

where $a=(z_1-a_1)$; $b=(z_2-a_2)$; $c=(z_1+b_1)$; $d=(z_2+b_2)$. Eqn.(5.5) gives the transfer function for 2-D digital bandstop filter.

5.3 Classification of 2-D Bandstop Filters

The 2-D bandstop filters are classified into four sets and each set is further classified into four cases. The classification of the four sets is formed based on the coefficients of the CFE and the classification of the four cases involved in each set is based on the coefficients of the generalized bilinear transformation. The same four sets as discussed in Chapters 2, 3 and 4 will be considered here and they are given in eqns.(4.1), (4.2), (4.3) and (4.4) respectively. Also, the same four cases in each set as discussed in Chapter 2 will be considered here as shown below.

Case 1:

$a_1=a_2 \quad , \quad k_1\neq k_2 \quad , \quad b_1=b_2=1$

Case 2:

$a_1\neq a_2 \quad , \quad k_1=k_2 \quad , \quad b_1=b_2=1$

Case 3:

$a_1 \neq a_2$, $k_1 \neq k_2$, $b_1 = b_2 = 1$

Case 4:

$a_1 = a_2$, $k_1 = k_2$, $b_1 = b_2 = 1$

The values of a_1 and a_2 vary from 0 to 1 and the values of k_1 and k_2 are greater than 0.

5.4 Frequency Responses of 2-D Digital Bandstop Filter

To investigate the manner in which each coefficient of the generalized bilinear transformation affects the magnitude response of the resulting 2-D bandstop filter, we change the value of some of the coefficients or fix some of the coefficients to specific values.

Let us consider the filter coefficients and the bilinear transformation coefficients to be unity, i.e., $a_1 = 1$, $a_2 = 1$, $b_1 = 1$, $b_2 = 1$, $k_1 = 1$, $k_2 = 1$, $a_{00} = 1$, $a_{10} = 1$, $a_{01} = 1$, $a_{11} = 1$, $b_{00} = 1$, $b_{10} = 1$, $b_{01} = 1$, $b_{11} = 1$. Under this condition, the 3-D amplitude-frequency response and contour response of the 2-D digital bandstop filter are shown in Fig. 5.1.

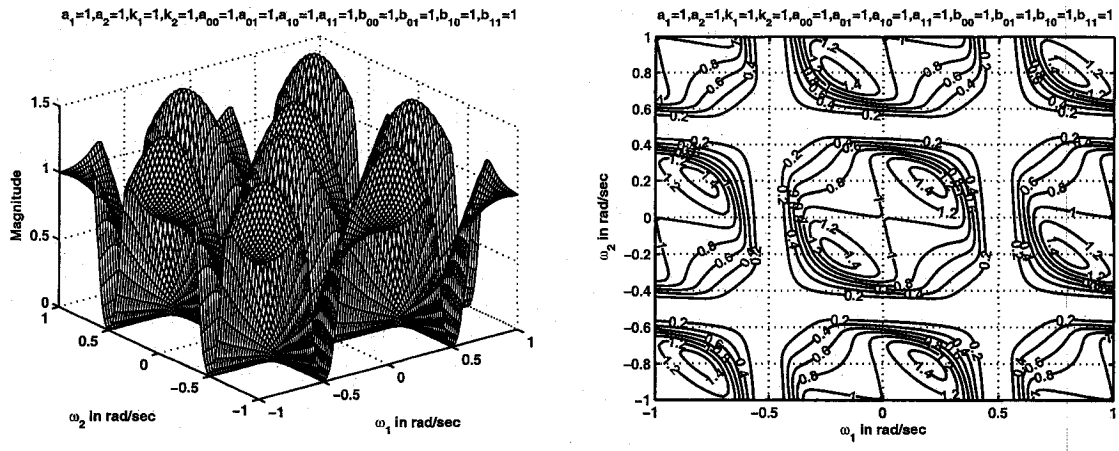

Figure 5.1: 3-D amplitude-frequency response and contour response of 2-D digital bandstop filter when all the coefficients are unity

It is observed that there are ripples in the lower and upper passband of the contour response. The ripples in the passband can be removed by reducing the values of a_1 and a_2

by a small fraction, i.e., from 1 to 0.75 as shown in Fig. 5.9 (a).

5.4.1 Frequency Response of 2-D Bandstop Filters in Set 1

In this section, we study the manner in which all the four cases in set 1 affect the frequency response behavior of the resulting 2-D bandstop filter. In this set, the values of all the coefficients of the reactance function are considered to be the same, i.e.,

$$a_{00} = a_{01} = a_{10} = a_{11} = b_{00} = b_{01} = b_{10} = b_{11} \tag{5.6}$$

Different contour plots are obtained by varying the values of a_1, a_2, k_1 and k_2.

In this set, it is observed in all the four cases that the coefficients k_1 and k_2 mainly affect the passband width and the coefficients a_1 and a_2 mainly affect the gain of the amplitude-frequency response. As k_1 and k_2 values are increased, the cut-off frequency of the lower passband decreases, the cut-off frequency of the upper passband increases and the bandwidth of the stopband of 2-D bandstop filter increases. In addition, the magnitude of the contour response also decreases. For values of k_1, $k_2 > 1$, it can be noticed that there is rounding of contour edges and hence the transition band of 2-D bandstop filter cannot be clearly defined and is less visible. As a_1 and a_2 values are increased, the magnitude of the lower and upper passband of 2-D bandstop filter increases. Also, the cut-off frequency of the lower passband decreases, the cut-off frequency of the upper passband increases and the bandwidth of the stopband of 2-D bandstop filter increases. Overall, the cut-off frequency of lower passband decreases , the cut-off frequency of the upper passband increases and the bandwidth of the stopband of 2-D bandstop filter increases when a_1, a_2, k_1 and k_2 values are increased.

5.4.1.1 Case 1

In this case,

$$a_1 = a_2 \quad , \quad k_1 \neq k_2 \quad , \quad b_1 = b_2 = 1$$

As discussed above, the coefficients k_1 and k_2 affect the passband width of 2-D bandstop filter. In Fig. 5.2 (a), (b), the cut-off frequency of lower passband decreases, the cut-off frequency of upper passband increases and the bandwidth of the stopband increases as the values of k_1 and k_2 are increased from 0.25, 0.5 to 0.5, 1 respectively for the same values of $a_1 = a_2 = 0.25$. In addition, the magnitude of the passband decreases for the same. When the values of k_1 and k_2 are greater than 1, there is rounding of contour edges and the transition band of the 2-D bandstop filter cannot be clearly defined. It is observed that the transition band is clearly marked in Figs. 5.2 (a) and (b), while the transition band is less visible in the case of Fig. 5.2 (c) and Fig. 5.3 (a), (c).

The coefficients a_1 and a_2 affect the gain of the amplitude-frequency response of 2-D bandstop filter. In Fig. 5.2 (a) and Fig. 5.3 (b) as a_1 and a_2 values are increased from 0.25 to 0.75, for the same values of $k_1 = 0.25$, $k_2 = 0.5$, the magnitude of the lower passband increases from 0.6 to 1 and the magnitude of the upper passband increases from 1 to 1.2. Also, the cut-off frequency of lower passband decreases, the cut-off frequency of upper passband increases and the bandwidth of the stopband of 2-D bandstop filter increases. It can be seen that there are ripples in the lower passband of the 2-D bandstop filters when $a_1 = a_2 \geq 0.75$ and when one or both of the k_1 and k_2 values are less than 0.5 as shown in Fig. 5.3 (b).

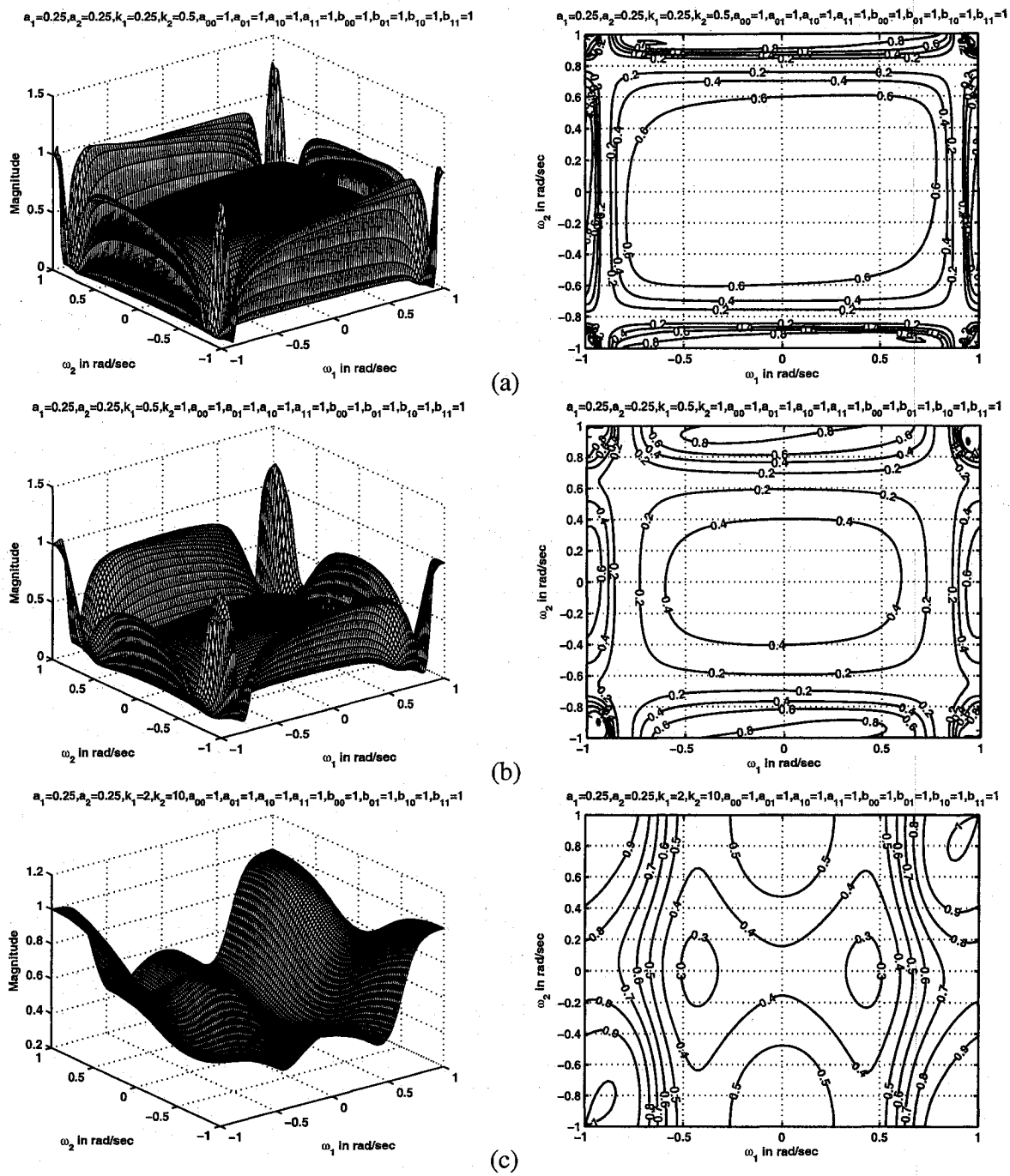

Figure 5.2: 3-D amplitude-frequency response and contour response of 2-D digital band-stop filter in case 1 of set 1 (when $a_1 = a_2 = 0.25$)

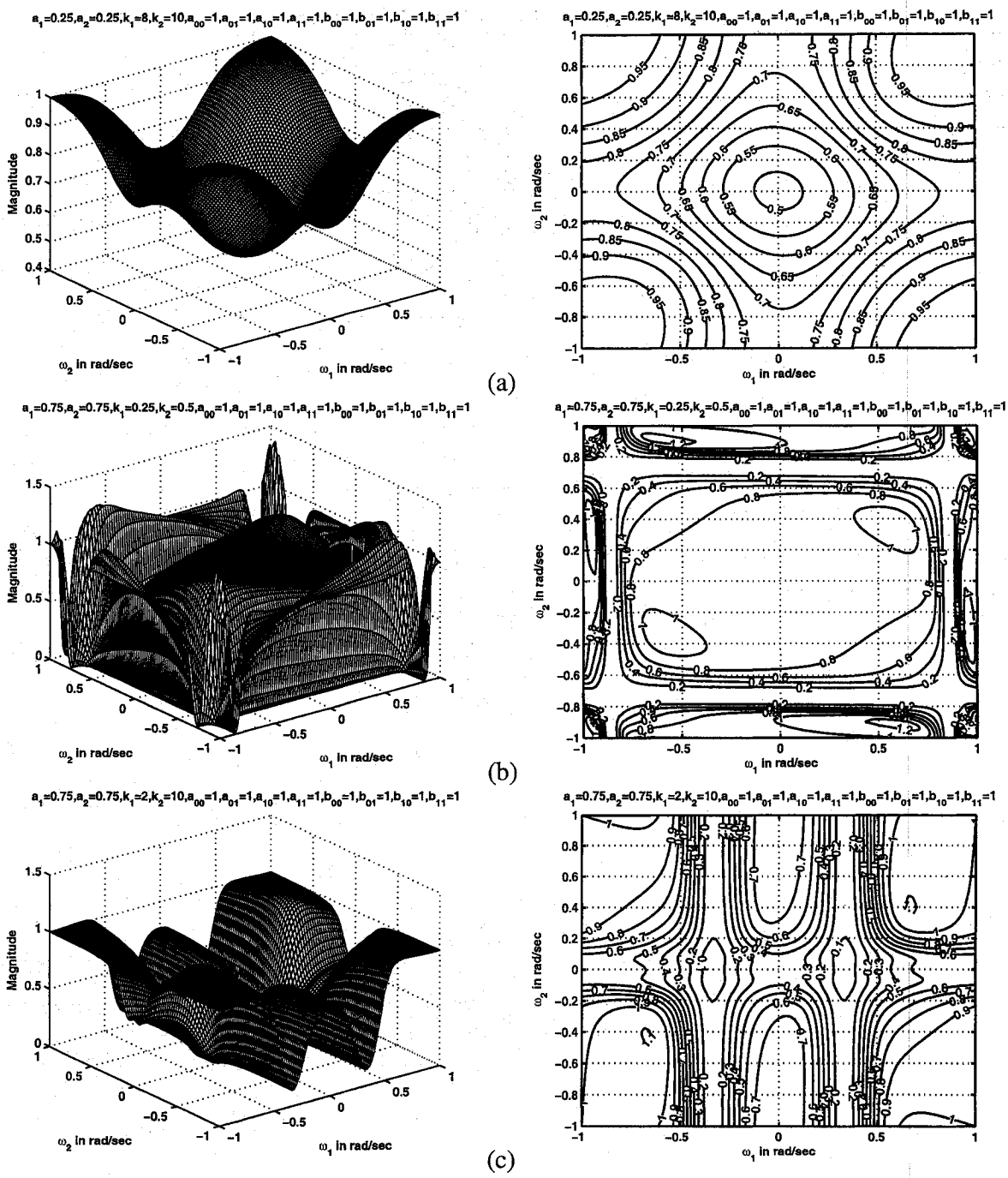

Figure 5.3: 3-D amplitude-frequency response and contour response of 2-D digital band-stop filter in case 1 of set 1 (when $a_1 = a_2 = 0.25,\ 0.75$)

5.4.1.2 Case 2

In this case,

$$a_1 \neq a_2 \quad , \quad k_1 = k_2 \quad , \quad b_1 = b_2 = 1$$

The coefficients k_1 and k_2 affect the passband width of the 2-D bandstop filter. In Fig. 5.4 (b) and Fig. 5.5 (a), the cut-off frequency of lower passband decreases, the cut-off frequency of upper passband increases and the bandwidth of the stopband increases as the values of k_1 and k_2 are increased from 0.5 to 1 for the same values of $a_1 = 0.5$, $a_2 = 0.75$. At the same time, there is also a decrease in the magnitude of the lower passband for the same. When the values of $k_1 = k_2 > 1$, there is rounding of contour edges and the transtion band of the 2-D bandstop filter cannot be clearly defined as shown in Fig. 5.5 (b), (c). This is because the outer contour of the lower passband merges with the inner contour of the upper passband of the 2-D bandstop filter. The transition band is visible for lower values of k_1 and k_2 as shown in Fig. 5.4 (a) and (b).

The coefficients a_1 and a_2 affect the gain of the amplitude-frequency response of the 2-D bandstop filter. In Fig. 5.4 (a), (b), as a_1 and a_2 values are increased from 0.25, 0.5 to 0.5, 0.75 respectively, for the same values of $k_1 = k_2 = 0.5$, the magnitude of the lower passband increases from 0.6 to 0.8. Also, the cut-off frequency of lower passband decreases, the cut-off frequency of upper passband increases and the bandwidth of the stopband of 2-D bandstop filter increases.

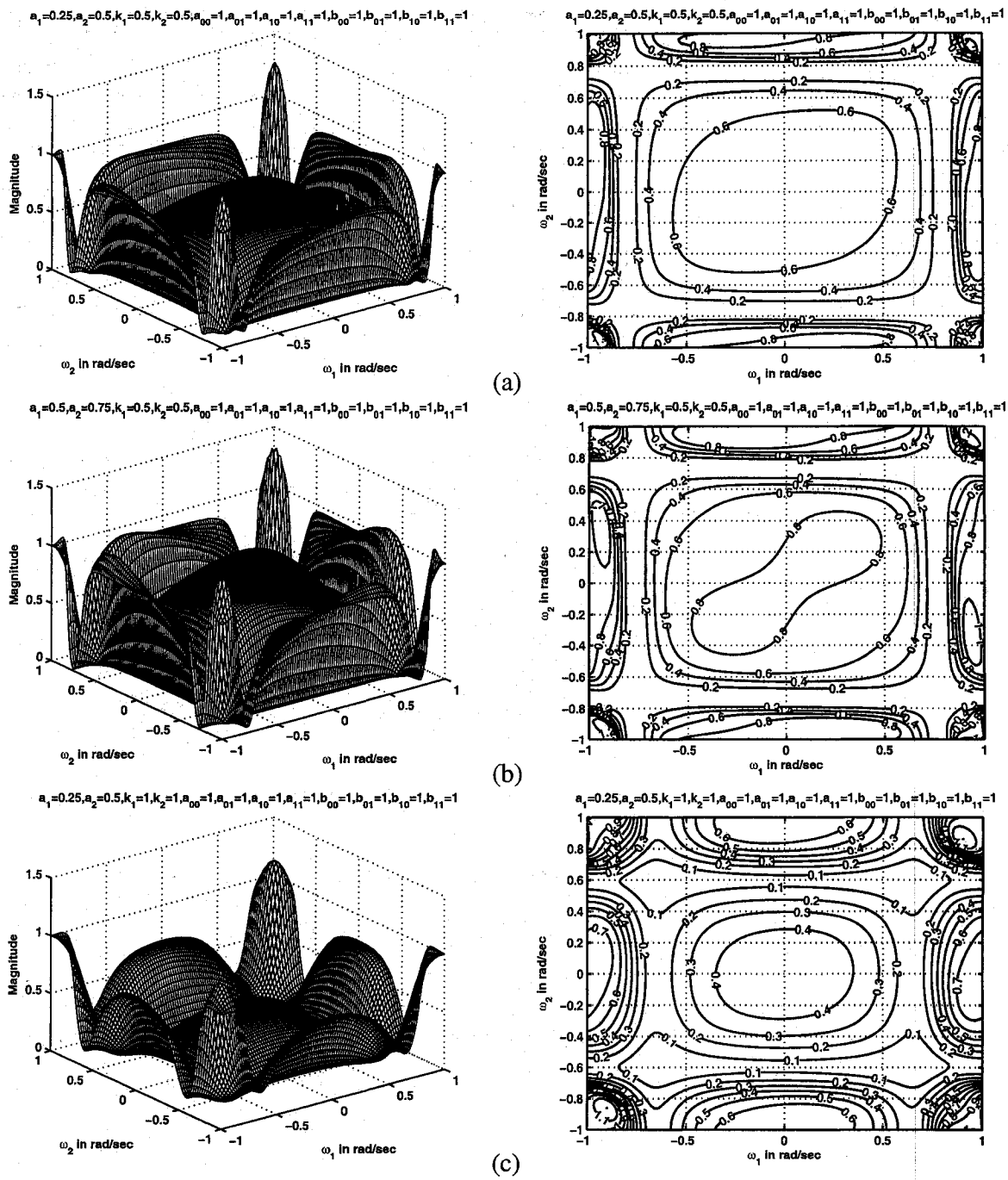

Figure 5.4: 3-D amplitude-frequency response and contour response of 2-D digital band-stop filter in case 2 of set 1 (when $k_1 = k_2 = 0.5,\ 1$)

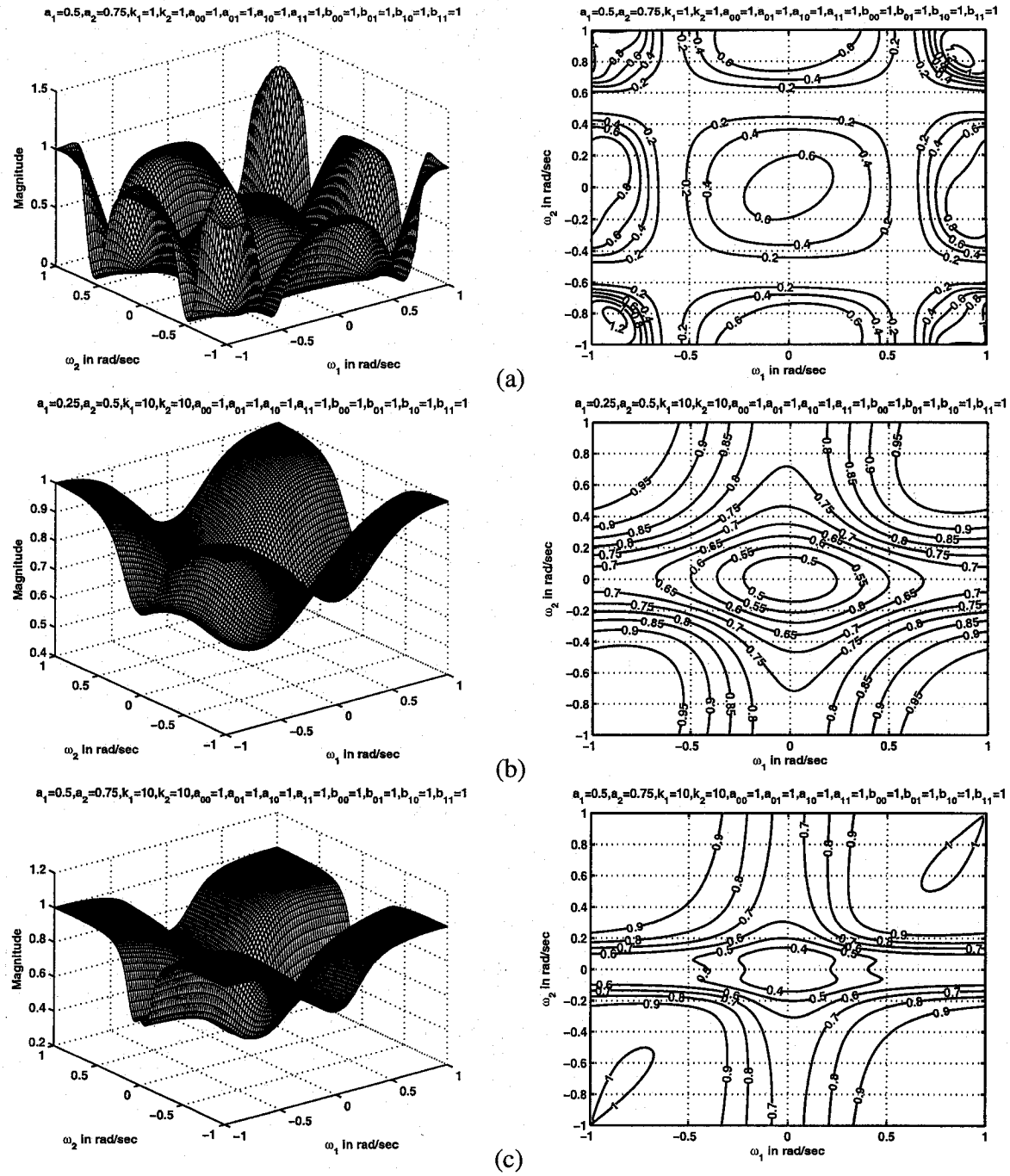

Figure 5.5: 3-D amplitude-frequency response and contour response of 2-D digital band-stop filter in case 2 of set 1 (when $k_1 = k_2 = 1,\ 10$)

5.4.1.3 Case 3

In this case,

$$a_1 \neq a_2 \quad , \quad k_1 \neq k_2 \quad , \quad b_1 = b_2 = 1$$

The coefficients k_1 and k_2 affect the passband width of the 2-D bandstop filter. As k_1 and k_2 values are increased, the cut-off frequency of lower passband decreases, the cut-off frequency of upper passband increases and the bandwidth of the stopband of 2-D bandstop filter increases. In addition, the magnitude of the contour response also decreases. For values of k_1, $k_2 > 1$, it can be noticed that there is rounding of contour edges and hence the transition band of 2-D bandstop filter cannot be clearly defined as seen in Fig. 5.6 (c) and Fig. 5.7 (a). This is because the outer contour of the lower passband merges with the inner contour of the upper passband of the 2-D bandstop filter. The transition band is visible for lower values of k_1 and k_2 as shown in Fig. 5.6 (a) and (b).

The coefficients a_1 and a_2 affect the gain of the amplitude-frequency response of the 2-D bandstop filter. In Fig. 5.6 (a), (b), as a_1 and a_2 values are increased from 0.25, 0.5 to 0.5, 0.75 respectively, for the same values of $k_1 = 0.5$, $k_2 = 1$, the magnitude of the lower and upper passband increases . Also, the cut-off frequency of lower passband decreases, the cut-off frequency of upper passband increases and the bandwidth of the stopband of 2-D bandstop filter increases.

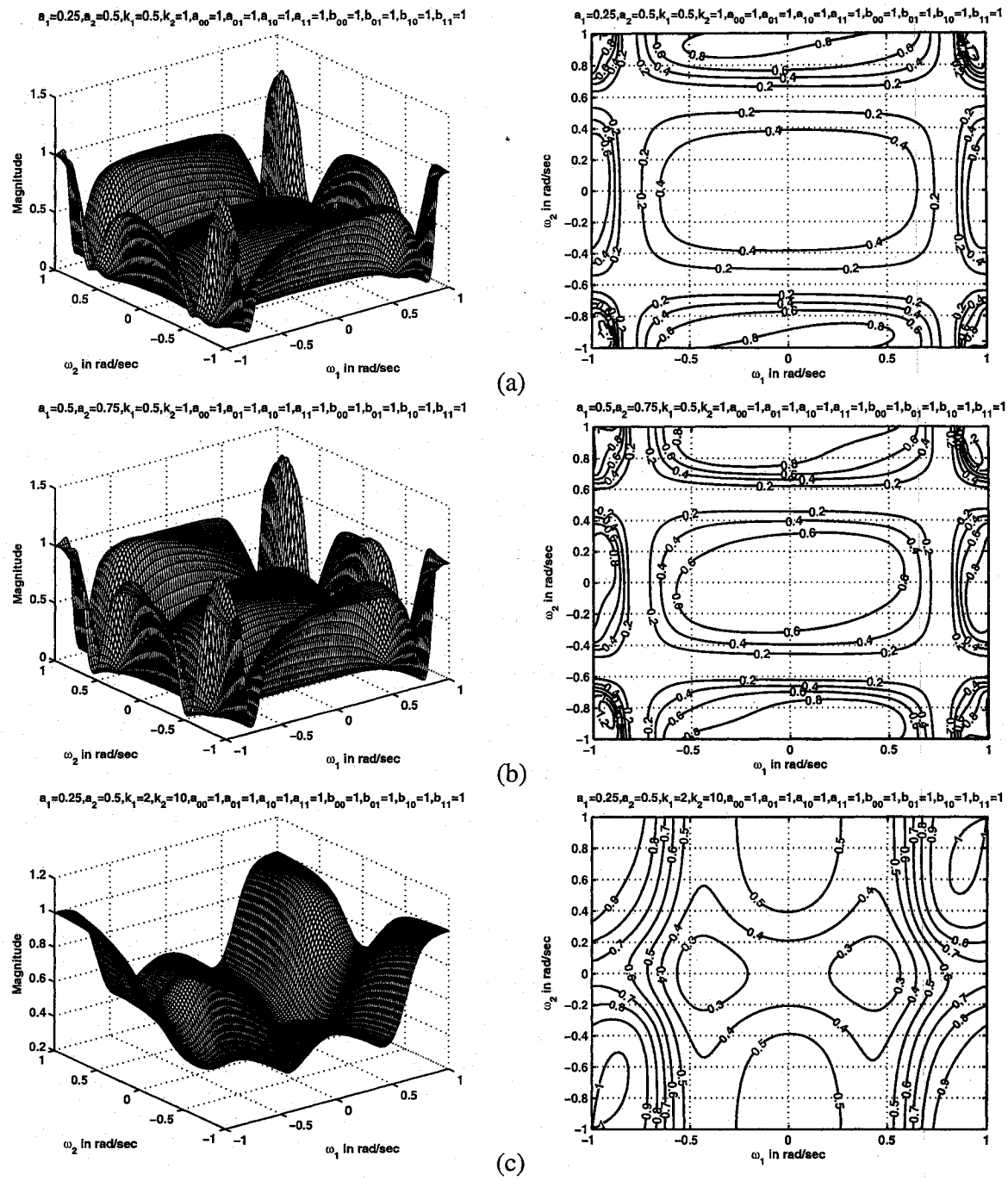

Figure 5.6: 3-D amplitude-frequency response and contour response of 2-D digital band-stop filter in case 3 of set 1 (when $k_1 = 0.5,\ 2,\ k_2 = 1,\ 10$)

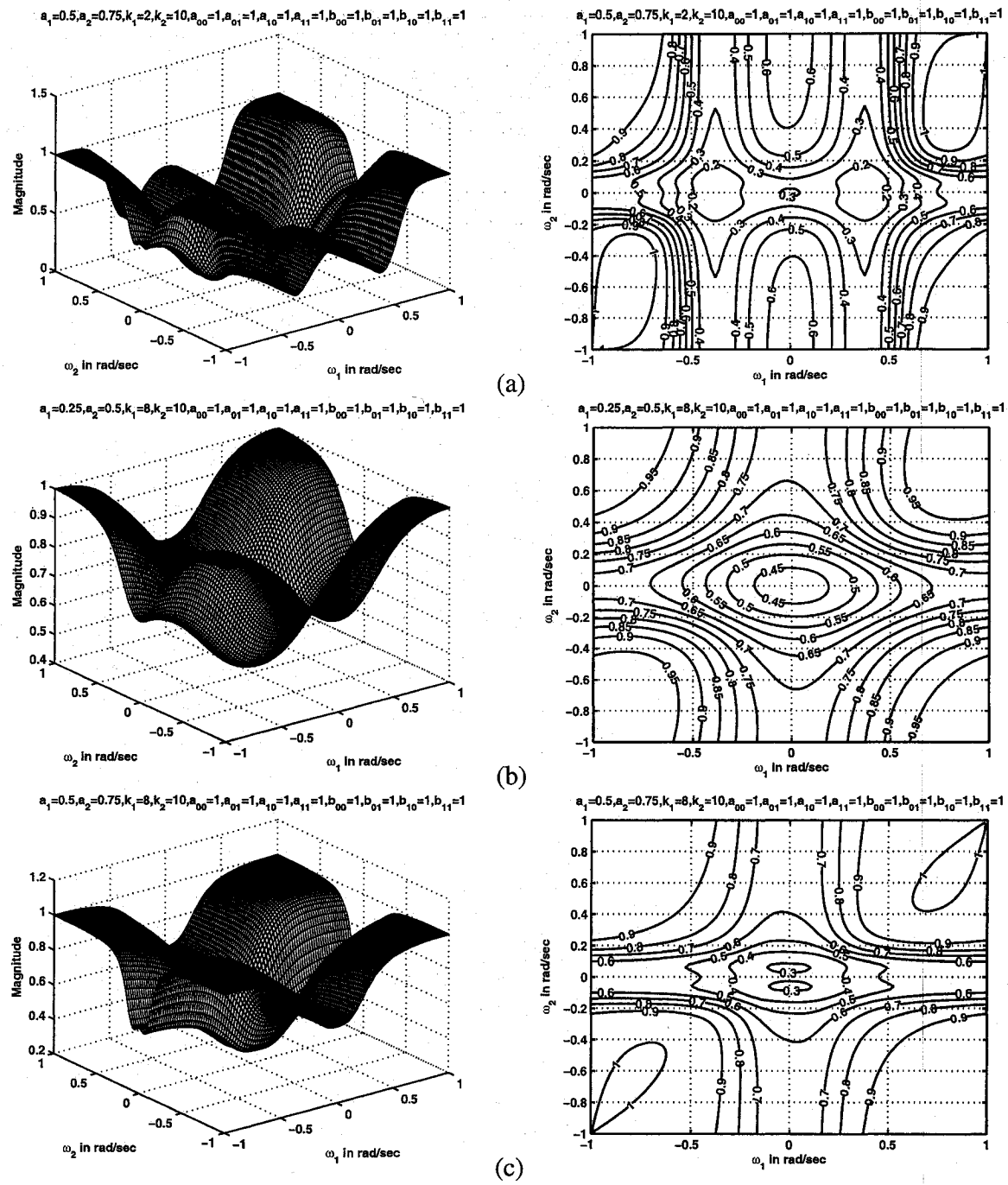

Figure 5.7: 3-D amplitude-frequency response and contour response of 2-D digital band-stop filter in case 3 of set 1 (when $k_1 = 2,\ 8,\ k_2 = 10$)

5.4.1.4 Case 4

In this case,

$$a_1 = a_2 \quad , \quad k_1 = k_2 \quad , \quad b_1 = b_2 = 1$$

The coefficients k_1 and k_2 affect the passband width of the 2-D bandstop filter. In Fig. 5.8 (b), Fig. 5.9 (a), the cut-off frequency of lower passband decreases, the cut-off frequency of upper passband increases and the bandwidth of the stopband increases as the values of k_1 and k_2 are increased from 0.5 to 1 for the same values of $a_1 = a_2 = 0.25$. At the same time, there is also a decrease in the magnitude of the lower passband for the same. When the values of $k_1 = k_2 > 1$, there is rounding of contour edges and the transition band of the 2-D bandstop filter cannot be clearly defined as shown in Fig. 5.9 (b), (c). Also in Fig. 5.8 (c), where $a_1 = a_2 = 0.25$ and $k_1 = k_2 = 1$, the stopband of the 2-D bandstop filter cannot be clearly defined because the outer contour of the lower passband merges with the inner contour of the upper passband of the 2-D bandstop filter. The transition band is visible for lower values of k_1 and k_2 as shown in Fig. 5.8 (a) and (b).

The coefficients a_1 and a_2 affect the gain of the amplitude-frequency response. In Fig. 5.8 (a), (b), as a_1 and a_2 values are increased from 0.25 to 0.75 respectively, for the same values of $k_1 = k_2 = 0.5$, the magnitude of the lower passband increases from 0.6 to 0.8. Also, the cut-off frequency of lower passband decreases, the cut-off frequency of upper passband increases and the bandwidth of the stopband of 2-D bandstop filter increases.

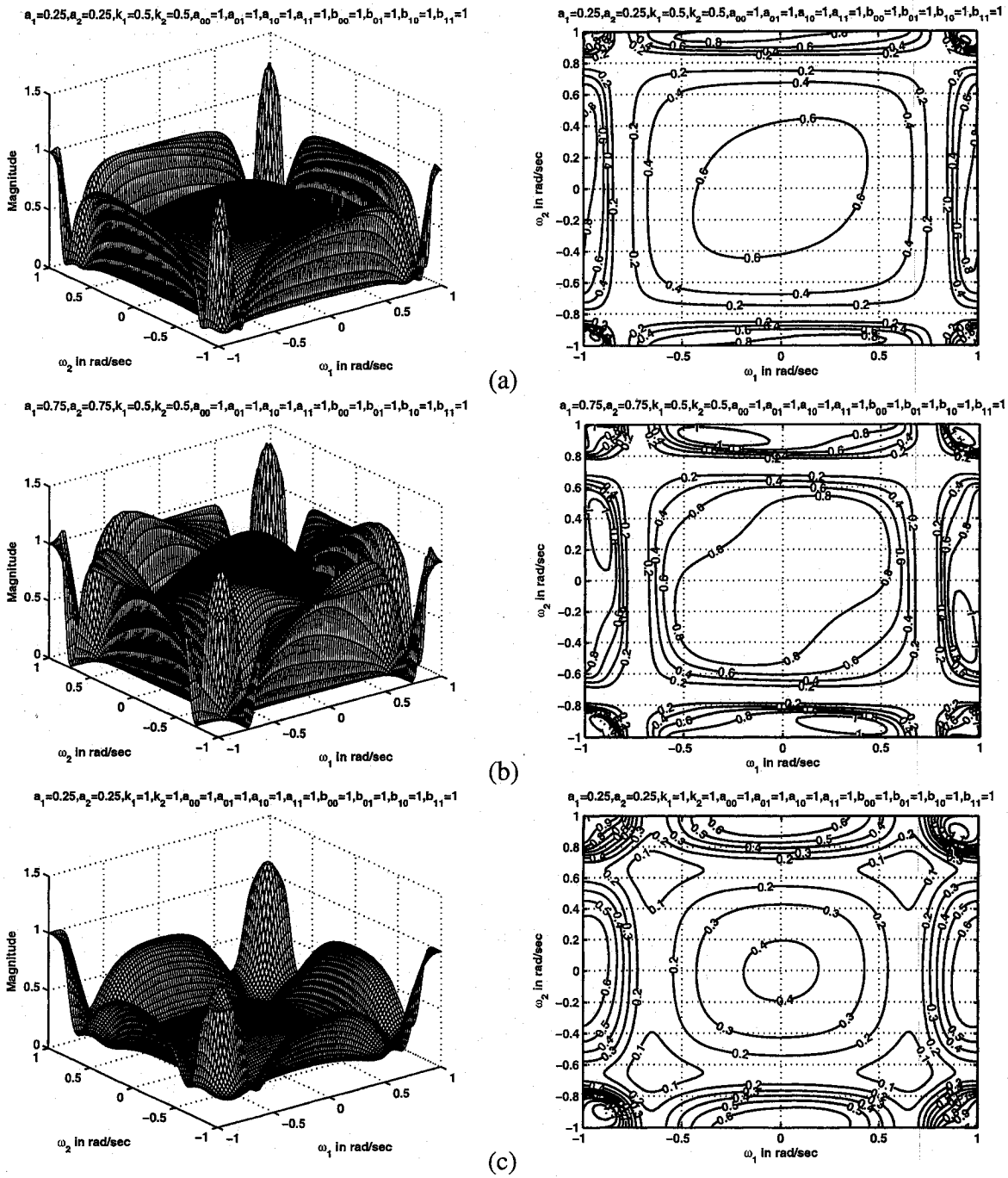

Figure 5.8: 3-D amplitude-frequency response and contour response of 2-D digital band-stop filter in case 4 of set 1 (when $k_1 = k_2 = 0.5,\ 1$)

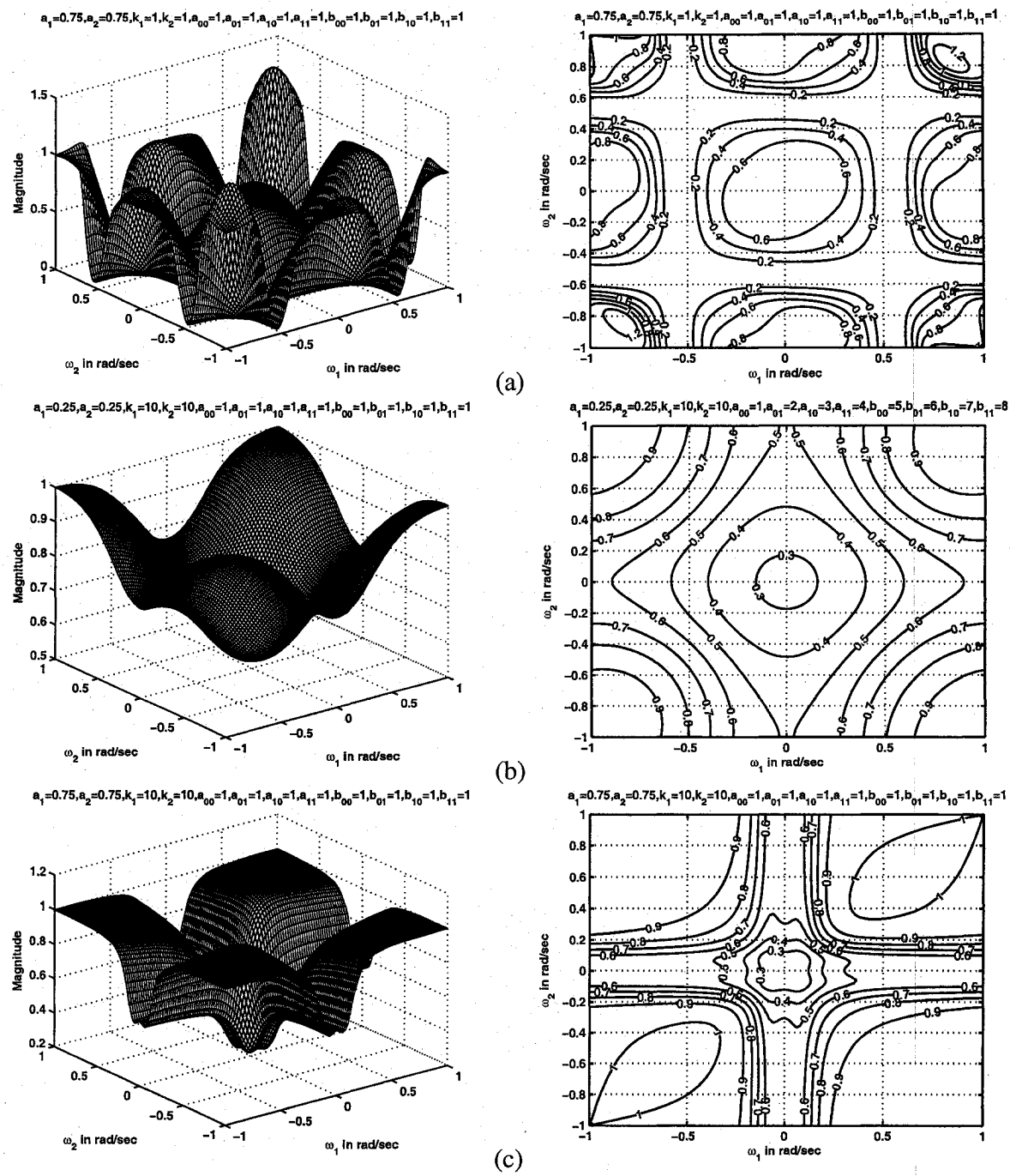

Figure 5.9: 3-D amplitude-frequency response and contour response of 2-D digital band-stop filter in case 4 of set 1 (when $k_1 = k_2 = 1,\ 10$)

5.4.2 Frequency Response of 2-D Bandstop Filters in Set 2

In this set,

$$\begin{aligned} a_{00} &= a_{01} = a_{10} = a_{11} \\ b_{00} &= b_{01} = b_{10} = b_{11} \end{aligned} \tag{5.7}$$

When the above combination of coefficients are substituted in the transfer function of 2-D bandstop filter, the resulting transfer function is the same as the one used in set 1 as the transfer function does not depend on the coefficients of the VSHP polynomial. It only depends on the coefficients of the bilinear transformation. Hence the frequency response of 2-D bandstop filters in set 2 is the same as that of set 1.

5.4.3 Frequency Response of 2-D Bandstop Filters in Set 3

In this section, we study the manner in which all the four cases in set 3 affect the frequency response behavior of the resulting 2-D bandstop filter. In this set,

$$\begin{aligned} a_{00} &= a_{11} \\ a_{01} &= a_{10} \\ b_{00} &= b_{11} \\ b_{01} &= b_{10} \end{aligned} \tag{5.8}$$

Different contour plots are obtained by varying the values of a_1, a_2, k_1 and k_2.

Similar to set 1, in set 3, it is observed in all the four cases that the coefficients k_1 and k_2 affect the passband width and the coefficients a_1 and a_2 affect the gain of the amplitude-frequency response. As k_1 and k_2 values are increased, the cut-off frequency of lower passband decreases, the cut-off frequency of upper passband increases and the bandwidth of the stopband of 2-D bandstop filter increases. In addition, the magnitude of the contour response also decreases. For values of k_1, $k_2 > 1$, it can be noticed that there is rounding of contour edges and hence the transition band of 2-D bandstop filter cannot be clearly defined

and is less visible. As a_1 and a_2 values are increased, the magnitude of the lower and upper passband of 2-D bandstop filter increases. Also, the cut-off frequency of lower passband decreases, the cut-off frequency of upper passband increases and the bandwidth of the stopband of 2-D bandstop filter increases. Overall, the lower passband width decreases, the upper passband width increases and the bandwidth of the stopband of 2-D bandstop filter increases when a_1, a_2, k_1 and k_2 values are increased.

The magnitude of the passband is low when compared to set 1 for the same values of a_1, a_2, k_1 and k_2. Otherwise, the responses are more or less similar to set 1 for all values of a_1 and a_2. There are no ripples in the contour response for all values of a_1, a_2, k_1 and k_2.

5.4.3.1 Case 1

In this case,

$$a_1 = a_2 \quad , \quad k_1 \neq k_2 \quad , \quad b_1 = b_2 = 1$$

It is observed in this case that the coefficients k_1 and k_2 affect the passband width and the coefficients a_1 and a_2 affect the gain of the amplitude-frequency response. As k_1 and k_2 values are increased, the cut-off frequency of lower passband decreases, the cut-off frequency of upper passband increases and the bandwidth of the stopband of 2-D bandstop filter increases. In addition, the magnitude of the contour response also decreases. For values of k_1, $k_2 > 1$, it can be noticed that there is rounding of contour edges and hence the transition band of 2-D bandstop filter cannot be clearly defined and is less visible. As a_1 and a_2 values are increased, the magnitude of the lower and upper passband of 2-D bandstop filter increases. Also, the cut-off frequency of lower passband decreases, the cut-off frequency of upper passband increases and the bandwidth of the stopband of 2-D bandstop filter increases.

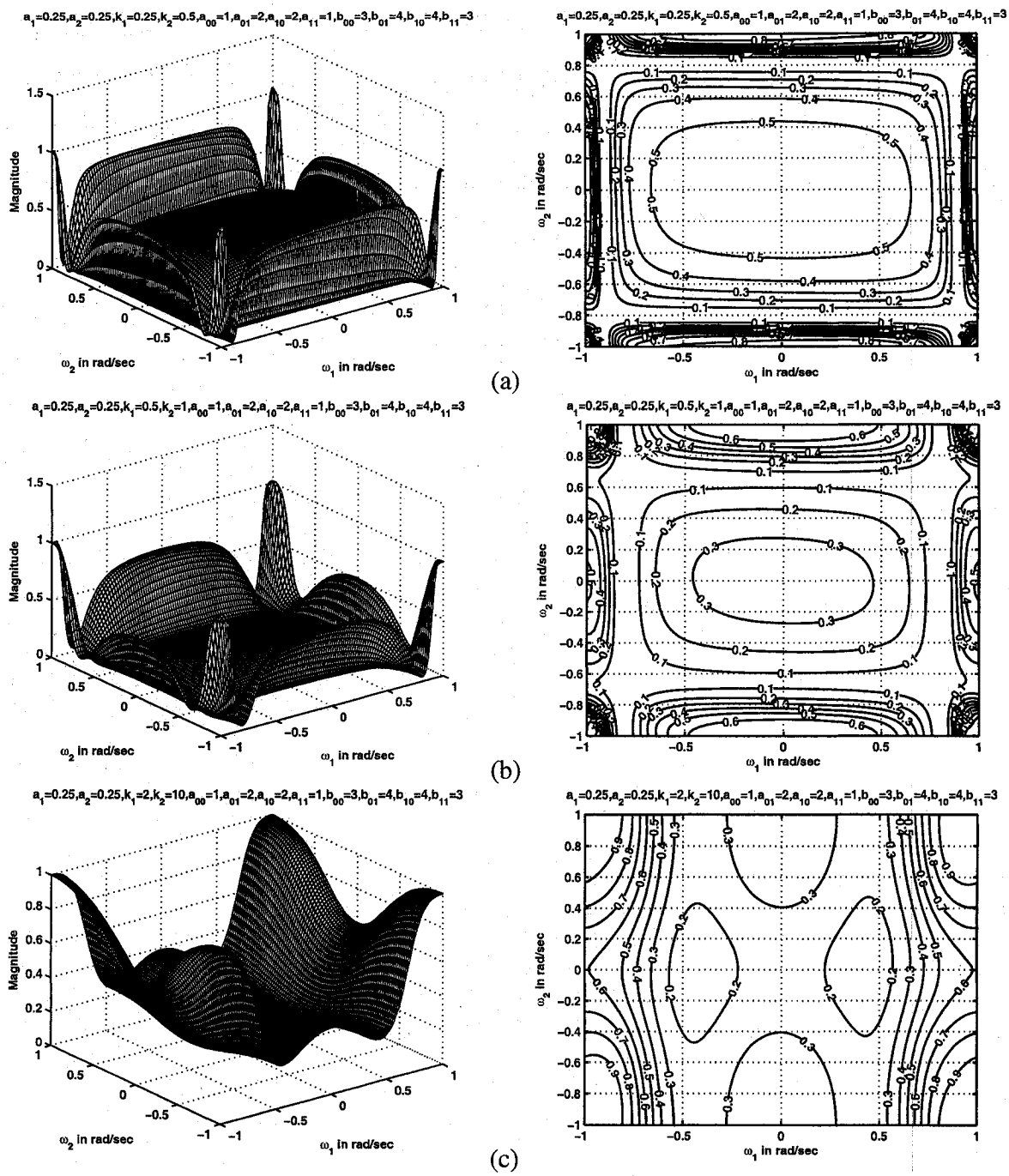

Figure 5.10: 3-D amplitude-frequency response and contour response of 2-D digital band-stop filter in case 1 of set 3 (when $a_1 = a_2 = 0.25$)

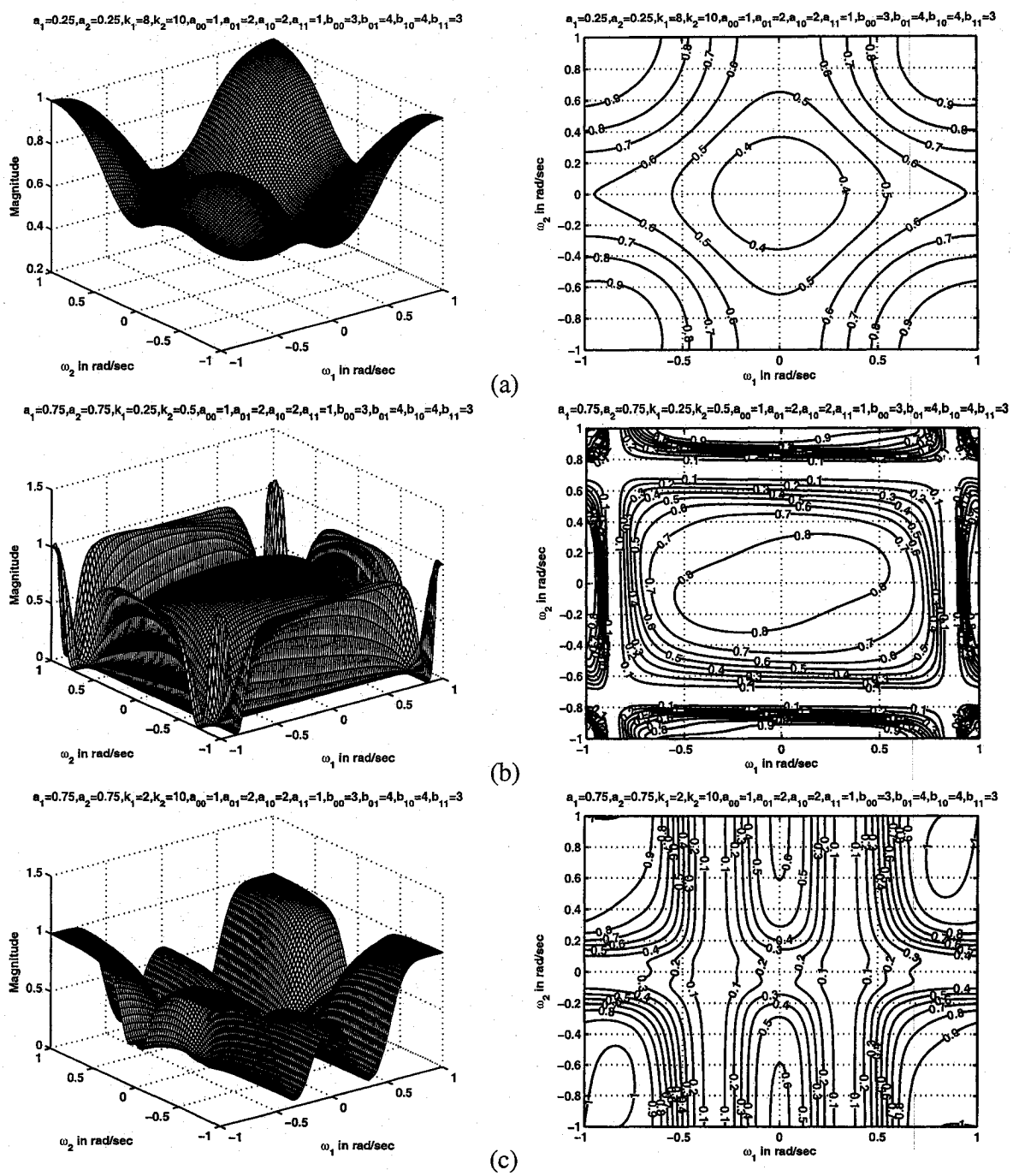

Figure 5.11: 3-D amplitude-frequency response and contour response of 2-D digital band-stop filter in case 1 of set 3 (when $a_1 = a_2 = 0.25,\ 0.75$)

The magnitude of the passband is lower than that of the contour responses in case 1 of set 1 for the same values of a_1, a_2, k_1 and k_2. The magnitude of the lower passband in Fig. 5.10 (a) is 0.5 which is lower than the magnitude in Fig. 5.2 (a) for the same values of $k_1 = 0.25$, $k_2 = 0.5$, $a_1 = a_2 = 0.25$. Unlike in set 1, there are no ripples in the contour response for higher values of a_1 and a_2. The ripples present in Fig. 5.3 (b) is absent in Fig. 5.11 (b) for the same values of a_1, a_2, k_1 and k_2.

5.4.3.2 Case 2

In this case,

$$a_1 \neq a_2 \quad , \quad k_1 = k_2 \quad , \quad b_1 = b_2 = 1$$

It is observed in this case that the coefficients k_1 and k_2 affect the passband width and the coefficients a_1 and a_2 affect the gain of the amplitude-frequency response of 2-D bandstop filter. As k_1 and k_2 values are increased, the cut-off frequency of lower passband decreases, the cut-off frequency of upper passband increases and the bandwidth of the stop-band of 2-D bandstop filter increases. In addition, the magnitude of the contour response also decreases. For values of k_1, $k_2 > 1$, it can be noticed that there is rounding of contour edges and hence the transition band of 2-D bandstop filter cannot be clearly defined and is less visible as shown in Fig. 5.13 (b) and (c). This is because the outer contour of the lower passband merges with the inner contour of the upper passband of the 2-D bandstop filter. As a_1 and a_2 values are increased, the magnitude of the lower and upper passband of 2-D bandstop filter increases. Also, the cut-off frequency of lower passband decreases, the cut-off frequency of upper passband increases and the bandwidth of the stopband of 2-D bandstop filter increases.

The magnitude of the passband is lower than that of the magnitude in case 2 of set 1 for the same values of a_1, a_2, k_1 and k_2. The magnitude of the lower passband in Fig.

5.12 (b) is 0.6 which is smaller than the magnitude in Fig. 5.4 (b) for the same values of $a_1 = 0.25$, $a_2 = 0.5$, $k_1 = k_2 = 0.5$.

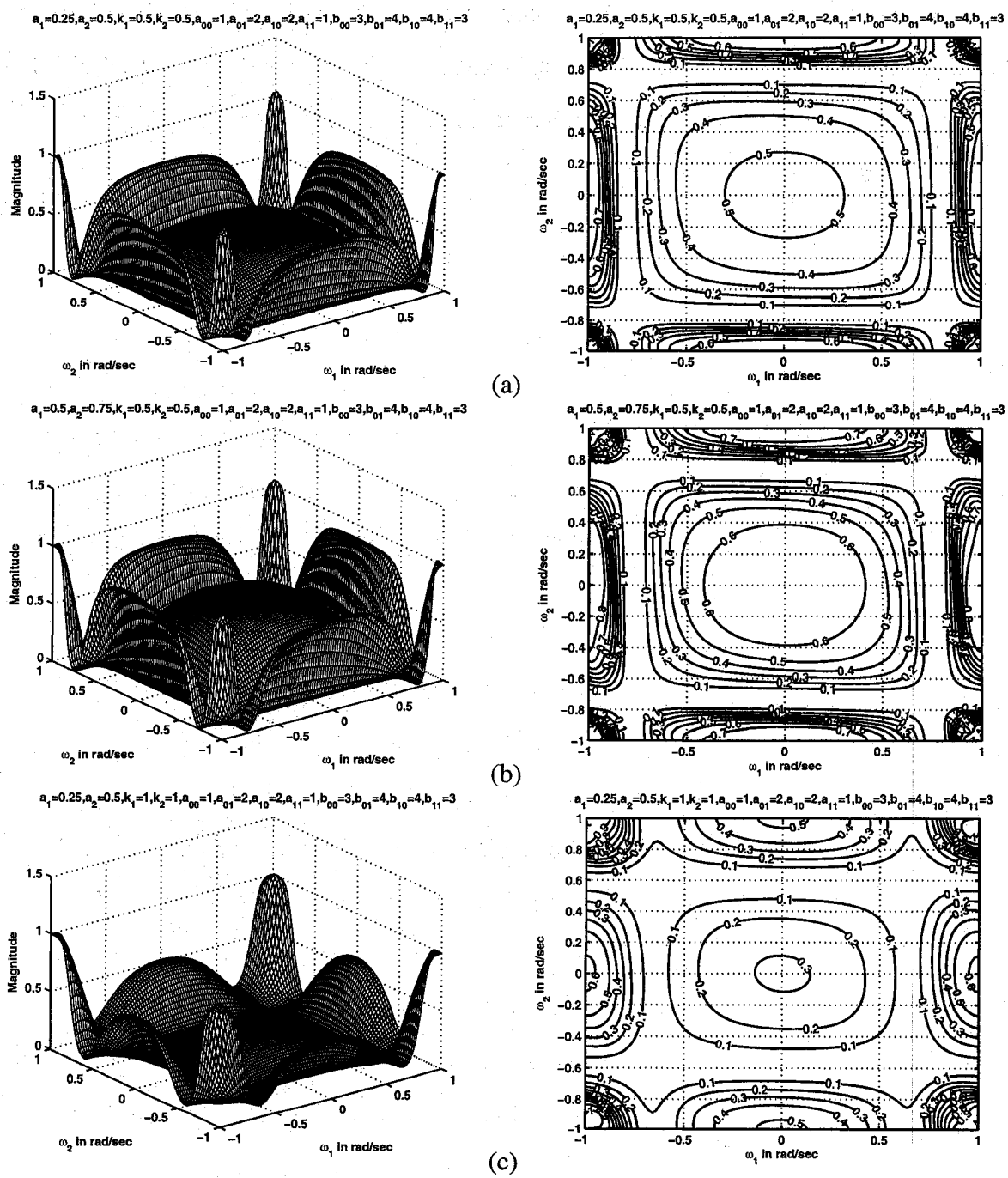

Figure 5.12: 3-D amplitude-frequency response and contour response of 2-D digital band-stop filter in case 2 of set 3 (when $k_1 = k_2 = 0.5,\ 1$)

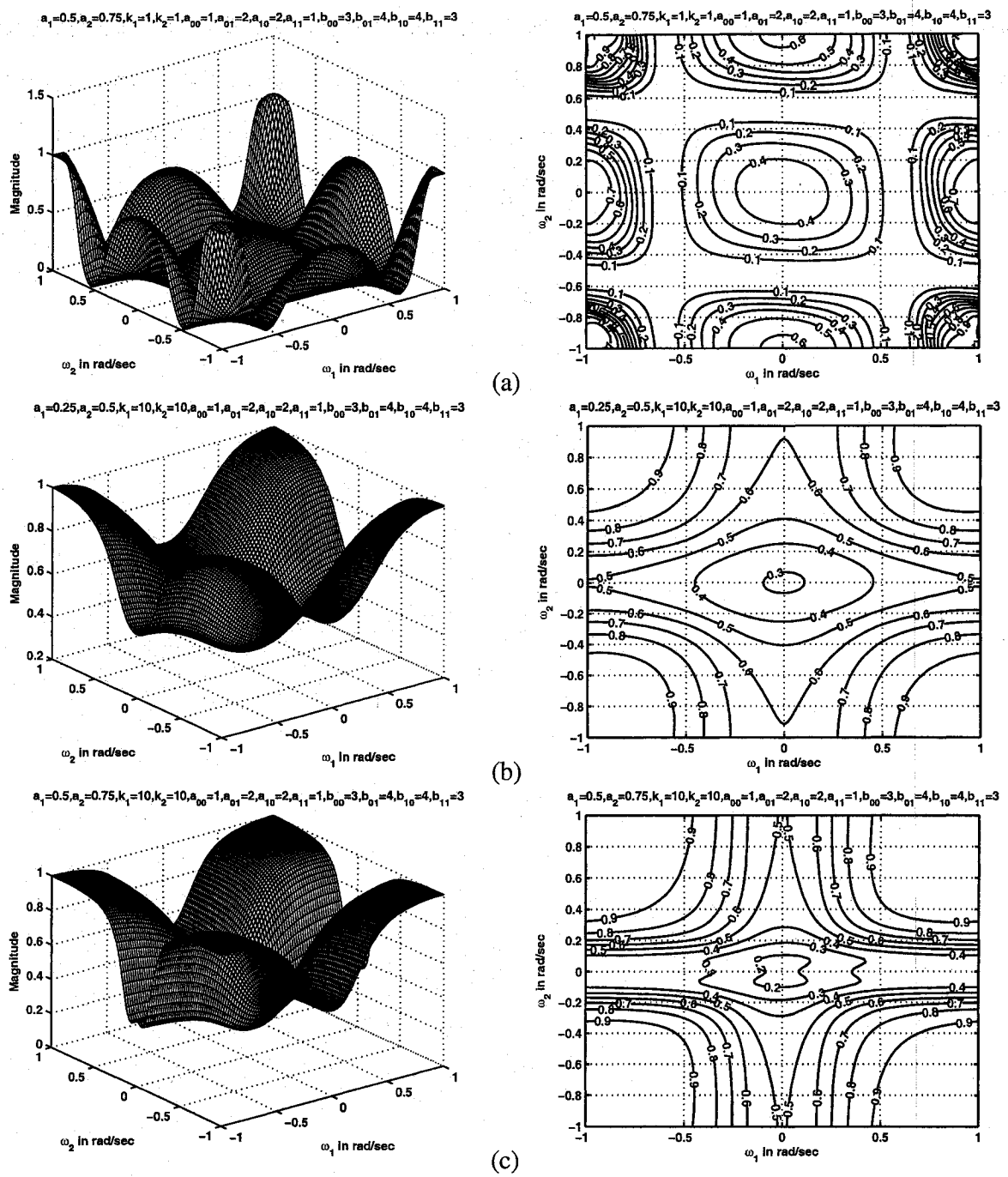

Figure 5.13: 3-D amplitude-frequency response and contour response of 2-D digital band-stop filter in case 2 of set 3 (when $k_1 = k_2 = 1,\ 10$)

5.4.3.3 Case 3

In this case,

$$a_1 \neq a_2 \quad , \quad k_1 \neq k_2 \quad , \quad b_1 = b_2 = 1$$

It is observed in this case that the coefficients k_1 and k_2 affect the passband width and a_1 and a_2 affect the gain of the amplitude-frequency response. As k_1 and k_2 values are increased, the cut-off frequency of lower passband decreases, the cut-off frequency of upper passband increases and the bandwidth of the stopband of 2-D bandstop filter increases. In addition, the magnitude of the contour response also decreases. For values of k_1, $k_2 > 1$, it can be noticed that there is rounding of contour edges and hence the transition band of 2-D bandstop filter cannot be clearly defined and is less visible as shown in Fig. 5.15 (b) and (c). This is because the outer contour of the lower passband merges with the inner contour of the upper passband of the 2-D bandstop filter. As a_1 and a_2 values are increased, the magnitude of the lower and upper passband of 2-D bandstop filter increases. Also, the cut-off frequency of lower passband decreases, the cut-off frequency of upper passband increases and the bandwidth of the stopband of 2-D bandstop filter increases.

The magnitude of the passband is lower than that of the magnitude in case 3 of set 1 for the same values of a_1, a_2, k_1 and k_2. For example, the magnitude of the passband in Fig. 5.14 (b) is smaller than the magnitude of the passband in Fig. 5.6 (b) for the same values of $k_1 = 0.5$, $k_2 = 1$, $a_1 = 0.25$, $a_2 = 0.5$.

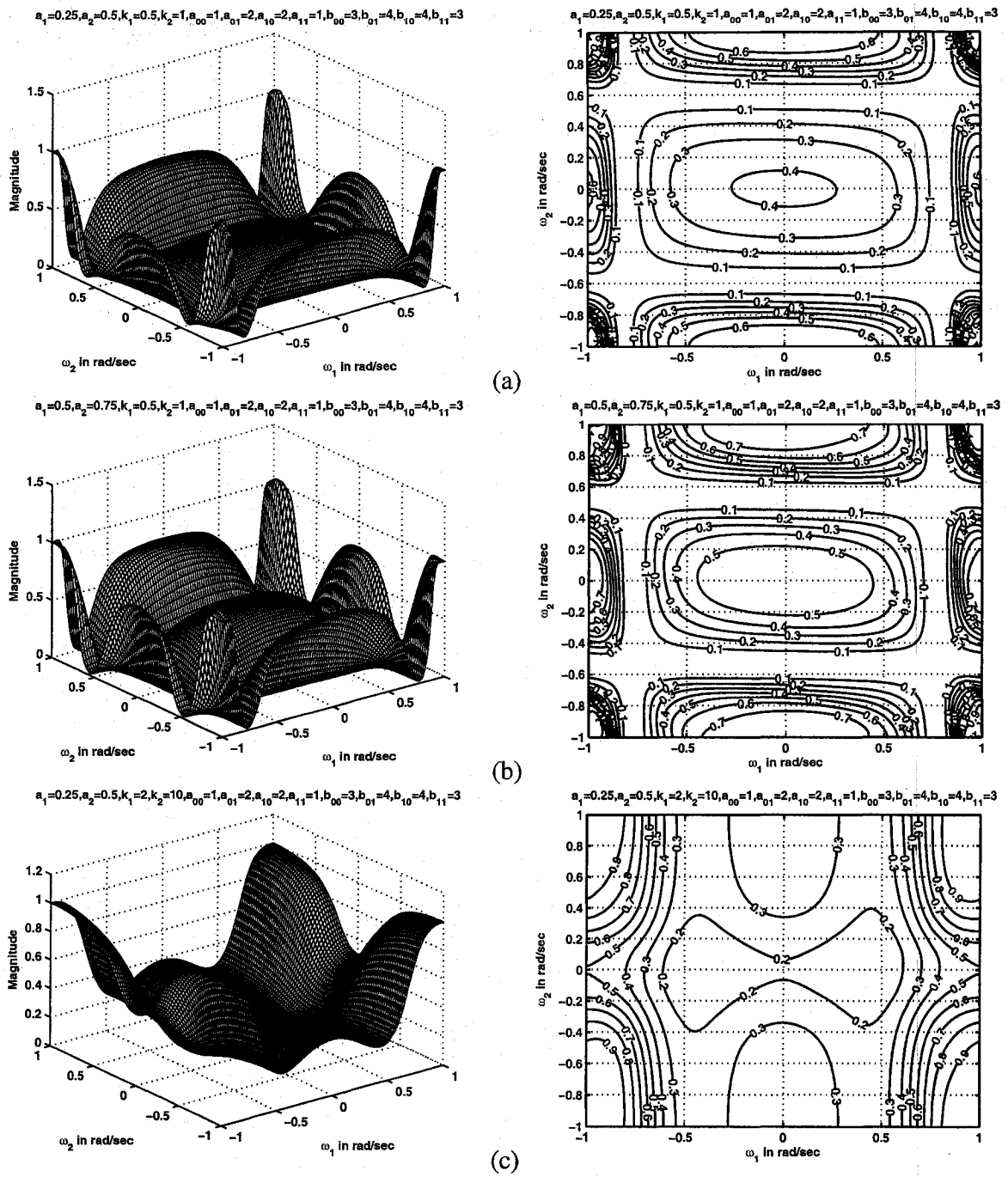

Figure 5.14: 3-D amplitude-frequency response and contour response of 2-D digital band-stop filter in case 3 of set 3 (when $k_1 = 0.5,\ 2,\ k_2 = 1,\ 10$)

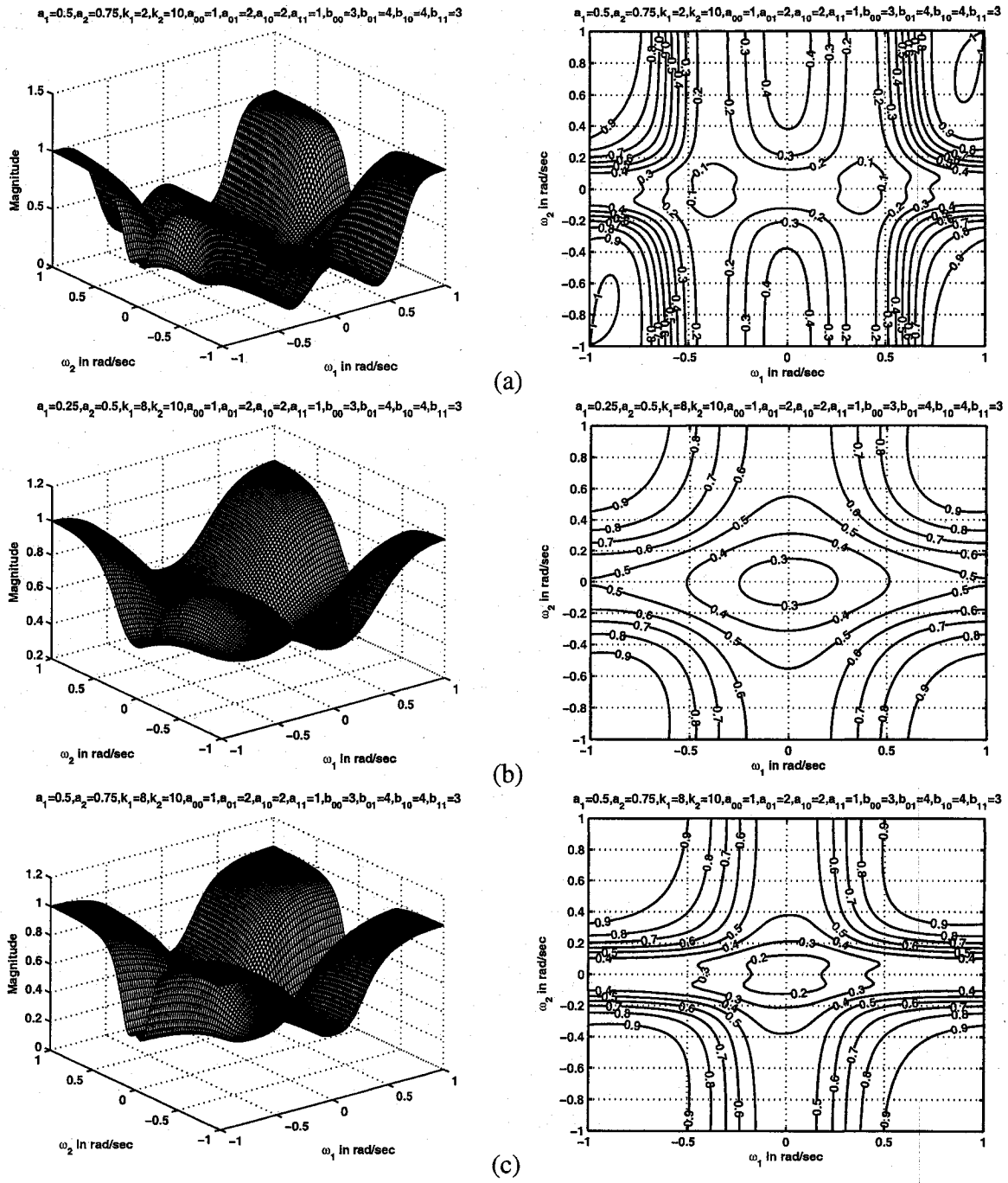

Figure 5.15: 3-D amplitude-frequency response and contour response of 2-D digital band-stop filter in case 3 of set 3 (when $k_1 = 2,\ 8,\ k_2 = 10$)

5.4.3.4 Case 4

In this case,

$$a_1 = a_2 \qquad k_1 = k_2 \qquad b_1 = b_2 = 1$$

It is observed in this case that the coefficients k_1 and k_2 affect the passband width and a_1 and a_2 affect the gain of the amplitude-frequency response. As k_1 and k_2 values are increased, the cut-off frequency of lower passband decreases, the cut-off frequency of upper passband increases and the bandwidth of the stopband of 2-D bandstop filter increases. In addition, the magnitude of the contour response also decreases. For values of k_1, $k_2 > 1$, it can be noticed that there is rounding of contour edges and hence the transition band of 2-D bandstop filter cannot be clearly defined and is less visible. Also, in Fig. 5.16 (c), where $a_1 = a_2 = 0.25$ and $k_1 = k_2 = 1$, the stopband of the 2-D bandstop filter cannot be clearly defined because the outer contour of the lower passband merges with the inner contour of the upper passband of the 2-D bandstop filter. As a_1 and a_2 values are increased, the magnitude of the lower and upper passband of 2-D bandstop filter increases. Also, the cut-off frequency of lower passband decreases, the cut-off frequency of upper passband increases and the bandwidth of the stopband of 2-D bandstop filter increases.

The magnitude of the passband is lower than that of the magnitude in case 4 of set 1 for the same values of a_1, a_2, k_1 and k_2. The magnitude of the lower passband in Fig. 5.16 (a) is 0.4 which is smaller than the magnitude of the lower passband in Fig. 5.8 (a) for the same values of $k_1 = k_2 = 0.5$, $a_1 = a_2 = 0.25$.

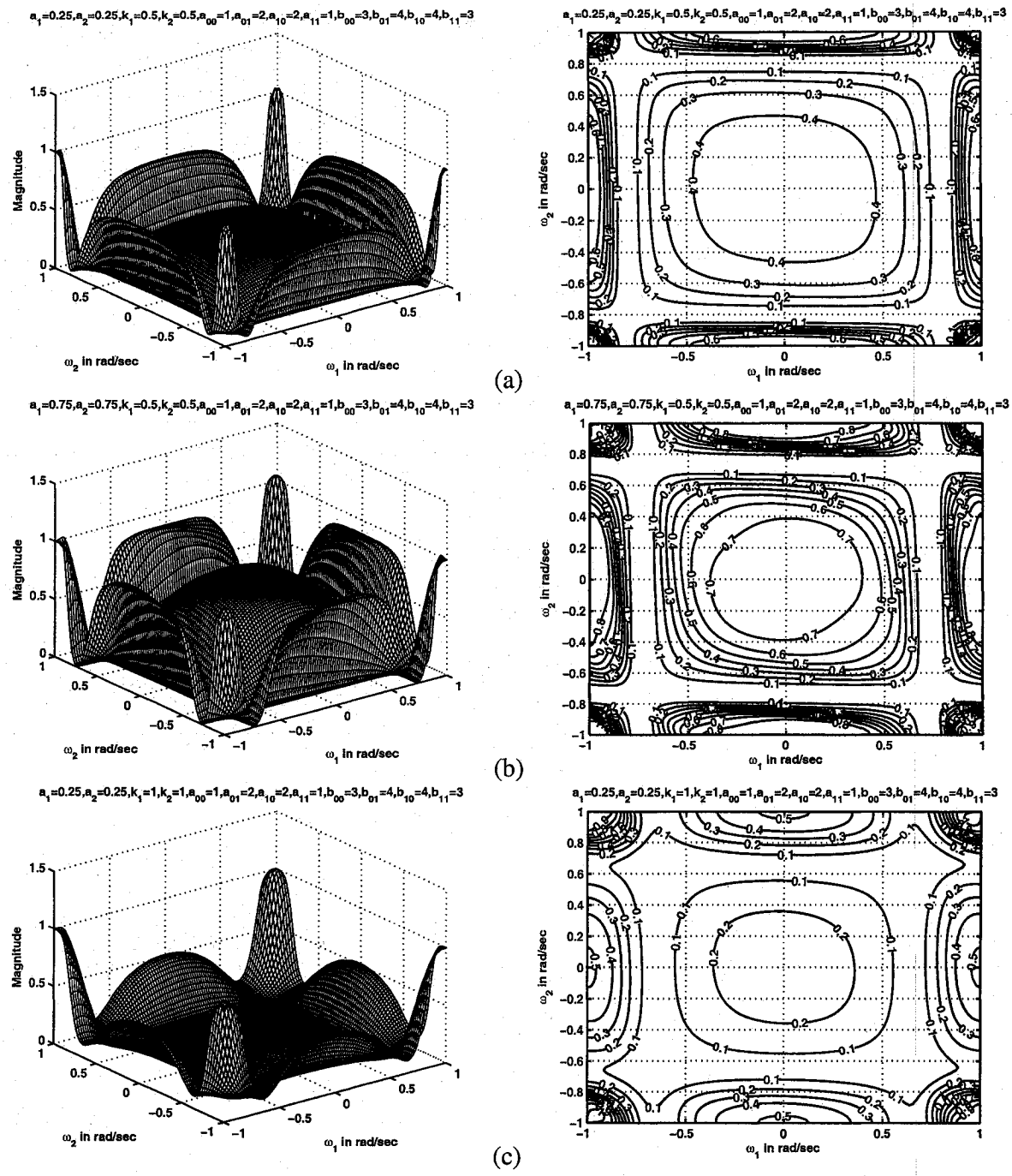

Figure 5.16: 3-D amplitude-frequency response and contour response of 2-D digital band-stop filter in case 4 of set 3 (when $k_1 = k_2 = 0.5,\ 1$)

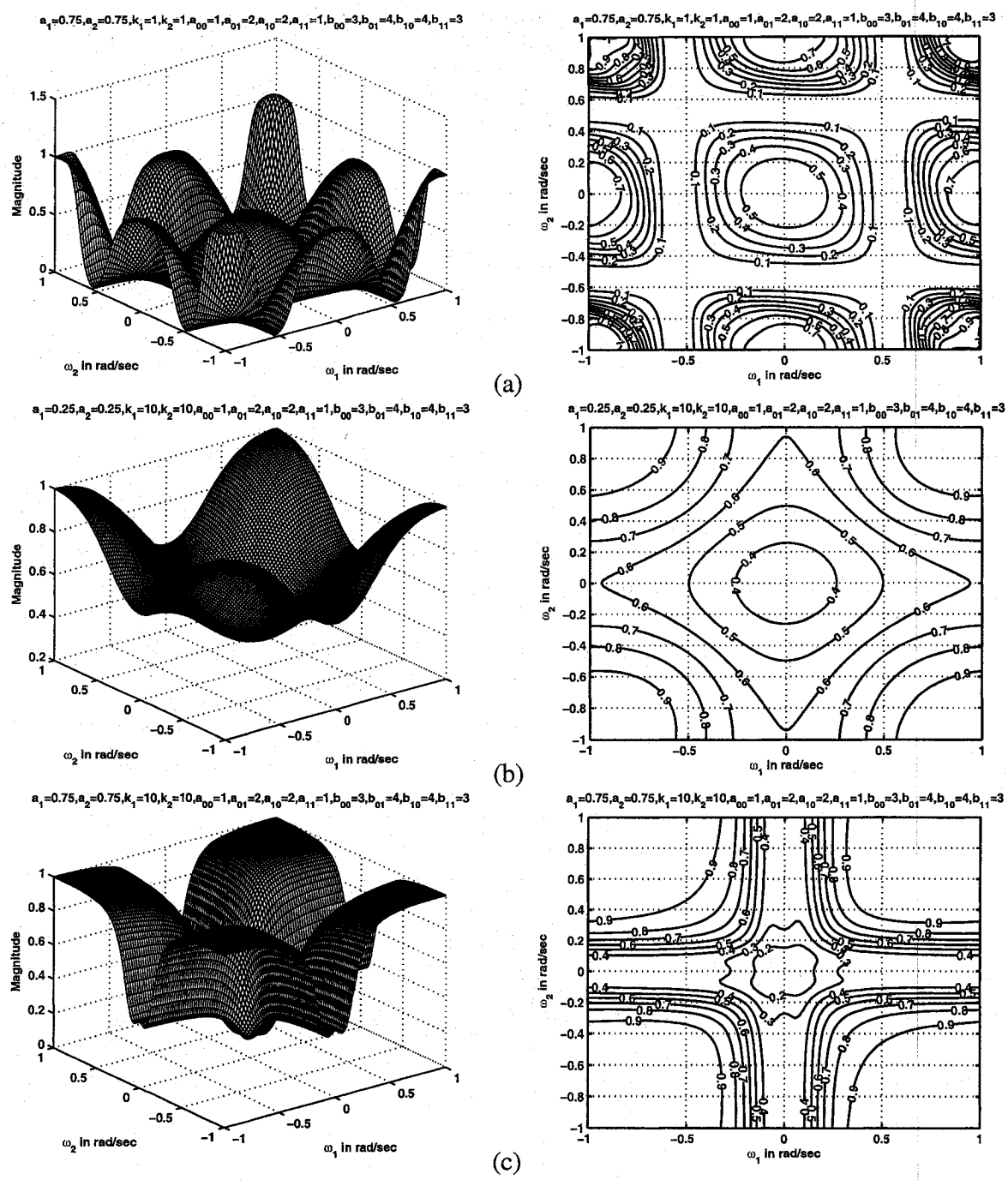

Figure 5.17: 3-D amplitude-frequency response and contour response of 2-D digital band-stop filter in case 4 of set 3 (when $k_1 = k_2 = 1,\ 10$)

5.4.4 Frequency Response of 2-D Bandstop Filters in Set 4

In this section, we study the manner in which all the four cases in set 4 affect the frequency response behavior of the resulting 2-D bandstop filter.In this set,

$$a_{00} \neq a_{01} \neq a_{10} \neq a_{11} \neq b_{00} \neq b_{01} \neq b_{10} \neq b_{11} \tag{5.9}$$

Different contour plots are obtained by varying the values of a_1, a_2, k_1 and k_2.

Similar to set 3, in set 4, it is observed in all the four cases that the coefficients k_1 and k_2 affect the passband width and the coefficients a_1 and a_2 affect the gain of the amplitude-frequency response. As k_1 and k_2 values are increased, the cut-off frequency of lower passband decreases, the cut-off frequency of upper passband increases and the bandwidth of the stopband of 2-D bandstop filter increases. In addition, the magnitude of the contour response also decreases. For values of k_1, $k_2 > 1$, it can be noticed that there is rounding of contour edges and hence the transition band of 2-D bandstop filter cannot be clearly defined and is less visible. As a_1 and a_2 values are increased, the magnitude of the lower and upper passband of 2-D bandstop filter increases. Also, the cut-off frequency of lower passband decreases, the cut-off frequency of upper passband increases and the bandwidth of the stopband of 2-D bandstop filter increases. Overall, the cut-off frequency of lower passband decreases , the cut-off frequency of upper passband increases and the bandwidth of the stopband of 2-D bandstop filter increases when a_1, a_2, k_1 and k_2 values are increased.

In set 4, the magnitude of the passband is smaller in the contour responses when compared to that of set 3 for the same values of a_1, a_2, k_1 and k_2.

5.4.4.1 Case 1

In this case,

$$a_1 = a_2 \quad , \quad k_1 \neq k_2 \quad , \quad b_1 = b_2 = 1$$

It is observed in this case that the coefficients k_1 and k_2 affect the passband width and a_1 and a_2 affect the gain of the amplitude-frequency response. As k_1 and k_2 values are increased, the cut-off frequency of lower passband decreases, the cut-off frequency of upper passband increases and the bandwidth of the stopband of 2-D bandstop filter increases. In addition, the magnitude of the contour response also decreases. For values of k_1, $k_2 > 1$, it can be noticed that there is rounding of contour edges and hence the transition band of 2-D bandstop filter cannot be clearly defined. This is because the outer contour of the lower passband merges with the inner contour of the upper passband of the 2-D bandstop filter. As a_1 and a_2 values are increased, the magnitude of the lower and upper passband of 2-D bandstop filter increases. Also, the cut-off frequency of lower passband decreases, the cut-off frequency of upper passband increases and the bandwidth of the stopband of 2-D bandstop filter increases.

In this case, the magnitude of the passband is lower than that of the contour responses in case 1 of set 3 for the same values of a_1, a_2, k_1 and k_2. The magnitude of the lower passband in Fig. 5.18 (b) is 0.2 which is lower than the magnitude of the lower passband in Fig. 5.10 (b) for the same values of $k_1 = 0.5$, $k_2 = 1$, $a_1 = a_2 = 0.25$.

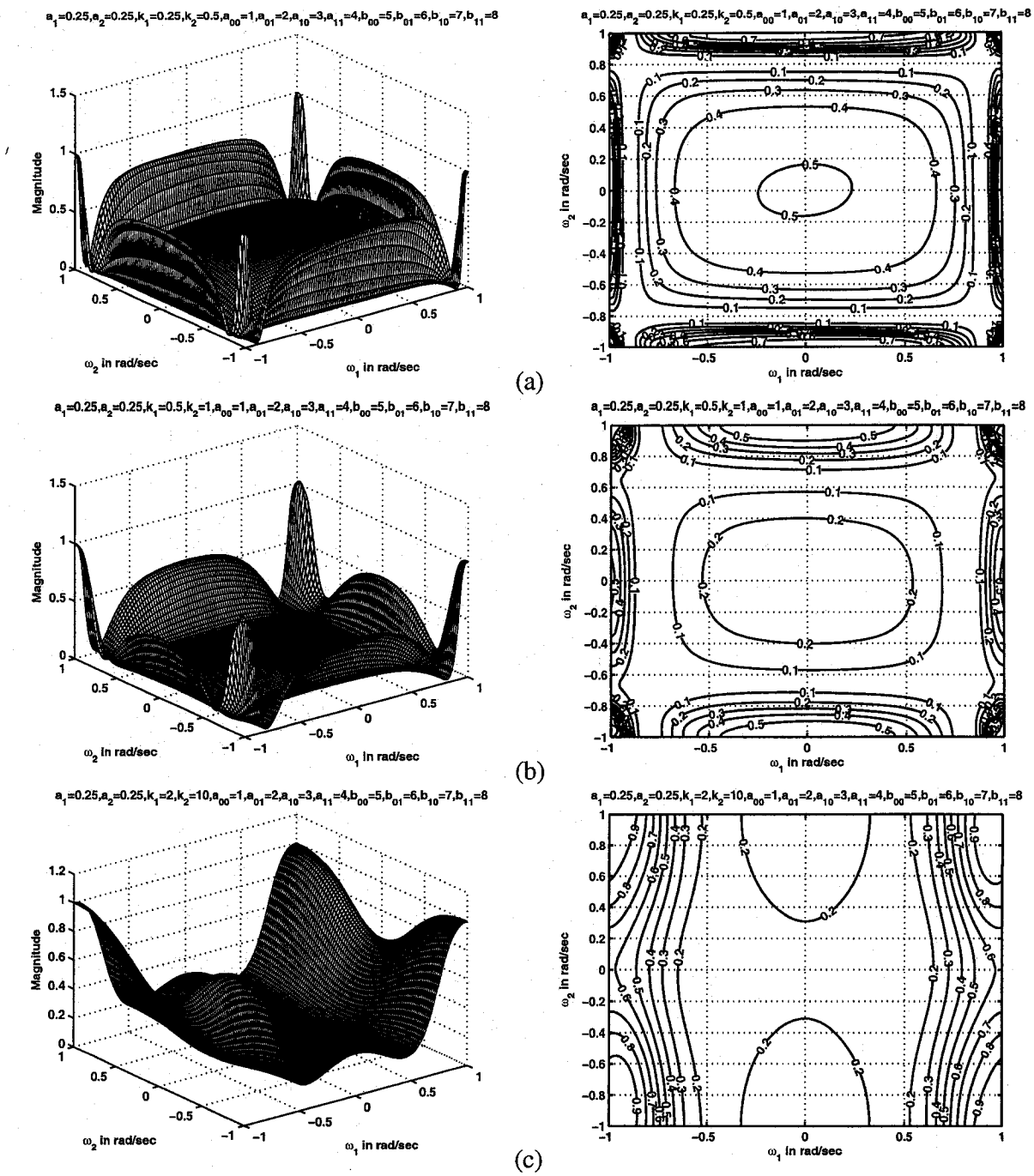

Figure 5.18: 3-D amplitude-frequency response and contour response of 2-D digital band-stop filter in case 1 of set 4 (when $a_1 = a_2 = 0.25$)

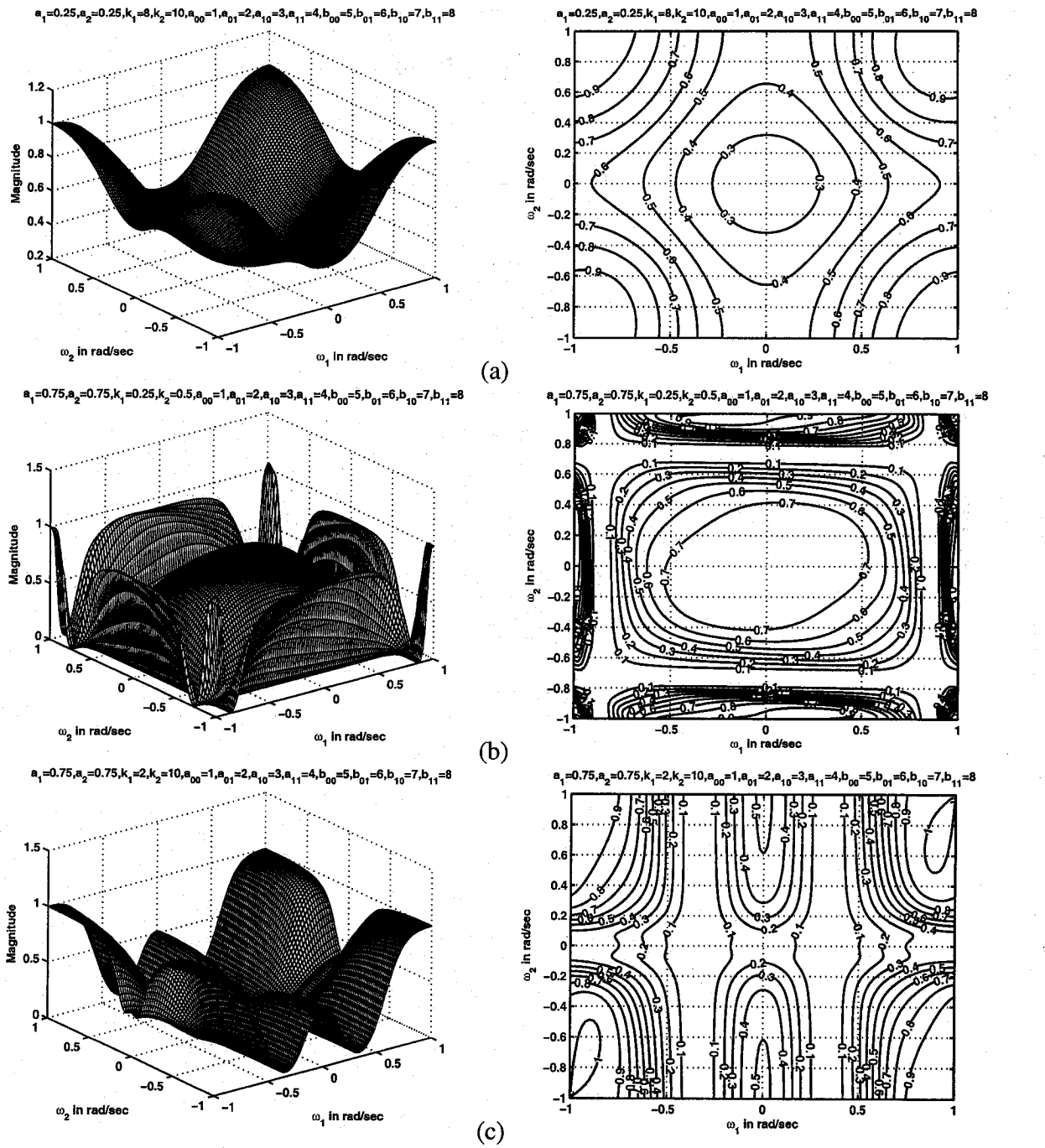

Figure 5.19: 3-D amplitude-frequency response and contour response of 2-D digital band-stop filter in case 1 of set 4 (when $a_1 = a_2 = 0.25,\ 0.75$)

5.4.4.2 Case 2

In this case,

$$a_1 \neq a_2 \quad , \quad k_1 = k_2 \quad , \quad b_1 = b_2 = 1$$

It is observed in this case that the coefficients k_1 and k_2 affect the passband width and the coefficients a_1 and a_2 affect the gain of the amplitude-frequency response. As k_1 and k_2 values are increased, the cut-off frequency of lower passband decreases, the cut-off frequency of upper passband increases and the bandwidth of the stopband of 2-D bandstop filter increases. In addition, the magnitude of the contour response also decreases. For values of k_1, $k_2 > 1$, it can be noticed that there is rounding of contour edges and hence the transition band of 2-D bandstop filter cannot be clearly defined. This is because the outer contour of the lower passband merges with the inner contour of the upper passband of the 2-D bandstop filter. As a_1 and a_2 values are increased, the magnitude of the lower and upper passband of 2-D bandstop filter increases. Also, the cut-off frequency of lower passband decreases, the cut-off frequency of upper passband increases and the bandwidth of the stopband of 2-D bandstop filter increases.

The magnitude of the passband is lower than that of the magnitude in case 2 of set 3 for the same values of a_1, a_2, k_1 and k_2. The magnitude of the lower passband in Fig. 5.20 (a) is 0.4 which is smaller than the magnitude of the lower passband in Fig. 5.12 (a) for the same values of $a_1 = 0.25$, $a_2 = 0.5$, $k_1 = k_2 = 0.5$.

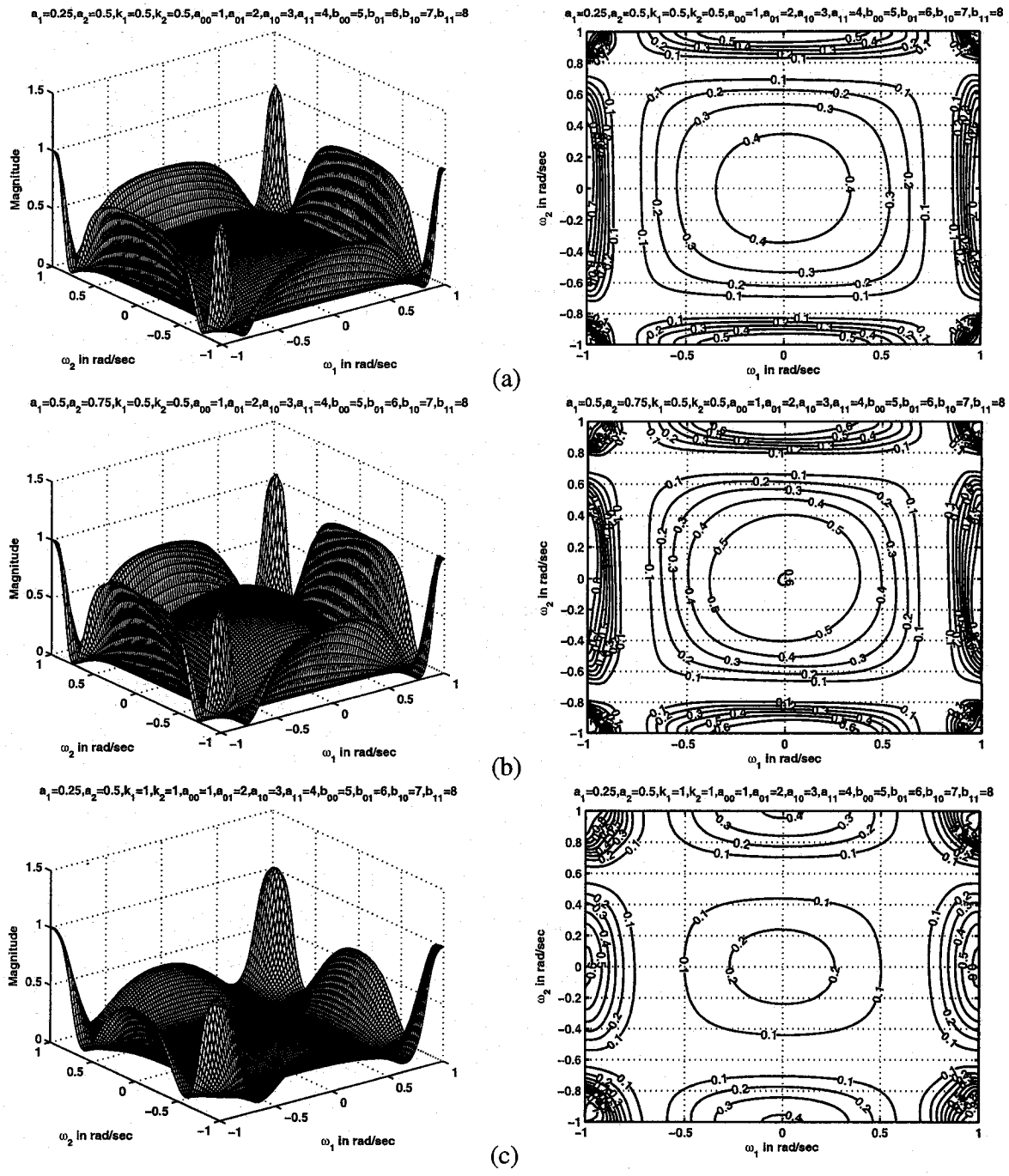

Figure 5.20: 3-D amplitude-frequency response and contour response of 2-D digital band-stop filter in case 2 of set 4 (when $k_1 = k_2 = 0.5,\ 1$)

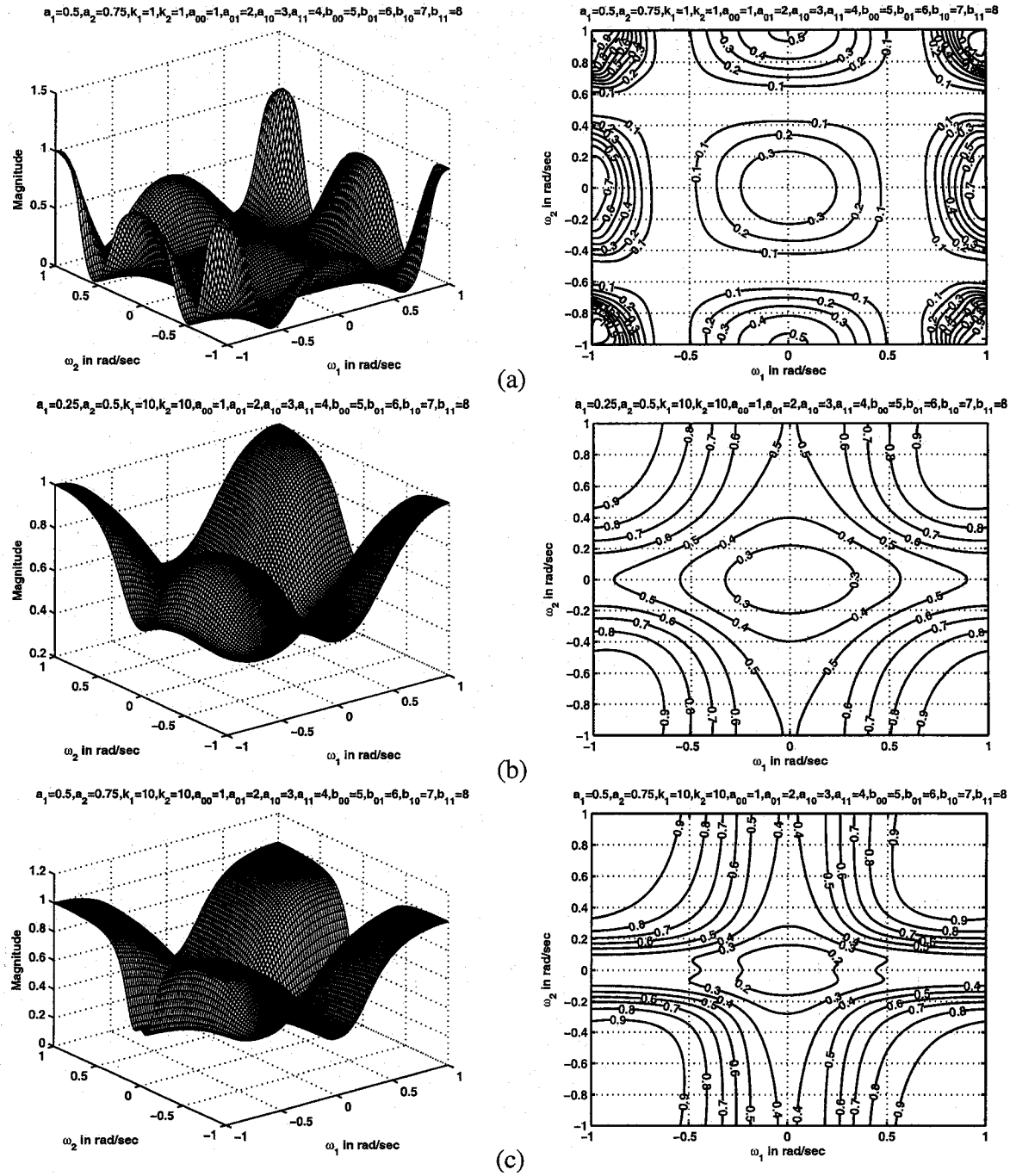

Figure 5.21: 3-D amplitude-frequency response and contour response of 2-D digital band-stop filter in case 2 of set 4 (when $k_1 = k_2 = 1,\ 10$)

5.4.4.3 Case 3

In this case,

$$a_1 \neq a_2 \quad , \quad k_1 \neq k_2 \quad , \quad b_1 = b_2 = 1$$

It is observed in this case that the coefficients k_1 and k_2 affect the passband width and the coefficients a_1 and a_2 affect the gain of the amplitude-frequency response. As k_1 and k_2 values are increased, the cut-off frequency of lower passband decreases, the cut-off frequency of upper passband increases and the bandwidth of the stopband of 2-D bandstop filter increases. In addition, the magnitude of the contour response also decreases. For values of k_1, $k_2 > 1$, it can be noticed that, there is rounding of contour edges and hence the transition band of 2-D bandstop filter cannot be clearly defined. This is because the outer contour of the lower passband merges with the inner contour of the upper passband of the 2-D bandstop filter. As a_1 and a_2 values are increased, the magnitude of the lower and upper passband of 2-D bandstop filter increases. Also, the lower passband decreases, the upper passband increases and the bandwidth of the stopband of 2-D bandstop filter increases.

The magnitude of the passband is lower than that of the magnitude in case 3 of set 3 for the same values of a_1, a_2, k_1 and k_2. The magnitude of the lower passband in Fig. 5.22 (a) is 0.3 which is smaller than the magnitude of the lower passband in Fig. 5.14 (a) for the same values of $k_1 = 0.5$, $k_2 = 1$, $a_1 = 0.25$, $a_2 = 0.5$.

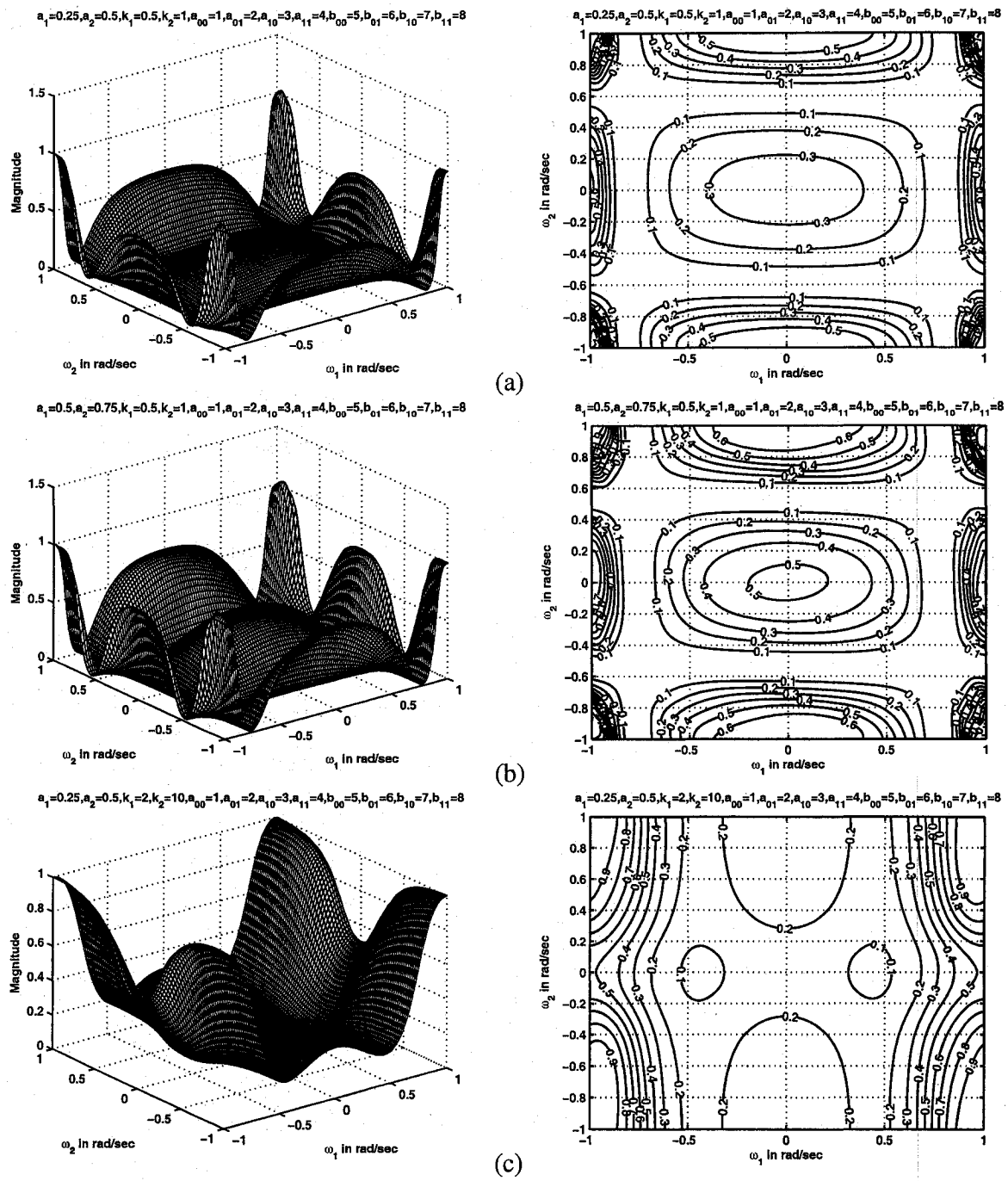

Figure 5.22: 3-D amplitude-frequency response and contour response of 2-D digital band-stop filter in case 3 of set 4 (when $k_1 = 0.5,\ 2,\ k_2 = 1,\ 10$)

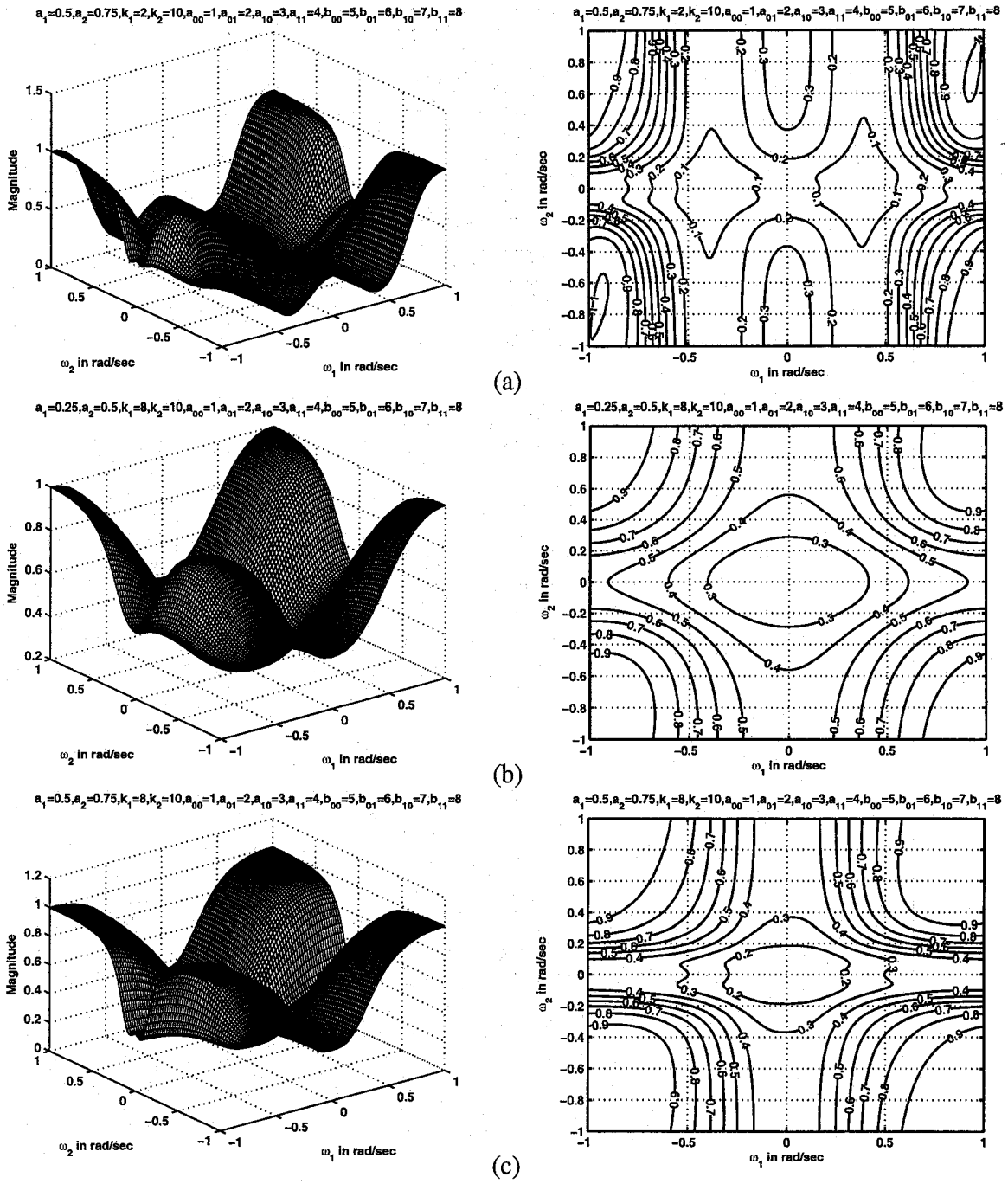

Figure 5.23: 3-D amplitude-frequency response and contour response of 2-D digital band-stop filter in case 3 of set 4 (when $k_1 = 2,\ 8,\ k_2 = 10$)

5.4.4.4 Case 4

In this case,

$$a_1 = a_2 \quad , \quad k_1 = k_2 \quad , \quad b_1 = b_2 = 1$$

It is observed in this case that the coefficients k_1 and k_2 affect the passband width and the coefficients a_1 and a_2 affect the gain of the amplitude-frequency response. As k_1 and k_2 values are increased, the cut-off frequency of lower passband decreases, the cut-off frequency of upper passband increases and the bandwidth of the stopband of 2-D bandstop filter increases. In addition, the magnitude of the contour response also decreases. For values of k_1, $k_2 > 1$, it can be noticed that there is rounding of contour edges and hence the transition band of 2-D bandstop filter cannot be clearly defined and is less visible. This is because the outer contour of the lower passband merges with the inner contour of the upper passband of the 2-D bandstop filter. As a_1 and a_2 values are increased, the magnitude of the lower and upper passband of 2-D bandstop filter increases. Also, the cut-off frequency of lower passband decreases, the cut-off frequency of upper passband increases and the bandwidth of the stopband of 2-D bandstop filter increases.

The magnitude of the passband is lower than that of the magnitude in case 4 of set 3 for the same values of a_1, a_2, k_1 and k_2. For example, the magnitude of the lower passband in Fig. 5.24 (a) is 0.3 which is smaller than the magnitude of the lower passband in Fig. 5.16 (a) for the same values of $k_1 = k_2 = 0.5$, $a_1 = a_2 = 0.25$.

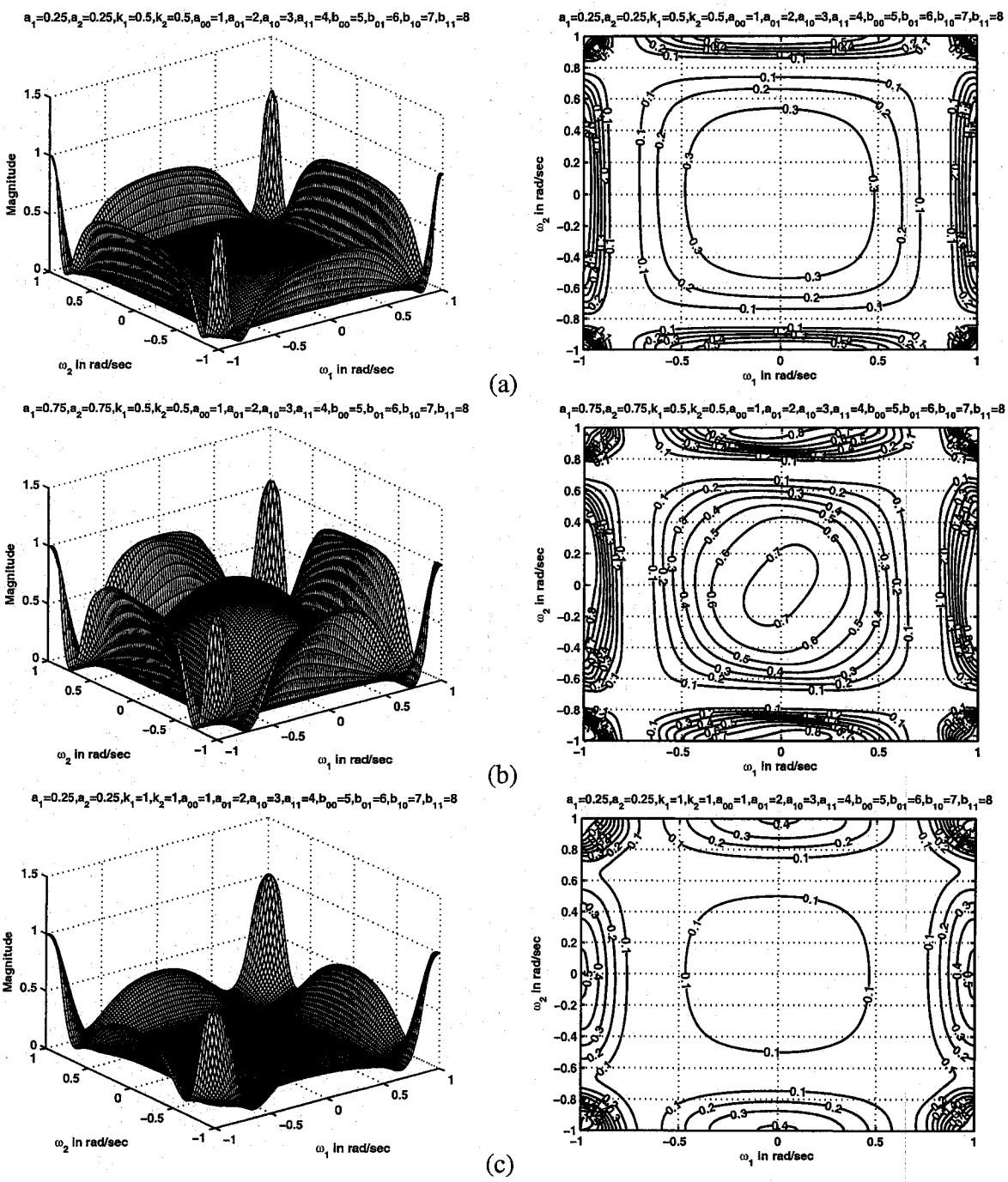

Figure 5.24: 3-D amplitude-frequency response and contour response of 2-D digital band-stop filter in case 4 of set 4 (when $k_1 = k_2 = 0.5,\ 1$)

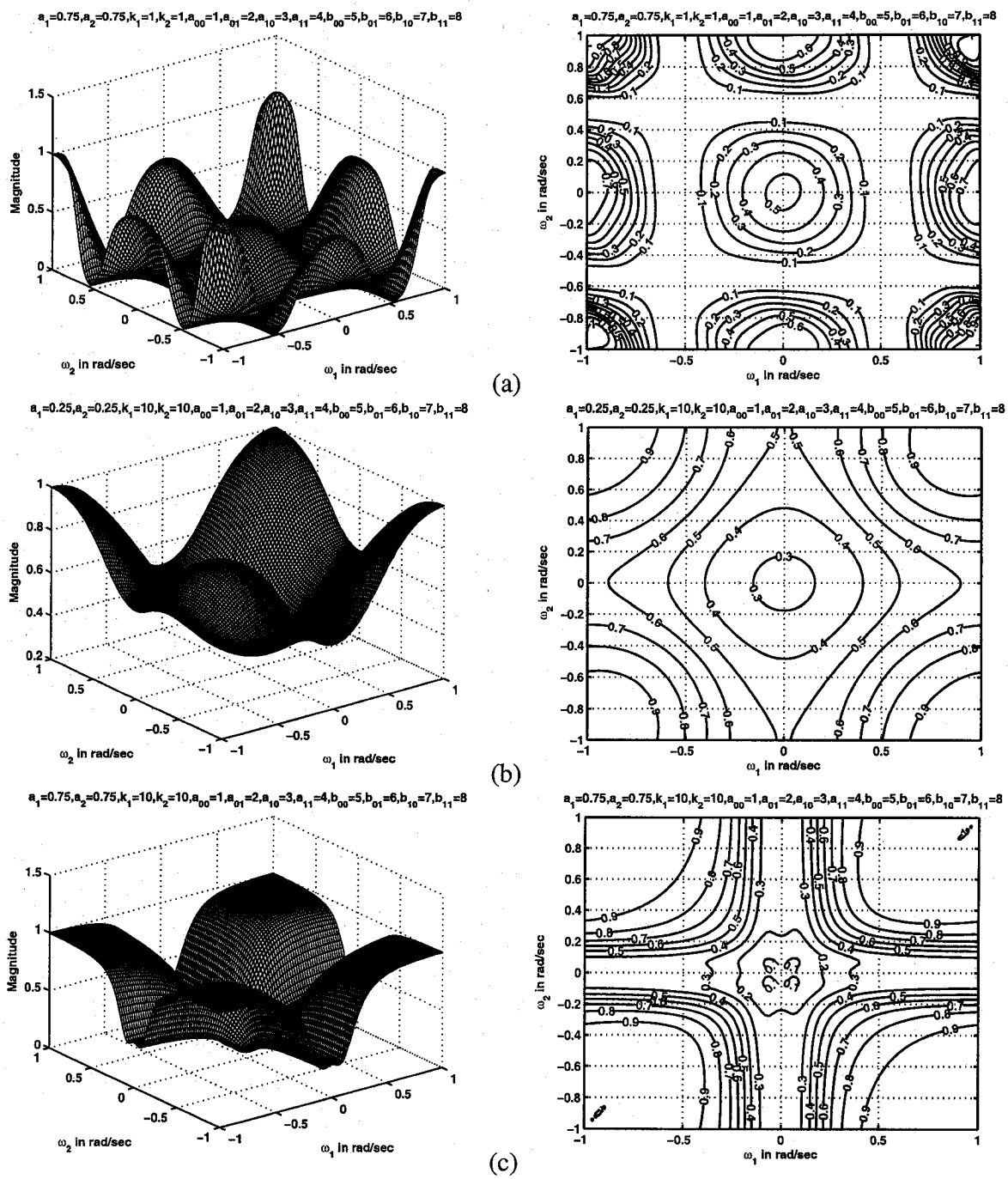

Figure 5.25: 3-D amplitude-frequency response and contour response of 2-D digital band-stop filter in case 4 of set 4 (when $k_1 = k_2 = 1,\ 10$)

5.5 Summary

In this chapter, inorder to investigate the manner in which each coefficient of the generalized bilinear transformation and CFE affects the magnitude response of the resulting 2-D bandstop filter, we changed the value of some of the coefficients of the filter to some fixed values.

It is observed in all the four cases of each set that the coefficients k_1 and k_2 mainly affect the passband width and the coefficients a_1 and a_2 mainly affect the gain of the amplitude-frequency response. As k_1 and k_2 values are increased, the cut-off frequency of lower passband decreases, the cut-off frequency of upper passband increases and the bandwidth of the stopband of 2-D bandstop filter increases. In addition, the magnitude of the contour response also decreases. For values of $k_1,\ k_2 > 1$, it can be noticed that there is rounding of contour edges and hence the transition band of 2-D bandstop filter cannot be clearly defined and is less visible. This is because the outer contour of the lower passband merges with the inner contour of the upper passband of the 2-D bandstop filter. As a_1 and a_2 values are increased, the magnitude of the lower and upper passband of 2-D bandstop filter increases. Also, the cut-off frequency of lower passband decreases, the cut-off frequency of upper passband increases and the bandwidth of the stopband of 2-D bandstop filter increases. In all the cases, values of k_1 and k_2 upto 10 have been studied. Higher values are not reported because the responses exhibit a tendency to repeat themselves.

In case 1 of set 1, it can be seen that there are ripples in the lower passband of the 2-D bandstop filters when $a_1 = a_2 \geq 0.75$ and when one or both of the k_1 and k_2 values are less than 0.5.

An important obervation to be noted is that the responses for set 2 is the same as that of set 1. This is because of the resulting transfer function for set 2 is the same as the one used in set 1 as the transfer function does not depend on the coefficients of the VSHP polynomial. It only depends on the coefficients of the bilinear transformation.

In set 3, the magnitude of the passband is low when compared to set 1 for the same

values of a_1, a_2, k_1 and k_2. There are no ripples in the contour response for all values of a_1, a_2, k_1 and k_2.

In set 4, the magnitude of the passband is low in the contour responses when compared to that of set 3 for the same values of a_1, a_2, k_1 and k_2. There are no ripples in the contour response for all values of a_1, a_2, k_1 and k_2.

Chapter 6

2-D digital filter application in image processing

6.1 Introduction

The application of digital signal processing techniques in general and of digital filtering in particular has expanded in many important areas such as speech signal processing, digital telephony and communications, facsimile and TV image processing, radar-sonar systems, biomedicine, space research and operative systems, geoscience, etc. Digital filters are widely applied to 1-D and multi-dimensional signals. Techniques used for 2-D systems can generally be extended to multi-dimensional systems. Examples of 2-D systems include image processing, seismic signal processing, meteorology, etc. This chapter discusses about the application of digital filters in image processing [34].

An image may be defined as a 2-D function, $f(x, y)$, where x and y are spatial co-ordinates, and the amplitude of $f(x, y)$ at any pair of co-ordinates (x, y) is called the intensity or gray level of the image at that point [2]. When these values are all finite and discrete quantities, the image is called a digital image.

Fourier transforms are widely used in the field of image processing, where one com-

monly describes an image in terms of intensity values in a 2-D matrix. The 2-D digital filters can be applied in frequency domain for various standard applications, like image enhancement, image restoration, etc., [2, 3]. The 2-D fourier transforms are effective tools for image processing. The 2-D Discrete Fourier Transform (DFT) of an image $f(x, y)$ of size M×N is given by,

$$F(\omega_1, \omega_2) = \frac{1}{MN} \sum_{x=0}^{M-1} \sum_{y=0}^{N-1} f(x, y) e^{-j2\pi(x\omega_1/M + y\omega_2/N)} \tag{6.1}$$

As in the 1-D case, this expression must be computed for values of $\omega_1 = 0, 1, 2, \ldots, M-1$ and also for $\omega_2 = 0, 1, 2, \ldots, N-1$. Similarly, for a given $F(\omega_1, \omega_2)$, we can obtain $f(x, y)$ via the 2-D Inverse Discrete Fourier Transform (IDFT), given by the expression

$$f(x, y) = \sum_{\omega_1=0}^{M-1} \sum_{\omega_2=0}^{N-1} F(\omega_1, \omega_2) e^{j2\pi(x\omega_1/M + y\omega_2/N)} \tag{6.2}$$

Also, one half of the convolution theorem for image, $f(x, y)$ and 2-D digital filter, $h_d(x, y)$, with Fourier transforms, $F(\omega_1, \omega_2)$ and $H_d(\omega_1, \omega_2)$, can be stated as

$$f(x, y) * h_d(x, y) \Leftrightarrow F(\omega_1, \omega_2) H_d(\omega_1, \omega_2) \tag{6.3}$$

In this chapter, we will show some examples in image processing by using standard images. In Sec. 6.2, we will study the effect of 2-D digital lowpass filtering in image restoration, by applying it on images corrupted with known amount of noise. We will use Gaussian noise and vary its variance to see the effect of filtering on images and discuss the results. In Sec. 6.3, we will show an example of extracting different frequency bands/components by applying 2-D digital lowpass filters.

6.2 Application of 2-D digital lowpass filters in image restoration

The ultimate goal of image restoration techniques is to improve an image in some predefined sense. Restoration attempts to reconstruct or recover an image that has been degraded by using apriori knowledge of the degradation phenomenon. The restoration techniques are oriented towards modeling the degradation and applying the inverse process in order to recover the original image. The noise in digital images arises during image acquisition (digitization) and/or transmission. We introduce image degradation artificially by adding noise, which is assumed to be independent of spatial coordinates and uncorrelated with respect to the image itself, i.e., there is no correlation between the pixel values of the image and the values of noise components [2, 3]. The lowpass filter in the spatial domain is equivalent to that of a smoothing filter, as it blocks high frequencies corresponding to sharp intensity changes, i.e., to the fine-scale details and noise in the spatial domain image.

There are various noise models e.g., Gaussian noise, Rayleigh noise, Erlang (Gamma) noise, exponential noise, uniform noise, impulse (salt and pepper) noise, periodic noise etc., available in literature [2]. We will consider Gaussian noise model for our analysis, as its mathematical tractability in both spatial and frequency domains are used frequently. The Probability Density Function (PDF) of a Gaussian random variable, z is given by

$$p(z) = \frac{1}{\sqrt{2\pi}\sigma} e^{-(z-\mu)^2/2\sigma^2} \tag{6.4}$$

where z represents gray level, μ is the mean of average value of z and σ is its standard deviation. The standard deviation squared, σ^2 is called the variance of z. Gaussian noise with zero mean, $n(x, y)$ is added to the image, $f(x, y)$ to get the degraded image, $f_d(x, y)$ i.e.,

$$f_d(x, y) = f(x, y) + n(x, y) \tag{6.5}$$

We can apply any 2-D lowpass filter proposed in Chapter 2 to remove/reduce the effect of noise. Let us use the 2-D digital lowpass filter obtained from CFE, $H_d(\omega_1, \omega_2)$ with $z_1 = e^{j\omega_1}$ and $z_2 = e^{j\omega_2}$, proposed in Chapter 2. By applying 2-D IDFT to $H_d(\omega_1, \omega_2)$, we get the 2-D filter function, $h_d(x, y)$ in spatial domain. There are two approaches to apply the 2-D filter.

(a) By convolution of the 2-D lowpass filter, $h_d(x, y)$ with the degraded image, $f_d(x, y)$ in the spatial domain, we expect to recover the image, $f_r(x, y)$

$$f_r(x, y) = f_d(x, y) * h_d(x, y) \tag{6.6}$$

(b) By multiplication of the filter, $H_d(\omega_1, \omega_2)$ and the degraded image, $F_d(x, y) = DFT\,[f_d(x, y)]$ in the frequency domain, and then 2-D IDFT to get the filtered image

$$f_r(x, y) = IDFT\,[F_d(\omega_1, \omega_2).H_d(\omega_1, \omega_2)] \tag{6.7}$$

where the recovered image is close to the original image i.e., $f_r(x, y) \approx f(x, y)$.

Although various quality measures are available in literature, those that correlate well with visual perception are quite complicated to compute. Most image processing systems of today are designed to minimise the Mean Square Error (MSE), the quantitative measure between two images, $f_1(x, y)$, $f_2(x, y)$ which is defined as

$$MSE = \frac{1}{MN} \sum_{x=0}^{M-1} \sum_{y=0}^{N-1} [f_1(x, y) - f_2(x, y)]^2 \tag{6.8}$$

where M×N is the image dimension and its product gives total number of pixels in the image. Instead of the MSE, the Peak Signal-to-Noise Ratio (PSNR) in decibels (dB) is more often used as a quality measure. The PSNR is defined as

$$PSNR = 10 \log_{10} \frac{\Psi_{max}^2}{MSE} \tag{6.9}$$

where Ψ_{max} is the peak (maximum) intensity value of the image. For the most common eight bit gray image, $\Psi_{max} = 255$.

We have considered images of 8-bit gray levels and corrupted them by additive Gaussian noise with zero mean and standard deviation of $\sigma \times 255$ gray levels. The corrupted image is then passed through the 2-D digital lowpass filter based on the first approach. The Original image, Degraded image and the Recovered/ filtered output images for different noise levels are shown in Figs. 6.1 and 6.2. The MSE and PSNR of the output and corrupted images are calculated with respect to the original image as reference. It is observed in the corrupted image that the MSE decreases and the PSNR increases with decrease in the noise level (i.e., Standard deviation σ or noise variation σ^2) of the added Gaussian noise. In 2-D lowpass filtering, the recovered image loses its sharpness at the edges. This is because the high frequency content of an image constitute the edges. It is also noted that when the noise level i.e., σ is not high, the MSE and PSNR of the corrupted and output recovered image are closer to each other with small improvement in the recovered image. For example, in Fig. 6.1, the noise level is not high (i.e., σ is a smaller value), and the MSE= 652.32 and 412.45 for the degraded and recovered image respectively. Since we are applying 2-D lowpass filtering, the sharpness of the image goes down and it can be easily seen in the edges of the Lenna image. But the influence of the noise is reduced considerably with a blurring effect in the output recovered image. When σ is increased, there is a higher level of degradation (noise variance σ^2) in the image and the filtered results have considerable amount of improvement with the 2-D lowpass filtering. For example, in Fig. 6.2, since noise level is high (i.e., σ is comparatively large value), the MSE = 7957.9 and 977.16 for the degraded and recovered image respectively. In this example, there is significant amount of improvement in the recovered image and the effectiveness of the 2-D lowpass digital filtering can be easily observed in terms of quantitative measure. To get a better filtered output, such lower order lowpass filters can be further cascaded.

Figure 6.1: The output of Lena image (Size: 256x256) when degraded by added Gaussian noise and passed through 2-D digital Lowpass filter; Standard Deviation σ of gaussian noise = 0.1
(a)Original Image
(b)Degraded Image, MSE = 652.32 and PSNR = 19.99 db
(c) Output Image, MSE = 412.45 and PSNR = 21.98 db

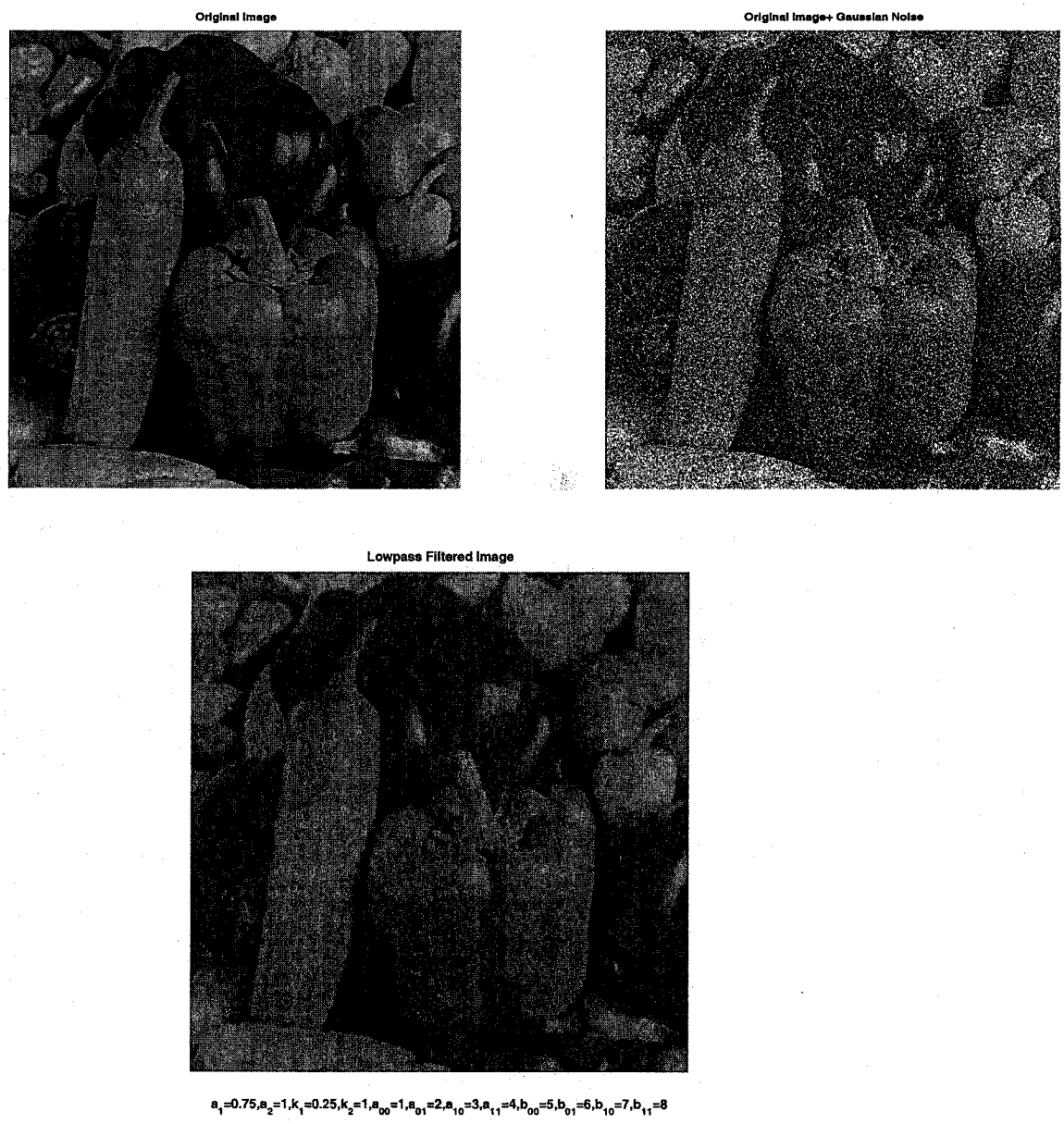

Figure 6.2: The output of Peppers image (Size: 256x256) when degraded by added Gaussian noise and passed through 2-D digital Lowpass filter; Standard Deviation σ of gaussian noise = 0.35
(a)Original Image
(b)Degraded Image, MSE = 7957.9 and PSNR = 9.13 db
(c) Output Image, MSE = 977.16 and PSNR = 18.23 db

6.3 Summary and Discussions

In image processing it is observed that most of the energy of a typical image is located at the low frequencies. On the other hand, energy of the noise is often spread across the frequency axes (e.g. white noise) or in the higher frequency range depending on its distribution function. One should expect to obtain good noise removal properties from 2-D lowpass filters. The high frequency content of an image constitutes the edges and applying 2-D lowpass filtering will result in losing the sharpness of the recovered image.

In Sec. 6.2, standard images are corrupted by additive Gaussian noise with known variance and mean. The 2-D digital lowpass filter with the given coefficients is used to remove noise from each corrupted image. The MSE and PSNR of the corrupted and recovered images are compared for quantitative measures of the image restoration.

Chapter 7

Conclusions

In this thesis, a new technique for generating 2-D digital filters having variable magnitude characteristics has been proposed. The approach used to generate 2-D filters is to start with a singly terminated network. So, we considered a Continued Fraction Expansion (CFE) obtained from the singly terminated network, defined its stability conditions and designed it as a stable 2-D digital lowpass filter. All the 2-D lowpass filters were further extended to 2-D digital highpass, bandpass and bandstop filters. In the end, we showed a few basic examples of 2-D filter application in image processing.

In Chapter 2, we generated 2-D digital lowpass filters from a new type of Continued Fraction Expansion (CFE) obtained from singly terminated network and studied their characteristics. The stability conditions of the 2-D analog lowpass filters have been obtained and proved by checking the transfer function denominator polynomial to be a Very Strict Hurwitz Polynomial (VSHP). The 2-D analog lowpass filters were transformed to digital domain by applying the generalized lowpass bilinear transformation. The 2-D digital lowpass filters were classified into four sets. Each set was further classified into four cases. The classification of four sets were based on the coefficients of the Continued Fraction Expansion (CFE); and the classification of four cases in each set were based on the coefficients of the generalized bilinear transformation. The effect of the coefficients of the generalized

bilinear transformation in each case and the effect of the coefficients of the Continued Fraction Expansion (CFE) in each set on the amplitude frequency response have been studied.

In Chapters 3 and 4 ,we generated 2-D digital highpass filters and 2-D digital bandpass filters respectively from their equivalent 2-D digital lowpass filters discussed in Chapter 2. Similar to 2-D digital lowpass filters, the four different sets and four cases involved in each set proposed earlier in Chapter 2 were classified and the effect of the coefficients on the amplitude frequency response were studied.

In Chapter 5, we generated 2-D digital bandstop filters from 2-D analog lowpass filter used in Chapter 2. The 2-D analog lowpass filter is transformed to 2-D analog bandstop filter using lowpass to bandstop transformation. The 2-D digital bandstop filter was then generated by applying the generalized bilinear transformation to the 2-D analog bandstop filter. Similar to Chapters 2, 3 and 4, the 2-D digital bandstop filters were classified into four sets and each set was further classified into four different cases and the effect of the coefficients on the amplitude frequency response were studied.

In all the four 2-D digital filters namely lowpass, highpass, bandpass and bandstop filters, it was observed that in general, the coefficients k_1, k_2 mainly affected the passband width and a_1, a_2 mainly affected the gain of the amplitude-frequency response. For 2-D digital lowpass filters, as k_1 and k_2 values were increased, the passband width of the 2-D filter decreased and also the amplitude of the contour response decreased. As a_1 and a_2 values were increased, the magnitude of the amplitude-frequency response of the 2-D lowpass filter increased and also the passband width decreased. Overall, the passband width decreased when k_1, k_2, a_1 and a_2 values were increased. For 2-D digital highpass filters, as k_1 and k_2 values were increased, the stopband width of the 2-D highpass filter increased, i.e., the cut-off frequencies changed and also the magnitude of the amplitude-frequency response decreased. As a_1 and a_2 values were increased, the magnitude of the amplitude-frequency response of the 2-D highpass filter increased and the stopband width increased. Overall, the cut-off frequencies of the 2-D highpass filter changed when k_1, k_2, a_1 and

a_2 values were increased. Also, the contours in the first and third quadrants were mirror images of one another and the contours in the second and fourth quadrants were mirror images of one another.

For 2-D digital bandpass filters, as k_1 and k_2 values were increased, the passband width increased and decreased periodically (only for case 1 and case 3) and the magnitude of the contour response decreased. As a_1 and a_2 values were increased, the magnitude of the amplitude-frequency response of the 2-D bandpass filter increased and also the passband width decreased. It was observed that the first and third quadrants of the contour response of the 2-D bandpass filters had the same passband width and magnitude whereas the second and fourth quadrants of the contour response had the same passband width and magnitude. For 2-D digital bandstop filters, as k_1 and k_2 values were increased, the cut-off frequency of lower passband decreased, the cut-off frequency of upper passband increased and the bandwidth of the stopband of 2-D bandstop filter increased. In addition, the magnitude of the contour response decreased. For values of k_1, $k_2 > 1$, it was noticed that there was rounding of contour edges and hence the transition band of 2-D bandstop filter could not be clearly defined. This was because the outer contour of the lower passband merged with the inner contour of the upper passband of the 2-D bandstop filter. As a_1 and a_2 values were increased, the magnitude of the lower and upper passband of 2-D bandstop filter increased. In additon, the cut-off frequency of lower passband decreased, the cut-off frequency of upper passband increased and the bandwidth of the stopband of 2-D bandstop filter increased.

In all the four cases, the values of k_1 and k_2 upto 10 were studied. Higher values were not reported because the responses exhibited a tendency to repeat themselves.

An important conclusion that was found when forming the four sets is that the responses for set 2 was the same as that of set 1. This was because of the resulting transfer function for set 2 was the same as the one used in set 1 as the transfer function did not depend on the coefficients of the Continued Fraction Expansion (CFE) . It only depended on the

coefficients of the generalized bilinear transformation.

In set 1, there were ripples in the contour response for smaller values of k_1 and k_2 and for larger values of a_1 and a_2. In set 3, it was observed that there were not many ripples in the contour responses when compared to set 1. Also the magnitude of the contour response was low when compared to set 1 for the same values of k_1, k_2, a_1 and a_2. In set 4, the passband width of the contour response was small and the magnitude of the contour response was low when compared to set 3. Also, it was observed that the ripples present in set 3 were removed.

In Chapter 6, we have shown examples of the application of 2-D digital lowpass filter in image processing. The 2-D digital lowpass filters were used to remove the added Gaussian noise corrupting standard images.

Scope for future work

In this thesis, we have limited ourselves to four types of sets. Different combinations of the coefficients of the CFE can be used to form other types of sets and the effect of the coefficients on the amplitude frequency response can be studied. We have used singly terminated network in the CFE to generate 2-D digital filters. Doubly terminated network can also be used in the CFE. We can study the effect of the coefficients of 2-D digital filters obtained from other types of transformations, e.g., impulse invariance method etc., The phase response of the filters are not studied in this thesis and they can be explored in future. All-pass filters and their combinations can also be considered to generate stable 2-D digital filters.

Depending on the combination of properties like symmetry, amplitude characteristics (monotonic responses, responses with ripples) and the response in the stop band, suitable values for the coefficients of the generalized bilinear transformation and the CFE can to be determined. This looks possible by adopting suitable optimization technique. It is envis-

aged that these types of 2-D filters have potential applications in other areas like speech processing, video transmission, identification of moving objects etc.,

Chapter 8

Appendix

8.1 MATLAB code to plot the 3-D amplitude-frequency response and contour response of the 2-D digital low-pass filter obtained from CFE

```
w1=-pi:pi/50:pi;
    w2=-pi:pi/50:pi;
    z1=exp(-j*w1);
    z2=exp(-j*w2);
    [Z1,Z2]=meshgrid(z1,z2);
    a00=input('Give the value of the constant a00=>');
    a01=input('Give the value of the constant a01=>');
    a10=input('Give the value of the constant a10=>');
    a11=input('Give the value of the constant a11=>');
    b00=input('Give the value of the constant b00=>');
    b01=input('Give the value of the constant b01=>');
    b10=input('Give the value of the constant b10=>');
```

```
b11=input('Give the value of the constant b11=>');
%input the values of the constants in the LP bilinear transformation.
k1=input('Give the value of the constant k1 for the bilinear LP transformation=>');
k2=input('Give the value of the constant k2 for the bilinear LP transformation=>');
a1=input('Give the value of the constant a1 for the bilinear LP transformation=>');
a2=input('Give the value of the constant a2 for the bilinear LP transformation=>');
a=Z1-a1; b=Z2-a2;
c=Z1+1; d=Z2+1;
H1=((k1^2).*(a.^2)).*(((a11*b11*k2^2).*(b.^2))+(((a10*b11)*k2).*b.*d)+
((a10*b10).*d.^2));
H2=(k1.*a).*((((a01*b11)*k2^2).*(b.^2).*c)+(((a00*b11+a10*b01+a01*b10+
a11*b00)*k2).*b.*d.*c)+((a10*b00).*c.*d.^2));
H3=((a01*b01*k2^2).*(b.^2).*(c.^2))+(((a01*b00)*k2).*b.*d.*(c.^2))+
((a00*b00).*(c.^2).*(d.^2));
H=(a00.*b00.*(c.^2).*(d.^2))./(H1+H2+H3);
figure;
mesh(w1/pi,w2/pi,abs(H));
grid on;
xlabel('\omega_1 in rad/sec');
ylabel('\omega_2 in rad/sec');
zlabel('Magnitude');
title(['a_1=',num2str(a1),',','a_2=',num2str(a2),',','k_1=',num2str(k1),',','k_2=',
num2str(k2),',','a_0_0=',num2str(a00),',','a_0_1=',num2str(a01),',','a_1_0=',
num2str(a10),',','a_1_1=',num2str(a11),',','b_0_0=',num2str(b00),',','b_0_1='
,num2str(b01),',','b_1_0=',num2str(b10),',','b_1_1=',num2str(b11)]);
  figure;
%to plot the magnitude values of countour
```

```
[c1,c2]=contour(w1/pi,w2/pi,abs(H));
clabel(c1,c2);
grid on;
xlabel('\omega_1 in rad/sec');
ylabel('\omega_2 in rad/sec');
title(['a_1=',num2str(a1),',','a_2=',num2str(a2),',','k_1=',num2str(k1),',','k_2=',
num2str(k2),',','a_0_0=',num2str(a00),',','a_0_1=',num2str(a01),',','a_1_0=',
num2str(a10),',','a_1_1=',num2str(a11),',','b_0_0=',num2str(b00),',','b_0_1=',
num2str(b01),',','b_1_0=',num2str(b10),',','b_1_1=',num2str(b11)]);
```

8.2 MATLAB code to plot the 3-D amplitude-frequency response and contour response of the 2-D digital high-pass filter obtained from CFE

```
w1=-pi:pi/50:pi;
w2=-pi:pi/50:pi;
z1=exp(-j*w1);
z2=exp(-j*w2);
[Z1,Z2]=meshgrid(z1,z2);
a00=1;
a01=1;
a10=1;
a11=1;
b00=1;
b01=1;
b10=1;
```

```
b11=1;
%input the values of the constants in the LP bilinear transformation.
k1=input('Give the value of the constant k1 for the bilinear LP transformation=>');
k2=input('Give the value of the constant k2 for the bilinear LP transformation=>');
a1=input('Give the value of the constant a1 for the bilinear LP transformation=>');
a2=input('Give the value of the constant a2 for the bilinear LP transformation=>');
a=Z1+a1; b=Z2+a2;
c=Z1-1; d=Z2-1;
H1=((k1^2).*(a.^2)).*(((a11*b11*k2^2).*(b.^2))+(((a10*b11)*k2).*b.*d)+
((a10*b10).*d.^2));
H2=(k1.*a).*((((a01*b11)*k2^2).*(b.^2).*c)+(((a00*b11+a10*b01+a01*
b10+a11*b00)*k2).*b.*d.*c)+((a10*b00).*c.*d.^2));
H3=((a01*b01*k2^2).*(b.^2).*(c.^2))+(((a01*b00)*k2).*b.*d.*(c.^2))+
((a00*b00).*(c.^2).*(d.^2));
H=(a00.*b00.*(c.^2).*(d.^2))./(H1+H2+H3);
figure;
mesh(w1/pi,w2/pi,abs(H));
grid on;
xlabel('\omega_1 in rad/sec');
ylabel('\omega_2 in rad/sec');
zlabel('Magnitude');
title(['a_1=',num2str(a1),',','a_2=',num2str(a2),',','k_1=',num2str(k1),',','
k_2=',num2str(k2),',','a_0_0=',num2str(a00),',','a_0_1=',num2str(a01),',','
a_1_0=',num2str(a10),',','a_1_1=',num2str(a11),',','b_0_0=',num2str(b00),',','
b_0_1=',num2str(b01),',','b_1_0=',num2str(b10),',','b_1_1=',num2str(b11)]);
figure;
%to plot the magnitude values of countour
```

```
[c1,c2]=contour(w1/pi,w2/pi,abs(H));
clabel(c1,c2);
grid on;
xlabel('\omega_1 in rad/sec');
ylabel('\omega_2 in rad/sec');
title(['a_1=',num2str(a1),',','a_2=',num2str(a2),',','k_1=',num2str(k1),',','
k_2=',num2str(k2),',','a_0_0=',num2str(a00),',','a_0_1=',num2str(a01),',',
'a_1_0=',num2str(a10),',','a_1_1=',num2str(a11),',','b_0_0=',num2str(b00),',','
b_0_1=',num2str(b01),',','b_1_0=',num2str(b10),',','b_1_1=',num2str(b11)]);
```

8.3 MATLAB code to plot the 3-D amplitude-frequency response and contour response of the 2-D digital band-pass filter obtained from CFE

```
w1=-pi:pi/50:pi;
w2=-pi:pi/50:pi;
z1=exp(-j*w1);
z2=exp(-j*w2);
[Z1,Z2]=meshgrid(z1,z2);
a00=input('Give the value of the constant a00=>');
a01=input('Give the value of the constant a01=>');
a10=input('Give the value of the constant a10=>');
a11=input('Give the value of the constant a11=>');
b00=input('Give the value of the constant b00=>');
b01=input('Give the value of the constant b01=>');
b10=input('Give the value of the constant b10=>');
```

```
b11=input('Give the value of the constant b11=>');
%input the values of the constants in the LP bilinear transformation.
k1=input('Give the value of the constant k1 for the bilinear transformation=>');
k2=input('Give the value of the constant k2 for the bilinear transformation=>');
a1=input('Give the value of the constant a1 for the bilinear transformation=>');
a2=input('Give the value of the constant a2 for the bilinear transformation=>');
%Lowpass filter
a=Z1-a1; b=Z2-a2;
c=Z1+1; d=Z2+1;
HL1=((k1^2).*(a.^2)).*(((a11*b11*k2^2).*(b.^2))+(((a10*b11)*k2).*b.*d)+
((a10*b10).*d.^2));
HL2=(k1.*a).*((((a01*b11)*k2^2).*(b.^2).*c)+(((a00*b11+a10*b01+a01*
b10+a11*b00)*k2).*b.*d.*c)+((a10*b00).*c.*d.^2));
HL3=((a01*b01*k2^2).*(b.^2).*(c.^2))+(((a01*b00)*k2).*b.*d.*(c.^2))+
((a00*b00).*(c.^2).*(d.^2));
HL=(a00.*b00.*(c.^2).*(d.^2))./(HL1+HL2+HL3);
%Highpass filter
e=Z1+a1; f=Z2+a2;
g=Z1-1; h=Z2-1;
HH1=((k1^2).*(e.^2)).*(((a11*b11*k2^2).*(f.^2))+(((a10*b11)*k2).*f.*h)+
((a10*b10).*h.^2));
HH2=(k1.*e).*((((a01*b11)*k2^2).*(f.^2).*g)+(((a00*b11+a10*b01+a01*
b10+a11*b00)*k2).
*f.*h.*g)+((a10*b00).*g.*h.^2));
HH3=((a01*b01*k2^2).*(f.^2).*(g.^2))+(((a01*b00)*k2).*f.*h.*(g.^2))+
((a00*b00).*(g.^2).*(h.^2));
HH=(a00.*b00.*(g.^2).*(h.^2))./(HH1+HH2+HH3);
```

```
%Bandpass filter
HB=HL.*HH;
figure;
mesh(w1/pi,w2/pi,abs(HB));
grid on;
xlabel('\omega_1 in rad/sec');
ylabel('\omega_2 in rad/sec');
zlabel('Magnitude');
title(['a_1=',num2str(a1),',','a_2=',num2str(a2),',','k_1=',num2str(k1),',',
k_2=',num2str(k2),',','a_0_0=',num2str(a00),',','a_0_1=',num2str(a01),',',
a_1_0=',num2str(a10),',','a_1_1=',num2str(a11),',','b_0_0=',num2str(b00),',',
b_0_1=',num2str(b01),',','b_1_0=',num2str(b10),',','b_1_1=',num2str(b11)]);
figure;
%to plot the magnitude values of countour
[c1,c2]=contour(w1/pi,w2/pi,abs(HB));
clabel(c1,c2);
grid on;
xlabel('\omega_1 in rad/sec');
ylabel('\omega_2 in rad/sec');
title(['a_1=',num2str(a1),',','a_2=',num2str(a2),',','k_1=',num2str(k1),',',
k_2=',num2str(k2),',','a_0_0=',num2str(a00),',','a_0_1=',num2str(a01),',',
a_1_0=',num2str(a10),',','a_1_1=',num2str(a11),',','b_0_0=',num2str(b00),',',
b_0_1=',num2str(b01),',','b_1_0=',num2str(b10),',','b_1_1=',num2str(b11)]);
```

8.4 MATLAB code to plot the 3-D amplitude-frequency response and contour response of the 2-D digital band-stop filter obtained from CFE

```
w1=-pi:pi/50:pi;
    w2=-pi:pi/50:pi;
    z1=exp(-j*w1);
    z2=exp(-j*w2);
    [Z1,Z2]=meshgrid(z1,z2);
    a00=input('Give the value of the constant a00=>');
    a01=input('Give the value of the constant a01=>');
    a10=input('Give the value of the constant a10=>');
    a11=input('Give the value of the constant a11=>');
    b00=input('Give the value of the constant b00=>');
    b01=input('Give the value of the constant b01=>');
    b10=input('Give the value of the constant b10=>');
    b11=input('Give the value of the constant b11=>');
    %input the values of the constants in the LP bilinear transformation.
    k1=input('Give the value of the constant k1 for the bilinear LP transformation=>');
    k2=input('Give the value of the constant k2 for the bilinear LP transformation=>');
    a1=input('Give the value of the constant a1 for the bilinear LP transformation=>');
    a2=input('Give the value of the constant a2 for the bilinear LP transformation=>');
    b1=1;
    b2=1;
    a=Z1-a1; b=Z2-a2;
    c=Z1+b1; d=Z2+b2;
    H1=(a00.*b00.*(((k1^2.*(a.^2./c.^2))+1).^2).*(((k2^2.*(b.^2./d.^2))+1).^2));
```

```
H2=((k1^2.*(a.^2./c.^2)).*((a11*b11.*(k2^2.*(b.^2./d.^2)))+(a10*b11.*(k2
.*(b./d)).*((k2^2.*(b.^2./d.^2))+1))+(a10*b10.*((k2^2.*(b.^2./d.^2))+1).^2)));
H3=((k1.*(a./c).*((k1^2.*(a.^2./c.^2))+1)).*((a01*b11.*(k2^2.*(b.^2./d.^2)))+
((a11*b00+a00*b11+a10*b01+a01*b10).*(k2.*(b./d)).*((k2^2.*(b.^2./d.^2))+1))
+(a10*b00.*((k2^2.*(b.^2./d.^2))+1).^2)));
H4=((((k1^2.*(a.^2./c.^2))+1).^2).*((a01*b01.*(k2^2.*(b.^2./d.^2)))+(a01*b00
.*(k2.*(b./d)).*((k2^2.*(b.^2./d.^2))+1))+(a00*b00.*((k2^2.*(b.^2./d.^2))+1).^2)));
H=H1./(H2+H3+H4);
figure;
mesh(w1/pi,w2/pi,abs(H));
grid on;
xlabel('\omega_1 in rad/sec');
ylabel('\omega_2 in rad/sec');
zlabel('Magnitude');
title(['a_1=',num2str(a1),',','a_2=',num2str(a2),',','k_1=',num2str(k1),',','k_2=',
num2str(k2),',','a_0_0=',num2str(a00),',','a_0_1=',num2str(a01),',','a_1_0=',
num2str(a10),',','a_1_1=',num2str(a11),',','b_0_0=',num2str(b00),',','
b_0_1=',num2str(b01),',','b_1_0=',num2str(b10),',','b_1_1=',num2str(b11)]);
figure;
%to plot the magnitude values of countour
[c1,c2]=contour(w1/pi,w2/pi,abs(H));
clabel(c1,c2);
grid on;
xlabel('\omega_1 in rad/sec');
ylabel('\omega_2 in rad/sec');
title(['a_1=',num2str(a1),',','a_2=',num2str(a2),',','k_1=',num2str(k1),',','k_2=',
num2str(k2),',','a_0_0=',num2str(a00),',','a_0_1=',num2str(a01),',','a_1_0=',
```

```
num2str(a10),',','a_1_1=',num2str(a11),',','b_0_0=',num2str(b00),',','b_0_1=',
num2str(b01),',','b_1_0=',num2str(b10),',','b_1_1=',num2str(b11)]);
```

8.5 MATLAB code to corrupt the image by adding Gaussian Noise and recover the image using 2-D digital low-pass filter

```
%Image restoration by using 2-D digital lowpass filter
clc;
clear all;
L=5; W=5; miss=floor(L/2);
%Read the image and get pixel values between 0 and 1 value
imgTemp=imread('peppers.gif','gif'); img=double(imgTemp)./255;
%Display the original image/Frame
figure(1); imshow(img);
title('Original Image');
mxSize=size(img); M=mxSize(1); N=mxSize(2);
%Introducing Gaussian noise with standard deviation-SD and mean-0
SD=0.35; imgdeg=img+SD*randn(M,N);
%Display the degraded image with known noise value
figure(2); imshow(imgdeg);
title('Original Image+ Gaussian Noise');
tot=0; for i=1:M
for j=1:N
tot=tot+(imgdeg(i,j)*255-img(i,j)*255)^2;
end; end; mserror=tot*(1/(M*N))
```

```
psnr=10*log10((255^2)/mserror)
[w1,w2]=meshgrid(0:((2*pi)/N):(2*pi)-((2*pi)/N),0:((2*pi)/M):(2*pi)-((2*pi)/M));
%Creates 2-D square matrix (mesh grid) of angular frequency w1 and w2
%Apply z1=r1*exp(jw1) and z2=r2*exp(jw2) with r1=r2=1
Z1=exp(j.*w1); Z2=exp(j.*w2);
%H1lpf is the required digital transfer function and its value is evaluated as
%follows
a00=input('Give the value of the constant a00=>');
a01=input('Give the value of the constant a01=>');
a10=input('Give the value of the constant a10=>');
a11=input('Give the value of the constant a11=>');
b00=input('Give the value of the constant b00=>');
b01=input('Give the value of the constant b01=>');
b10=input('Give the value of the constant b10=>');
b11=input('Give the value of the constant b11=>');
%input the values of the constants in the LP bilinear transformation.
k1=input('Give the value of the constant k1 for the bilinear LP transformation=>');
k2=input('Give the value of the constant k2 for the bilinear LP transformation=>');
a1=input('Give the value of the constant a1 for the bilinear LP transformation=>');
a2=input('Give the value of the constant a2 for the bilinear LP transformation=>');
a=Z1-a1; b=Z2-a2;
c=Z1+1; d=Z2+1;
H1=((k1^2).*(a.^2)).*(((a11*b11*k2^2).*(b.^2))+(((a10*b11)*k2).*b.*d)+
((a10*b10).*d.^2));
H2=(k1.*a).*((((a01*b11)*k2^2).*(b.^2).*c)+(((a00*b11+a10*b01+a01*b10
+a11*b00)*k2).*b.*d.*c)+((a10*b00).*c.*d.^2));
H3=((a01*b01*k2^2).*(b.^2).*(c.^2))+(((a01*b00)*k2).*b.*d.*(c.^2))+((a00*b00)
```

```
.*(c.^2).*(d.^2));
%Transfer function of the lowpass filter
Hlpf=(a00.*b00.*(c.^2).*(d.^2))./(H1+H2+H3);
H1lpf=abs(Hlpf);
%Taking IFFT of the digital lowpass filter
imgLPF_S=real(ifft2(Hlpf,L,W));
%Convoluting degraded image and lowpass filter in spatial domain
img_out=conv2(imgdeg,imgLPF_S);
%Extracting the image from the enlarged image because of convolution
sz=size(img_out); imgLowpassFiltered=[];
imgLowpassFiltered=img_out(miss+1:sz(1)-miss,1+miss:sz(2)-miss);
figure(3); imshow(imgLowpassFiltered);
title('Lowpass Filtered Image');
xlabel(['a_1=',num2str(a1),',','a_2=',num2str(a2),',','k_1=',num2str(k1)
,',','k_2=',num2str(k2),',','a_0_0=',num2str(a00),',','a_0_1=',num2str(a01)
,',','a_1_0=',num2str(a10),',','a_1_1=',num2str(a11),',','b_0_0=',num2str(b00)
,',','b_0_1=',num2str(b01),',','b_1_0=',num2str(b10),',','b_1_1=',num2str(b11)]);
total=0;total1=0; for p=1:M
for q=1:N
total=total+(imgLowpassFiltered(p,q)*255-img(p,q)*255)^2;
total1=total1+(imgdeg(p,q)*255-imgLowpassFiltered(p,q)*255)^2;
end; end; mse_LP=total*(1/(M*N))
psnr_LP=10*log10((255^2)/mse_LP)
```

Bibliography

[1] R.L. Rabiner and B. Gold, "Theory and Application of Digital Signal Processing", Prentice Hall, 1975.

[2] Rafael C. Gonzalez and Richard E.Woods, "Digital Image Processing", Pearson Education, Inc., Second Edition, 2002.

[3] Tamal Bose, "Digital Signal and Image Processing", John Wiley and Sons, Inc., 2004.

[4] E.I. Jury, "Inners and stability of dynamic systems", John Wiley and Sons, 1974.

[5] V. Ramachandran and C.S. Gargour, "Generation of very strict hurwitz polynomials and applications to 2-D filter design", *Control and Dynamic systems, Multidimensional Systems: Signal Processing and Modeling Techniques, Academic Press Inc.,Vol.69, pg 211-254,1995.*

[6] C.S. Gargour, V. Ramachandran, Ravi P. Ramachandran and F.Awad, "Variable Magnitude characteristics of 1-D IIR discrete filters by a generalized bilinear transformation", Proceedings of the IEEE Canadian Conference on Electrical and Computer Engineering, pp.1036-1039, 2002.

[7] D. Goodman, "Some stability properties of two-dimensional linear shift-invariant digital filters", IEEE Transactions on Circuits and Systems, Vol. CAS-24, No.4, pp.201-208, April 1977.

[8] D. Goodman, "Some difficulties with double bilinear transformations in 2-D digital filter design", Proc.IEEE, vol.66, No.7, pp.796-797, July 1978.

[9] M.N.S. Swamy, L.M. Roytman and N.Marinovic, "A necessary condition for the BIBO stability of 2-D filters", IEEE Transactions on Circuits and Systems II: Analog and Digital Signal Processing, vol. 39, Issue: 7, pp.475-476, July 1992.

[10] J.L. Shanks, S. Treitel and J.H. Justice, "Stability and Synthesis of two-dimensional Recursive filters", IEEE Trans. Audio-Acoustics, vol. AU-20, June 1972.

[11] C.S. Gargour, V. Ramachandran and Ravi P. Ramachandran, "Generation of a class of 2-D transfer function yielding variable magnitude and contour characteristics", ISCAS 2001, pp.797-800, Sydney, Australia, May 2001.

[12] E. Dubois and M.L. Blostein, "A circuit analog method for the design of recursive two-dimensional digital filters", Proc. IEEE Internet. Symp. Circuits Syst., pp.451-454, 1975.

[13] P.A. Ramamoorthy and L.T. Bruton, "Frequency Domain Approximation of stable multi-dimensional discrete filters", Proc. IEEE Internet. Symp. Circuits Syst., pp.654-657, 1977.

[14] Richard E. Twogood and Sanjit K.Mitra, "Computer-aided design of separable two-dimensional digital filters", Proc. IEEE Trans. Acoust., Speech, Signal Process. Vol. ASSP-25(2), pp.165-169, 1977.

[15] S. Basu and A. Fettweis, "Test for two dimensional scattering Hurwitz polynomials", Circuits, Syst., Signal Processing, vol.3, no.2, pp.225-242, 1984.

[16] H.C. Reddy at al., "Generation of two-dimensional digital transfer functions without nonessential singularities of the second kind", Proc. IEEE Int. Conf. Acoust., Speech, Signal Processing, pp.13-19, April 1979.

[17] H.C. Reddy and P.K. Rajan, "A comprehensive study of two-variable Hurwitz polynomials", IEEE Transactions on Education, vol.32, Issue: 3, pp.198-209, Aug. 1989.

[18] V. Ramachandran, "Some similarities and dissimilarities between single-variable and two-variable reactance functions", IEEE Circuits and Systems Newsletter, vol. 10, N0.1, pp 11-14,February 1976.

[19] M. Marden, "Geometry of Polynomials", American Mathematical Society, pp.22, 1966.

[20] V. Ramachandran and C.S. Gargour, "Generation of stable 2-D transfer functions having variable magnitude characteristics", Control and Dynamic systems,*Multidimensional Systems: Signal Processing and Modeling Techniques, Academic Press Inc.,* vol.69, pp. 255-297, 1995.

[21] V. Ramachandran and M. Ahmadi, "Design of 2-D stable recursive filters by generation of VSHP using Terminated n-port Gyrator Networks", Journal of the Franklin Institute, vol. 316, no.5, pp. 373-380, November 1983.

[22] M.A.Abiri, V.Ramachandran and M.Ahmadi,"An alternative approach in generating a 2-Variable Very Strict Hurwitz Polynomial (VSHP) and its applications", Journal of the Franklin Institute, vol. 324, no. 2, pp.187-203, 1987.

[23] V. Ramachandran, M. Ahmedi, "Design of 2-D stable analog and recursive digital filters using properties of the derivatives of even or odd parts of Hurwitz Polynomials", Journal of the Franklin Institute, vol. 315, no. 4, pp. 259-267, April 1983.

[24] M. Ahmedi, S. Golikeri and V. Ramachandran, "A new method for the design of 2-D stable recursive digital filters satisfying prescribed magnitude and group delay response", IEEE International Conference on Acoustics, Speech and Signal Processing, ICASSP'83, vol.8, pp.399-402, April 1983.

[25] P. Kavitharajan and M.N.S. Swamy, "Some results on the nature of 2-Dimensional filter functions possessing certain symmetry in its magnitude response", IEEE Journal on Electronic Circuits and Systems, vol.2, no.5, pp.147-153, September, 1978.

[26] S.G. Tzafestas, "Multidimensional systems: Techniques and Applications", 1986.

[27] P. Kavitharajan and M.N.S. Swamy, "Some results on the nature of a two dimensional filter function possessing certain symmetry in its amplitude response", IEEE jounal on Electronic Circuits and Systems, vol.2, no.5, pp.147-153, September 1978.

[28] P. Kavitharajan and M.N.S. Swamy, "Symmetry constraints on 2-D half plane digital transfer functions", IEEE Transactions on Acoustics, Speech and Signal Processing, vol.27, no.5, pp. 506-511, 1979.

[29] V. Ramachandran, Ravi P. Ramachandran and C.S. Gargour, "Some properties of the z-domain Continued Fraction Expansion of 1-D discrete reactance functions, IEEE International Symposium on Circuits and Systems, (ISCAS), Sydney, Australia, 2001, vol 2, pp.841-844.

[30] Ling Luo, "A new z-domain continued fraction expansion and its use in the generation of stable transfer functions", M.A.Sc. Thesis, Concordia University, Montreal, QC, H3G 1M8, June 2003.

[31] V. Ramachandran and A. Sreenivasa Rao, "A Multivariable array and its applications to ladder networks", IEEE *Trans. on Circuit Theory, vol.CT-20, no.5, September 1973.*

[32] C.S. Gargour, V. Ramachandran and Ravi P. Ramachndran, "Modification of filter responses by the generalized bilinear transformations and the inverse bilinear transformations", *Electrical and Computer Engineering, 2003. IEEE CCECE 2003, Canadian Conference on, vol. 3, pp.2043-2046, May 4-7, 2003*

[33] James H. McClellan, "The design of two-dimensional digital filters by transformations", *Proceeding of 7thAnnual Princeton Conference on Information Sciences and Systems, pp.247-251, 1973.*

[34] V. Cappellini, A.G. Constantinides and P. Emilliani, "Digital filters and their applications", 1978, Academic Press.

[17] H.C. Reddy and P.K. Rajan, "A comprehensive study of two-variable Hurwitz polynomials", IEEE Transactions on Education, vol.32, Issue: 3, pp.198-209, Aug. 1989.

[18] V. Ramachandran, "Some similarities and dissimilarities between single-variable and two-variable reactance functions", IEEE Circuits and Systems Newsletter, vol. 10, N0.1, pp 11-14,February 1976.

[19] M. Marden, "Geometry of Polynomials", American Mathematical Society, pp.22, 1966.

[20] V. Ramachandran and C.S. Gargour, "Generation of stable 2-D transfer functions having variable magnitude characteristics", Control and Dynamic systems,*Multidimensional Systems: Signal Processing and Modeling Techniques, Academic Press Inc.,* vol.69, pp. 255-297, 1995.

[21] V. Ramachandran and M. Ahmadi, "Design of 2-D stable recursive filters by generation of VSHP using Terminated n-port Gyrator Networks", Journal of the Franklin Institute, vol. 316, no.5, pp. 373-380, November 1983.

[22] M.A.Abiri, V.Ramachandran and M.Ahmadi,"An alternative approach in generating a 2-Variable Very Strict Hurwitz Polynomial (VSHP) and its applications", Journal of the Franklin Institute, vol. 324, no. 2, pp.187-203, 1987.

[23] V. Ramachandran, M. Ahmedi, "Design of 2-D stable analog and recursive digital filters using properties of the derivatives of even or odd parts of Hurwitz Polynomials", Journal of the Franklin Institute, vol. 315, no. 4, pp. 259-267, April 1983.

[24] M. Ahmedi, S. Golikeri and V. Ramachandran, "A new method for the design of 2-D stable recursive digital filters satisfying prescribed magnitude and group delay response", IEEE International Conference on Acoustics, Speech and Signal Processing, ICASSP'83, vol.8, pp.399-402, April 1983.

[25] P. Kavitharajan and M.N.S. Swamy, "Some results on the nature of 2-Dimensional filter functions possessing certain symmetry in its magnitude response", IEEE Journal on Electronic Circuits and Systems, vol.2, no.5, pp.147-153, September, 1978.

[26] S.G. Tzafestas, "Multidimensional systems: Techniques and Applications", 1986.

[27] P. Kavitharajan and M.N.S. Swamy, "Some results on the nature of a two dimensional filter function possessing certain symmetry in its amplitude response", IEEE jounal on Electronic Circuits and Systems, vol.2, no.5, pp.147-153, September 1978.

[28] P. Kavitharajan and M.N.S. Swamy, "Symmetry constraints on 2-D half plane digital transfer functions", IEEE Transactions on Acoustics, Speech and Signal Processing, vol.27, no.5, pp. 506-511, 1979.

[29] V. Ramachandran, Ravi P. Ramachandran and C.S. Gargour, "Some properties of the z-domain Continued Fraction Expansion of 1-D discrete reactance functions, IEEE International Symposium on Circuits and Systems, (ISCAS), Sydney, Australia, 2001, vol 2, pp.841-844.

[30] Ling Luo, "A new z-domain continued fraction expansion and its use in the generation of stable transfer functions", M.A.Sc. Thesis, Concordia University, Montreal, QC, H3G 1M8, June 2003.

[31] V. Ramachandran and A. Sreenivasa Rao, "A Multivariable array and its applications to ladder networks", IEEE *Trans. on Circuit Theory, vol.CT-20, no.5, September 1973.*

[32] C.S. Gargour, V. Ramachandran and Ravi P. Ramachndran, "Modification of filter responses by the generalized bilinear transformations and the inverse bilinear transformations", *Electrical and Computer Engineering, 2003. IEEE CCECE 2003, Canadian Conference on, vol. 3, pp.2043-2046, May 4-7, 2003*

[33] James H. McClellan, "The design of two-dimensional digital filters by transformations", *Proceeding of 7thAnnual Princeton Conference on Information Sciences and Systems, pp.247-251, 1973.*

[34] V. Cappellini, A.G. Constantinides and P. Emilliani, "Digital filters and their applications", 1978, Academic Press.